Design, synthesis and biological evaluation of small molecules for controlling cellular development

HAFFEZ, HESHAM,RAFFAT,SHAWKY

Department of Chemistry

&

School of Biological and Biomedical Sciences

Design, synthesis and biological evaluation of small molecules for controlling cellular development

Hesham Raffat Shawky Haffez

A thesis submitted for the degree of Doctor of Philosophy

2015-2016

Declaration

The work described here was carried out in the Department of Chemistry and the Department of Biological and Biomedical Sciences, University of Durham between March 2012 and November 2015. All of the work is my own, except where specifically stated otherwise. No part has previously been submitted for a degree at this or any other university.

Statement of Copyright

Acknowledgments

Firstly, I would like to express my sincere gratitude to my advisor Prof. Andy Whiting for the continuous support of my Ph.D. study and research, for his patience, motivation, and immense knowledge. His guidance helped me in all the time of research and writing of this thesis. I could not have imagined having a better advisor and mentor for my Ph.D. study. Also, I would like to thank the rest of my thesis committee: Prof. Stefan Przyborski, Dr. Chris Redfern and Dr. Ehmke Pohl for their insightful comments and encouragement, to join their team as intern, to give access to the laboratory and research facilities which help me to widen my research from various perspectives.

I take this opportunity to express gratitude to all of my labmates in National Institute of Cancer Research of Newcastle University, Whiting's and Przyborski's groups in Durham University for their help and support. I can't forget the Egyptian Cultural centre and Educational bureau for their generous funding support to the research discussed in this dissertation.

Last but not the least; I would like to dedicate this thesis to my family; my father and spirit of my mother, to Amel my wife for supporting me spiritually throughout writing this thesis. For the past six months, Amel kept on reminding me 'Hesham, go to Library and write your dissertation'. To my lovely twins Yasseen and Karma who are able to make me smile.

I also place on record, my sense of gratitude to one and all, who directly or indirectly, have provided help in this venture.

Abstract

Cellular differentiation is a process directed by a wide range of controlling signaling molecules and pathways. All-*trans*-retinoic acid (ATRA) is one such compound that shows a wide range of biological activity. The endogenous effects of ATRA have the potential to be translated into many *in vitro* and *in vivo* applications; however, its administration is associated with many drawbacks. Consequently, a large group of synthetic analogues known as synthetic retinoids - that are structurally similar to ATRA have been prepared and tested *in vitro* in the search for higher stability and more potency.

A small library of stable synthetic retinoids known as EC and GZ derivatives were prepared and their biological activity investigated using TERA2.cl.SP12 human embryonal carcinoma (EC) stem cells and SHSY5Y neuroblastoma cells. Two compounds, EC23 and GZ25 were found to inhibit cellular proliferation and induce neural differentiation in both cell lines. EC_{50s} showed higher binding affinity of these two analogues to all RAR types and was confirmed by how they fit into the binding pocket of the different RARs. They bind into the binding pocket through a hydrophilic network of carboxylate group with Arg (salt bridge) and Ser (two hydrogen bonds) residues similar to ATRA.

These effects were thoroughly characterized and quantified by monitoring the phenotypic changes of both cell lines and the gene expression markers such as RAR-β, PAX6, NeuroD1 which showed higher order of efficacy for induction of neuronal differentiation.In this study, the combined use of calculated chemical structures, molecular docking tools with receptor binding assays and biological characterization was useful to probe, and hence, understand the biological activity of certain synthetic retinoids with the ultimate goal of designing more specific synthetic retinoic acid derivatives.

List of Contents

Abbreviations

13-Cis RA= 14-CRA	13-*Cis*-retinoic acid
9-Cis RA= 9-CRA	9-*Cis*-retinoic acid
Å	Angstrom
ACTB	Beta-actin
ADP	Adenosine Diphosphate
AF-2	Activation factor-2
Ala	Alanine
AM1	Austin Model 1
APL	Acute promyelocytic leukemia
Arg	Arginine
ASP	Astex Statistical Potential
Asp	Aspartic acid
ATRA	All-*trans*-retinoic acid
BDNF	BDNF
BLAST	*Basic Local Alignment Search Tool*
BSA	Bovine serum albumin
cAMP	Cyclic- Adenine monophosphate
CARs	constitutively activated receptors
CCDC	Cambridge Crystallographic Data Centre
CD	cluster of differentiation
Ci/mol	Curi/ mole
CK-8	Cyto-Keratin 8
CKI	Cyto- Keratin 1
CPU	*Central processing unit*
CRABP	Cellular retinoic acid binding protein
CYP26	Cytochrome P450-26
DBD	DNA- binding domain
DMSO	Dimethyl sulfoxide
DNA	Deoxyribonucleic acid
DRIP	D-receptor interacting protein
DTT	Dithiotheritol
E.Coli	*Escherichia coli*
EC	Embryonic carcinoma

EC_{50}	50% Effective concentration
EGF	Epidermal growth factor
ES	Embryonic stem cells
*E*x	Excitation
F318A	Oleic acid
GA	Geometric algorithm
GABAA	Gamma- amino butyric acid
GAD	Glutamic acid decarboxylase
GADPH	Glyceraldehyde-3-Phosphate Dehydrogenase
Glu	Glutamic acid
Gly	Glycine
GRF	Growth- releasing factor
GST	Glutathione-S-Transferase
HAT	Histone acetyltransferases
HDACs	Histone deacetylase
HEPES	4-(2-Hydroxyethyl)-1-piperazineethanesulfonic acid
His	Histidine
HIV	Human immune deficient virus
hTERT	Human telomerase reverse transcriptase
hTR	Human telomerase
I.D.	Internal diameter
IgG	Immunoglobulin G
Ile	Isoleucine
iPSCs	Induced pluripotent stem cells
ITC	*Isothermal titration calorimetry*
LBD	Ligand-binding domain
Leu	Leucine
LRAT	Lecithin retinol acyltransferase
LSQ	Live show quality bioinformatics databas
LXRs	Liver X receptor
Lys	Lysine
MC	Mechanical calculation
MP3	Moller-Plasset-3
MP4	Moller-Plasset-4

MD	Molecular dynamics
MeOH	Methanol
Met.	Methionine
MMFF	Molecular mechanics free force calculation
MMFFaq	Molecular mechanics free force calculation in aqueous
MNDO	Modified neglect of differential overlap calculation
MRF-4	Myogenic regulatory factor- 4
MSCs	Mesenchymal stem cell
MyoD	Myogenin D
NCBI	*National Center for Biotechnology Information*
NCOR	Nuclear receptor co-repressor
nM	Nano molar
NMR	Nuclear magnetic resonance
NNE	Non- neuronal elastase
NPCs	Neuro progenitor cells
NSE	Neuron specific enolase
NT-3	Neurotrophin-3
NT-4/5	Neurotrophin-4/5
Pax	Paired box protein
PDB	Protein data bank
Phe	Phenylalanine
PLA2	Phospholipase A2
PM3	Parameterized Model number 3
PPARs	Peroxisome proliferator-activated receptor
QAC	Quaternary ammonium compound
QCI	*Quadratic configuration interaction*
QM	Quantum mechanics
QSAR	Quantitative Structure activity relationship
R.M.S.	Root mean square
R.M.S.D.	Root mean square of deviation
RA	Retinoic acid
RAR	Retinoic acid receptor
RBP-4	Retinol binding protein 4
RCSB	Research Collaboration for Structural Bioinformatics

RXR	Retinoic X receptor
SCID	Severe combined immunodeficient
Ser	Serine
SFD	Serum free differentiation
SIB	Swiss Institute of Bioinformatics
SIN3	Transcription regulatory factor protein
SMCC	Srb and mediator protein-containing complex
SMRT	Silencing mediator for retinoid or thyroid-hormone receptors
SSEA	Stage-specific embryonic antigen
SVZ	Subventricular zone
Thr	Threonine
TIRF	Total internal reflection
TRAP	Thyroid-hormone-receptor-associated protein
TR-FRET	Time-resolved fluorescence resonance energy transfer
TrkB	Tropomyosin receptor kinase B
TSH	Thyroid-stimulating hormone
TTR	Transthyretin
TUJ-1	βIII-Tubulin
Val	Valine

List of retinoid chemical structures

Compound	Chemical structure	Molecular weight (g/mol)
ATRA	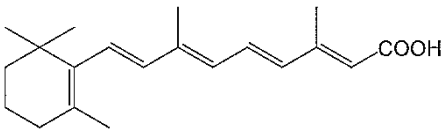	300.4
ATRA methyl ester	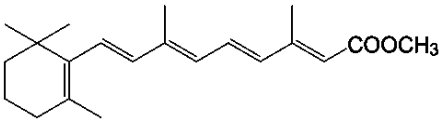	314.4
9-CRA	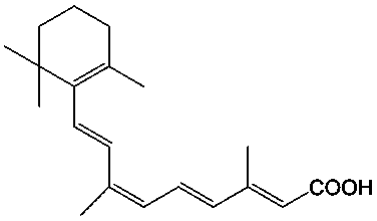	300.4
TTNBP	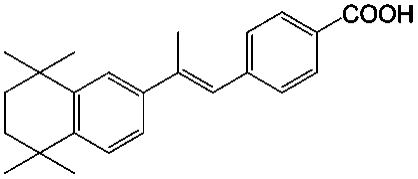	348.48
TTNN	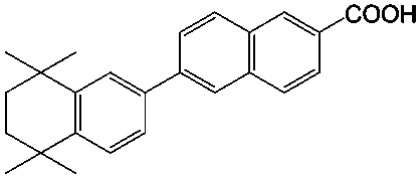	358.48
AM580	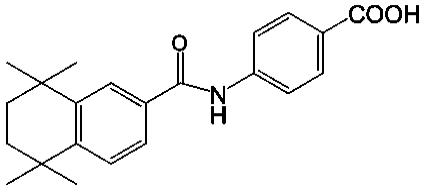	351.44
CD437	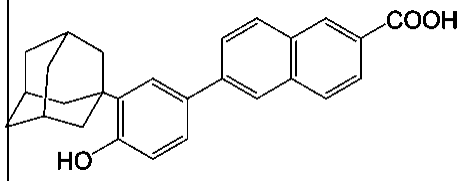	398.5
EC19	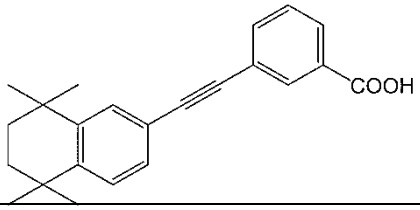	332.4

EC23	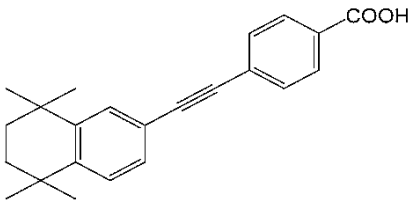	332.4
BMS195614	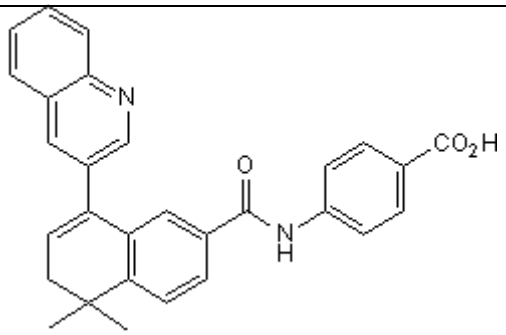	448.51
EC19 - methyl ester	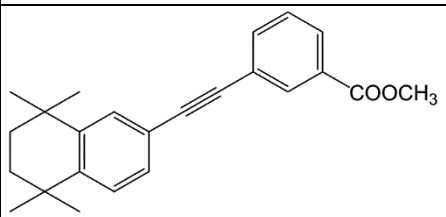	346.4
EC23 - methyl ester	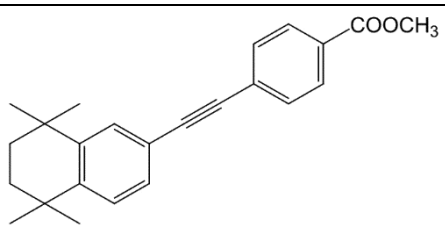	346.4
GZ18	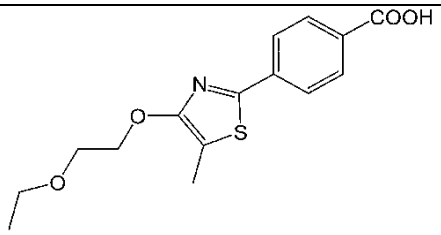	307.36
GZ22	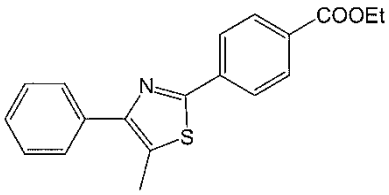	323.41

GZ23	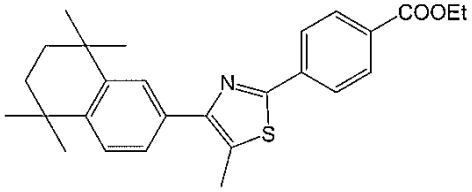	433.60
GZ24	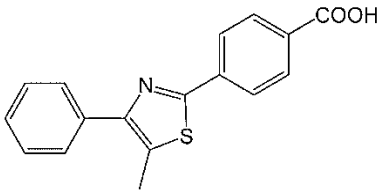	295.36
GZ25	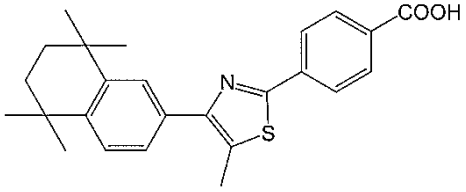	405.55

Chapter I

Molecular, cellular and binding activity of retinoids

Molecular, cellular and binding activity of retinoids

❖ Molecular activity of retinoids

1.1 Molecular docking

All pharmaceutical and biotech companies are facing enormous pressure from the market to apply all available techniques in the field of drug discovery in lower attrition rates and costs. Currently, one of the most widely applied techniques in drug discovery is computational chemistry and molecular modelling, which is centred on applying the fundamental laws of physics and chemistry to the study of molecules with the potential to be drugs. The ultimate aim for molecular modelling is to create models and simulations, which can help in the different stages of a discovery pipeline by predicting, rationalizing and estimating the properties of molecules and their interactions, thereby allowing a more rational approach to drug development. In this piece of research work, there is a combination between the molecular docking, receptor binding assay and biological evaluation of retinoids in a parallel way to understand the molecular binding interaction of retinoids with their cognate target.

The model building can be either simple or sophisticated, depending on the main purpose of construction. In practice, the molecular modelling of biomolecular interactions and binding processes has some limitations including the large amount of CPU time required and limitations in force field accuracy. However, modelling can fit in conjunction with other techniques, such as crystallography, to refine biomolecular modelling to provide accurate geometries, bond lengths and an insight into actual interactions and structure. Molecular modelling techniques are generally divided into two broad categories: 1) Ligand-based modelling which consists of a series of techniques, used for creating models and predictions based solely on the structure of the small organic compounds; 2) Structure-based drug design exploits the knowledge of the 3D structure of one or more biological receptors (targets, the ones sought to modulate and anti-targets, the ones sought not to interfere with) and or their macromolecular ligands.[1]

1.2 Receptor-ligand docking

To carry out receptor-ligand docking, it is assumed that a rigid molecule is used. The rigid protein representation greatly reduces the number of degrees of freedom sampled, enabling the development of algorithms for the rapid docking of large numbers of ligands. The problem with this approximation is that it ignores induced-fit effects.[2] Many docking programs work on this basic principle like that of DOCK, AutoDock,[3] ICM,[4] LigandFit[5] and Surflex.[6] On the other hand, a flexible docking theory was shown to be more efficient and convenient approach, generating many initial orientations (binding sites), for which at least one should be close to the correct structure. Many new programs work using this flexible principle such as FlexX,[7] GOLD[8] and Glide.[9]

1.3 Docking accuracy (Validation methods)

1.3.1 Self-Docking

The accuracy of a docking program can be assessed by comparing the predicted structures of protein-ligand complexes with crystallographic data. For rigid docking, the simplest comparisons are made by docking each ligand into its own cognate receptor conformation. This is referred to as self-docking.[10] It should be noted that these results are dependent on a few factors, including the experience of the individual performing the experiment, preparation of the individual protein and ligand structures prior to docking and average RMSD used as a measure of a docking accuracy. Hence, most data raised by self-docking was a round 1.5 Å according to Cambridge Database recommendations. In some cases, the polarized charges on the ligand have effect on the docking results with low RMSD orientations suggesting incorrect ligand orientation inside the binding site and the wrong hydrogen-bonding system and so it is recommended to use quantum calculations that apply a total ligand charge is zero.[11]

1.3.2 Cross-docking

Cross-Docking is a more complex and demanding test than self-docking and involves docking a ligand into a confirmation of the receptor that is not its cognate, but rather either the apo-structure of the receptor or one from co-crystallization with a different ligand.[12]

Cross-docking can generate reasonable ligand orientations, albeit usually not quite as accurate in details as obtained from self-docking. It can also introduce noise into the calculations with the effect of creating smaller energy gaps between experimentally observed and incorrect docking solutions, introducing an energetic preference for an incorrect solution.[13] This method is usually carried out by setting up rigid receptor docking. Given a setup of superimposed co-crystallized complexes of a given receptor, one simply takes all of the ligands and attempt to dock them into all, or some fraction, of the receptor conformations and records the ligand RMSDs. Some studies have used this procedure and referred to it as "ensemble docking".[14,15]

1.4 Nuclear receptors as a biological target

The nuclear hormone receptor super family includes receptors for thyroid and steroid hormones, retinoids, vitamin D as well as different “orphan” receptors of unknown ligand. Ligands for some of these receptors have been recently identified, showing that products of lipid metabolism such as fatty acids, prostaglandins, or cholesterol derivatives can regulate gene expression by binding to nuclear receptors. Nuclear receptors act as ligand-inducible transcription factors by directly interacting as monomers, homodimers, or heterodimers with the retinoid X receptor with DNA response elements of target genes, as well as by “cross-talking” to other signalling pathways. Most of these receptors bind co repressor factors and actively represses target gene expression in the absence of ligand[16] and once ligand activation happens, the transcription activity occurs through recruitment of coregulators. Since this initial finding, it has been shown that the RA signal can be transduced in cultured cells through two families of retinoid receptors. The RAR family (RAR-α, -β and -γ and their isoforms) are activated by both all-*trans*-RA and 9-*cis*-RA, whereas the RXR family (RXR-α, -β and -γ) are activated only by 9-cis-RA.[17, 18, 19, 20]

1.4.1 Retinoic Acid Receptors (RARs)

The biological effects of retinoids come through retinoic cid receptors. They were first identified in 1987 as three major types originated from three different genes; RAR-α (NR1B1), RAR-β (NR1B2) and RAR-γ (NR1B3).[21,22,23]

There are various isoforms for each RAR types which differ in the alternative splicing of the two promoters in their N-terminal region with P2 as the downstream promoter found in the retinoic acid response element (RARE).[24] The isomers of RARs are RAR-(α1 and α2), RAR-(β1 and β2) and RAR-(γ1 and γ3 initiated at the P1 promoter and γ2 and γ4 initiated at the P2 promoter).[25] The biologoical effect of RAR is driven through heterodimerization with other different nuclear receptors such as RXRs.[26] The resultant RXR-RAR heterodimers can bind to RARE DNA region found in many target genes responsible for cellular differentiation.[27,28] Examples of these target genes are Hox genes[29,30] which are responsible for cellular development especially in anteroposterior axis in embryo. Also, CYP26 genes especially CYP26A1 has this RARE region and responsible for the cellular metabolism of ATRA. [31] And finally, retinol binding protein I and CRABPII are the two genes which play key role in cellular transport and biological activity of retinoids inside the cells.

1.4.2 Retinoic X Receptors (RXRs)

Retinoid X receptors are the second class of retinoic acid receptor that discovered in 1990.[32] There are three RXR subtypes; RXR-α (NR2B1), RXR-β (NR2B2) and RXR-γ (NR2B3) and they originated from different genes.[33,34] Also there are two isoforms for each subtype; RXR-α (α1 and α2), RXR-β (β1 and β2), and RXR-γ (γ1 and γ2) which are different from each other in N-terminal and A/B domain.[35] 9-CRA, the isomer of retinoic acid was known to be the principle ligand acting on these receptors with higher binding affinity compared to ATRA.[36] In addition, these receptors can also heterodimerize with other different nuclear receptors such as vitamin D receptor (VDR), farnesoid X receptor (FXR) and constitutively activated receptors (CARs).

1.5 Impact of RAR-RXR complex on biological activity of retinoids

RAR and RXR actively involved in the retinoic acid mediated transcription[37], however they are not active in their monomeric forms. Also, RAR does not dimerize with itself but forms heterodimeric proteins with RXR (RAR-RXR). This RAR-RXR protein complex is the predominant receptor complex for retinoic acid signalling. In addition to forming heterodimers with RAR, RXR is able to homodimerize and also dimerize with other receptor proteins, including PPAR. The RAR-RXR protein complex binds to retinoic acid response elements (RAREs) or retinoid X response elements (RXREs), each of which are well-defined DNA sequences.[38] RXR enhances the binding of the RAR protein to the RARE sequences.5 In the absence of ligands at the ligand receptor binding sites, the apo-RAR:RXR heterodimer recruits corepressors, proteins and enzymes that interfere with the transcription process.[39] Many genes were strongly identified as being regulated by this classical pathway (either up-regulated or down-regulated).[40]

Another downstream biological processes occur in parallel to the activation mechanism of RAR-RXR, which is ubiquitination and phosphorylation as that are crucial for gene regulation and transcription.[38,39,41] This includes the degradation of RAR-RXR by the proteosome for the termination of retinoid signalling. Phosphorylation may also participate in proteosome degradation and affect the ability of the holo- RAR-RXR complex to associate with coregulators and general transcription factors.[39] Phosphorylation of the serine residues of RARγ has been shown to control both the RARγ transactivation function and the degradation of RARγ by the proteosome.[40]

1.6 Repression /derepression mechanism

The mechanism of depression and activation of retinoic acid receptors was suggested in absence of retinoic acid agonist, as the corepressor proteins NCoR or SMRT with histone deacetylases (HDACs) or DNA-methyl transferases binds to the RAR-RXR heterodimers. This complex induces the depression mechanism and hence, the condensed chromatin structure and transcription is inhibited.[42]

Upon activation, retinoic acid binds to the RAR type which induces some conformational change in the LBD which allows the coactivator binding and corepressor release. This is followed by activation of other different enzymes such as histone acetyltransferases or histone arginine methyltransferases which are responsible for actiation of gene transcription.[43,44] The process of binding of retinoic acid to RAR is key step in activation of these cascade reactions as RXR- ligands (rexinoids) can not activate the previousely mentioned complex formation without RAR- agonist. However, the activation of both RAR and RXR by binding to agonists at the same time was shown to have synergistic effect on the activation process which might suggest the co-transcriptional role of RXR as a partner in RAR-RXR heterodimers.[45]

Another mechanism is proposed in the absence of agonists, where corepressor links the receptor complex to histone deacetylases (HDACs) through SIN3, resulting in chromatin condensation and gene silencing. Upon agonist binding to the receptors, a conformational change is induced, destabilizing the corepressor complex and allowing co-activators to bind. Co-activators recruit histone acetyltransferases (HAT) resulting in acetylation of histone amino-terminal tails, thus, inducing chromatin decondensation. Finally, a third multi-subunit complex, termed Srb and mediator protein-containing complex (SMCC), or thyroid-hormone-receptor-associated protein (TRAP), or D-receptor interacting protein (DRIP) establishes contact with the basal transcriptional machinery, leading to increased transcription[46] (Fig. 1.1).

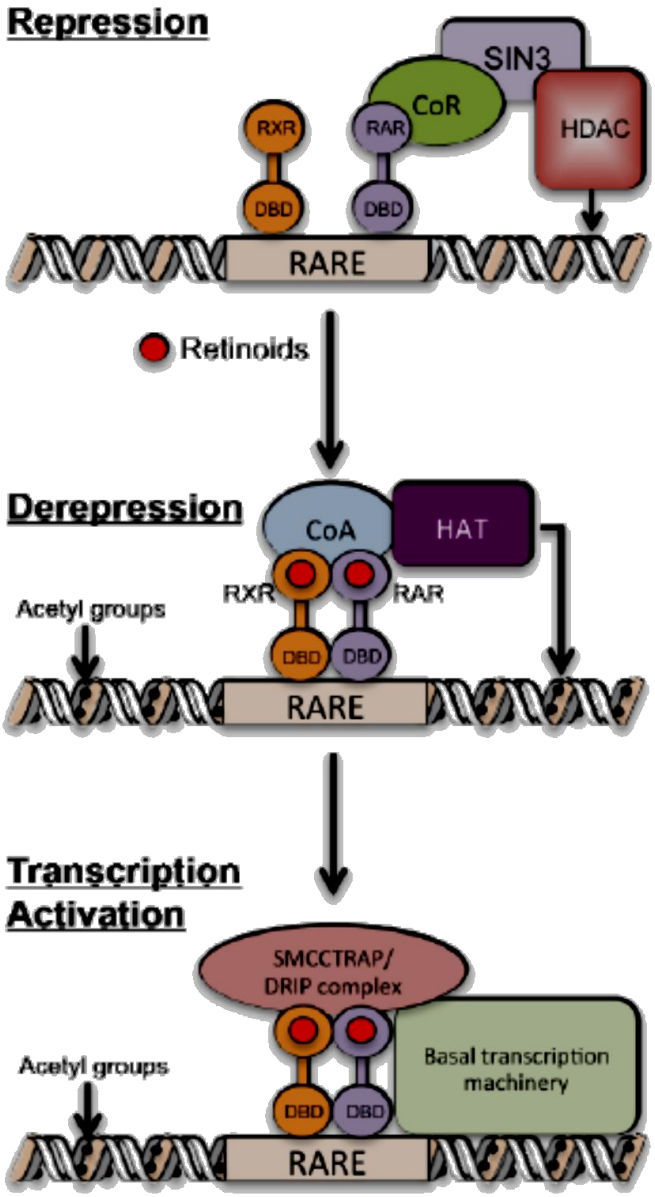

Figure 1.1: Mechanisms of repression, depression and activated transcription. In the repression state, ligand is absent and hence, co repressor (CoR) binds with histone deacetylases (HDACs) through another transcription protein, SIN3 resulting in silencing of gene transcription. Once retinoid ligand binds, CoR is removed due to conformational changes in the ligand binding pocket to allow co activator (CoA) binds. This will activate the recruitment of histone acetyltransferases (HAT) and acetylation of amino terminal occurs and hence, the induction of chromatin condensation. Another possibility for the activation mechanism is through the formation of multi-subunit complex co activators, SMCC or TRAP with DRIP complex to activate the basal transcriptional machinery and gene transcription.[46,47]

1.7 Crystal structure of RARs

Like other transcriptional regulators, nuclear receptors exhibit a modular structure with different regions corresponding to autonomous functional domains that can be interchanged between related receptors without loss of function. A typical nuclear receptor consists of a variable NH2-terminal region (A/B), a conserved DNA binding domain (DBD) or region C, a linker region D; and a conserved E region that contains the ligand-binding domain (LBD). Some receptors contain also a COOH terminal region (F) of unknown function. All RARs have two activation domains, N-terminal AF-1 which contributes to constitutive ligand independent transcriptional activation function and C-terminal AF-2 which is strictly ligand dependent and conserved among all members of the nuclear receptor superfamily[48] (Fig. 1.2).

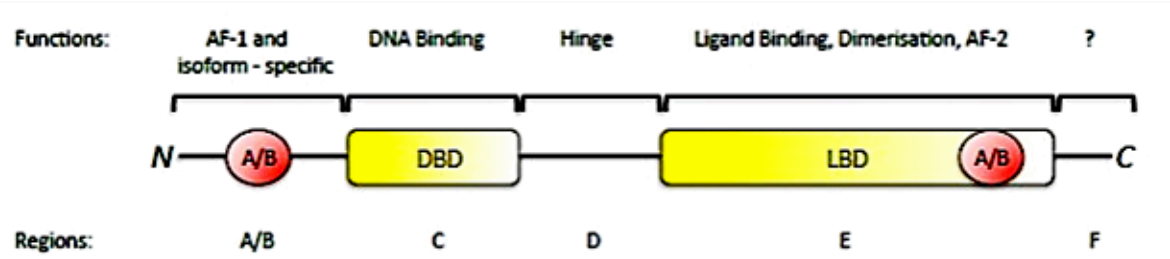

Figure 1.2: Structural and Functional domains of a retinoid receptor. There are 5 main domains; ligand-independent, DNA binding, hing, ligand dependent and F domains. Ligand binding domain (LBD) is the most important part for binding of RARs with its retinoid ligands. LBD contains AF-2 region which is reposnible for co activator binding and active transactivation process.[47]

Also, it was observed in a study using LSQ options with a RMS deviation 1.5Å that human RAR holo-LBD topology (Fig. 1.3) consists of twelve α-helices (H1 to H12), which are organized in a three-layer structure with H4, H5, H6, H8 and H9 sandwiched between H1 and H3 on one side, and H7, H10 and H11 on the other side. Two topologically conserved β-strands (S1-S2) form a β-turn inserted between loop 1-3 (connecting H1 to H3) and H3.[49] In addition, it is noted that H12 helix position is essential to seal the ligand binding pocket of the receptor. Also, this conformation generates a recognisition surface constituted of mostly hydrophobic residues from helices H3, H4 and H12 of RAR-β and RXR-α which allow, after the heterodimerization of the two receptors for the binding of coactivator peptide per protomer.[50]

Also amino acid sequence alignment of RAR-α, -β and –γ (Fig. 1.4) reveals that among all of these residues, only three positions were variable (marked with blue arrows): serine 232, alanine 225, and alanine 234 in H3, isoleucine 270, isoleucine 263 and methionine 272 in H5 and valine 395, valine 388 and alanine 397 in H11. These amino acid residues therefore became obvious candidates as key amino acids responsible for RAR-ligand selectivity.[51]

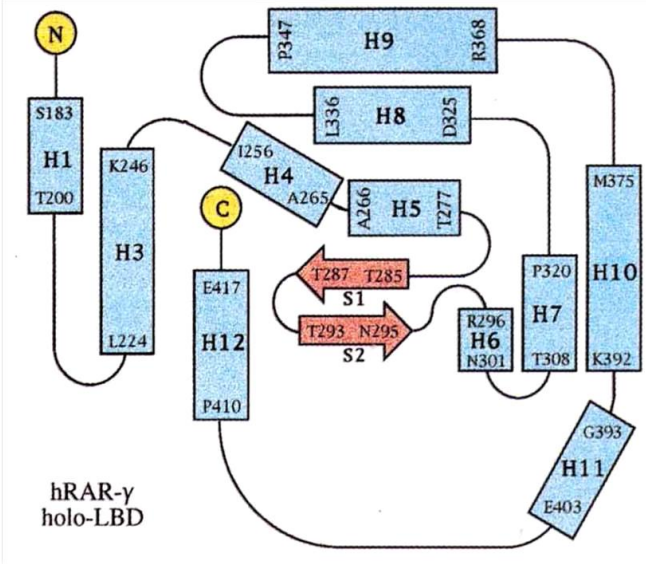

Figure 1.3: Schematic representation to RAR helices arrangement. RAR-γ LBD consists of twelve α-helices (H1 to H12) and two β-strands (S1-S2). The ligand binding pocket is buried between of H1, H3, H5, H7, H11 and H12.[47]

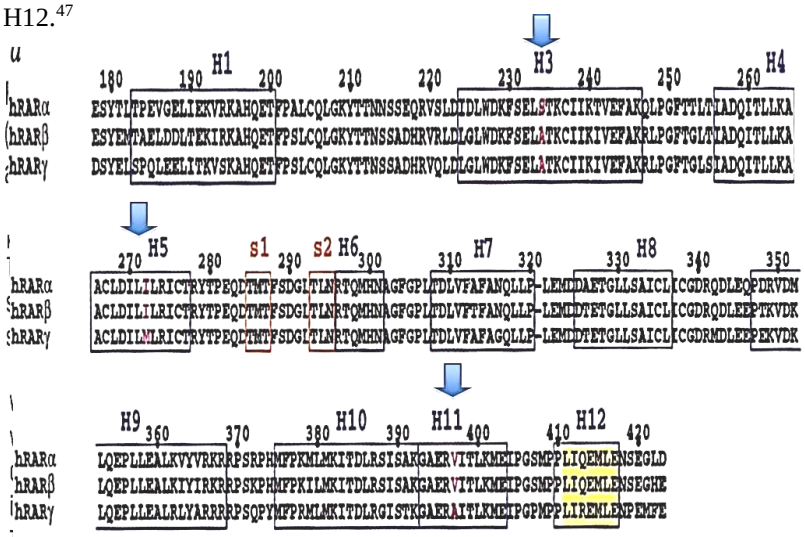

Figure 1.4: Amino acid alignment of RAR-α, -β and –γ LBD. Amino acid regions indicated by *blue arrows* represent residues that are different in RAR LBD and have direct effect on receptor-ligand interactions. In H3, serine amino acid in RAR-α is different than alanine in RAR-β and RAR-γ. In H5, methionine amino acid in RAR-γ is different than isoleucine in RAR-α and RAR-β. In H11, alanine amino acid in RAR-γ is different than valine in RAR-α and RAR-β.[52]

1.8 The retinoic acid-binding pocket

The studies showed that the ligand is completely buried within the ligand-binding pocket formed by residues located on helices H3, H5, H7, H11 and the β-turn. The majority of the contacts are van der Waals interactions except for the carboxylate group of the ligand that forms a salt bridge with the conserved Arg residue in helix H5, which participates in a network of hydrogen bonds with Ser (β-turn) and Lys or Leu residues.[53,54] Also sequence alignment of RAR-α,-β, and-γ shows that only three residues in the ligand-binding pocket are variable: Ala234 (Ser232 in -α and Ala225 in -β), Met272 (Ile270 in -α and Ile263 in -β), and Ala397 (Val395 in -α and Val388 in -β). These divergent residues are obvious candidates to account for the RAR selectivity of certain synthetic retinoids (Fig. 1.5). In RAR-γ, Ala234 and Met272 interact with the isoprene tail and Ala397 with the β-ionone ring. RAR-α and RAR-β differ only by one residue in the pocket [Ser232 (RAR-α) *versus* Ala225 (RAR-β) in H3].[55,56, 57] The orientation of H12 helix is vibrant and movable with changing the binding mode of LBD. In the unbound receptor, Phe282 (H3), Phe442 (H11) and Phe455 (H12) are almost completely solvent exposed and make very little or no contact at all with other LBD residues. Upon binding interaction with ligand, a concerted reorientation of these three phenylalanine side-chains occurred that become in close contact to H12 helix and the co-activator peptide.[58] This is consequently followed by forced rotation of Phe282 around the Cα-Cβ bond by 110° due to steric restrictions applied by Leu648 of the co activator peptide which consequently forces Phe455 from H12 to pivot by 104°.

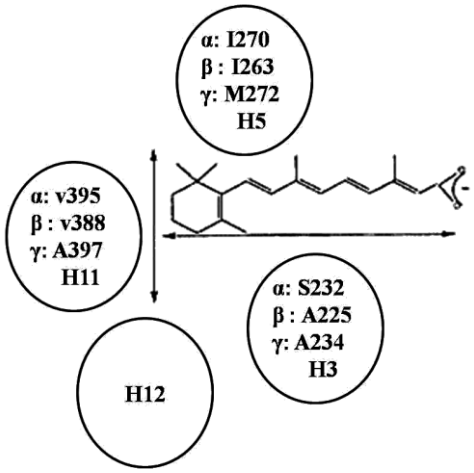

Figure 1.5: RAR ligand binding pocket with the main different active residues in LBD. In H3, S232 is thought to be responsible for the selectivity of RAR-α and makes the binding pocket more polar; While M272 and A397 in RAR-γ are thought to be responsible for preference of the pocket to the retinoid ligands with more hydrophobic side chains.[58]

A rigid-body translation of helix H12 towards H3 and the coactivator's peptide of almost 2.0Å allows Phe445 to be accommodated in a small hydrophobic pocket of residues composed from helices H3 (Phe282, Leu281, Leu285), H12 (Met459) and the peptide (Leu645, Met644, Leu648). Consequently, Phe442 (H11) flips by 112° to contact Leu460 (H12) and forms together with Phe282 of H3 an "aromatic clamp" that locks H12 in the optimal conformation.[59] The more compact structure of RAR-γ and other holo-LBDs which are different from the apo-structure in two major ways: (i) three helices, H3, H11 and the transactivation helix H12, undergo large conformational changes; and (ii) helix H12 of hRARapo-LBD is replaced by a disordered connecting peptide in an extended conformation that may be necessary to allow the N-terminal part of helix H3 to reach its new position[60] (Fig. 1.6). Upon ligand binding, H11 is repositioned in continuity with H10, and the concomitant hinging of H12 is accompanied by additional structural changes such as bending of H3 and folding of the H6-H7 loop. These conformational changes lead finally to the formation of specific ligand binding domain interface with coactivators.[61]

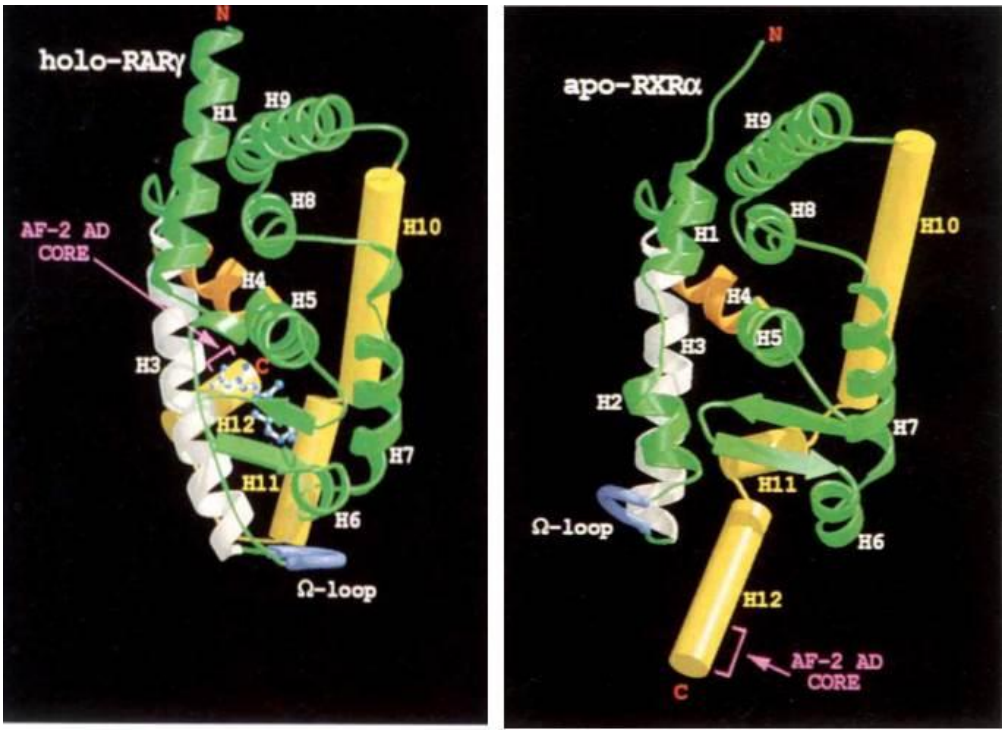

Figure 1.6: Schematic representation of hRXR-α apo-LBD (left) and hRAR-γ holo-LBD (right). RAR-γ is bound with ATRA (left) and H12 is able to move in apposition for binding with co activator and lock the ligand binding pocket. RXR-α is in the silence state (right) -without binding to the ligand- with H12 is flipping in the space.[60]

It was observed also that Lys236 in RAR-γ displays two equivalent possible conformations. This can help to coordinate since NH_3^+ of Lys236 interacts with the carboxyl group of ATRA and other retinoids when possible.[61] Furthermore, Leu266 can provide some information about the inside of the ligand binding pocket as it was found it plays important role for hydrophobic interaction with the 7-methyl-group of ATRA.[62] Also among the numerous residues that have important role inside RAR binding pockets are Phe302, which is in close contact with the adjacent C7 methenyl group (4.5Å cut-off).[62] Also Gly301 and Gly303 were shown to be critical for RAR-α specific van der Waal's interactions with ATRA.[63,64] In addition, studies emphasise that some amino acid residues from the N-terminal region of the LBD, such as Ser232 and Thr239 in RAR-α play a role in selectivity for polar retinoids by participating in a hydrogen bond with the amide linker of retinoids.[65] Also, Al225 and Ile232 in RAR-β inhert through different hydrophobic interactions and Met272 in RAR-γ, through the presence of a sulphur atom in the side-chain, which could account for weak hydrogen bonding with the hydroxyl group of some retinoid agonists and antagonists.[66] Finally, it should be noted that the interactions between RAR and RXR within the heterodimer work independently from each other, like their monomers, which is in agreement with many studies that showed that dimerization does not affect the structure of RAR and RXR LBDs or their affinities for different retinoids.[67]

1.9 Endogenous retinoids

The endogenous ligands for RAR and RXR receptors are ATRA, 9-CRA and 13-CRA. ATRA binds and activates only RARs, while 9-CRA acts as an agonist for both RARs and RXRs. 13-CRA has no approved significant biological activity as with its isomer 9-CRA. Crystallographic studies of the LBDs of both types of retinoic receptors showed that the shape of the LBP differs markedly between RARs and RXRs. RARs possess linear "I" shaped LBPs, whereas those of RXRs are a shorter and more restrictive "L" shape. As a result, the linear retinoid ATRA can act as a ligand only for RARs while the flexible 9-CRA can adopt both the linear and twisted conformations required for binding to both RARs and RXRs respectively[68, 69] (Fig.1.7). Also, the superposition of 9-CRA molecules from holohRXR-α (yellow) and hRAR-γ (red) showed a difference in binding affinity to different retinoic receptors[70, 71] (Fig. 1.8).

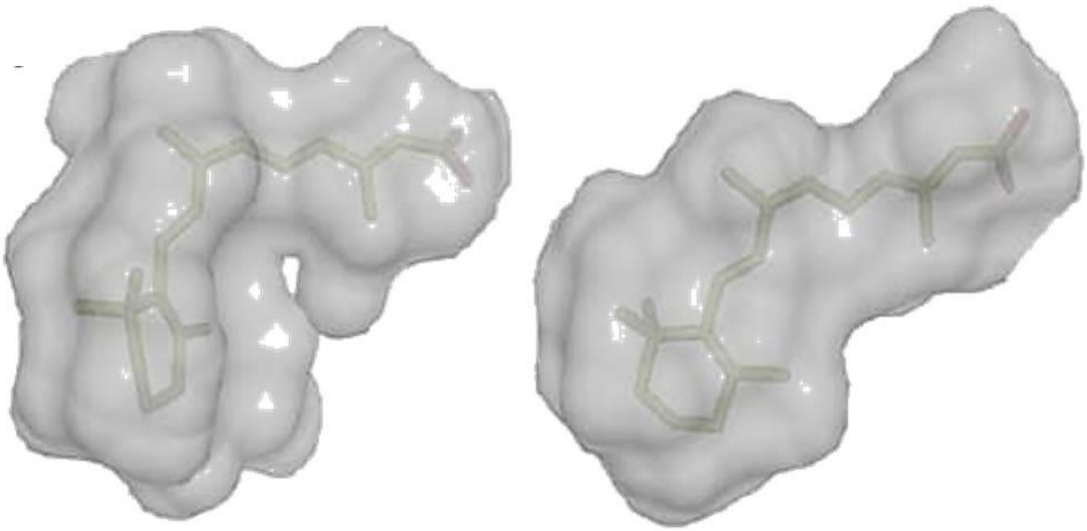

Figure 1.7: RAR and RXR cavities calculated by VOIDOO and MSMS[72] with a probe radius of 1.4 Å in white using DINO[73]occupied by 9-CRA.[60] The conformational bending structure of 9-CRA allows it to bind both the L-shaped pocket of RXR and the more elongated pocket of RAR.

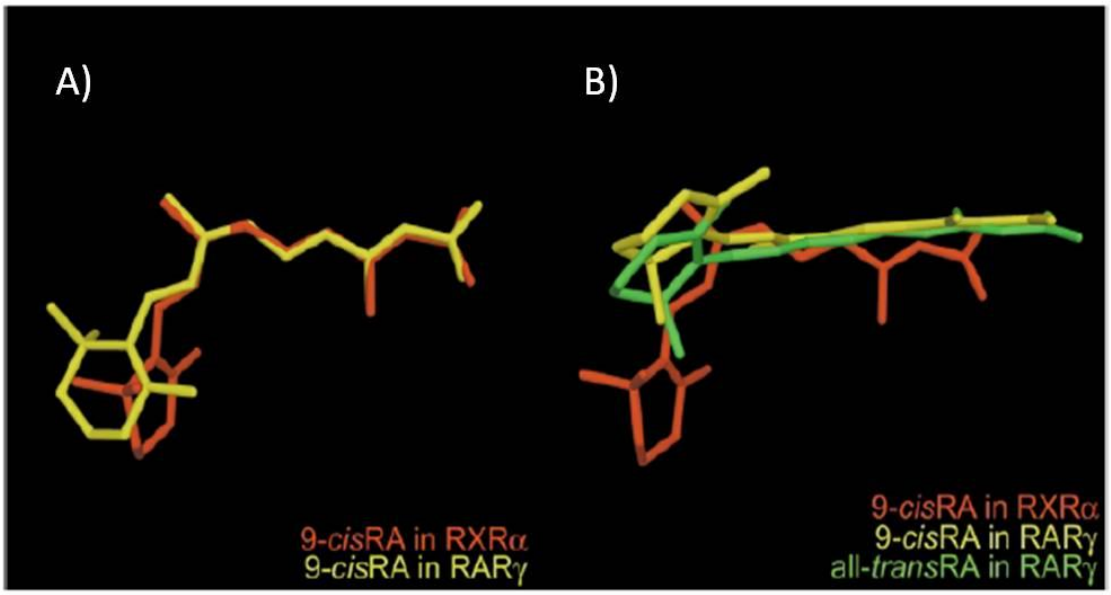

Figure1.8: Relative orientation of 9CRA and ATRA molecules after superimposition in both RXR and RAR. A) The superimposition of the 9-CRA before binding to the binding pocket of RAR and RX; B) the superimposition of 9-CRA and ATRA inside the binding pocket of RAR and RXR 9- CRA is able to adapt its conformational structure to bind both RAR and RXR, while ATRA is able only to bid the pocket of RAR.[60]

1.10 Synthetic retinoids analogues

Before talking about the different synthetic retinoid analogues, we should classify them according to the level of transcriptional activation of RAR[74] into:

- Complete agonist: they have good binding affinity to the RAR, induce coactivator recruitment and trigger the required response mimic to the action of a naturally occurring ATRA.
- Complete antagonist: this class of retinoids binds in the same fashion like agonists, however, the orientation of H12 helix is different than with ATRA or agonists and hence, cannot bind the co activator and the response would be different.
- Neutral antagonist has no activity in the absence of an agonist but can block the activity of it.
- Partial agonist: they bind to and activate RAR, but have only partial efficacy at the receptor relative to a full agonist. They may also be considered ligands which display both agonistic and antagonistic effects - when both a full agonist and partial agonist are present; the partial agonist actually acts as a competitive antagonist.
- Several studies tried to increase stability and activity of retinoids by replacement of two C=C double bonds in the conjugated polyene by other groups to decrease photo-induced isomerisation. Some examples of these classes are stilbene, tolan and biaryl arotenoids such as TTNPB,[75] EC23[76] and TTNN[77] respectively (Fig. 1.9).

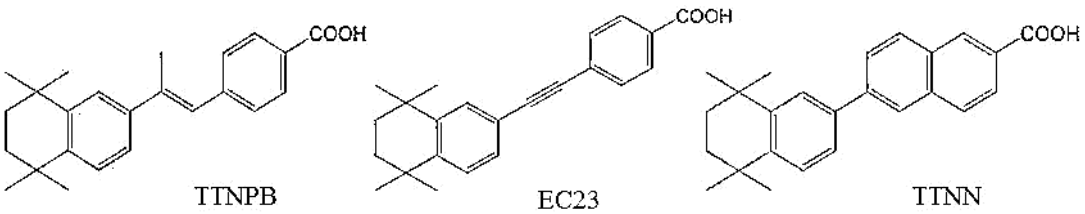

Figure 1.9: Different arotenoids with higher stability and activity than ATRA.

TTNPB is one example of a potent arotenoid (aromatic retinoid) analogue of ATRA that is modified in the 4-position of the hydrophobic ring as well as the polyene chain,[50] and it binds to all three nuclear retinoic acid receptors (RARs)[78,79] with higher binding affinity and is biologically more potent than ATRA[80,81] due to the higher stability profile. It is 100-times more effective at inhibiting the growth of breast cancer cells and 250-fold more potent in suppressing the growth of DMBA-induced skin papilloma in mice.[82] The modification in TTNPB carboxyl group with N-(4-hydroxyphenyl) amido (4HPTTNPB) or a 4-hydroxybenzyl (4HBTTNPB) group gave compounds with different biological activity, poor binding affinity to RARs but induces apoptosis in cancer cells. Even 4HPTTNPB is less toxic to developing embryos than the parent TTNPB (Fig. 1.10).

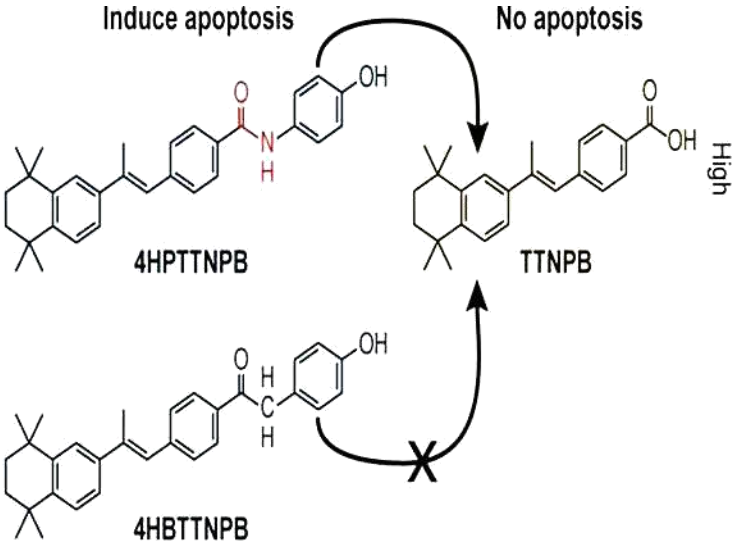

Figure 1.10: Two effective retinoids derivatives of TTNPB.[83]

Other examples of two selective potent RAR-α selective agonists are AM80 and AM580 which displayed a marked selectivity towards RAR-α. The K_d values of these compounds for RAR were 1 order of magnitude lower than the K_d for RAR-β and 2 orders of magnitude lower than the K_d for RAR-γ. This could be explained in terms of an additional Ser232 residue present inside, the RAR-α LBD pocket which can be oriented in a certain position suitable for the formation of additional hydrogen bonding to increase the selectivity and affinity of these compounds to RAR-α.[84] There is the same issue with BMS-185411, which is selectively bound to RAR through Ser232, although it is an antagonist which interferes with H12 transactivation.[85]

In contrast, BMS195614 (check the list of retinoid chemical structures) is an example of a neutral antagonist with selectivity for RAR-α and this can be explained in two parts: 1) the agonistic part is due to interaction between three divergent ligand-binding pocket residues that determine the RAR-α selectivity (Ser232 [H3], Ile270 [H5], and Val395 [H11]); 2) looking carefully into the interactions between these residues and BMS614 which was previously assumed to be responsible for the RAR-α specificity of BMS614, these are not observed in the crystal structure. This is the case for the Ser232 OH group, which is not hydrogen bonded with either the amide NH or carbonyl groups of BMS614, but with the aromatic CH (3.1° A**)** located in the *meta*-position (relative to the carboxylate moiety) of ring E. The reasons for this change in interaction and shift in activity is assumed to be due to BMS614 being a shorter molecule than ATRA, and also due to the location of the antagonistic extension of BMS614 between H3 and H11 which prevents the positioning of helix H12 in the "active" conformation.[55]

❖ Ligand–receptor binding interactions

The transcriptional response mediated by retinoic acid involves a complex series of events beginning with ligand recognition by a nuclear receptor. This step is important to recognize and see what factors are affecting retinoid binding to RARs, in terms of chemical structure modifications. Several studies have discussed the relative binding affinity of several retinoid derivatives, either naturally occurring or synthetic, to measure EC_{50}, K_d and Bmax, to explain how this chemical difference affects the binding affinity. Many other factors such as the relationship between the binding affinities of retinoids to RARs is correlated to heat of binding and thermodynamic entropy occurred inside ligand binding pocket need to be considered. In addition, there is still a need for explanations about the relative difference in binding affinities for different retinoids in terms of molecular modelling studies to give an indication about how the geometry of the binding pocket has impact on relative binding affinities.

1.11 Law of mass action

Ligand – Receptor binding experiments are usually analyzed according to the simple model of law of mass action:[86,87,88]

$$[R] + [L] \underset{k_{off}}{\overset{k_{on}}{\leftrightarrow}} [RL]$$

Where [R], [L] and [RL] represent the free concentrations of receptor, ligand, and receptor-ligand complex, respectively, and where it is assumed that the reaction components can freely diffuse within the medium. k_{on} and k_{off} are the rate constants for association and dissociation of the ligand-receptor complex.The reaction is driven by the concentration of the reacting agents. Equilibrium is reached when the rate at which ligand-receptor complexes are formed and dissociate are equal. At equilibrium, the following applies:

$$[R]\,[L]\,k_{on} = [RL]\,k_{off}$$

The equilibrium dissociation constant, K_d, a measure for binding affinity, is defined as:

$$K_d = \frac{k_{on}}{k_{off}} = \frac{[L]\,[R]}{[RL]}$$

These constants have the following units: k_{on}: $M^{-1} \cdot s^{-1}$; k_{off}: s^{-1}; K_d: M, where M stands for Molar or $mol \cdot L^{-1}$. When a receptor-binding experiment is performed, [LR] usually is the parameter needs to be determined.This implies, however, that only a minor fraction (<5%) of the total applied ligand should become bound (either by specific binding, nonspecific binding or adsorption to tissue and assay container) so that the free concentration is not altered.

1.12 Retinoids receptor binding assays

Retinoids need a specific receptor-binding assay especially when dealing with naturally occurring retinoids (ATRA and 9-CRA) to be sure that they are isomerically pure and of high specific activity. Some of the popular radio-receptor assays used are competitive binding assays which require high specific activity of radiolabelled [H3]-ATRA or 9-CRA (> 25 Ci/mol), coupled with a co transfection assay to identify the structural features of these retinoids and the impact on receptor selectiveness and ability to induce co-activators transactivation. The first example is a study carried out[89] to compare between the binding affinity of ATRA and 9-CRA to RARs in the different organs of rainbow trout tissues through inducing reproduction, body pattern formation and normal tissue maintenance. The different tissues were isolated, homogenized and the nuclear portion was extracted. Several centrifugation was done and The final pellet was transferred to a scintillation vial with 5 ml of scintillation cocktail and assayed for ^{3}H activity The results are shown in (Table 1.1) as ATRA showed general higher affinity in all types of tissues (lower K_d) compared to 9-CRA (higher K_d) while *visa versa* in terms of binding capacities (B_{max}). This means ATRA has higher binding affinity and can occupy a lot of free receptors available compared to 9-CRA.

Another radio-labelled receptor binding assay story[90] is that of receptor selectivity of TTNPB, LG100268 and 9-CRA. Table 1.4 shows the comparative abilities (K_d) of the RAR-selective retinoid agonist TTNPB, and the pan RAR-RXR agonist 9-CRA, to bind the different baculo virus-expressed retinoid receptors. The structures of these compounds are shown in (Fig. 1.11), as it was found that using a competitive binding assay, LG100268 binds strongly to RXR-α,-β, and-γ but not to RAR-α,-β, and-γ. Conversely, TTNPB binds with high affinity to RAR-α,-β, and-γ but not at all to RXR-α, -β, and-γ. The pan agonist 9-CRA binds with high affinity to both RARs and RXRs in this assay and that matches with the previous observation regarding twisting structure of 9CRA inside RAR and RXR LBDs[91] (Table 1.2).

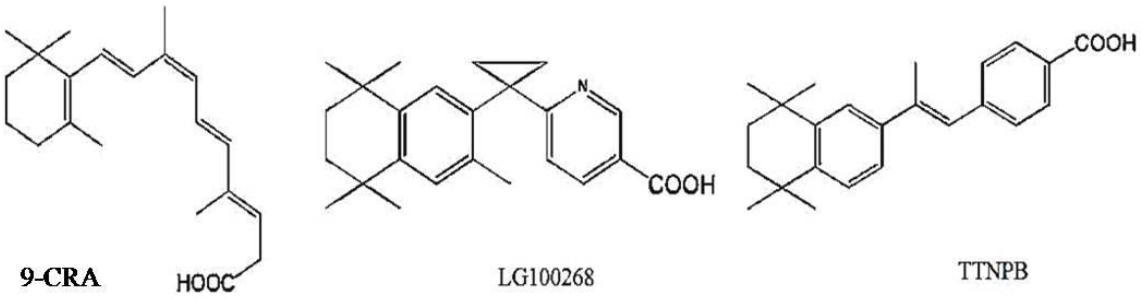

Figure 1.11: Chemical structures of 9-CRA, TTNPB and LG100268.

Table 1.1: Affinity (K_d) and binding capacity (B_{max}) of ATRA and 9-CRA in nuclear fraction of adult Rainbow Trout tissues.[89]

Tissue	**RA isomer**	**K_d(nM)**	**B_{max} (fmol/mg protein)**
Gill	ATRA 9CRA	1.0±0.1 7.0±0.2	175.6±16.8 214.3±29.1
Liver	ATRA 9CRA	2.5±0.1 51.2±2.9	74.7±5.3 1076±270
Eyed embryo	ATRA 9CRA	1.9±0.03 11.5±0.3	483.8±3.3 526.0±10.4
Post hatch fry	ATRA 9CRA	3.4±0.1 24.2±1.4	296.0±4.7 342.9±10.8
Swim-up fry	ATRA 9CRA	3.9±0.1 55.9±13.5	62.1±1.4 115.5±21.7

Table 1.2: $K_d$values for receptor selective ligands.[92]

Retinoid agonist	**Kd value (nM) for:**					
	RAR-α	RAR-β	RAR-γ	RXR-α	RXR-β	RXR-γ
9C-RA	93	97	148	8	15	14
TTNPB	20	39	51	8113	4093	2566
LG100268	10000	10000	10000	3	3	3

The comparison between different retinoid structures in terms of radio labelled binding affinity did not stop at natural retinoids but was extended to compare between different derivatives of the same synthetic retinoid to explore how structural modification has an impact on binding activity. This study was issued to compare ATRA, 9-CRA, TTNPB with derivatives of 3-methyl, 3-ethyl and 3-isopropyl TTNPB using competitive binding assay with [3H]-9-CRA (Fig.1.12). Table 1.5 shows how is ATRA is a good activator of RAR-α, -β, and -γ, however, it is less active at RXR-α, -β, and –γ. In contrast, 9-CRA is a potent activator of RXR-α, -β, and -γ. TTNPB functions as a potent activator of RAR-α,-β, and-γ but does not activate RXR-α, -β, and -γ in this co-transfection assay. Examination of 3-alkyl-substituted TTNPB derivatives show a different activation profile: in the co-transfection assay, 3-methyl-TTNPB is a (10-200)-fold weaker activator of the RARs than is its parent TTNPB. In contrast, 3-methyl- TTNPB activates all members of the RXR subfamily but not all members of the RAR subfamily.

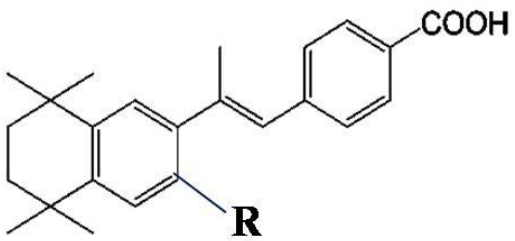

R= methyl

R= Ethyl

R= Isopropyl

Figure 1.12: Chemical structures of TTNBP analogues used in transactivation and competition assay.[51]

The results for 3-ethyl- and 3-isopropyl-TTNPB showed similar, albeit lower, activation profiles across all six receptors as 3-methyl-TTNPB, as was observed in the binding studies. It is still more interesting to know the reason in this difference in binding activity due to structural modification[93] (Table 1.3).

Table 1.3: Competitive assay from CV-1 cell.[93]

Retinoid agonist	**EC_{50} (nM)**					
	RAR-α	**RAR-β**	**RAR-γ**	**RXR-α**	**RXR-β**	**RXR-γ**
ATRA	350 ± 31	80 ± 9.0	10 ± 2.0	900 ± 70	1400 ± 130	1100 ± 85
9C-RA	191 ± 20	50 ± 17	45 ± 5.0	100 ± 25	200 ± 30	140 ± 13
TTNPB	30 ± 6.0	3 ± 2.0	2 ± 1.0	>10000	>10000	>10000
3-Methyl- TTNPB	340 ± 30	230 ± 28	180 ± 15	1200 ± 120	1175 ± 150	1500 ± 111
3-Ethyl- TTNPB	1700 ± 118	310 ± 29	23 ± 4.0	2900 ± 250	2000 ± 150	2600 ± 160
3-Isopropyl- TTNPB	>10000	>10000	270 ± 35	300 ± 32	>10000	2700 ± 240

The transactivation and competitive coupled transfection assay is used again to illustrate the binding activity of AM80, AM580, BMS-185411 and BMS-185354[51] (Fig.1.13). Retinoid efficacy was measured by the concentration of induced chloramphenicol acetyltransferase gene product obtained from transfected cells using the chloramphenicol acetyltransferase enzyme-linked immunosorbent assays kit. Activity was routinely normalized for transfection efficiency by β-galactosidase activity. Results (EC_{50}) are presented as the dose at which chloramphenicol acetyltransferase induction was half of the level observed for ATRA at 10^{-6} M (Table 1.4).

From Table 1.4, it was found that Am-580 is RAR-α selective agonist, BMS 185411 showed specific agonist activity for RAR-β while BMS-185354 selectively activated RAR-γ. Two sets of residues, serine232 (Ser232)/alanine225 (Ala225) and threonine239 (Thr239)/isoleucine232 (Ile232) in RAR-α and RAR-β were found to be essential for receptor-ligand-specific interactions. Ser232 in RAR-α may participate in a hydrogen bond with the amide linker of Am-580 and its analogs, which links the compound to α-helix H3. In RAR-β and RAR-γ, alanine residues at positions225 and 234, respectively, correspond to Ser232 in RAR-α. The presence of a hydrophilic linker, as seen in Am-580, in close proximity to a hydrophobic amino acid (Ala225 or Ala234) may result in negative interactions between the receptor and retinoid manifested as decreased affinity of the compound for both RAR-β and -γ.

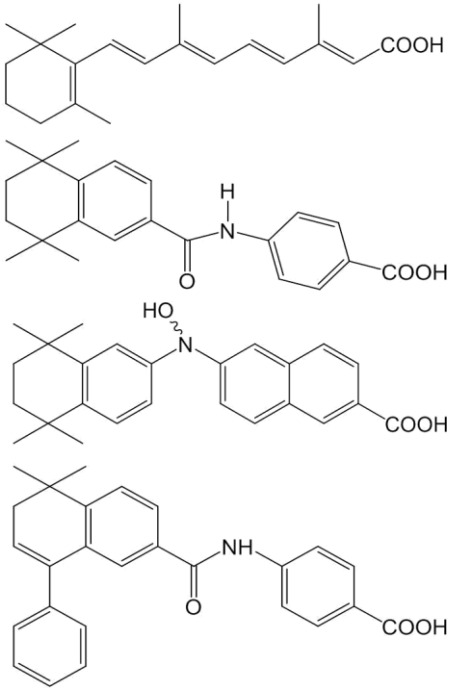

Figure 1.13: Chemical structures of the ligands used in transactivation and competition assay.[51]

Table 1.4: Competitive-transfection assay from Hela cells.[51]

Receptor	**EC_{50} (nM)**			
	ATRA	**AM-580**	**BMS-185411**	**BMS-185354**
Wild type RAR-α	17 ± 5	3.2 ± 1	NA	NA
Wild type RAR-β	23 ± 6	200 ± 90	34 ± 13	280 ± 84
Wild type RAR-γ	12 ± 6	400 ± 120	>10000	28 ± 7.5

❖ Cellular activity of retinoids

1.13 Introduction

Developing systems exhibit a dynamic balance between cell proliferation and differentiation, and although this equilibrium is important, it is a poorly understanding question in development. This model holds interactions between proliferation factors, and those promoting differentiation to regulate the developmental patterning processes.[94] Two important terminologies related to developmental potential are related here, determination (cell fate) and differentiation.

When a cell “chooses” a particular fate, it is said to be determined, although it still "looks" just like its undetermined neighbours, however this process is irreversible. Determination implies a stable change while the fate of determined cells does not change. While differentiation follows determination, as the cell elaborates a cell-specific developmental program results in the presence of cell types that have clear-cut identities, such as muscle cells, nerve cells and skin cells[95] etc. Once differentiation occurs, cell size and shape change dramatically, as does its ability to respond to signalling molecules through specific combination of genes that are turned on or off (expressed or repressed), and this is what dictates how cells function.[96]

1.14 Retinoids are biologically active molecules

Vitamin A (retinol) and its naturally occurring and synthetic derivatives collectively are referred to as retinoids, a family which consists of poly-isoprenoid lipids with variety of profound effects in cell proliferation, cell differentiation and embryonic development.[97] These observations were followed by numerous studies focused on the metabolism and pharmacological action of these retinoids in the skin, leading to the establishment of retinoic acid treatment for some of the skin diseases.[98,99] Also, they are useful therapy for someof the precancerous lesions, including the treatment of acute promyelocytic leukemia (APL) through its agonist activity on RARs which consequently induces myeloid differentiation at the promyelocytic stage.[100] ATRA also had useful clinical use with other therapy for treatment of malignancies in high-risk cancer groups.[101,102,103] These biological functions of retinoids based on its own profile and pharmacological properties that determine its usefulness in clinical dermatology or oncology since their biological activities are usually associated with clinical disadvantages such as toxicity and teratogenicity.[92, 104]

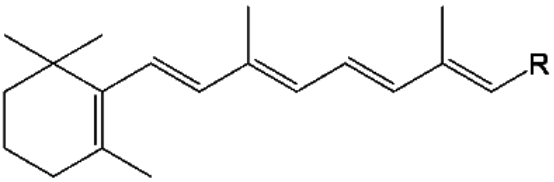

R) –CHO Retinaldhyde

R) –CHOH Retinol

R) –COOH Retinoic acid

Figure 1.14: Chemical structure of parent retinoid with its derivatives.

From Fig. 1.14, it can be noted that the vitamin-A molecule (retinol) is composed of three main building units: the cyclic end group (hydrophobic end); the polyene side-chain; and the polar end group.[105,106] Changing the polar end group from an alcohol to an acid gives the active form of vitamin A, retinoic acid or all-*trans*-retinoic acid (ATRA). The polyene linker in naturally occurring retinoids is highly conjugated and it is this region that gives the ability to absorb light (at a frequency of 300-400 nm depending on the solvent.[107] Modification of the structure results in many varieties of synthetic retinoid analogues with different biological activity. For example, the active form of retinoid is the free carboxylic acid because in several *in vitro* systems the retinoids with a carboxylic acid end group are more active than the corresponding analogues with a modified end group such as alcohols, aldehydes, esters and amines.[108,109]

Even for some derivatives with ethyl ester or etretinate analogues which are inactive, could be activated by esterase, which in turn, converted the retinoid into its free acid form.[110] Also, a drastic improvement in activity was observed in analogues with various forms of ring involving either a hydrophobic end group or polyene side-chain, in particular, such as indane and tetraline derivatives.[111] Recently, a new class of arotinoids with substitution of the polyene linker by other stable groups as acetylene showed activity of up to 10 times greater than naturally occurring retinoids.[112, 113]

1.15 Biosynthesis, transport and storage of vitamin A in human body

The vitamin A that is obtained from the diet is stored in the liver in the form of retinyl esters.[114] To release this stored form the esters, it is hydrolysed to retinol, which is released into the bloodstream for transport round the body bound to plasma retinol-binding protein. Cells which require retinoic acid take up retinol and convert it to retinoic acid through the action of two types of enzymes. The first type of enzyme, the retinol dehydrogenases (ROLDH), convert retinol to retinaldehyde which is used in the visual cycle, and the second type of enzyme, the retinal dehydrogenases (RALDH), convert retinaldehyde to retinoic acid.

Retinol (ROH) is transported in serum to the target cells as a complex by specific retinol-binding proteins CRBPII which protect it from metabolic oxidation into retinoic acid and allows it to be reduced into retinol by microsomal retinal (RCHO) reductase.[115,116]

Also, CRBP II–retinol complex serves as a substrate for the conversion of retinol into R-FA (retinyl esters) by the enzyme lecithin: retinol acyltransferase (LRAT) which is incorporated into lipoprotein particles (called chylomicrons in humans)in which it is carried to be stored in the main storage organ, the liver.[117] A specific circulatory transport system for retinol is mediated by serum retinol-binding protein (RBP-4). In plasma, holo-RBP circulates as a 1:1 molar complex with transthyretin (TTR) which is able to bind retinol from its storage source into target cells.[118,119] Numerous target cells have a receptor for TTR-RBP to facilitate the uptake of TTR-RBP-retinol and in the target cell, retinol undergoes metabolic activation, ultimately supporting the biosynthesis to active retinoids, RA and 9-CRA.[120,121] Also, esterification proceeds at a rate sufficient to store excess retinol as retinyl esters in target cells as a second storage source of retinol, while maintaining intracellular non-esterified retinol concentrations sufficient to initiate different biological activities and biosynthesis of other hormones[122] (Fig. 1.15).

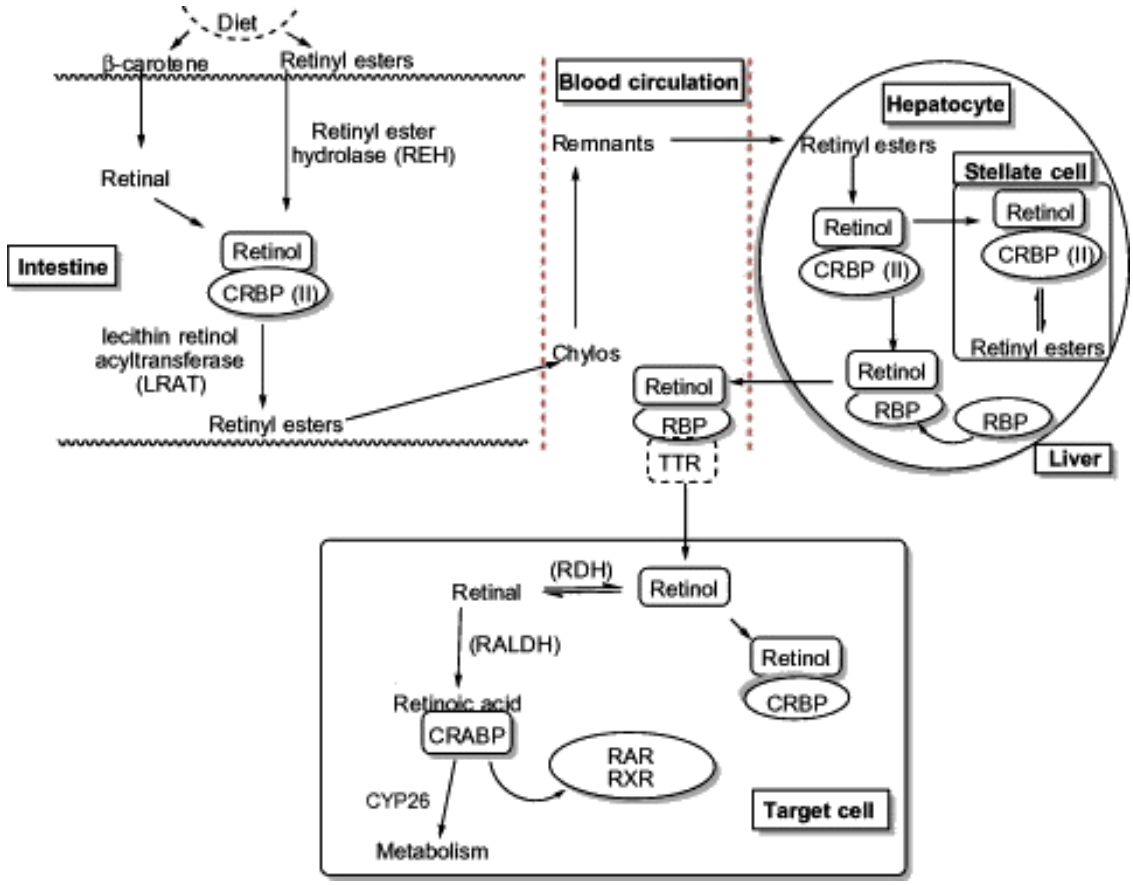

Figure 1.15: Absorption, transport and activation of naturally occurring retinoids. Carotenoids or other retinoids are biochemically converted to retinoic acid (RA), which is essential for modulating a wide range of biological processes. first in the intestine, then the liver, and finally in target cells with the support of various binding proteins including cellular retinol-binding proteins (CRBPs), retinol-binding proteins (RBPs), and cellular retinoic acid binding proteins (CRABPs).[123]

1.16 Cellular metabolism of retinoids

The oxidative metabolism of retinoids and especially RA by certain enzymes helps to maintain tissue retinoid concentrations within appropriate bounds. Recent studies have provided new insight into the processes by which RA is catabolized. It is speculated that RA might be metabolized with at least three pathways.[124] One of these pathways, which accounts for nearly two-thirds of RA metabolism, involves the excretion of the retinoid with an intact isoprenoid side-chain, which is assumed to include retinoyl-β-glucuronic acid. The remaining two pathways apparently involve oxidative loss of the C-14 and C-15 positions.[125,126,127] Recent studies suggested that RA metabolism is catalyzed by an enzyme, or enzymes, with properties similar to cytochrome P450–mediated monooxgenase systems, however, gene expression and protein analysis showed that the predicted cytochrome P450 protein had less than 40% amino acid identity to other known cytochrome P450s that binds retinoic acid, and therefore, the gene was classified as a member of a new cytochrome P450 gene family, designated CYP26 with P450RAI becoming CYP26A1[128,129] (Fig. 1.16).

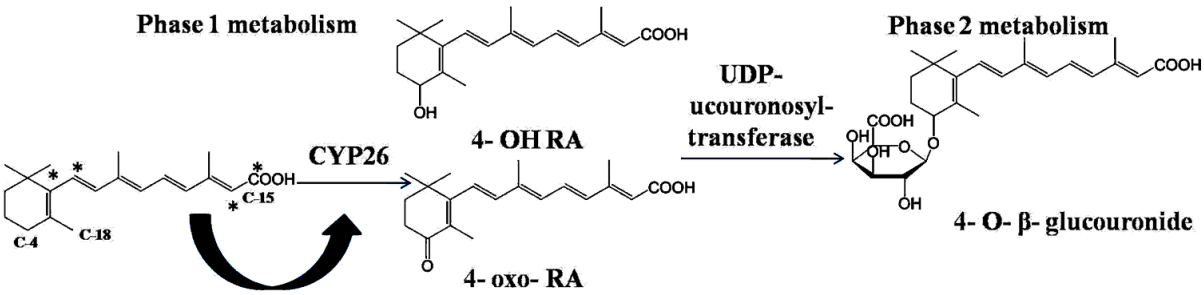

Figures 1.16: The major metabolic pathway of vitamin A is through CYP26 enzyme with oxidation at 4-position. These oxo- products are easily excreted through glucouridination.[124]

1.17 Biological function of retinoids

The retinoids regulate a wide range of biological processes including development, differentiation,[130] proliferation and apoptosis.[131] which is summarized in Fig.1.17. Some biological functions of β-carotene include anti-oxidant properties, increasing natural killer cell (NK-cell) activity and improving lung function.[132]

Also, retinoic acid shows its activity for inducing differentiation on different types of cells, including neural differentiation in the neural plate of developing embryos through attenuating fibroblast growth factor (FGF) signaling.[133] It has been shown that retinoids are able to inhibit mammary carcinogenesis[134] in experimental animals and other different types of tumours[100,135] interfering a variety of biochemical pathways[136,137,] such as cell proliferation AKT pathway [138,139] which is necessary for tumour overgrowth. Also retinoic acid can inhibit the tumour growth through activation of RARs especially RAR-β gene and hence, changing their behaviour. Another proposed mechanism in neuroblastoma is through to be through the cell-cycle arrest at G1 which is mediated by increased expression of the p21/WAF1 gene.[140]

Moreover, retinoids have other essential *in vivo* functions in reproduction, spermatogenesis through induction of differentiation of type A spematogonia, conception through induction of oocyte development and placental formation through stimulation of human gonadotropin hormone in trophoblast.[141,142]

Vitamin A and its precursor β-carotene also have impact in neurodegenerative diseases including Alzheimer's disease (AD) and Parkinson's disease (PD). They inhibit the formation of amyloid-β (Aβ) fibrils in a dose-dependent manner. Furthermore, they destabilize the pre-formation of Aβ fibrils *in vitro*.[143] Oligomerization of Aβ40 and Aβ42 can also be prevented by vitamin A and β-carotene. One study showed that 9-CRA could provide neuroprotection in CNS injury in a transient focal ischemia model due to the activation of bone morphogenetic proteins (BMPs).[144] Retinoid-dependent expression of BMP7 was found to protect neurons against injuries caused or induced by neurotoxins, free radicals, and ischemia *in vitro* and *in vivo*.[145]

Retinoic acid is necessary for renal development and even mild gestational vitamin A deficiency can affect nephron endowment. This was first demonstrated by feeding pregnant rats a vitamin A-deficient diet that caused reduced vitamin A levels in the fetal circulation leading to a significant reduction in nephron number and severe renal defects in the newborn rats.[146]

Another studies in the mouse showed a requirement for retinoic acid signalling in the normal development of the ventral retina and optic nerve through its activities in the neural crest cell-derived peri-ocular mesenchyme, dependent on the activities of various retinoid receptors RAR-α,-β,-γ and RXR-α,-β,-γ. Retinoic acid-synthesizing enzyme (RALDH) and retinoic acid-degrading enzymes (CYP26) also have critical roles in embryonic eye development.[147]

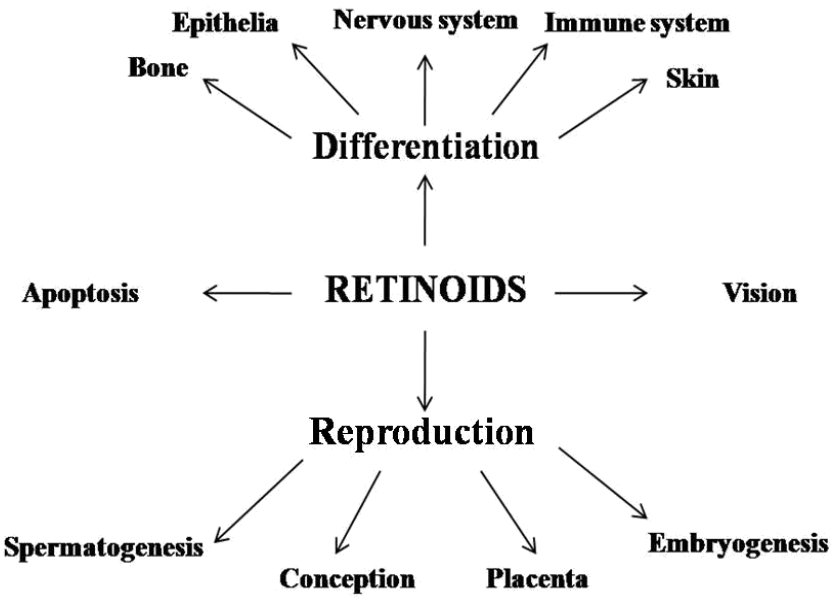

Figure 1.17: Summary of the biological functions of retinoids.[83]

1.18 Retinoic acid signalling during early embryonic development

Retinoic acid was known as important molecule for induction of cellular development in different species includes human.[148] The activity of retinoids starts early at the embryo stage and has been shown to include several process;

1.18.1 Axis formation

One of the important pathways that has significant implication on dorso-ventral axis formation is Nodal signalling pathway.[149] Retinoic acid was shown to interact with this pathway through the similar region of RARE in intron 1 and this might suggest the early effect of retinoic acid at this stage.[150]

Experiments in zebra fish embryos indicate that reduction of retinoic acid by ectopic cyp26 decreased the expression of posterior genes *meis3*.[151] This was confirmed by knockdown model of of cyp26 which affect on the expression of *meis3*. On the other way, FGF/Wnt signalling was shown to suppress the expression of cyp26, and hence, the specification of posterior trunk during the gastrulation.[152] This can conclude that both retinoic acid and FGF/Wnt signalling have a significant effect on the regulation of the antero-posterior axis formation in gastrula embryos.[153]

1.18.2 Neuronal differentiation

Neuronal differention is the second stage in embryo development and it was shown that Neurogenein 2 (Neurog2), the pro-neuronal induction factor has important role in early development of the primary sensory neurons. Neurog2 has two RARE sequences in its promoter region and hence, this might suggest the biologicl effect of retinoic acid onthe level of expression of Neurog2 and its activity and hence, neuronal differentiation.[154]

1.18.3 Hindbrain development

In vertebrate hindbrain, there was shown a correlation between several rhombomeres and Hox genes.[155] This correlation comes through the link between RARE and the promoter region in some of Hox genes which are required for the restricted expression in rhombomere.[156] This was confirmed by several studies in mouse and fish embryos which showed that retinoids could induce ectopic expression of both Hoxa1 and Hoxb1, which caused a rhombomere 2 to 4 transformation.[157] In addition, another signalling pathway of Hnf1b was shown to suppres Hoxb1 expression in rhombomere 5 was also regulated by the retinoic acid signalling. These data might suggest that the retinoic acid signalling is involved in hindbrain patterning.[158]

1.18.4 Development of internal organs

The retinoic acid signalling also plays essential roles in both endoderm and gastrulation development as was observed in several studies in frog, avian, and mice.[159] Retinoic acid signalling is essential for pancrease development include dorsal and ventral region formation.[160] Cdx4 and XPDIp were shown to be essential genes under the control of retinoic acid signalling for the development of posterior boundary of dorsal pancreatic territory and exocrine portion of both dorsal and ventral pancreas respectively.[161] The formation of cardiac progenitors, the correct modelling of the early heart field and the anteroposterior patterning were also under the regulatory effect of retinoic acid.[162] Specific link between retinoic acid inductions of Raldh2 gene can explain the biological role of retinoic acid in heart development.[163] Moreover, studies in *Xenopus* and zebrafish have demonstrated that ectopic production of retinoic acid increased the size of the kidney field, while blocking the pathway inhibited the kidney specification.[164] This is due to both *pax8* and *lhx1* are both under control of the retinoic acid signalling.[165]

Also, *in vivo* study was done to evaluate the biological activity of new synthetic retinoid analogue; EC23 compared to retinoic acid for embryo development. EC23 has very similar biological effects to retinoic acid within the appropriate concentration as well as the added benefit of being more stable. In addition, when higher doses of EC23 were applied, some novel phenotypes were produced compared with ATRA; in particular, a novel type of digit duplication was observed (Fig. 1.18).[166]

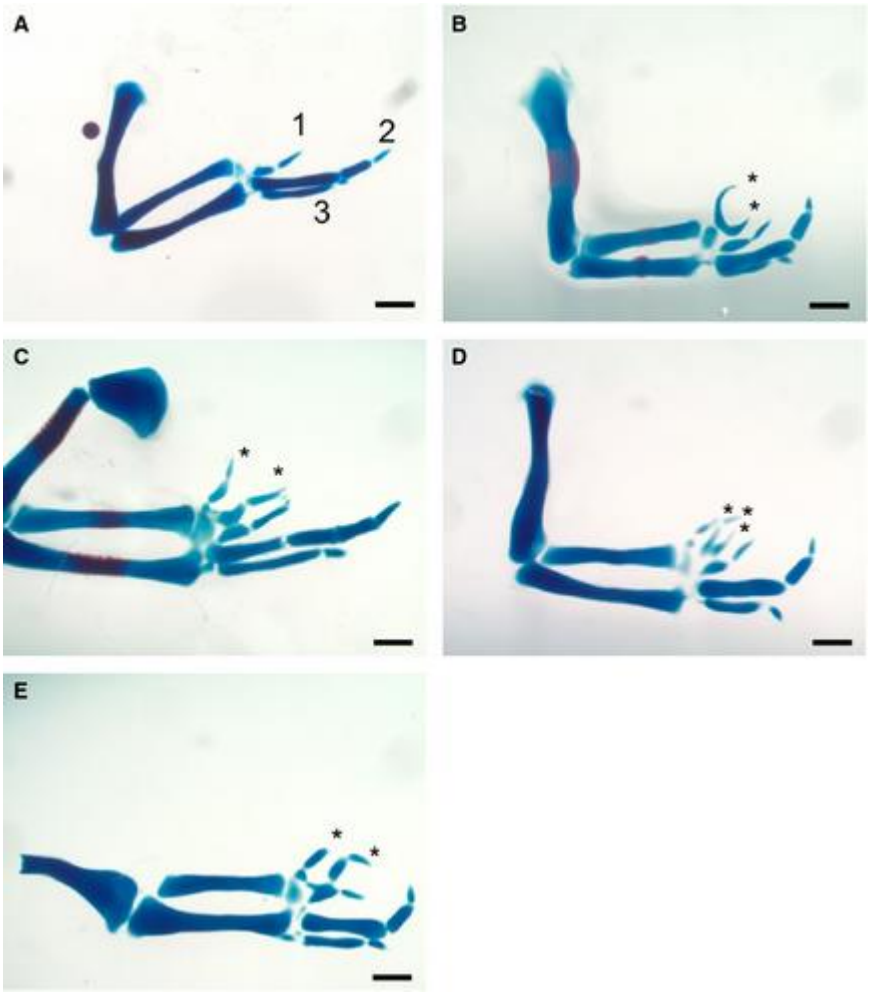

Figure 1.18: The effect of 0.01mg.ml^{-1} of EC23 on chick wing development. A) The normal digit development, 123 was produced by DMSO and acts as control and B-E) represents the multiplication of the wing digits generated by EC23. The whole mount skeletal view is dorsal. The additional digits are highlighted by asterisks. [167]

1.19 Stability of retinoids

Naturally occurring retinoids, including ATRA, 9-CRA and 13-CRA, can be described as chromophores because of the highly conjugated polyene linker region that gives the ability to absorb light. This makes these molecules particularly susceptible to photo-isomerisation and can degrade into a mixture of different retinoic acid isomers and decomposition products.[105, 106] The resulting concentration of retinoid levels in cells has also been shown to decrease markedly over time in culture and this could be a consequence of both their degradation and metabolism.[135] Moreover, ATRA is temperature sensitive and is known to oxidize readily. A paper warning cell biologists of this issue of stability has been published relating to using retinoic acids as inducers of cell differentiation and that the isomers of ATRA differentially affect the ability of mammalian stem cells to differentiate along alternative lineages and stated that extreme care should be taken to protect retinoic acid from isomerisation in such experiments.[106] To reduce such variability in differentiation response and improve reproducibility, it is essential that whatever compound is used to induce cell differentiation to be sure it is in the same form and concentration every time is used.

Currently, this cannot be guaranteed when using reagents such as ATRA and its stereoisomers, all of which are light and heat sensitive and are prone to undergo isomerisation under sample preparation, under storage of stock solution and in culture conditions. It is because the different isomers have diverse effects on cells that some attempts have been made to control ATRA's sensitivity and tendency to isomerise. For example, a number of additives preventing *cis-trans* interconversion or oxidation of retinoic acids have been evaluated, including bovine serum albumin (BSA), fibrogen, lysozyme, phosphatidylcholine *N*-ethylmaleimide and vitamin C.[130] However, the addition of such molecules to cell culture media is often not possible and such additives may affect cell behaviour in their own way, and none of these additives can completely prevent isomerisation. The use of BSA, for example, would not be possible also in serum free culture media.

1.20 Cellular differentiation

Cell differentiation is an important biological phenomenon that is involved in numerous physiological and pathological significant processes occurs during multiple stages of development.[168] Once cell differentiate, phenotypic characters change dramatically in response to signalling molecules to generate a new genotypic characters characterized by specific combination of genes that are turned on or off (expressed or repressed) once cells become specialized. Retinoid derivatives are one of the most potent agents known for induction of cellular differentiation as they exert highly di-versified effects on cells irreversibly at nano-molar concentration. This effect is thought to be mediated through two classes of nuclear receptors; the retinoic acid receptors (RARs) and the retinoid X receptors (RXRs).[22] These ligand-regularly nuclear receptor complexes modulate expression of their target genes by binding to *cis*-regulatory DNA sequences to initiate the cellular differentiation process. RXRs can act as transcriptional co-regulator with its cognate RARs, or *other* receptors as thyroid hormone receptors to form heterodimers complexes.[169] ATRA, as well as its natural isomer 9-CRA, are widely used to direct the *in vitro* differentiation of many cell lines including stem cells.[170]

Cellular differentiation by the vitamin A derivative ATRA has been studied with different undifferentiated cell lines including pluripotent embryonic carcinoma (EC) [171] and embryonic stem (ES)[172] cells *in vitro*. Both cellular systems are suitable for the study of differentiation of other cell types, because they recapitulate the early stages of mouse embryogenesis. *In vivo*, ATRA was identified as a signalling molecule influencing gene expression in a complex manner *via* a family of RA receptors.[173] Thus, *In vitro* cellular differentiation offers several advantages over comparable approaches in the whole embryo for many reasons. First, the generation of mature lineages from ES cells in culture provides access to populations of early precursors that are difficult, if not impossible, to access *in vivo*.[174] Second, the developmental potential of ES cells carrying targeted mutations of genes essential for embryonic development can be determined in culture. Analyses of these mutations *in vivo* are often complicated by early death of the embryo in uterus.[175] So here, it is susceptible to *in vitro* differentiation studies to demonstrate the diverse activity of ATRA on various cell lines and possible mechanisms for the induction of neuronal differentiation.

1.21 In vitro neuronal differentiation

1.21.1 Stem cells modulation

1.21.1.1 Human embryonic stem cells (ES)

In vitro differentiation of embryonic stem cells (ES) has attracted wide interest as an experimental system to investigate cell development/differentiation.[176] In addition, the isolation of human ES cells[177] has raised the possibility that differentiation may provide a novel source of cells for tissue replacement or repair.[178] Therapeutic use of ES cells will require robust and reliable methods for producing specific neural cell types. Early work on ES celldifferentiation found that aggregation of cells into embryoid bodies, combined with exposure to RA, enhanced the efficiency of ES cells conversion to a neural phenotype.[179,180,181] Although ES cells can differentiate spontaneously or with serum free differentiation (SFD) media, into many other cell lineages, however, cells with a brief exposure to RA were able to differentiate, lose stem cell identity, adopt a neural fate, and acquire mature axonal/dendritic polarity more rapidly than cells induced with SFD medium alone.[182]

There are many advantages to using ATRA in ES cells for neuronal differentiation such as the conversion of neural progenitor cells to postmitotic neurons which undergo their final mitosis at an earlier time point than cells induced spontaneously or with SFD medium alone.[183] Also ATRA directly induces genes associated with neuronal maturation at early stages so that young neurons are able to initiate formation and outgrowth of neurites that ultimately become axons and dendrites in structure.[184]

Many gene level changes occur upon neuronal differentiation of ESs with retinoids, including an increase in the expression of tumour suppressor gene p53,[185,186] cyclin-dependent kinase inhibitor(p21)[187] and CKI genes,[188] that is the likely cause of cell cycle arrest which stops proliferation at the expense of differentiation.[189] In addition, many other genes which are implicated directly in the process of neuronal differentiation are over expressed such as SoxII,[190] Pax6,[191] Nestin,[192] neurofilament L,[193] (GAD_{67}, GAD_{65})[194] and MashI.[195] On the other hand, ATRA reduces gene expression of Nanog,[196] one of the genes required for the maintenance of pluripotency and suppression of cyclin genes to control the progression of cells through the cell cycle.

1.21.1.2 Haematopoietic stem cells (HSCs)

Although ATRA signaling is known to accelerate the differentiation of generated hematopoietic progenitors to more mature blood cells, its role in hematopoiesis and HSC biology in particular, is still unclear. Based on its ability to differentiate both normal[197] and malignant[198] promyelocytes, studies using murine or human umbilical cord blood HSCs show apparent contradictory roles for ATRA signaling.[199] Murine models have shown that HSC expansion can be achieved either by activation of the ATRA pathway[200] or its inhibition *via* retroviral-mediated expression of dominant negative RARα.[201] This difference in such activity may be explained due to ATRA's pleiotropic effects on different hematopoietic progenitors and RAR subtypes, since RAR signaling is down-regulated in $CD34^{+}CD38^{-}$ cells compared with the more differentiated $CD34^{+}CD38^{+}$ cells.[202] Also, it is hypothesized that CYP26-mediated lowering of retinoid levels might also be an important physiologic mechanism for determining HSC fate. Thus, blood development depends on an ATRA concentration since at low level with activity of CYP26 enzymes will lead to cellular development while at higher concentration this differentiation will be abolished.[203]

1.21.1.3 Mesenchymal Stem Cells (MSCs)

Mesenchymal stem cells (MSCs) are pluripotent adult stem cells that can be induced to differentiate into various mesenchymal lineages, including osteocytes,[205] chondrocytes [204] and adipocytes.[205] Because of their ability to *trans*-differentiate across embryonic boundaries into neuronal cells, MSCs are considered good potential candidates for treating neurodegenerative disorders and nerve injury diseases.[206] It was found that RA pre-treatment could improve neuronal differentiation efficiency of MSCs and promote neuronal differentiation and survival of MSCs after transplantation into an animal model of hypoxic-ischemic brain damage.[207] This could indicate that MSCs became "sensitized cells", that are sensitive to neuronal induction microenvironments following pre-induction by RA to display a distinct neuronal shape, express neuronal markers and acquire neuron-like functional characteristics. RA pre-induction of MSCs was closely related to the activation of RAR-β signalling because of it is a neural specific receptor, highly expressed in neural tissues to regulate the physiological functions of nervous system and nerve regeneration.[206]

1.21.1.4 Induced pluripotent stem cells (iPSCs)

Human induced pluripotent stem cells (hiPSCs) are considered to be suitable tools to study basic molecular and cellular mechanisms of neurodevelopment. The directed differentiation of hiPSCs *via* the generation of a self-renewable neuronal precursor cell line allows the standardization of defined differentiation protocols. It was found that ATRA treatment of hiPSCs leads to higher yields of neurons *vs.* glia cells and longer axons than unconditioned controls, glutamatergic activation and depolarization.[208,209,210] However, there are diversity in protocols and methods used for the induction of neuronal differentiation using RA from hiPSCs which depends on applied concentrations, starting time point of application and the duration of treatment during neuronal differentiation. However, without doubt, retinoic acid treatment at the early stages of neurolation phase in hiPSCswill increase the yield of neuronal phenotypes, but does not have impact on the functionality of the terminally differentiated neuronal cells.[211] Many methods have been used to confirm cellular and functional aspects of generated cells such as quantification of neurite length, soma size, synaptic connectivity, cell-type specification and neuronal excitability.[212, 213, 214] Also, cell differentiation of hiPSCs into neurons is pre-programmed and co-ordinated by down-regulation of pluripotent genes and concomitant up-regulation of neurons-specific lineage genes such as Nanog and Oct4 are down-regulated before Pax6 becomes over-expressed.[215, 216]

1.21.2 Cancerous cells neuronal modulation

1.21.2.1 Embryonal carcinoma stem Cells (EC)

Embryonal carcinoma (EC) cells are the stem cells of teratocarcinoma. They are deriven from the inner cell mass of blastocyst of human or mice embryos.[217] There are many advantages in using these cells *in vitro* as they are adaptive to any condition changes, proliferating faster and becoming easier to maintain with time in culture. Furthermore, these adaptive cells can be inoculated into a SCID (severe combined immunodeficient) mouse, teratocarcinoma to obtain histologically recognizable stem cells with similar properties to the starting ES cells.[217] There are many examples of EC stem cells such as F9 teratocarcinoma,[218] P19 embryonal carcinoma[219] and NTERA-2.cl.D1.[220]

Many of these EC cell lines have some practical difficulties for their routine use especially when it is necessary to expand cultures and produce larger amounts of cell material. Furthermore, it is well known that suboptimal culture conditions can lead to spontaneous differentiation of human ES cells, introducing contaminating cell types.[221] The independently derived TERA-2.cl.SP12 teratoma cells[222] can provide a robust and simple culture systems to study certain aspects of cellular differentiation in a pertinent to human embryogenesis. It is also a good model used for the study and biological evaluation of the potency of synthetic derivatives of retinoic acid.[223,224] RA was found to induce ectoderm differentiation and the formation of neuronal cell types.[225] Also, this has helped to understand the cellular and molecular mechanisms that control the growth and differentiation of neural tissues. The mechanisms by which RA induces differentiation suggest binding to nuclear receptors, especially RAR-β[226] mediated by a cytoplasmic receptor proteins as CRABPI and CRABPII.[227] Moreover, many genes were reported to be over-expressed at early stages of differentiation, driven by RA under serum-free conditions like neural (Mash-1)[228] and neuroectodermal (Pax-6),[229] endodermal (GATA-4, alpha-fetoprotein).[230]

1.21.2.1 Neuroblastoma (NB)

Neuroblastoma originates from precursor neuroblasts of the sympathetic nervous system. Unlike most other cancer types, neuroblastoma is characterized by a unique capacity for spontaneous complete regression, at least partly through neuronal differentiation, in a proportion of patients, and is therefore, regarded as a cancer due to cell differentiation blocking.[231,232] The differentiated neuroblastoma cells show an increased expression of noradrenalin, adrenaline and neuron-specific enolase (NSE), differentiation markers which are employed for the diagnosis of neuroblastoma in patients.[233] Using differentiation therapy shows minimal side-effects on normal cells, because normal non-malignant cells are already differentiated. Many types of neuroblastoma are identified and they are classified basically according to cellular phenotypic characteristics into three types; sympathoadrenal neuroblasts (N), non-neuronal precursor cells (S) and third type (I) type. N-type is characterized as grow poorly attached aggregates of small, rounded cells with short neuritic processes, immature nerve cells and usually reliable for retinoic acid differentiation effect. Non-neuronal precursor cells (S) are flattened multipotent precursors to Schwann cells, melanocytes and glial cells and form the non-neuronal lineage of the neural crest.

I-type cells are intermediate with respect to N- and S-type cells in terms of morphology and biochemical markers represent either a stem cell or an intermediate stage in the *trans*-differentiation between N- and S-type cells.[234] SHSY5Y cell is the most popular cell line used for retinoic acid differentiation and can act as a good model for evaluation and understand the mechanism of cellular differentiation in neuroblastoma cell lines.[235,236] ATRA was shown to induce concentration dependent morphologic differentiation and growth inhibition even despite removal of ATRA from media.[237] The effects of retinoids in neuroblastoma cell lines are mediated by two classes of non-steroid nuclear hormone receptors, the retinoic acid and the retinoic X receptors and mainly RAR-β.[238,239] Retinoic acid induces SHSY5Y cellular differentiation through many possible mechanisms, including induction of RAR-β and CRABP-II genes expression for cellular differentiation and cellular metabolism control respectively.[240] The activity of RAR-β receptor is not a single activity but it was found that it works as heterodimer complex with RXR-α to induce cellular differentiation.[238,241]

Furthermore, ATRA stimulates nerve growth factor (NGF)-dependent survival in sympathetic neurones which responsible for neurites outgrowth after prolonged retinoids treatment.[237] Also, it induces the expression of TrkB, the receptor for the neurotrophins BDNF, NT-3 and NT-4/5 which are responsible for mature and functional neurons.[242] On the other hand, ATRA is able to inhibit the cellular growth of neuroblastoma and SHSY5Y, specifically through induction of apoptosis pathway.[138,243] Moreover, the cell cycle blockage occur in G1/S phase through high protein levels of cyclin-dependent kinase inhibitors, p21 and p27Kip which inhibit cell proliferation after RA treatment.[244]

1.21.2.3 PC12 cell line

Pheochromocytoma of rat adrenal medulla-derived cell lines can be induced to express a sympathetic neuroblast-like phenotype by nerve growth factor treatment.[245] A single exposure to RA was sufficient to cause neurite formation and inhibit cell division for a period of greater than 3 weeks, suggesting that ATRA may cause a long-term, stable change in the state of these cells.[246] In contrast to the differentiating effects of nerve growth factor, retinoic acid treatment has a negligible effect on cellular morphology, however it enhanced the survival of PC12 cells following oxidative injury generated by H_2O_2 treatment in a manner that is qualitatively similar to that observed after nerve growth factor treatment.[247]

1.22 Cancerous cells non-neuronal modulation

1.22.1 Acute promyelocytic leukaemia (APL)

Acute promyelocytic leukaemia was first defined by a specific morphological feature and by a bleeding diathesis. Two features specifically define the disease: the morphology of the malignant cells; and the pathology of coagulation (coagulopathy).[248] Retinoids are able to induce terminal differentiation of leukemic cell lines, such as HL60 and U937 with high remission percentage.[249] However, some limitations were observed with retinoids upon treatment of APL, which includes secondary resistance occurring in all patients treated with ATRA after a short time and relapsing within 6 months.[250] Also, lower plasma concentrations were initially noted at the time of relapse in patients with APL causing a shift in the ATRA dose-response curve *in vitro* because of up regulation in the expression of CRABP in relapsed patients.[251] In addition there had been reported several adverse effects after clinical application of RA.[252] Many approaches now try to solve these problems by either combining ATRA with other intensive chemotherapies[253] to decrease resistance, or by using other RA isomers such as 9-CRA which is more potent than ATRA at lower doses to minimize adverse effects.[254]

1.23 Neuronal cell markers

Neurons are the basic signalling components of the nervous system. Consequently, a fundamental part of any attempt to understand how neurons work as a network enquires the investigation of functionally distinct cell types. For this point, immunohistochemical markers have emerged as one of the most valuable tools available to neuroscientists for studying cells expressing a neuronal phenotype, and moreover, collect information regarding their morphological characteristics and expression of specific proteins. In this section, some examples of neuro markers are explained that have some impact on the characterization and functionality of mature differentiated neurons.

1.23.1 Neuron specific enolase (NSE)

NSE is a glycolytic isoenzyme which is located in central and peripheral neurons, and neuroendocrine cells. There is also another enolase isoenzyme, non-neuronal enolase (NNE) found in glial cells. During the development of nervous system, NNE is dominant at the first stages of developing brain and later NSE is ascendant.[255]

ATRA is able to induce over-expression of mRNA for the gamma isoform of the neuronal glycolytic enzyme enolase in mouse neuroblastoma cells, in addition to extension of long neurites.[256] Even pre-induction of SHSY5Y with ATRA improved neuronal differentiation of rat MSCs for a short time (24 hours) which was sufficient to induce high levels of NSE supporting that ATRA pre-induction promotes maturation and function of derived neurons at early stages.[257] Sequential treatment of SH-SY5Y cells with retinoic acid and brain-derived neurotrophic factor was also very useful and sufficiently potent to give rise to fully differentiated, neurotrophic factor-dependent, human neuron-like cells with high level of NSE.[258] NSE is also a very useful marker for the diagnosis of damaged neurons since the amount of chloride ion entering such damaged neurons is reduced affecting the activation and stability of NSE, and consequently there damaged cells will not need more for such NSE with reduced depolarization.[255]

1.23.2 Neuronal nuclei (NeuN)

It is a neuronal specific nuclear protein which is detected in most neuronal cell types throughout the central and peripheral nervous systems of adult mice. The appearance of the NeuN corresponds temporally to the withdrawal of neuronal cells from the cell cycle and/or with initiation of terminal differentiation.[259] It is usually found complexed with Fox-3; a protein involved in the regulation of mRNA splicing and is expressed exclusively by neurons suggesting that NeuN plays a role in regulating neural cell differentiation and nervous system development.[260] This marker secretion is characteristic for late stage maturation of neurons in the nervous system which can be related to the establishment of electrical polarity of the neural membrane, the onset of biosynthesis and release of neurotransmitter substances, and the establishment of synaptic circuitry.[261] There is no specific correlation between the secretion of NeuN and ATRA activity on cells, except that ATRA can induce the release of arachidonic acid and its metabolites during differentiation and apoptosis in LAN-1 cells. Arachidonic acid is mainly released by the action of phospholipase A2 (PLA2) and phospholipase C (PLC)/diacylglycerol lipase pathways which are based mainly through nuclear stimulation signal. So it is suggested that retinoic acid-induced stimulation of phospholipase A2 activity is a retinoic acid receptor-mediated process that correlated with other nuclear stimulation includes NeuN.[262]

1.23.3 Microtubule associated protein-2 (MAP-2)

This protein is related to a group of microtubule associated proteins and it is mainly found in the dendrites of neurons as it stabilizes microtubules in the dendrites of postmitotic neurons.[263] It is also found in primary melanoma and could disrupt the dynamic instability of microtubules, inhibit cell division and prevent or delay tumour progression.[264] ATRA induces cellular differentiation of P19 cells with higher level of MAP-2 due to several possible mechanism include the high level of acetylated P53 which activate the promotor region of MAP-2, [265] synergistic activity of CRABP-II/RAR[266] and high level of SOX6 gene expression through Wnt-1 pathway of cell differentiation. [267]

1.23.4 β-Tubulin III (TUJ-1)

Tubulins are a major building block of the microtubules, which are structural components of the cytoskeleton, attributed with roles in cell structure maintenance, mitosis, meiosis and intracellular transport among others. It is thought to be involved specifically during differentiation of neuronal cell types. [268] TuJ1 is found in the cell bodies, dendrites, axons and axonal terminations of immature neurons. One of the significant advantages associated with the use of immunohistochemical detection of TuJ1 is the degree to which it reveals the fine details of axons and terminations, and how it can be co-expressed with other early neuromarkers such as nestin for the indication of cellular differentiation. [269] It is also found that β-tubulin isotypes play a role in cell proliferation during neuronal differentiation.

Cell viability in differentiated cells was examined after knocking down a specific β-isotype before and after ATRA treatment of neuroblastoma cells, and it was found that undifferentiated cells, knocking down any single isotype, had no effect on viability. In differentiated cells, in contrast, the viability of cells in which βI was knocked down decreased by 53% compared to the control cells, which were transfected with negative control siRNA, while silencing βII or βIII had no effect on viability as shown by trypan blue assay. [270] Also, in P19 embryonal carcinoma cell lines after ATRA differentiation, TUJ-1 was increased in mRNA in the mitotic spindle of neuroblasts indicating early cellular differentiation. [271]

1.23.5 Neurogenic differentiation 1 (NeuroD-1)

The ability to generate new neurons provides the brain with an important level of plasticity for maintaining cellular homeostasis and potentially underlies a response to injury. However, cell-intrinsic transcription factors are also required to generate and promote the survival of newborn neurons that have not been yet fully elucidated. [272] So, NeuroD1 is one of the neuro markers predominantly expressed in the nervous system late in development, and is therefore, more likely to be involved in terminal differentiation, neuronal maturation and survival. [273] Various cell lines express NeuroD while being differentiated into neurons. For example, expression of NeuroD is observed during the differentiation of P19 teratocarcinoma cells, F11 human neuroblastoma cells, and HC2S3 immortalized neuronal progenitor cells and in murine cerebral cortical neurons. [272] In the case of the human neuroblastoma cell lines, the neurotrophin receptor TrkB (cognate receptor for BDNF neurotrophin) and the cyclin dependent kinase inhibitor p21 (Cip1) are concomitantly expressed. These two genes contain E-box elements within their promoters and can be activated by NeuroD and E47 in the absence of retinoic acid treatment. [274] In Cushing's disease, ATRA was found to be an effective treatment for regulation of ACTH secretion as RA, or synthetic retinoid AM-80, were able to activate RAR-α which consequently increases the expression of NeuroD1 and Tpit binding elements which activate the proopiomelanocortin (Pomc) gene expression to control secretion of ACTH secretion. [275]

1.23.6 Nestin

Nestin is an intermediate filament protein that is known as a neural stem/progenitor cell marker. It is expressed in undifferentiated CNS cells during development, but also in normal adult CNS and in CNS tumour cells, however it is expressed in neural stem/progenitor cells and was downregulated upon differentiation. [276] Nestin also has an important function for proper survival and self-renewal of multipotent neural stem cells (NSCs) uncoupled with any of cytoskeleton neuromarkers. [277] Also, because nestin has a role in cell signalling, organogenesis and cell metabolism, it was found that it is a strong prognostic marker for glioma malignancy as it has been detected in primary CNS tumours but not in carcinoma metastases. [278] Studies showed that mouse ES cells can be differentiated into neural cells with low concentrations of ATRA within 2 days of differentiation with enhanced expression of nestin indicating early cellular differentiation. [279]

Interestingly, in some cases such as neuroblastoma, combined therapy of ATRA and a proteasome inhibitor was effective at inducing cellular differentiation and inhibiting cell growth. However, after 5 days of recovery, both chemicals were withdrawn and the expression of stem cell markers such as Nestin, Sox2, and Oct4 were reduced, indicating a relapse and resistance occur which means early indication of stopping cellular differentiation.[280]

1.23.7 Retinoic acid receptor–β (RAR-β)

The retinoic acid receptor beta (RAR-beta) gene is a member of the family of retinoic acid/thyroid hormone receptor genes, encoding retinoic acid-inducible transcription factors. [281] It was shown that RA is a morphogen that has a development effect on many mammalian organs including CNS, limbs, craniofacial and the central axial skeleton. At early stages in the formation of an organ, the expression patterns were different in the epithelium, the adjacent mesenchyme and in mesenchyme more distant from the epithelium, suggesting a role for ATRA and RARs in epithelial-mesenchymal tissue interactions. RAR-β plays a role in mediating retinoid effects on the differentiated stage of these epithelia.

CRBP expression domains showed a high degree of overlap with RAR-β and RAR-γ, and mutual exclusivity with CRABP expression domains where it can help with RAR-β to store and release retinol where high levels of ATRA are required for specific morphogenetic processes. [282] ATRA induces both a greater number of neurites as well as increased neurite length, as well as being capable of dictating their direction of growth and because ATRA is acting on the transcription level, it is observed that RAR-β2 plays a crucial role in ATRA signal transduction, cellular differentiation and neurite outgrowth rather than a RAR-α or a RAR-γ specifically. [283] This was also confirmed by studying NGF, NT-3 and BDNF dependent neurons, isolated from recently developed embryo and by addition of RA to each of the neuronal classes only the NGF and NT-3 dependent neurons responded by extending neurites due to the presence of RAR-β2 which consequently was found over-expressed. [284]

RAR-β can work sequentially with other RAR types as RAR-α for the induction of cellular differentiation of adult forebrain neural progenitor cells. This was shown to occur through stimulation of fibroblast growth factor (FGF) and Sonic hedgehog (Shh) signalling pathways to promote neurogenesis in the SVZ region of the brain. [285]

Also the order and timing of expression of these retinoic acid receptors was found to be essential during the neuronal cell differentiation from NPCs as astrocytes and oligodendrocytes are predominantly formed in the presence of activated RAR-α, whereas motoneurons are formed when RAR-β is activated. Two transcription factors involved in neuronal fate especially islet-1 and islet-2, which are members of the LIM homeodomain family. [286] Activated RAR-β up-regulates islet-1 expression, whereas activation of RAR-α can either act in combination with RAR-β signalling to maintain islet-1 expression or induce islet-2 expression in the absence of activated RAR-β. RAR-γ cannot directly regulate islet-1/2 but can down-regulate RAR-β expression, which results in loss of islet-1 expression. [287]

The RAR-β2 isoform also has been associated with the tumour-suppressive effects of the retinoids due to use of the RAR-β gene promoter P2 which contains a strong RAR element, suggesting that RAR-β expression is up-regulated by retinoic acid and places RAR-β2 as a potential target gene underlying the growth-suppressive effects of retinoic acid.[23, 288, 289] Furthermore, the loss of the RAR-β2 expression was reported during the early phases of cancer development including breast and lung tumors. [290] In contrast, the expression of RAR-α and RAR-γ as well as RXR-α are mostly unaltered in malignant tissues. This was confirmed by using ATRA or RAR-α/-β selective agonists with taxol to dramatically lower the effective dose of taxol needed to induce cytotoxicity of a wide range of tumour cell lines.[291]

1.24 Raman spectroscopy analysis

The ability to analyze single cells for their biochemical composition in terms of small molecule content, their proteomic and genomic content, or possibly even their epigenome has become increasingly more important as we continue to improve our understanding of cellular biology. Furthermore, most diseases initially start at the level of single cells (the initial cell that stopped responding to apoptosis signals, the initial point of a bacterial or viral infection). [292] Electron microscopy has a similarly wide range of analytical capabilities and achieves even higher spatial resolution, but a lack of a similarly wide range of contrast agents and typical sample preparation steps have limited it to providing snapshots of cells, rather than supporting extended live-cell imaging. [293] Secondary ion-mass spectrometry, another analytical imaging technique, destroys cells during the imaging process. [294]

Raman micro spectroscopy is based on the dispersion and detection of photons that are in elastic scattering by molecular vibrations. When a monochromatic laser is used to probe a sample, most of the interacting photons undergo elastic scattering, while just a small fraction of photons scatters in elastically off molecular bonds and thereby exchanges energy with the vibrational energy levels of the molecules in the sample. [295]

1.24.1 Recent development in instrumentation for single cell Raman spectroscopy

Sir Raman observed the first spectra of light that was scattered by molecular bonds by focusing sunlight into a sample by using a telescope with an 18 cm–diameter large lens. [296] For filters, he used colored glasses. Even though in further experiments he began using mercury vapor lamps and more compact spectrometers to observe the inelastic light-scattering properties of gases and liquids. The performance of these components has changed remarkably. A lot of development in lasers, high-quality optical filters, and modern charge-coupled device (CCD) cameras and similar detectors had been occurred. Raman spectra can now be acquired directly from almost any biological sample, with little difficulty. [297, 298] To acquire Raman spectra of biological samples, there are some key requirements that have to be satisfied. Auto fluorescence from the sample and the sample substrate has to be minimized or creative ways for isolating the different signals have to be developed, and sample damage has to be avoided. The majority of Raman microspectroscopy systems are designed in a confocal-like optical arrangement, which helps acquire Raman spectra from very small volumes, on the order of 1 femtoliter (fL), and allows us to reject signals that are not generated in the very focus of the laser beam. Many biological applications of this technique are now implemented *in vitro* for the non-invasive characterization of specific metabolic states of eukaryotic cells, the identification and characterization of stem cells, and the rapid identification of bacterial cells. [299,300]

1.25 Conclusion

This review has shown three dimensional levels for the activity of retinoids toward their cognate target; retinoic acid receptors. The molecular level showed the crystallographic structure of these receptors, their ligand binding region, sequence alignment between the different RAR residues inside the binding sites responsible for their differential selectivity. The retinoid-receptor binding interaction level showed the overall dynamic rearrangement of this complex to mediate the biological activity of retinoids. Also, the impact of chemical structure modification in retinoids was studied and how this had effect on the difference in binding affinities to RAR and RXRs. The cellular and biological level also has shown the wide varieties and essential roles of retinoids as small molecules for the induction of cellular differentiation, highlighting the basic role of retinoids and their physiological roles in *in vivo* system. Natural retinoids have also some limitations for use *in vitro,* and this is why synthetic retinoids approaches become an essential step for the enhancement of stability and biological potency. Some members of these synthetic retinoids, in addition to the parent ATRA, have been shown to have potential therapeutic applications such as chemotherapy and chemo-preventive for cases as APL and neuroblastoma. Understanding the differences in biological activity between these molecules based on understanding the level of molecular interactions is essential for the future design and synthesis of further analogues of high potency and selective activity which can be used for clinical treatments.

1.26 Project aims

This work aims to combine theoretical and practical tools in order to understand the relative differences between the new synthetic retinoid derivatives. In particular, this help in the design of new synthetic analogues with higher stability and potency. The compounds presented in this thesis are new synthetic derivatives with known higher laboratory stability to overcome the highlighted problems mentioned previously with ATRA and its isomers.

The first part of this research will focus on the investigation of the molecular binding interactions of these compounds and their relative binding affinities to RARs using the combined molecular docking and receptor binding assay studies. All software will be updated and under the license of Chemistry Department, Durham University. Optimization of procedure will depend on ATRA and other characterized synthetic retinoid derivatives.

The second part will evaluate the biological potency of these compounds in both prolonged time of exposure using TERA-2.cl.SP12 stem cells and short time of exposure using neuroblastoma cells. The compounds will be evaluated for their ability to induce cellular differentiation using many different biological assays. The major aim is to find a correlation between the investigated molecular binding interactions and the actual biological response.

Chapter II

Materials and methods

Materials and methods

2.1 Molecular modelling study of small synthetic retinoids into ligand binding domain of retinoic acid receptors (RARs)

2.1.1 General procedures

In this study, a combination between Spartan10 (Wavefunction Inc., Irvine, CA)[301] and GOLDsuite 5.3[302] modeling programs was carried out for preparation of files and docking processes. Also, visualization of the docked complexes and images captions were processed through the UCSF Chimera program.[303]

2.1.2 Choosing PDB files from database

All PDB files used for crystal structures of different RAR types were obtained from RCSB protein data bank website. PDB files for RAR subtypes were 3KMR for RAR-α, 1XAP for RAR-β and 2LBD for RAR-γ. The selection of these files was based on specific parameters, suchas the quality of the atomic model obtained from the crystallographic data (R-Value and free R-value) and the diffraction pattern to show the fine details of the crystal (resolution value).

2.1.3 Protein Sequence alignment

Expasy SIB Bioinformatics Resource Portal and UniportKBwebsites were used for protein sequence alignments between the different isomers of RARs (-α, -β and –γ) to check for areas of similarities and differences inside the ligand binding domains, and also to find any deletion or insertion in PDB files used. The sequence alignment was expressed as percentage of the homology, sites of homology and classification of different amino acid types inside each sequence.

2.1.4 Preparation of. Mol2 files

Spartan10 was used to draw the 3D-structures of these synthetic retinoids compounds based on understanding their chemical structures provided and crystal structures available for some of them.

Computational calculation was the second step to provide a gateway for prediction of the different conformational states and identification of the lowest energy conformation. Semi-empirical molecular orbital model methods were 2-3 times faster for equilibrium and transition-state geometry calculations than quantum chemical methods, and hence, it was employed in conjunction with the Monte Carlo methods for calculation. The different conformational states based on calculation in vacuum using the AM1 method applied to systems with 100-200 atoms. The lowest energy conformation structure was saved as Mol2 files for further docking processes and it was checked that all bond types were correct and no bonds were missed.

2.1.5 Setting up the protein files

3.1.5.1 Protein hydrogen atoms, ionization states and tautomeric states

All hydrogen atoms were added and geometric positions of residue were automatically optimized by the GOLD suite program. This step was useful since it allowed the GOLD suite program to control the protonation and tautomeric state of Asp, Glu and His residues during docking process.

2.1.5.2 Handling water

All water molecules were removed, including those inside the ligand binding domain, since by inspection, it was found that they were generally not linear/or >120° and > 2 **Å**.[304]

2.1.5.3 Flexible Side Chains

The flexibility of the protein side-chain in RARs files was not explicitly controlled as this could give false positive results and increase the search space that must be explored, however, the GOLD program can allow torsional rotation of one or more residues around one or more of its acyclic bonds.

2.1.6 Setting up the ligand files

2.1.6.1 Essential steps in setting up a ligand

The correct entry of all bond types was ensured and that no dummy atoms were present although this did not affect the docking prediction process.

The starting geometry of the ligand should be reasonably low in energy, since GOLD will not alter bond lengths or angles, or rotate *rigid* bonds such as amide linkages, double bonds and certain other iterations, such as trigonal nitrogen.

2.1.6.2 Ligand hydrogen atoms, ionization states and tautomeric States

The Spartan 10 program adds hydrogen atoms in the right positions to ligand structures, hence, GOLD deduces hydrogen-bonding abilities and ionization states of carboxylic and amide groups from the presence or absence of hydrogen atoms during the docking process. Although it is important to note that the negative charge on the carboxylic acid terminal group was considered during calculation to be de-localized rather than protonated as this is more realistic with respect to physiological environments.

2.1.6.3 Ligand geometry, conformation and stereochemistry

The ligand conformation was varied by GOLD during the docking process so that the starting conformation therefore did not matter. However, it was essential to start with the minimum energy conformation.

2.1.6.4 Ligand flexibility

Allowing ligand bond flexibility was similar to the naturally occurring systems in nature either by flipping ring corners, amide bonds, planar bonds, pyramidal nitrogen and protonated carboxylic acid.

2.1.7 Setting and releasing constraints

Specific bond constrains were not added or specified between ligand and RAR protein residues to allow free binding interactions for the accurate determination of different binding possibilities.

2.1.8 Choice of geometric algorithm

GOLD offers a lot of different algorithms: GoldScore, ChemScore**,** ASP, protease inhibitors, etc. Chemkinase was chosen as the genetic algorithm function to allow details detection of Population Size, Selection Pressure, Number of Operations, Number of Islands, Niche Size and van der Waals and Hydrogen Bonding Annealing Parameters.

2.1.9 Sumaary for the steps used for ligand, protein and docking preparations:

❖ **For the retinoid structuretion preparation:**

1- Retinoic acid and the synthetic analogues were drawn using ChemDraw and transformed into 3D-structures using Spartan 10 software.

2- Semi-empirical molecular orbital modelling using geometric distribution was applied to calculate potential energies, molecular structures, geometry optimizations, atom co-ordinates, bond length and bond angles.

3- AM1 method of calculation was used in vaccum for 100 cycles and all structures were calculated with neutral charge. The lowest energy conformations for each structure were saved as a Mol2 file for further examination in GOLD suite software to avoid any un-defined atoms in the structure.

4- The calculated lowest energy conformations were compared to the X-ray crystal structures to find out that the starting point of ligand docking to receptors.

❖ **For the protein structure preparation:**

1- All Pdb files were checked for resolution, R- and free R- values to ensure that they are within the standard values.

2- All water molecules were removed, including those inside the ligand binding domain.

3- All hydrogen atoms were added and geometric positions of residue were automatically optimized by the GOLD suite program.

4- The binding site sizes of different RARs were identified based on the structure already present ligands inside the receptor within range of 15 Å.

❖ **For the docking of both ligand and protein files using GOLD suite software:**

1- Chemplp was chosen as the fitness scoring function and Chemkinase as the genetic algorithm function to allow detailed detection of hydrogen bonding, torsion angles, van der Waals forces and any short contacts.

2- The detection of the centre for the ligand binding pocket was based on the previousely identified docked retinoid structure in the choosen Pdb files.

3- Early termination was not allowed so that the program could find all available solutions within 10,000 population sizes. A Cluster size of 2 was also specified to increase the gap between different diverse solutions but within the acceptable range of 2.0 Å.

4- Each retinoid- RAR docked complex was export as Pdb file and explored using Chimera software.

2.2 Receptor binding assay of small synthetic retinoids molecules to their retinoic acid receptors (RARs)

2.2.1 General procedure

All reactions were performed under air, in a dark room to avoid degradation of retinoic acid. RAR kits were stored under the conditions stated by the manufacturer.

2.2.2 LanthaScreen™ TR-FRET retinoic acid receptor coactivator assay

All reagents were purchased from Life Technologies®and used without further purification. Dry DMSO was purchased from Sigma Aldrich as molecular biology grade with purity ≥99.9%.

2.2.3 Analytical techniques

The TR-FRET analyses were performed on a PHERAstar FS Microplate Reader using a dedicated UV-laser for TR-FRET measurements, validated in March 2012. The assays were performed in black, 384-well assay plates, low-volume and round-bottom (non-binding surface) assay plates from Thermo Scientific's Nunc ® range.

2.2.3.1 Principle of FRET and TR-FRET assay

The principle of the TRFRET assay is based on using suitable pairs of fluorophores which are brought within close proximity of oneanother. Excitation of the first fluorophore (the donor) can result in energy transfer to the second fluorophore (the acceptor).

This energy transfer is detected by an increase in the fluorescence emission of the acceptor and a decrease in the fluorescence emission of the donor. The TR-FRET assay uses a long-lifetime lanthanide chelate as the donor species. Lanthanide chelates are unique in that their excited-state lifetime (the average time that the molecule spends in the excited state after accepting a photon) can be of the order of a millisecond or longer. TR-FRET assays are performed by measuring FRET after a suitable delay, typically 50 to 100 microseconds after excitation by a flash lamp excitation source in a microtiter plate reader.

This delay not only overcomes interference from background fluorescence or light scatter, but also avoids interference from direct excitation due to the non-instantaneous nature of the flash lamp excitation source.The lanthanide used here in these TR-FRET assays for HTS is terbium and the common fluorophore is fluorescein as the acceptor. (Fig.2.1).

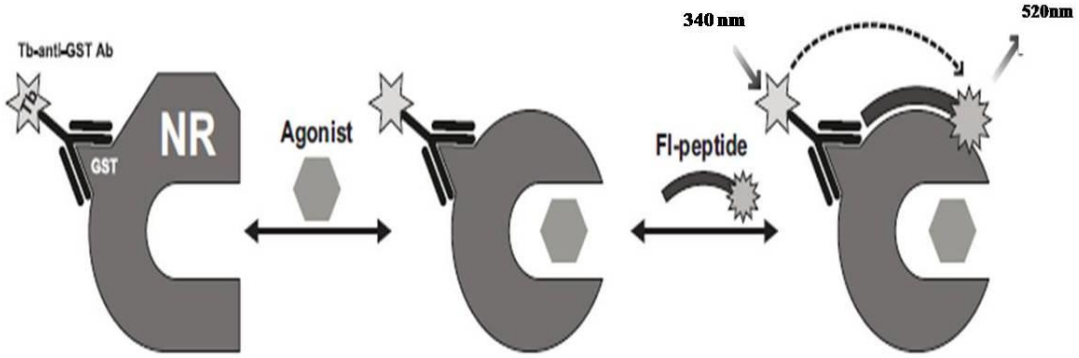

Figure 2.1: Principle of the nuclear receptor (NR) agonist dependent co-activator peptide recruitment assay. The purified ligand binding domain of RAR is tagged with GST which is attached with terbium anti-GST antibody and upon binding with retinoid ligand, induction of conformational change occurs in the ligand binding pocket. This allows the second consequent event to occure, where the tagged co activator with fluorescen attaches the ligand bind domain surface. The close proximity between fluorescen and terbium allows the excitation-emission signal to propagate and hence, can be measured as indication for binding interaction of retinoids with RAR LBD. The figure adopted from the kit manual at Invitrogen website.

2.2.4 Kits components: According to (Table 2.1)

Table 2.1: Kit component for the three RARs-types (-α,-β and-γ).

Component	Composition	Amount	Storage temperature
*Fluorescein coactivator[305]	100 µM in 10 mM Na_2CO_3, pH 11.0 Sequence: LPYEGSLLLKLLRAPVEEV	100 µl	–20°C
**RAR LBD, GST	RAR ligand-binding domain in a buffer (pH 8.0) containing protein stabilizing reagents and glycerol. See Certificate of Analysis for the recommended molar concentration for this kit.	75 pmol	-80°C
LanthaScreen™ Tb anti-GST antibody	Terbium labeled anti-GST antibody in HEPES buffered saline (137 mMNaCl, 2.7 mMKCl, 10 mM HEPES pH 7.5). See Certificate of Analysis for lot specific concentration	25 µg	–20°C
***TR-FRET Co-regulator Buffer	Proprietary buffer (pH 7.5) including 20% glycerol	25 ml	4°C
DTT, 1 M	In water	1 ml	–20°C or –80°C

* Fluorescein-D22 (RAR-α), Fluorescein-SRC2-2 (RAR-β), Fluorescein-PGC1a (RAR-γ).
** RAR LBD (-α,-β and-γ).
*** Buffer D (RAR-α), Buffer E (RAR-β), Buffer C (RAR-γ).

General settings:

Excitation	340 nm filter (30 nm bandwidth)
Emission	520 nm filter (25 nm bandwidth)
Emission	490 or 495 nm filter (10 nm bandwidth)
Delay time	100 µS
Integration time	200 µS

2.2.5 Testing up the instrument (Kit validation)

2.2.5.1 Setting up the instrument

Instructions were available from (www.invitrogen.com/insrumentsetup) to obtain the specific set-up guide for the instrument. The settings are shown here, were optimized specifically for LanthaScreen® TR-FRET assays.

2.2.5.2 Preparation of the Acceptor (LanthaScreen® fluorescein substrate or peptide)

1- Preparation of 30 µM acceptor stock solutions:

Fluorescein substrate/ peptide	**Stock concentration**	**Dilution to prepare a 30 µM solution**
Fluorescein-poly GT	30 µM	No dilution needed
Fluorescein-poly GAT	30 µM	No dilution needed
Fluorescein peptides for kinases	Various	Add 6µL of 1mg/mL peptide stock to 94µL of TR-FRET dilution buffer.(1mg/mL with a MW =2KDa= 500µM
Fluorescein Co-regulator peptides for NRs	100 µM	Add 30µL of 100 µM peptide stock to 70µL of TR-FRET Co-regulator buffer. Do not add DTT

2- Preparation of 120 µL of each 2X acceptor concentration from the 30 µM stock

96- well plate	**A1**	**B1**	**C1**	**D1**	**E1**
2X acceptor concentration	10,000 nM	5,000 nM	2,500 nM	1,250 nM	400 nM
Final 1X acceptor concentration	5,000 nM	2,500 nM	1,250 nM	625 nM	200 nM
Volume TR-FRET dilution buffer or NR Co-regulator buffer	80 µL	100 µL	110 µL	115 µL	117.5 µL
Volume 30 µM acceptor (prepared above)	40 µL	20 µL	10 µL	5 µL	2.5 µL

2.2.5.3 Preparation of the donor (Tb-chelates labelled antibody)

A 2X stock solution of Tb-chelates at 125 nM was prepared that resulted in a final assay concentration of 62.5 nM. This method relied on the concentration of Tb-chelates, NOT on the concentration of antibody.

Example calculation: for preparation of 1,000 µL of Tb-chelate:

Tb-antibody = 0.5 mg/mL (3.3 µM) with a chelate: antibody ratio of 11

Chelate: stock = 3.3 µM x 11 = 36.3 µM = 36,300 nM. ⟶ 1X = 62.5 nM; 2X = 125 nM

Hence, 3.4 µL of 36,300 nM of stock solution was added to 996.6 µL of TR-FRET dilution buffer or NR co-regulator buffer.

2.2.5.4 Addition of the reagents to the 384-well plate and read

For the donor, 10 µL of 2X Tb-chelates was transferred to rows A through J and columns 1 through 5 of the 384-well assay plate. Since only a single concentration was required this solution was transferred with a multichannel pipette from a basin to all 50 wells.

For the acceptor, 10 µL of the indicated concentration of 2X acceptor was transferred to the rows A-J of the corresponding column of the 384-well. Then the specified wavelengths were recorded. The raw data was plotted (ratios vs. acceptor concentration nM) and normalized data (normalized ratio vs. acceptor concentration nM) and finally calculation of the "assay window" in terms of Z'-factor.[306]

2.2.6 Agonist assay (for RAR-α,-β and-γ)

3.2.6.1 Preparation of complete TR-FRET co-regulator buffer and agonist controls

Note: The RAR-LBD was thawed prior to use and all other components were equilibrated to room temperature.

1. A complete TR-FRET co-regulator buffer was prepared by adding 1 M DTT to TR-FRET co-regulator buffer for a final concentration of 5 mM DTT. This was prepared fresh daily as required.

Note: complete TR-FRET co-regulator buffer was kept at room temperature for the preparation of all reagents except for 4X RAR -LBD, which was prepared with cold buffer.

An appropriate volume of buffer was reserved on ice for preparation of 4X RAR alpha-LBD (see step 8 for concentrations and example volumes needed).

2. For the “no agonist” controls, DMSO was added to Complete TR-FRET Co-regulator Buffer for a final concentration of 2% DMSO. 10 µl of this solution was added to row C, columns 1–24 of a 384-well assay plate

For example: Add 10 µl of DMSO to 490 µl of Complete TR-FRET Co-regulator Buffer D.

3. Preparation of control agonist solution (all-*trans* retinoic acid is recommended) was done at 100X of the final desired maximum starting concentration-using DMSO.

For example: If the final desired maximum starting concentration of agonist is 1 µM, so a solution of 100 µM agonist was prepared in DMSO.

4. For the "maximum agonist" controls, 100 X agonist solution from step 3 was diluted to 2X using Complete TR-FRET Co-regulator Buffer. 10 µl of this solution was added to row D, columns 1–24 in the 384-well assay plate.

For example: 10 µl of 100X agonist solution was added to 490 µl of Complete TR-FRET Co-regulator Buffer.

2.2.6.2 Preparation of 2X agonist dilution series

Note: Although steps 5 and 6 below required more pipetting than other methods of preparing a serial dilution of agonist, it has been found that this approach provided a robust method for preparation of the dilution series without problems due to agonist solubility.

5. Preparation of 12-point 100X dilution series of agonist in a 96-well plate was done by serially diluting the 100X agonist solution from step 3 three-fold using DMSO.

For example: 20 µl of DMSO was added to wells A2–A12 in a 96-well polypropylene plate. To well A1, 30 µl of the 100X agonist solution prepared in step 3 was added.

Three-fold serial dilution was performed by transferring 10 µl of the 100X agonist solution from well A1 to the 20 µl of DMSO in well A2, mixed by pipetting up and down and repeated for wells A2–A12.

6. Each 100X agonist serial dilution from step 5 was diluted to 2X using Complete TR-FRET Co-regulator Buffer.

For example: 5 µl of each of the 100X agonist serial dilutions from row A of the 96-well plate (wells A1–A12) was transferred to row B (wells B1–B12).

245 µl of Complete TR-FRET Co-regulator Buffer D was added to each well in row B of the 96-well plate and mixed by pipetting up and down.

7. 10 µl of each of the 2X agonist serial dilutions was transferred to duplicate columns of rows A and B of a 384-well assay plate.

For example: columns 1 and 2 of rows A and B of the 384-well assay plate received 10-µl aliquots from well B1 of the 96-well assay plate, wells A and B in columns 3 and 4 of the 384-well assay plate received 10-µl aliquots from well B2 of the 96-well assay plate, and so on.

2.2.6.3 Preparation of 4X RAR –LBD (differ from-α,-β,-γ)

8. 4X RAR-LBD was prepared using cold Complete TR-FRET co-regulator buffer in step 1. The recommended molar concentration of RAR for the kit was listed on the Certificate of Analysis (Table 2.2).

Table 2.2: Molar concentration for the three RARs-types (-α,-β and-γ).

RAR type	Stock solution	Recommended final solution	Preparation procedure
RAR-α	7900nM	3.5nM	4X concentration=14nM Dilution factor 1RARα: 564.3 buffer
RAR-β	6100nM	2.5nM	4X concentration=10nM Dilution factor 1RARβ: 610 buffer
RAR-γ	5430nM	3nM	4X concentration=12nM Dilution factor 1RARγ: 452.5 buffer

Note: RAR-LBD stock or dilutions was not vortexed. It was mixed by pipetting or gentle inversion. This solution was kept on ice until needed for use in the assay.

9. 5 µl of 4X RAR -LBD was added to rows A–D, columns 1–24 of the 384-well assay plate.

2.2.6.4 Preparation of 4X specific Fluorescein type / 4X Tb anti-GST Antibody (differ from α, β, γ)

10. Solution containing 200 nM specific fluorescein type (4X) and 20 nM Tb anti-GST antibody (4X) was prepared using Complete TR-FRET Co-regulator Buffer at room temperature. This stock concentration of fluorescein differs according to RAR types in (Table 2.3).

Table 2.3: stock concentration of fluorescein for the three RARs-types (-α,-β and-γ).

Fluorescein type	Stock solution	Recommended final solution	Preparation procedure
Fluorescein-D22 (RAR-α)	100 µM	50nM	4X concentration=200nM Dilution factor 1D22: 500 buffer
Fluorescein-SRC2-2 (RAR-β)	100 µM	0.125 µM	4X concentration=0.5 µM Dilution factor 1SRC2-2: 200 buffer
Fluorescein-PGC1a (RAR-γ)	100 µM	0.25 µM	4X concentration=1µM Dilution factor 1PGC1a: 100 buffer

Also the concentration of Tb anti-GST antibody is indicated on both the vial label and the Certificate of Analysis of RAR types kits (1 mg/ml = ~6.7 µM antibody).

For example in RAR-α: Add 4 µl of 100 µM fluorescein-D22 and 6 µl of 6.7 µM Tb anti-GST antibody to 1990 µl of Complete TR-FRET Coregulator Buffer D.

11. Add 5 µl of 4X peptide/4X antibody solution to rows A–D, columns 1–24 of the 384-well assay plate.

2.2.6.5 Plate incubation and reading

12. Gently mix the 384-well plate on a plate shaker and incubate at room temperature protected from light. The plate may be sealed with a cover to minimize evaporation.

13. Read the plate after 4-6 hours at wavelengths of 520 nm and 495 nm, using the instrument settings.

2.2.7.6 Agonist assay—data analysis

The TR-FRET ratio was calculated by dividing the emission signal at 520 nm by the emission signal at 495 nm. Then, a binding curve was generated by plotting the emission ratio vs. the log [ligand]. The data was expressed as a ratio of signal at 520 nm and 490 nmfitted to a three-parameter ligand-binding sigmoid equation shown below using Sigmaplot (version 12.5, Systat Software Inc., San Jose CA) and normalized to the lower asymptote of each binding curve. The symmetrical sigmoidcurves produced were varied in the location of the mid-point (EC_{50}) and upper asymptote.

$$f = min + (max-min)/(1+10^{(logEC50-x)})$$

2.3 Biochemical model of the TR-FRET binding assay

The readout of the LanthaScreen TR-FRET binding assay was based on the signal generated from the interaction between a terbium-labelled anti-glutathione-S-transferase (GST) antibody and a fluorescein-labelled coactivator peptide terbium-labelled anti-GST bind the LBD fusion protein, thus the output of the assay relied on two binding interactions: ligand with LBD and ligand-bound LBD with the co-activator peptide. As both interactions were affected by the fit of ligand to the binding pocket of the LBD, biochemical pathway simulator COPASI[307] was used to build a simple model of how the FRET signal output in the assay varied according to differential changes in the kinetics of the two binding interactions. Reactions were modelled deterministically using mass-action kinetics described by ordinary differential equations (ODE) within COPASI.

The species in the model:

Ligand (L), Receptor (R), Ligand-Receptor complex (LR), Co-activator (Co.A) and Ligand-Receptor Co-activator complex (LRCo.A).

The model is based on two reversible reactions

$$L+R \underset{*k_2}{\overset{*k_1}{\rightleftharpoons}} LR \qquad LR+CO.A \underset{*k_4}{\overset{*k_3}{\rightleftharpoons}} LRCO.A \quad \ldots\ldots\ldots\ldots\ldots\ldots (\mathbf{1})$$

* Where k_1, k_2 and k_3, k_4 are the rate constants controlling the rate of LR and LR.CO.A complex formation, respectively.

Thus:

$k_1 [L] [R] = k_2 [LR]$

And $k_1/k_2 = [L] [R]/[LR]$

Similarly $k_3 [LR] [CO.A] = k_4 [LRCO.A]$

And therefore $k_3/k_4 (K_d) = [LR] [CO.A]/[LRCO.A]$ …….…….. (**2**)[308]

All species concentrations were expressed as µmol. L^{-1} and changed during the simulation by dynamic evaluation of ODEs

Starting concentrations;

L= 10 µmol. L^{-1} to 0.03 nmol. L^{-1}, R= 0.0035 µmol. L^{-1} (defined by the TR-FRET assay formulation), CO.A = 30 µmol. L^{-1} (defined by the TR-FRET assay formulation), LR = 0 µmol. L^{-1} and LRCo.A = 0 µmol. L^{-1}.Steady states for LRCo.A were derived from the range of ligand starting concentrations (10 µmol. L^{-1} to 0.03 nmol. L^{-1}) using the Steady State and Parameter Scan functions within COPASI.

2.4 Biological characterization of small synthetic retinoids molecules

2.4.1 General procedure

All laboratory research work was done under safe laboratory practice guidelines to minimize any chemical and biological hazardous. Handling and dosing of synthetic retinoids especially retinoic acid occurred using latex double gloves and only under reduced light to prevent isomerization and degradation.

2.4.2 Retinoid stock solutions

All retinoid compounds were prepared using tissue culture grade DMSO solvent (Sigma) as 1 ml of 10 mM stock solutions of soluble compounds. Small aliquots of ~ 300 µL in each tube were stored either at -80 ˚C for long time storage or at -20 ˚C for short time storage and thoroughly defrosted in a water bath set at 37 °C prior to use. Overview of different synthetic retinoids used in this study in addition to the molecular modeling is mentioned in the list of retinoid chemical structures.

2.4.3 Cell cultures

2.4.3.1 TERA2.cl.SP12 EC stem cells

Human pluripotent TERA2.cl.SP12 embryonic carcinoma stem cells were cultured as 2D in T25 (BD falcon) flasks using the standard protcol.[309,221] The components of growing matrix media wereDulbecco's modified Eagle's medium (DMEM, high glucose, Lonza BE12 614F) supplemented with 10 % fetal calf serum (Sigma 10270), 2mM L-glutamine (Lonza BE17 605F) and 100 active units of Penicillin and Streptomycin (Lonza DE17 602F). Cells were incubated at 37 °C in a 5 % CO_2 humidified atmosphere. Media was kept in water bath at 37 °C before use for feeding cells every day till after 3-4 days the cells will reach 95% confluence and must be passage during acid washed sterile glass beads (Fisher Scientific G/0300/50) in 3ml fresh warm media and split 1:3 into T75 flasks for further incubation and proliferation. Cell Passage numbers from 20 to 36 were used as these passages were readily available in the laboratory at the time of carrying out this research using this cell type and all the passages showed the same characteristic embryonic carcinoma stem cell morphology.

2.4.3.2 SHSY5Y neuroblastoma cells

SHSY5Y cells were cultured according to standard procedure,[310] in brief the components of matrix media are Dulbecco's modification of Eagle's medium F12-Ham containing 2mM L-glutamine, supplemented with 10% fetal bovine serum (FBS) and were grown at 37 °C with 5% CO_2 in air. For cell suspensions, cell flasks were treated with 3ml sterile PBS and incubate flasks at cell incubator at 37 °C for 3-5 minutes for cell detachment. Centrifugation of the cell suspensions were done at 1000 rpm for 3 minutes, PBS was removed , re-suspended in fresh media and split into 1:3 into T75 flasks (Sigma) and incubated for further cell proliferation. Cell passage numbers from 20 to 30 were used experimentally without difference in reproducible data.

2.4.3.3 Storage of cells

Once cell growth reached 95% confluence, passaging of cells was carried out using either acid washed glass beads for TERA-2.cl.SP12 or sterile PBS solution for SHSY5Y to get single cell suspension solution in 15 ml falcon tubes.

Centrifugation was done at 1000 rpm for 3 min at 4 ˚C and any media was carefully aspirated leaving cell pellets in the bottom of the tube. The cell pellets were re-suspended in freezing solution (FBS supplemented with 10% DMSO) with good dispersion very well. Frozen solution contains 1ml of each cells were transferred into cryovials and slowly frozen at – 80 ˚C for one day using Dr.freeze (filled with 95% isopropanol) and then transferred to permanent storage at -150 ˚C.

2.4.4 Preparation of control cells for mono-layer 2D cell cultures

Control cells represent those were treated with DMSO organic solvent at concentration not more than 0.1%. The dilution factor used for DMSO all over the experiments was similar to that used for dilution of retinoid solutions. After 95% confluency of cells, either TERA-2.cl.SP12 or SHSY5Y cells were seeded with the recommended starting concentration of cells for another 24 hours in new T25 flask under the same incubation conditions. The next day, cells were treated with 0.1% DMSO and kept for the time required for each individual experiment with changing the media with fresh DMSO when necessarily.

2.4.4 Induction of differentiation protocol for mono-layer 2D cell cultures using different retinoids compounds

2.4.4.1 For TERA-2.cl.SP12 stem cell line

At 95% confluence, cells in T75 flasks, single cell suspension were obtained as mentioned previously and counted using haemocytometer using trypan blue dye and specific number of cells (as well be mentioned for each experiment) was seeded in warm media 37 °C into either T25 flask (for flow cytometry and gene expression experiments) or 6-well Nunc ®plates (for Immunecytochemistry, cytotoxicity and florescent imaging experiments) and incubated at 37 °C in a 5% CO_2 humidified atmosphere for 12-24 hours before cellular induction of differentiation. Cell flasks/plates were observed next day for attachment with the same morphology of EC stem cell without any spontaneous differentiation. Dilution of 10 mM of each synthetic retinoids solutions were done inside the tissue culture hood to 10 µM working solution using pre-wormed tissue culture media. The old media were aspirated and fresh retinoids media were added to each flask/well with incubation in standard condition mentioned before and changing media every 3-4 days for 7, 14 and 21 days according to each experiment requirement. Each experiment was done in triplicate for three independent experiments.

2.4.4.1 For SHSY5Y cell line

Single cell suspensions were obtained by previously mentioned techniques and single cells were counted by haemocytometer using trypan blue dye and specific number of cells (as well be mentioned for each experiment) was seeded in warm media 37 °C into either T25 flask (for gene expression and Raman analysis experiments) or 6-well Nunc ®plates (for cytotoxicity experiment) and incubated at 37 °C in a 5% CO_2 humidified atmosphere for 12-24 hours before cellular induction of differentiation. Cell flasks/plates were observed next day for attachment with the same morphology of polygon shape of N-type SHSY5Y neuroblastoma cells. Dilution of 10 mM of each synthetic retinoid solutions were done inside the tissue culture hood to different working concentration solutions using pre-wormed tissue culture media. The old media were aspirated and fresh retinoids media were added to each flask/well with incubation in standard condition mentioned before and changing media every 3-4 days for the definite time scale of each experiment.

2.4.5 Flow cytometry analysis of TERA-2.cl.SP12 stem cell line

Cell surface antigens expression specific for TERA2.cl.SP12 stem cells and their retinoids induced differentiation derivatives were analysed by extracellular flow cytometry. Primary monoclonal antibodies specific to the antigens associated with pluripotent stem cells globoseries glycolipid (SSEA-3, University of Iowa Hybridoma Bank), keratan sulfate-related (TRA-1-60, Abcam) and neural cell marker (A2B5, R&D Systems)were used to investigate the differentiation status of EC cells and their derivatives grown in media enriched with test retinoids. A suspension of 0.25 x 10^6 live cells was used as a starting population in each T25 flask for induction of cellular differentiation and after 7 days for retinoid treatment or 0.1% DMSO control cells, single EC cell suspensions were obtained and centrifuged at 1000 rpm and re-suspend in wash buffer (0.1% BSA in PBS) and added to a 96-well plate at concentration of 0.2 x 10^6 cells with round bottom as a suspension for incubation with primary antibodies according to (Table 3.4). This was followed by several washes with wash buffer and then incubation with FITC-conjugated secondary antibody IgM (Sigma, 1:128). Labelled cells were analysed in a Guave EasyCyte Plus System (Millipore) flow cytometer. Thresholds determining the numbers of positively expressing cells were set against the negative control antibody P3X (generous gift from Prof. P. Andrews, University of Sheffield). Guava Express Pro and WinMDI flow cytometry software were used for data acquisition and analysis respectively.

Table 3.4: Primary antibodies and its corresponding working dilutions for extracellular flow cytometry analysis

Primary monoclonal antibody	Dilution
SSEA-3	1:10
TRA-1-60	1:50
A2B5	1:40

2.4.6 Genes expression analysis of both TERA-2.cl.SP12 stem cell and SHSY5Y neuroblastoma cell lines

Real time PCR was carried out on both cell lines lysates immediately after treatment with 0.25% trypsin–EDTA. For TERA-2.cl.SP12, cells were seeded at a density of 1x10^6 cells per 25 cm^2 flask (BD falcon) 12-24 hours before treatment with different retinoids solutions at concentration of 10 µM for 3, 5 and 7 days. Control cells had the same treatment condition with 0.1% DMSO.

For SHSY5Y, cells were seeded at a density of 1 x 10^6 cells per 25 cm^2 flask (Sigma) 12-24 hours before treatment with different retinoids solutions or DMSO as control cells at different concentrations (1, 0.1, 0.01 and 0.001 µM) and at different time scales 2-12 hours. Commercial RNA extraction kits (Qiagen) and reverse transcription (Applied Biosystems) kits were purchased and procedures used according to manufacturer instructions.Purity of RNA samples were determined using nanodrop absorbance at 230, 260 and 280 nm. 260/280 and 260/230 ratios were measured and should be 1.8-2.2 and any samples higher or lower than this were removed and repeated.

RNA integrity was also checked using formaldehyde denaturated agarose gel. This was followed by reverse transcription to obtain cDNA. Also, real time PCR was performed using the TaqMan® Universal PCR master Mix (Life technologies) and TaqMan® gene expression system (Applied Biosystems) based on probe sets to the specific genes to be analysed. PAX-6, NeuroD1 were used for TERA-2.cl.SP12 cell genes analysis.RAR-β, CYP26-A1, RAR-α and RAR-γ were used for SHSY5Y cell genes analysis. GADPH and ACTB were used as internal reference genes for TERA-2.cl.SP12 and SHSY5Y, respectively. Data were normalized against both the internal reference genes and control cells based on $2^{-\Delta\Delta Ct}$ method and equation as follow;

$$Ct_{GOI\ s} - Ct_{norm\ s} = \Delta Ct_{sample}$$

$$Ct_{GOI\ c} - Ct_{norm\ c} = \Delta Ct_{calibrator}$$

$$\Delta Ct_{sample} - \Delta Ct_{calibrator} = \Delta\Delta Ct$$

$$\text{Fold difference} = 2^{-\Delta\Delta Ct}$$

Where; $Ct_{GOI\ s}$ (Ct value of unknown sample of gene of interst), $Ct_{norm\ s}$ (Ct value of internal normalizing gene) and $Ct_{GOI\ c}$ (Ct value of control sample of gene of interst).

2.4.7 Immunocytochemistry analysis of TERA-2.cl.SP12 stem cells

TERA-2.cl.SP12 cells grown on poly-D-lysine (25µg/ml) coated cover slips 22 x 22 mm, high precision (170 ± 5µm) in 6-well plates for 12-24 hour at 5000 cells per well 12-24 hours before treatment with either 0.1% DMSO as positive control or 10µM of different retinoids solution for 7, 14 and 21 dayswith changing media ever 3-4 days. The cells then were fixed in 4% *para*-formaldehyde (PFA) in PBS for 30 min at room temperature and rinsed with PBS. One set of experiment used for extracellular marker A2B5 (R&D systems diluted 1: 100) staining and the other set used for intracellular staining as the cell membranes were permeabilised by treatment with 1% Triton- X-100 (Sigma) in PBS for 10 min at room temperature. Nonspecific labelling was blocked by incubation on a bench-top shaker (Fischer Scientific) for 1 h at room temperature with a solution of 1% goat serum (Sigma) containing 0.2% Tween-20 (Sigma) in PBS. Primary antibodies were diluted in blocking solution and incubated with cells for 1 h at room temperature according to (Table 2.5). After washing three times for 15 min with PBS, cells were incubated for 1 hour in the dark with secondary antibody according to (Table 2.6). Hoechst 33342 nuclear staining dye (Molecular Probes, 1:1000) was used in blocking solution after secondary antibody staining step for nucleus staining.Stained coverslips were inverted and mounted on microscope slides in Vectashield Mounting Medium (Vector Laboratories) and the coverslips sealed using nail varnish. Stained cover-slips were examined using a fluorescence confocal microscope (Leica SP5CLSM FLIM FCCS).

Table 2.5: Primary antibodies and its corresponding working dilutions, sources for immunocytochemistry staining.

Primary monoclonal antibody	Dilution	Source
β-III tubulin antibody (TUJ-1)	1:200	Affymetrix eBioscience
Cytokeratin-8 (CK-8)	1:500	Affymetrix eBioscience

Table 2.6: Secondary antibodies and its corresponding working dilutions, sources for immunocytochemistry staining.

Secondary monoclonal antibody	Dilution	Source
Anti-mouseFITC-conjugated secondary antibody IgM for A2B5	1:128	Sigma
Anti-mouse Alexafluor®488 IgG for TUJ-1 and CK-8 (green florescence)	1:600	Invitrogen

2.4.7.1 Leica SP5 confocal laser scanning microscope

All experiments were done on poly-D-lysine (25 µg/ml) coated cover slips 22 x 22 mm, high precision (170 ± 5 µm) in 6-well plates for specific time and concentration scale (as mentioned for each experiment). After the experiments finished, cells were then fixed in 4% para-formaldehyde (PFA) in PBS for 30 min at room temperature and rinsed with PBS. Coverslips were inverted and mounted on microscope slides in Vectashield Mounting Medium (Vector Laboratories) and the coverslips sealed using nail varnish. Stained cover-slips were examined using oil-immersion fluorescence confocal microscope (LeicaSP5CLSM FLIM FCCS).

The following specifications were set up during the acquisition of images;

Laser excitation wavelength: 50 mW - Diode laser (405nm), 50 mW - Argon laser (488 nm and 458, 477, 514 nm), 10 mW - Helium Neon laser (633 nm).

Laser power: 60% on all experiments.

Acquisition mode: xyz (for images acquisition)

Filters: fully adjustable, 3 sequential (400-450 nm), (450-600 nm) and (600-775 nm).

Lens used: 63X HCX PL APO Oil immersion UV.

Image resolution: laser speed rate 100 HZ and resolution of 1024x1024

Pinhole size: 200 µm, 1 Airy unit, bidirectional laser beam

Zoom 1.5, line average 5 and Accuracy 1.

2.4. 8 Raman spectroscopy analysis of SHSY5Y cells

2.4.8.1 Experimental set-up for Raman spectroscopy analysis of SHSY5Y cells

SHSY5Y cells were seeded at density of 2 x 10^6 cells per 25 cm^2 flask (Sigma) and incubated at standard conditions for 12-24 hrs before treatment with different synthetic retinoids at concentration of 10 µM for 3 days as one shot treatment without changing media. Then cells were de-attached from the reservoir flask using pre-warmed PBS solution, centrifuged at low speed and fixed using 4% *para*-formaldehyde. Instrumental set-up, validation, analysis and recording data were done by Graeme Clemens at Chemistry Department, University of Central Lancashire.

2.4.8.2 Samples preparation (cytospinning onto 1 mm CaF_2 plates)

100 Microliters of fixed SHSY5Y treated or control cellssolutions were dispensed into individual labelled cytospinning cuvettes. The loaded cuvettes were spun at 950 rpm for five minutes firing a number of SHSY5Y onto the CaF_2 substrate window. The micro-slides were left to dry overnight, dipped carefully into double distilled water to remove any residual salt and left to air dry.

2.4.9 X-gal assay

Sil-15 cells were plated in a 0.1% gelatin-coated 96-well plate and grown to about 85-90% confluence in Dulbecco's modified Eagle's medium (DMEM) containing 10% fetal calf serum (Invitrogen/Gibco) and 0.8mg/ml G418 sulfate (Sigma) for selection.Serial dilutions of ATRA, EC23 and EC19 were prepared from the stock solutions. Standard curve of RA was included in the experiment as positive control. All retinoid dilutions were added to the seeded Sil-15 cells in the 96-well plate and then the plate was wrapped with aluminum foil and incubated overnight in a humid atmosphere containing 5% CO_2 at 37°C. All the concentrations for ATRA and the two synthetic retinoids were tested in triplicates. The next day, Sil-15 cells were washed twice with 1X PBS, fixed with 100 µl per well of 1%glutaraldehyde fixation solution for 15 minutes, washed again two times with 1X PBS and finally β-galactosidase activity was visualized by adding 100 µl of a freshly prepared X-Gal developing solution (5-bromo-4-chloro-3-indolyl-β-d-galactopyranoside)to each well. The plate was incubated overnight at 37°C in 5% CO_2. The plate was read on an Emax microplate reader at 650 nm.

2.4. 10 Neurite outgrowth assay of SHSY5Y cells

13 Mm diameter cover slips (Agar Scientific) were acid treated in a mixture of 70% nitric acid (VWR) and 37 % hydrochloric acid (VWR) in a 2:1 ratio for two hours. The cover slips were then washed extensively with distilled water until the pH of the water reached levels of 5.5-6. Until needed, the cover slips were stored in a jar containing 70% ethanol. The cover slips were sterilized by putting them on a 70% ethanol soaked tissue paper under the cell culture hood for 5 minutes. Then, the cover slips were placed in 12well plates. After that they were coated by adding 1 ml of poly-L-lysine solution above each cover slip in the well.

The final concentration of poly-L-lysine solution used for coating was 0.002% and the incubation time was 2 hours at 37 °C. Two washes with sterile 1X PBS followed and afterwards the cover slips were air dried in the cell culture hood. SH-SY5Y cells were first grown in T-25 culture flask in Dulbecco's modified Eagle's medium (DMEM) containing 10% fetal calf serum. Then, the cells were removed from the flask by the standard PBS protocol and were plated at an approximate density of 10000 cells per well in 12-well plates containing acid treated/Poly-L-Lysine coated cover slips. The plates were maintained at 37°C in a humid atmosphere containing 5% CO_2 for 24 hours. The next day, two dilutions (0.1 and 10 µM) of EC23 and EC19 were prepared from the given stock solutions in DMEM medium. DMSO containing DMEM medium was used as a control. The dilutions were added above the seeded SH-SY5Y cells in the 12-well plates and then the plates were wrapped with aluminium foil and incubated for 5 days in a humid atmosphere containing 5% CO_2 at 37°C. All the concentrations for the two chemicals and the controls were tested in triplicates.

SH-SY5Y cells grown on cover slips were washed two times in 1X PBS before fixing them in 4% *para*-formaldehyde for 20 minutes at room temperature, and then they were washed again two times with 1X PBS. The plates were stored at 4 °C in 1X PBS until use. Prior to immunocytochemical staining, the cells on cover slips were washed three times in 1X PBS before blocking them in 10% donkey serum, 0.1% triton X-100 in PBS for 1 hour at room temperature. The cells were then labelled by incubating them overnight at 4°C with β-III tubulin primary antibody (1:1000; Sigma) diluted in the blocking buffer. Next day, the cells were washed three times with PBS containing 0.1% triton X-100 before incubating them with anti-mouse monoclonal secondary antibody (1:300 in PBS with 0.1% triton X-100; Jackson Immunoresearch) for 2 hours at room temperature. Finally after 3 washes in PBS containing 0.1% triton X-100 and a final wash in 1X PBS, the cover slips to which the cells were attached were mounted on slides in mounting medium (1 mg/ml bisbenzimide (Pierce) in 1:1 glycerol (Sigma): 4% PFA and 2.5% 1, 4-Diazabicyclo [2.2.2] octane solution – DABCO (Sigma) and sealed with nail polish.

For each neurite outgrowth experiment, 3 cover slips (in 3 wells) were used. 10 different randomly selected images were taken for each cover slip and the numbers of neurites were counted and traced them in each of the 10 images. After that, the average neurite length for each picture was calculated by dividing the total neurite length by the total number of neurites in that picture. This is ended up with 10 values for the average neurite length for each cover slip; the average of the 10 values was taken to get one value for the average neurite length in each cover slip. By the end of experiment, 3 values of average neurite length; one value per each cover slip of the three.

The tracing was done using a semi-automatic NeuronJ plugin in ImageJ software (Fig. 3.2). The mouse anti β-III tubulin secondary antibody was used for fluorescent labelling of neurites. After taking the images using the microscope, each image was converted into an 8-bit image then the image was subsequently optimised using brightness and contrast tool in GIMP (GNU Image Manipulation Program). After that, individual traces were drawn for each visible clearly identifiable neurites in the image using the tracing tool in NeuronJ plugin in ImageJ software. The length was measured by pixels and then it was transformed from pixel value into the corresponding length in µm depending on the magnification used.

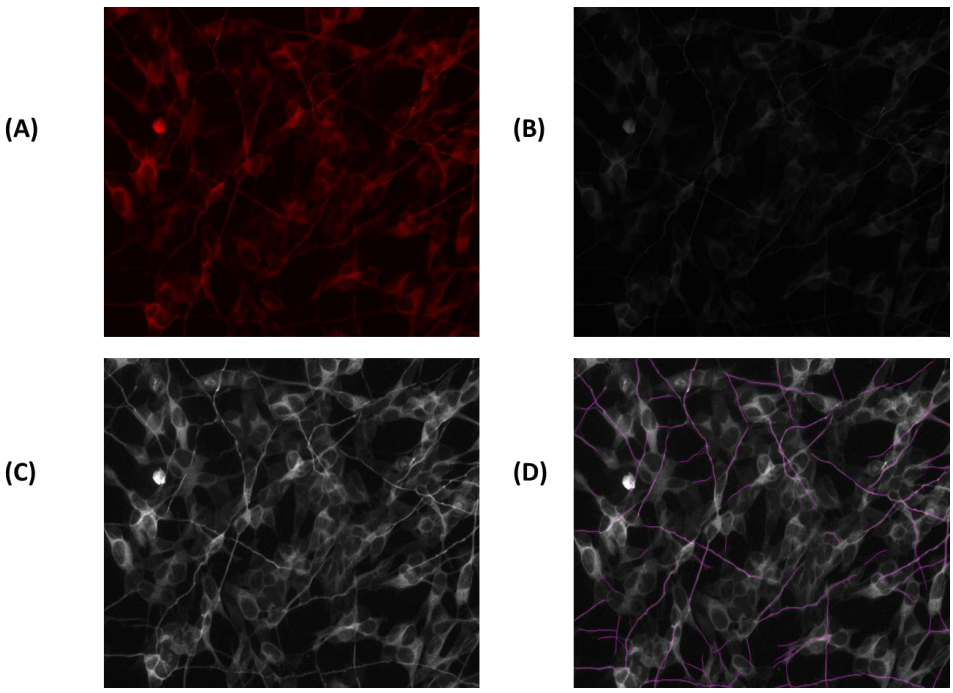

Figure 3.2: Measuring of total neurite length using NeuronJ. (A) The original picture; (B) The picture was converted into an 8-bit image; (C) The brightness and contrast of the 8-bit image was changed for easily and accurate identification of neuritis and (D) Traces were individually drawn above the neurites and then were quantified using ImageJ software.

Chapter III

Investigation of the molecular interactions between novel synthetic retinoids and the ligand-binding domains of retinoic acid receptors

Investigation of the molecular interactions between novel synthetic retinoids and the ligand-binding domains of retinoic acid receptors

3.1 Introduction

Retinoids interact with their cognate protein receptors (RARs) through consequence of different intermolecular interactions. These interactions include specific interactions binding in the LBD site as well as dynamic conformational changes outside the binding pocket. The complexity of interactions between these proteins and target retinoids is determined by the considerable selectivity between retinoid ligand, the RAR binding site and the structural rearrangements that occur upon binding to form a minimal energy active complex structure that initiates signal transduction.A goal of many biophysical studies in the retinoid area is to determine the molecular forces that control biological interactions and to use this information to rationally design synthetic retinoids with higher binding affinities to RARs, which are then able to induce signal transduction successfully. Computational structure prediction of ligand-protein complexes using docking methods such as DOCK, FLEXx and GOLD[311,312,313] is useful to understand the molecular interaction of retinoids in the binding pocket of RARs.

In this chapter, the procedure for *in silico* molecular modelling of different synthetic retinoid molecules introduced into ligand binding domains of different types of RARs. This modelling is then compared to experimental estimates of binding affinities using receptor binding assays. This is a useful starting step for further investigations of the binding interactions of other synthetic retinoids with either selective interaction to one type of RAR or with broad binding interactions to all of them. By the end of this chapter, it is expected to be able to predict the characteristic features of binding affinities of these molecules based on their differences in binding interaction poses within the protein binding pockets of the RARs. A combination of different computational and docking software was used for optimization of both retinoids and proteins and for visualizing the complexes of docked structures. Also, bimolecular simulation software was used to correlate how the values of EC_{50} have impact on the binding affinities of the retinoids to the RARs.

3.2 Study of retinoic acid receptor (RAR) structure and sequence alignment.

Retinoic acid receptors mainly consist of three main regions; DNA binding domain (DBD), hinge region and ligand binding domain (LBD). The LBD consists of 220 amino acid residues and it is the essential part for retinoid binding interaction with its RARs to initiate the active conformational change in the proteins. Sequence alignment was the first step done to check the similarity and differences between LBDs in comparison with other regions of RARs. Protein sequences and sequence alignment was retrieved using UniportKB as a common alignment resource and the results are shown in (Fig. 3.1 and Fig. 3.2) .The first analysis of different amino acid sequences in LBDs and DBDs of RAR-α, -β and -γ receptors showed that major variations in amino acid sequences were found in the LBDs with 83% similarity compared to the most robust and conserved region in DBD of 94%, the residues responsible for these differences in LBD of each type of receptors are shown by blue arrows.

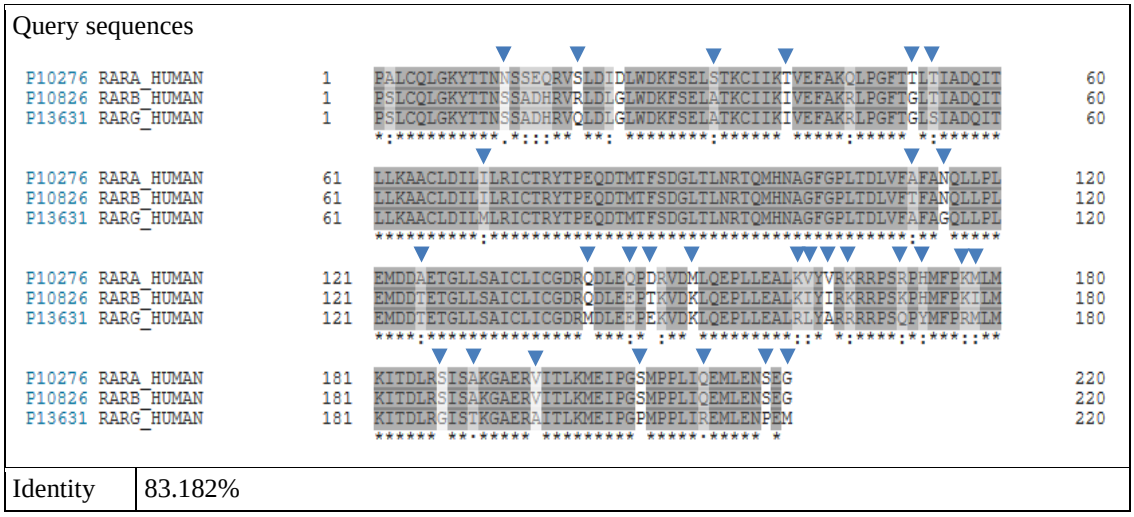

Figure 3.1: Sequence alignment in LBDs of RAR-α,-β and –γ. The green arrows represent the difference in amino acid sequences between different RARs. The similarity between LBD of RARs was shown to be 83%.

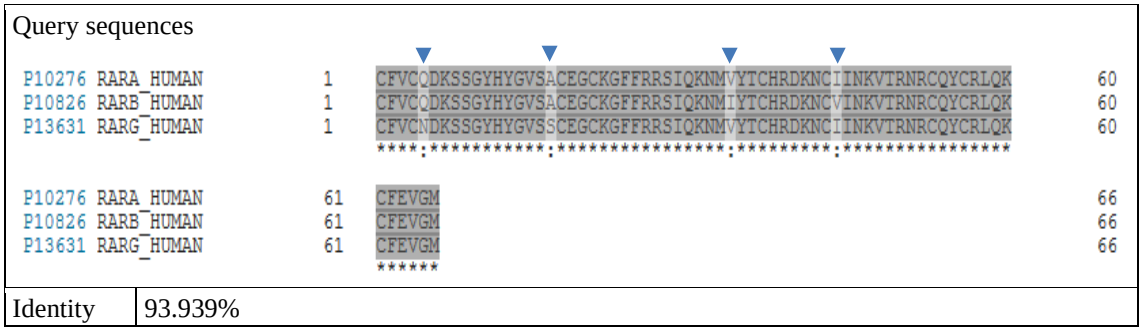

Figure 3.2: Sequence alignment in DBDs of RAR-α,-β and –γ. The blue arrows represent the difference in amino acid sequence between DNA binding domains of RAR. The similarity was greater than 90%.

PDB files necessary for molecular docking were retrieved from RCSB protein data bank website as shown (Table 3.1). The selection of these PDB files was based on the quality of the atomic model obtained from crystallographic data (R-Value and free R-value) and the diffraction pattern to show the fine detail of the crystal (resolution value).

Table 3.1: PDB file used for molecular docking of RARs retrieved from protein data bank showing the essential crystallographic parameters.

PDB files	R-Value	Free R-value	Resolution
1DKF	0.197	0.237	1.8
1XAP	0.213	0.253	2.10
2LBD	0.210	0.313	2.06

It is necessary to understand the topographic structure of the ligand binding domains of these receptors, Fig. 3.3 which shows how ATRA is buried in the hydrophobic pocket of RAR-γ formed by residues located in H1, H3, H5 helixes, β-turn and H11-H12 loops. Also, some hydrogen bonding and van der Waals contacts stabilize the bound ATRA molecule inside the pocket.

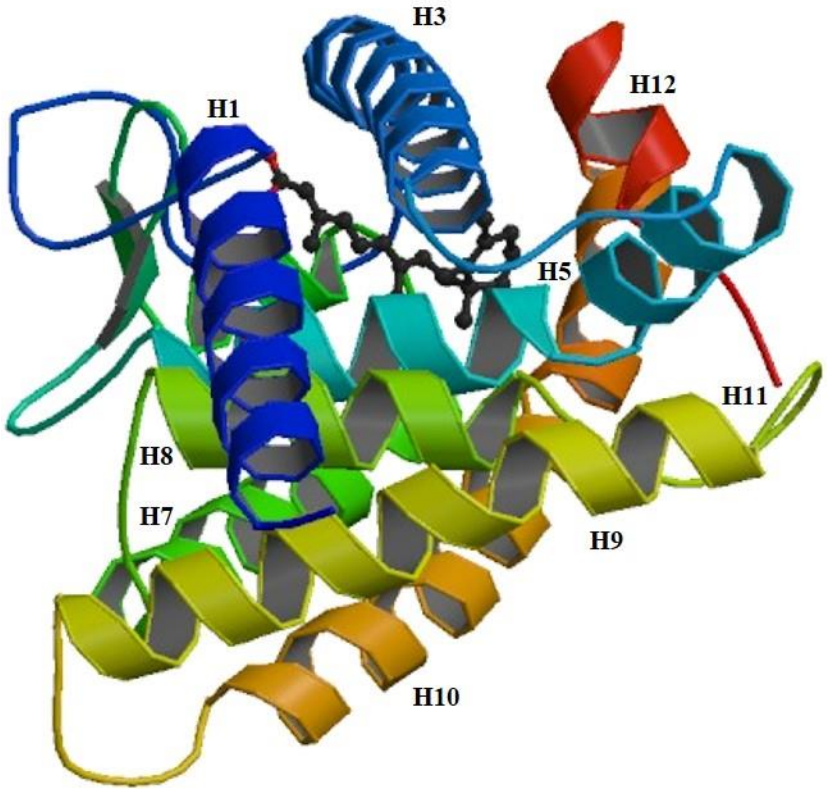

Figure 3.3: The crystal structure of RAR–γ bound to all-trans-retinoic acid. PDB accession code 2LBD. The ligand is ATRA bounded in the ligand binding pocket between H1, H3, H5, H7 and H12.[52]

3.3 Preparation of retinoid 3D molecules as .mol2 files

Preparation of mol2 files of the retinoid starting molecules was carried out using Spartan10 computational software. Molecules were prepared using the Spartan drawing facility which creates 3D structures. Semi-empirical calculations *in vacuum* were used to calculate the energy of each possible conformation, from which the lowest energy conformer was created. Table 3.2 and Table 3.3 show the calculated energies of the lowest energy conformers with other subsequent higher energy conformers. It was obvious that there were differences between lowest, 2nd lowest and highest energy conformers for the naturally occurring molecules of ATRA, ATRA methyl ester and 9-CRA because of the presence of conjugated double bonds which might have effect on the different possible energy conformations.

For ATRA, the methyl groups on the cyclohenyl ring consistently produced low energy conformations in which the conjugated polyene twists out of plane with the 6-membered ring. In addition, the lowest energy conformation adopts one *s-cis* sigma-bond rotation in the middle of the polyene, again seemingly relieving strain due to the presence of one of the methyl group substituents. A completely *s-trans*-conformation for ATRA was also found as the fourth lowest energy conformation at 288 kJ mol^{-1}, which was within around 3 $kJmol^{-1}$ of the lowest energy conformation. In fact, all these low energy conformation for ATRA all showed an out of plane twisting of the polyene from the plane of the cyclohexene ring and especially the *endo*-cyclic alkene. Otherwise, the conformations only differ in terms of which sigma bonds show *s-cis* conformations, and hence, all are selectable as possible structures that could bind to the receptor sites since all such conformations would exist at almost the same concentrations in solution at room temperature (Table 3.2).

For 9-CRA, the lowest energy conformation showed somewhat similar trends to that of ATRA, with the polyene section twisting out of plane from the cyclohenyl ring due to steric repulsion for the 6-ring methyl groups, and similar *s-cis* sigma bond rotation effects were also present. However, in the case of 9-CRA, two conformations were within 1 $kJmol^{-1}$ of each other, with the next lowest energy conformation being around 18 $kJmol^{-1}$ higher in energy, hence, it seems that 9-CRA exhibits lower conformation flexibility with only two major conformations being those that the receptors could select from in solution at room temperature(Table 3.2). Other synthetic retinoid analogues, this energy difference between different conformers was minimal, less than 1 kJ/mol, in many cases because of decreasing the degree of flexibility and rotation around bonds with using aromatic or hetero cyclic ring systems(Table 3.3).

3.3.1 Validation of calculated retinoid structures

Validation of lowest energy conformers in comparison to X-ray crystal structures is an essential step to be sure the starting point of docked retinoid molecules are similar.Calculated structures of EC19 and EC23 were initially superimposed onto the experimental crystal structures known for these two molecules (CCDC Ref code; 688680 KOHHIZ for EC23 and 688681 KOHHOF for EC19)[314] to validate the correct starting point for docking.

The calculated 3D structures and crystal structures had higher agreement in term of R.M.S.D, to conclude that these conformations as the most likely lowest energy (Fig. 3.4).

Table 3.2: Different conformers of ATRA and 9-CRA with calculated energy using Spartan 10

ATRA	Conformation	Energy ($kJmol^{-1}$)
(conformer-1) lowest energy	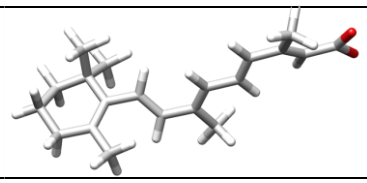	291.57
(conformer-2)	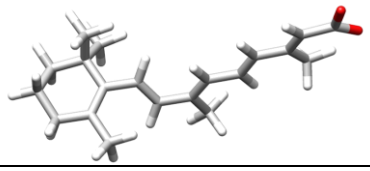	290.58
(conformer-3)	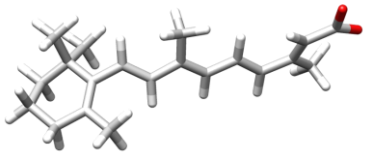	289.67
(conformer-4)	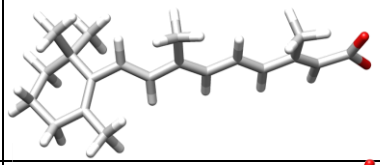	288.38
(conformer-5) highest energy	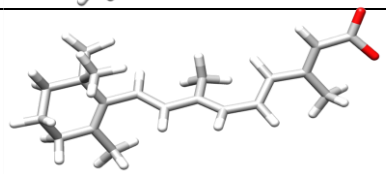	276.91
9-CRA	Conformation	Energy ($kJmol^{-1}$)
(conformer-1) lowest energy	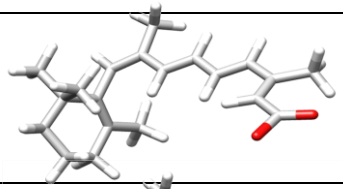	288.85
(conformer-2)	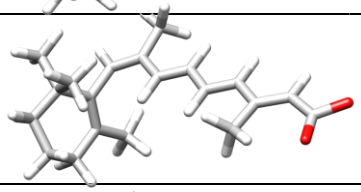	288.05
(conformer-3) highest energy	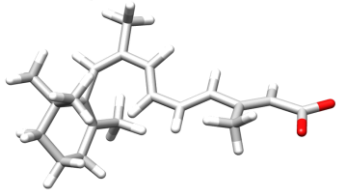	270.54

3.4 GOLD 5.2 suite program validation

The next step was to validate GOLD 5.2 program by extracting the docked retinoid structure from all three PDB files and re-dock them and superimpose both the original and docked structure and calculate R.M.S.D. All geometric functions were tried until ChemKinase was found as the best one to give minimal R.M.S.D. less than 1.5 Å. All hydrogen atoms were added to amino acid residues in RARs protein files and all H_2O molecules were removed from the binding pockets.

Also, there were no specific constrain through protein or ligand to allow the software to find all the available results. The pharmacophore binding size was detected based on the docked retinoids in the various PDB files within a range of 15 Å. Chemplp was chosen as the default fitness scoring function to allow detection of hydrogen binding, torsion angles, van der Waals force and any short contacts.

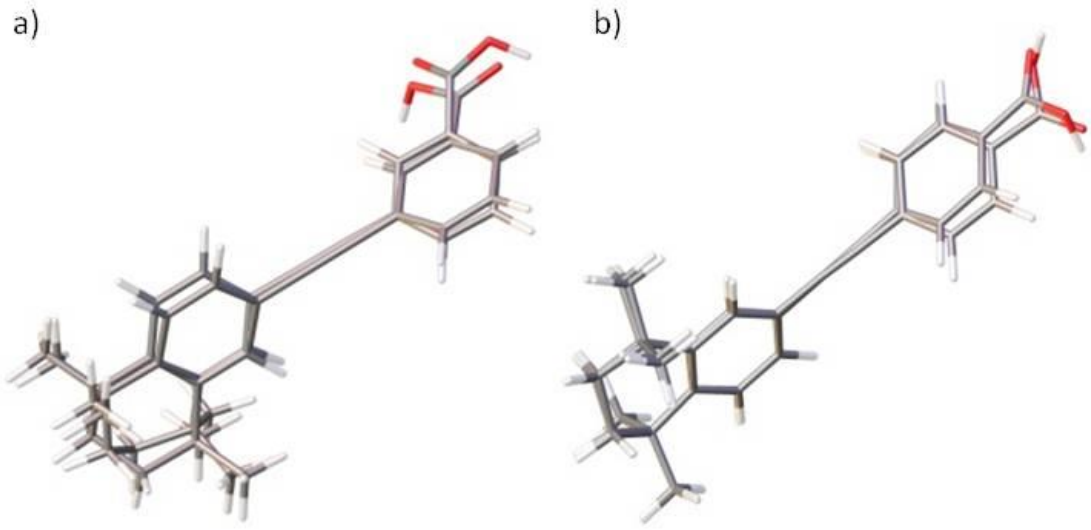

Figure 3.4: Calculated EC19 and EC23 Structure overlay with X-ray crystal structures; a) structure overlays for EC19 with R.M.S.D = 0.38 Å; and b) Structure overlays for EC23 with R.M.S.D. = 0.25 Å. All least squares superposition was calculated with Olex2.[315]

3.5 De-localization of carboxylate ion

It is important to note that the negative charge on the carboxylate terminal group was considered during calculation to be de-localized rather than protonated, as this is more realistic with respect to the physiological environment. Docking with the H-atom and a neutral carboxylate group led to unfavourable binding modes (Fig. 3.5).

Table 3.3: Lowest energy conformers of retinoids and other conformational energies.

Retinoid	Lowest energy conformation (K_J/mol)	2nd lowest energy confirmation (K_J/mol)	Highest energy confirmation (K_J/mol)
ATRA-methyl ester	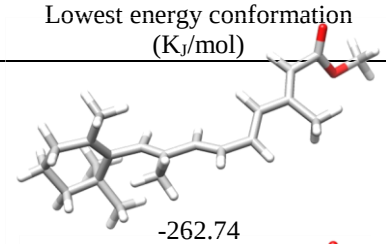 -262.74	-261.32	-247.07
TTNBP	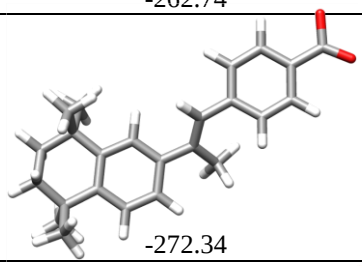 -272.34	-272.32	-272.21
TTNN	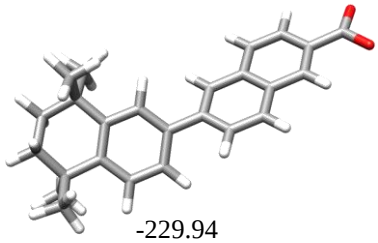 -229.94	-229.90	-229.87
AM580	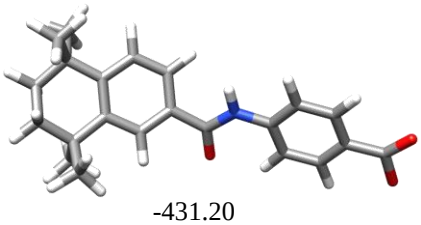 -431.20	-430.83	-418.53
CD437	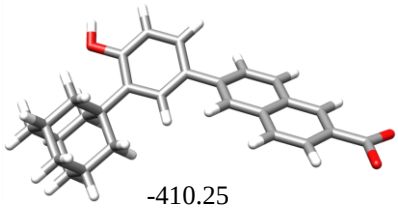 -410.25	-410.24	-397.25
EC19	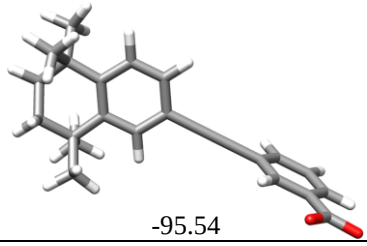 -95.54	-95.22	
EC23	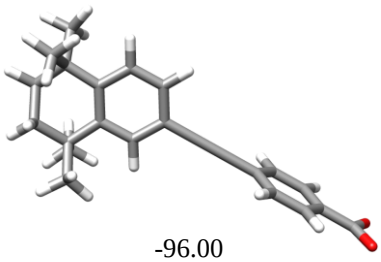 -96.00	-95.99	

EC19- methyl ester	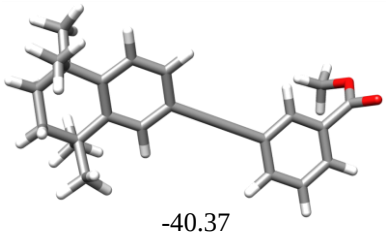 -40.37		
EC23- methyl ester	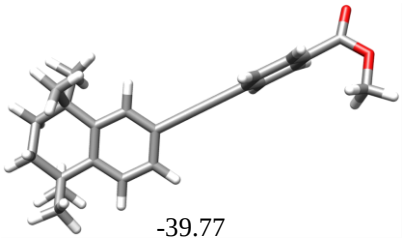 -39.77		
GZ18	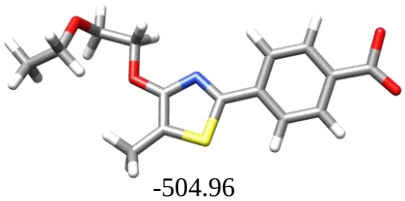 -504.96	-504.87	-492.90
GZ22	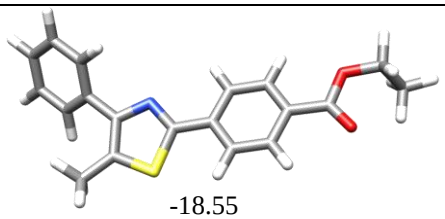 -18.55	-18.44	-17.98
GZ23	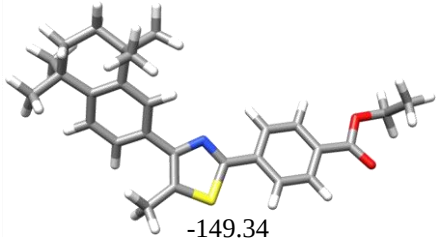 -149.34	-194.12	-148.49
GZ24	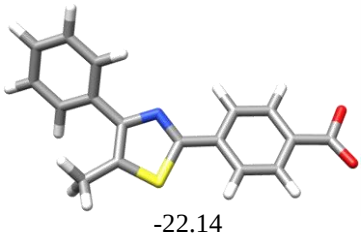 -22.14	-21.93	
GZ25	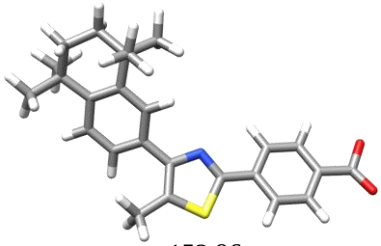 -152.96	-152.77	-152.48

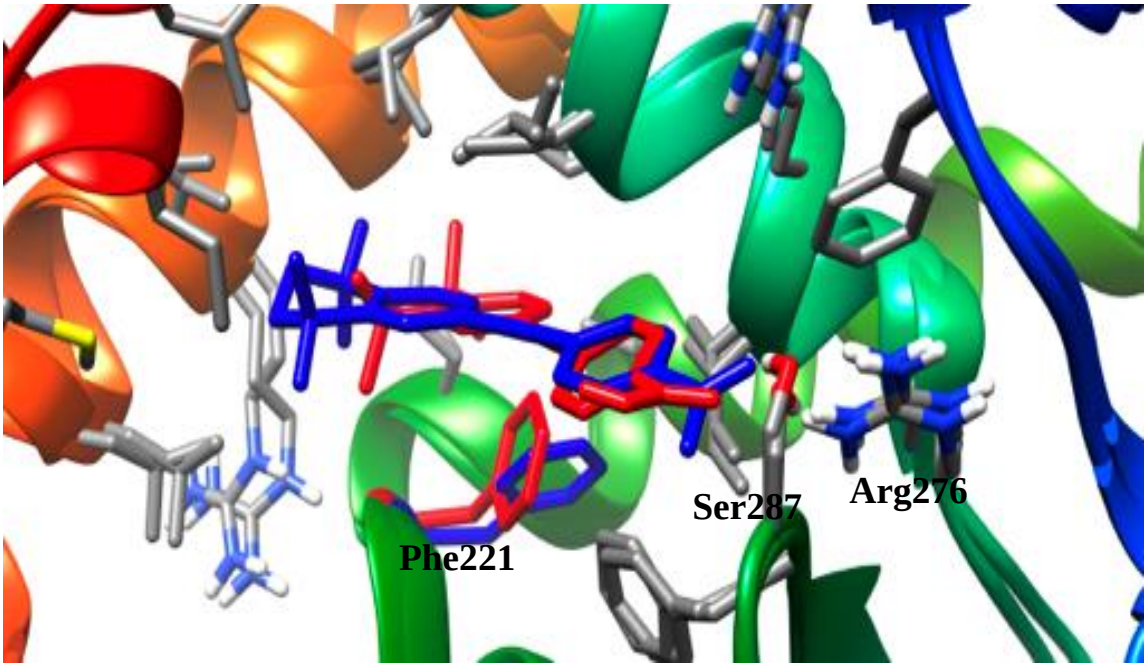

Figure 3.5: Least-squares superposition of the docked structures of EC23 in the ligand-binding pocket of RAR-α in the protonated form (red) and negatively delocalized charge (blue). The negatively charged carboxylate group of the retinoid might induce dynamic changes of some residues inside the binding pocket to produce, for example, a closer orientation of Ser287 and fewer steric clashes between the phenyl groups of EC23 and Phe221. UCSF CHIMERA[316] was used to produce this figure.

3.6 Molecular binding interactions of naturally occurring retinoid (ATRA) into RARs receptors

Validated procedures from the GOLD program were used for molecular docking of ATRA into three target RARs (-α, -β and –γ) for further comparison with other synthetic retinoids. Closer inspection of the highest binding score for the docked complexes of ATRA with different RAR-types revealed that the carboxylate ion plays a key role in interacting with some conserved residues in the RARs binding pocket. One carboxylate oxygen of ATRA formed a salt bridge with the protonated Arg residue in the LBD. In addition, the other oxygen of the carboxylate ion of ATRA formed hydrogen bonds with the hydrogen atoms of the hydroxyl group of Ser. Table 3.4 summarizes these binding interactions of ATRA with different residues in the RAR LBDs with measured distances in Å, which were in the expected range for salt bridges and hydrogen bonding.[317]

The results from the docked RAR-γ-ATRA complex structure parallels that of the known co-crystallized crystal structures deposited in the Protein Data Bank.[88] Furthermore, the binding mode appeared to be stabilized by hydrophobic interactions between the tri-methyl-cyclohexene moiety of ATRA with Leu270 (4.0 Å) and Val395 (3.5 Å) for RAR-α, Ile263 For RAR-β and Ala397, Leu416, Phe230, Ala234 for RAR-γ (Fig.3.6). In addition, it is noteworthy that there may be additional subtle effects operating particularly in relation to the shape, *i.e.* conformation, of these types of small molecules. In particular, comparing RAR-α and -β with RAR-γ. This can be seen by comparing Fig.3.6a and Fig. 3.6b, by examining the bound conformations of ATRA in the LBDs of each protein. The crystallography reports did not show the actual bound conformation of ATRA in the RAR protein binding sites. From these results, we tentatively propose that RAR-α and -β prefer to recognize a similar ATRA conformation, whereas RAR-γ prefers to recognize a more extended nearly all *s-trans*-conformation which might be a receptor selective interaction, specific to the conformation of ATRA.

Table 3.4: Molecular hydrophilic binding interactions and distances observed from molecular docking of ATRA and 9-CRA on different RAR LBDs

Retinoid analogue	Molecular binding interaction (Å)					
	RAR-α		RAR-β		RAR-γ	
	Arg276	Ser287	Arg269	Ser280	Arg278	Ser289
ATRA	2.9	2.8	2.9	2.6	3	2.8
9-CRA	3.7	2.6	3.8	2.5	3.7	2.7

3.6.1 Calculation of EC_{50} for ATRA with RARs receptors

The readout of the LanthaScreen TR-FRET binding assay was based on a Forster resonance energy transfer (FRET) signal generated from the interaction between a terbium-labeled anti-glutathione-S-transferase (GST) antibody fused with GST tagged RAR ligand- binding domain. The interaction between the LBD and the fluorescein-labeled coactivator peptide was driven by the binding of ligand to the LBD, and detected by the FRET signal from the terbium/fluorescein interaction when the terbium-labeled anti-GST binds the LBD fusion protein.

The output of the assay thus relied on two binding interactions: ligand with LBD and ligand-bound LBD with the coactivator peptide. As both the two consequent interactions are affected by the fit of retinoid ligand to the binding pocket of the RAR LBD, it was useful to calculate the sum of all these binding interactions as a total binding affinity (EC_{50}). All results were calculated compared to the blank DMSO solvent and graphs presented using Sigmaplot statistical software.

The results of the binding assays are summarized in Table 3.5 and Fig. 3.7, showing the measured EC_{50} for ATRA in the TR-FRET receptor binding assay for the different RARs. ATRA had similar binding affinities to all RAR-types, with slightly higher binding affinity to RAR-γ, which might be explained by the selective binding of the extended nearly all *s-trans*-conformation.

3.6.2 9-CRA molecular binding interaction *versus* ATRA

9-CRA was the second naturally occurring retinoid discovered and the predominant alternative isomer of ATRA with one *cis*-double bond that affects the molecule's length, although it has the same number of carbon atoms as ATRA, but is more bent in the ligand binding pocket. The EC_{50} of 9-CRA in all RAR types are slightly higher compared to ATRA which indicates that the binding affinity of 9-CRA is lower than ATRA (Table 3.4 and Fig.3.8). Also, molecular docking showed similar consistent effects for 9-CRA on all RARs LBDs, with one oxygen of the carboxylate group forming a hydrogen bond with the Ser residue in each RAR LBDs, because it is unable to hit the Arg to achieve an interaction to form salt bridge that would be stronger than the Ser hydrogen bond in all RARs binding pockets. This suggests that one *cis*-double bond effectively shortens the molecule and the carboxylate cannot quite reach the Arg residue which consequently affects the binding affinity and interaction of 9-CRA compared to ATRA. In addition, inside the ligand binding pocket of RAR-α and RAR-β, ATRA exists with in a single *s-cis* conformation which is ideal for best fit interactions with Arg and Ser residues compared to *s-trans* form of 9-CRA. While, in the ligand binding pocket of RAR-γ, ATRA and 9-CRA both exist in a mostly *s-trans* form with much better interactions for ATRA (Fig.3.9).

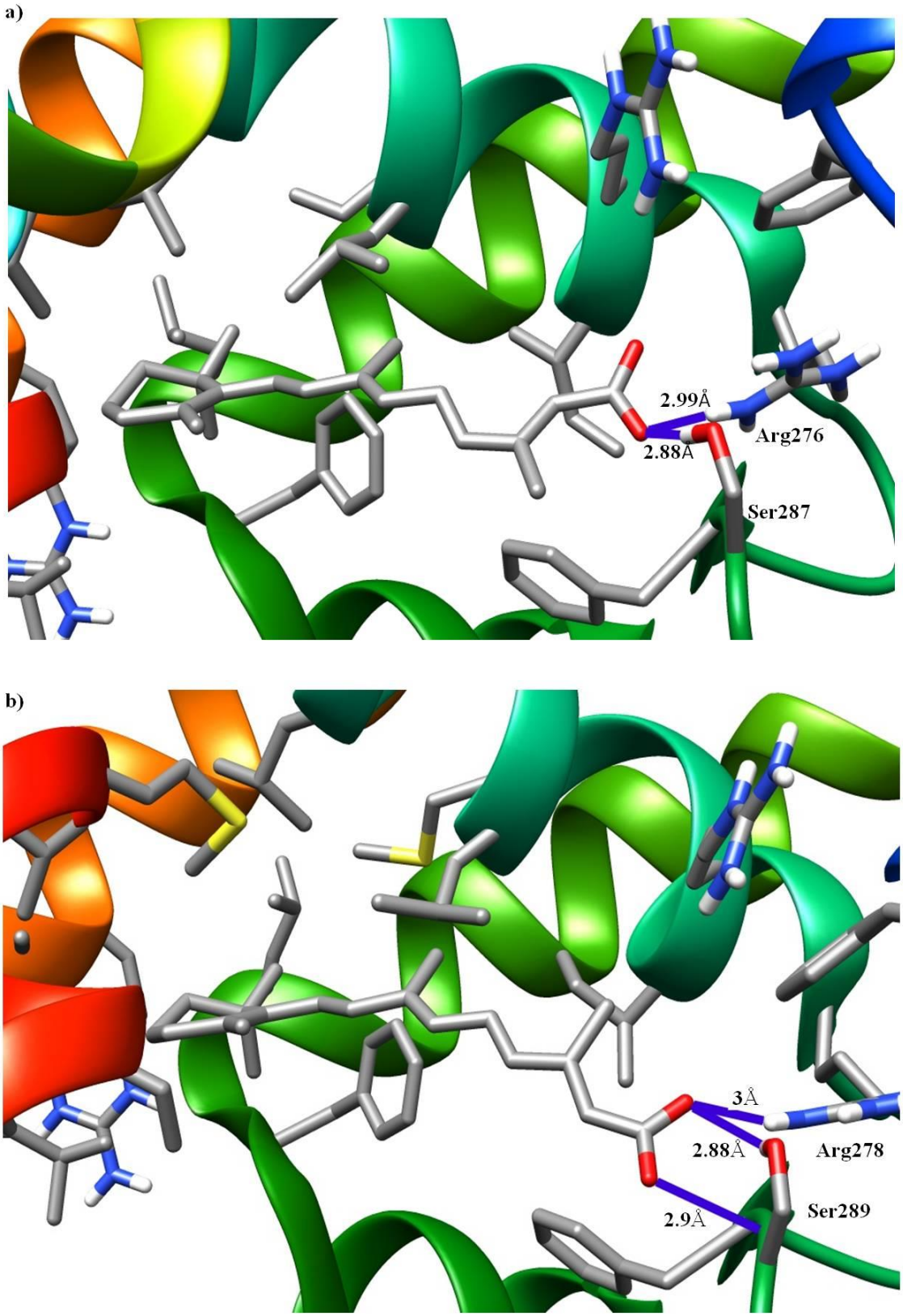

Figure 3.6: ATRA binding mode of interaction onto its cognate RARreceptors; a) ATRA bound to RAR-α showed hydrogen bond with Ser287 and salt bridge with Arg276; and b) ATRA bound to RAR-γ showed hydrogen bond with Ser289 and salt bridge with Arg278.

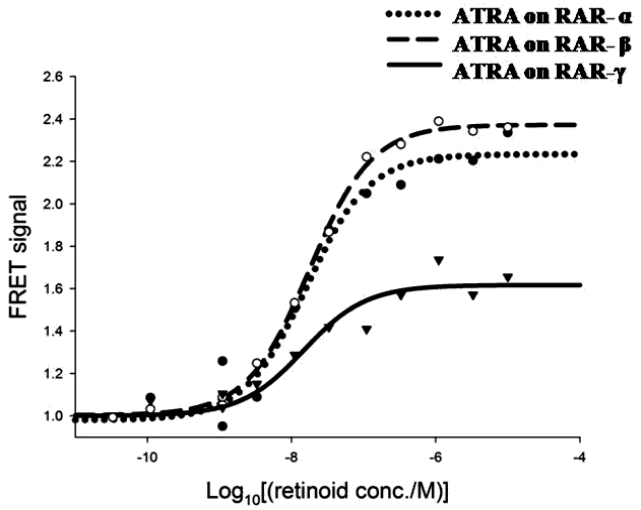

Figure 3.7: Sigmoid representation for the receptor binding assay for ATRA on all RAR-types for calculation of binding affinity (EC_{50}) which represented mid-point on graphs to produce 50% of FRET signal. Calculation was done using Sigmaplot statistical software and data normalized to lower asymptote values.

Table 3.5: Comparison between EC_{50} of ATRA for different RARs

Retinoid analogue	*EC_{50} (nM)		
	RAR-α	RAR-β	RAR-γ
ATRA	16 ± 1%	17.6 ± 3.1%	14.7 ± 2.2%
9-CRA	28.8 ± 0.7%	27 ± 0.7%	36.7 ± 1%

*(EC_{50}± % S.E.M)

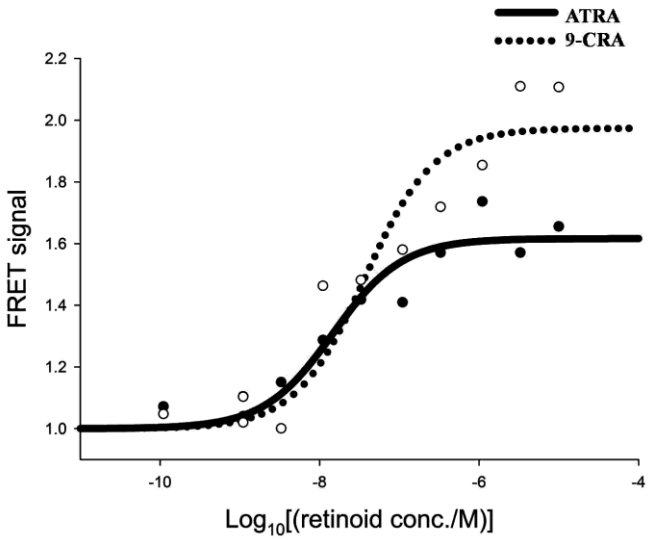

Figure 3.8: Sigmoid representation for the receptor binding assay of ATRA and 9-CRA on RAR-γ showed EC_{50} of ATRAwas 14.7 nM and 36.7 nM for 9-CRA which indicated ATRA binding affinity was approximately double that of 9-CRA.

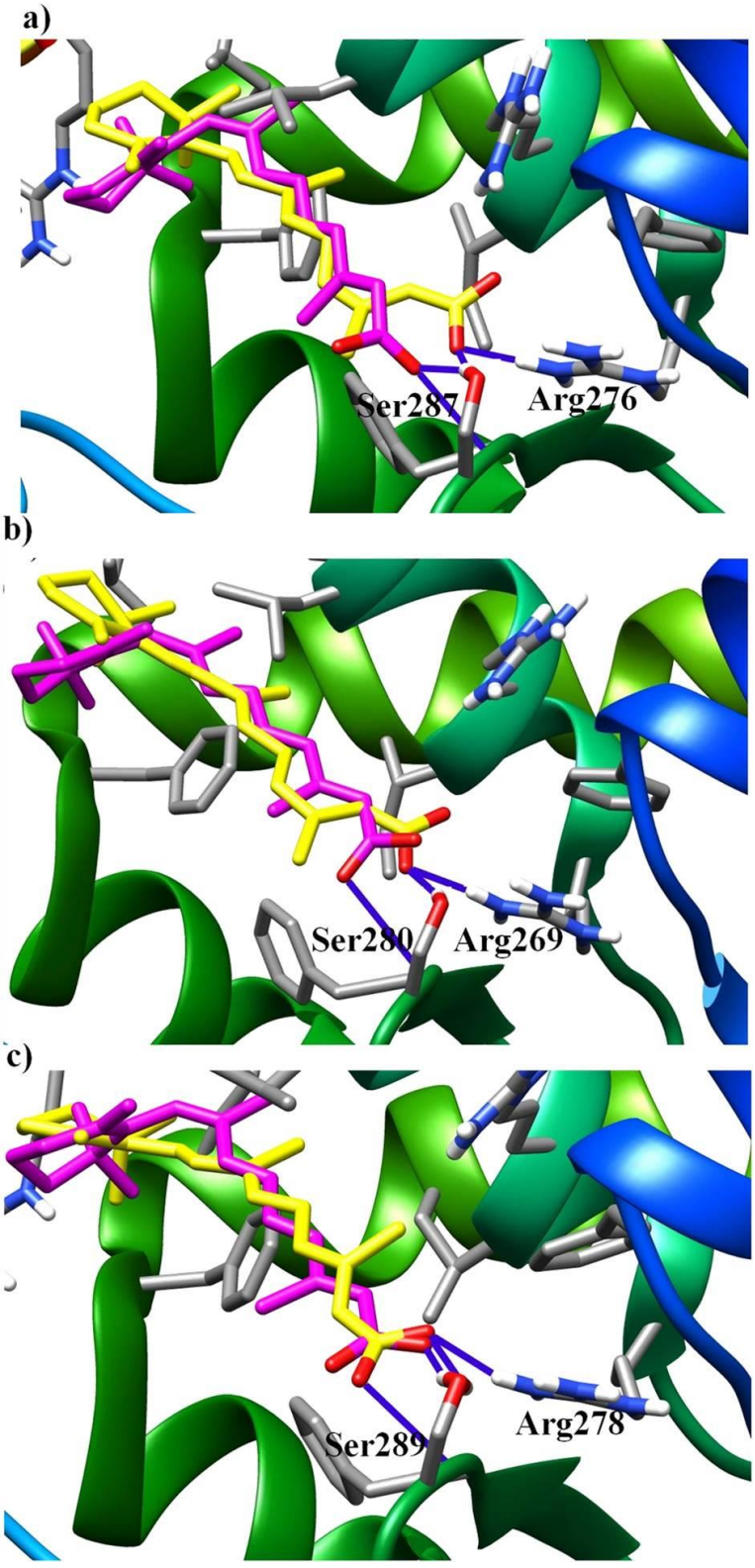

Figure 3.9: ATRA and 9-CRA binding mode and interactions into its cognate receptor RARs; a) RAR-α; b) RAR-β; and c) RAR-γ. ATRA bound through hydrogen bonds with Ser and salt bridge with Arg residues while 9-CRA bound only through hydrogen bond with Ser and away from Arg (~ 4.5 Å) to form salt bridge. Note the difference between *s-cis* form of ATRA in RAR-α and - β and *s-trans* form of ATRA in RAR-γ. ATRA is yellow and 9-CRA is magenta color.

3.6.3 Carboxylic acid terminal active group versus ester group

Methyl retinoate was another naturally occurring retinoid form which was thought to be a storage form of ATRA during the metabolism of retinoic acid. It was interesting to compare the free carboxylic acid form of retinoic acid to the methyl ester form of ATRA and find out if this has an impact upon the binding interaction poses in the LBD of the RARs. Molecular modelling of methyl retinoate had an overall lower fitness score compared to ATRA. The reason for this is suggested to be the presence of extra methyl group of the ester, which could direct the oxygen of carboxylate away from the binding pocket of all the RARs, so that there is no salt bridge formed with Arg residue, and hence, weaker binding than that of ATRA. This can be revealed from the distance between the oxygen of ATRA and Arg was on average of 2.8-3.0 Å while that of oxygen and Arg in methyl retinoate was 3.3 Å, and hence, there was a drop in the strength of binding interaction inside the binding pocket (Fig.3.10).

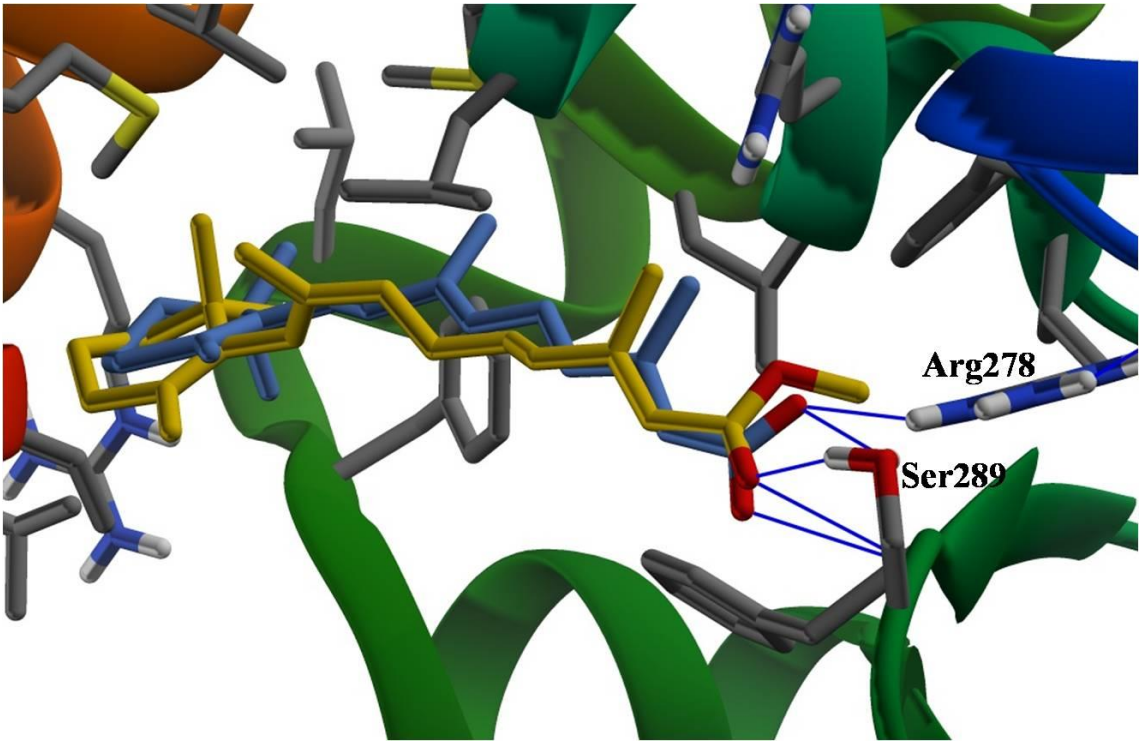

Figure 3.10: ATRA and methyl retinoate binding mode of interactions onto its cognate receptor RAR-γ, ATRA bound to RAR-γ through salt bridge with Arg278 with distance 3.0 Å while methyl retinoate was not able to bind to Arg278. ATRA is blue and methyl retinoate is gold color.

3.7 Molecular binding interaction of synthetic retinoids

There are some synthetic molecules in the literature have similar retinoids structures with replacement of conjugated double bonds system by more stable derivatives which have proposed biological activity as retinoids and more stability. This study compared the molecular binding affinities of these molecules to ATRA and highlighted the differences in molecular binding interactions between all of them.

3.7.1 Pan-RARs synthetic retinoids agonists (TTNBP and TTNN)

Chemically, the parent retinoid structure is defined as a di-terpenoid derived from a monocyclic compound with five carbon-carbon double bonds and a functional group at the terminus of a cyclic portion. However, this definition does not account for some new synthetic derivatives which are tri-cyclic or tetra-cyclic retinoidal benzoic acid derivatives (arotinoid acids) as TTNBP and TTNN. Such new synthetic derivatives can be modified in future to yield almost an unlimited number of retinoids with different potency compared to monocyclic parent retinoids.

Receptor binding assays studies showed that TTNBP has the lowest EC_{50} of all different RARs compared to ATRA and TTNN; 3-fold lower on RAR-α, 7-fold lower on RAR-β and 100-fold lower on RAR-γ compared to ATRA which indicated it had broad, higher binding affinities to all types of RARs. This receptor binding data matched with Table 1.3 in introduction chapter, since both ATRA and TTNBP are able to bind all RARs however, they have relatively higher binding affinity to RAR-γ. It might be suggested that the hydrophobic naphthalene side chain of TTNBP will favour the van der waals contacts in the more hydrophobic pocket of RAR-γ especially with Met residues in H11 and H12. TTNN was ranked with a lower binding affinity than TTNBP and ATRA on both RAR-α and RAR-γ, while it also had a higher binding affinity to RAR-β (2-fold higher than ATRA), this suggests its potential selectivity for RAR-β over other types (Table 3.6 and Fig.3.11).

Molecular docking of these arotinoids to the LBD of the RARs explained this higher binding affinity of TTNBP, since this molecule fitted in the binding pockets of RARs with the formation of two strong hydrogen bonds with the Ser residue (2.5, 2.2 Å for RAR-α), (2.02, 2.22 Å for RAR-β) and (2.5, 2.016 Å for RAR-γ).

Also, it was able to form one strong salt bridge with the Arg residue in the pocket (2.5 Å for RAR-α), (2.16 Å for RAR-β) and (3 Å for RAR-γ). TTNN had a higher fitness score than ATRA on molecular docking of RAR-β and also a lower EC_{50}, and the reason for this may be the stronger two hydrogen bonds formed with Ser280 (2.02, 2.218 Å) compared to ATRA, however, for RAR-α and RAR-γ the binding interactions were similar to ATRA and TTNBP, but more much reduced binding affinity than ATRA (Fig.3.12).

Table 3.6: Comparison between EC_{50} of ATRA, synthetic retinoids TTNBP and TTNN on different RARs

Retinoid analogue	*EC_{50} (nM)		
	RAR-α	RAR-β	RAR-γ
ATRA	16 ± 1%	17.6 ± 3.1%	14.7 ± 2.2%
TTNBP	5.7 ± 3.3%	2.7 ± 13.7	1.2 ± 0.5%
TTNN	20 ± 0.7%	8.2 ± 2%	70 ± 0.2%

*(EC_{50}± % S.E.M)

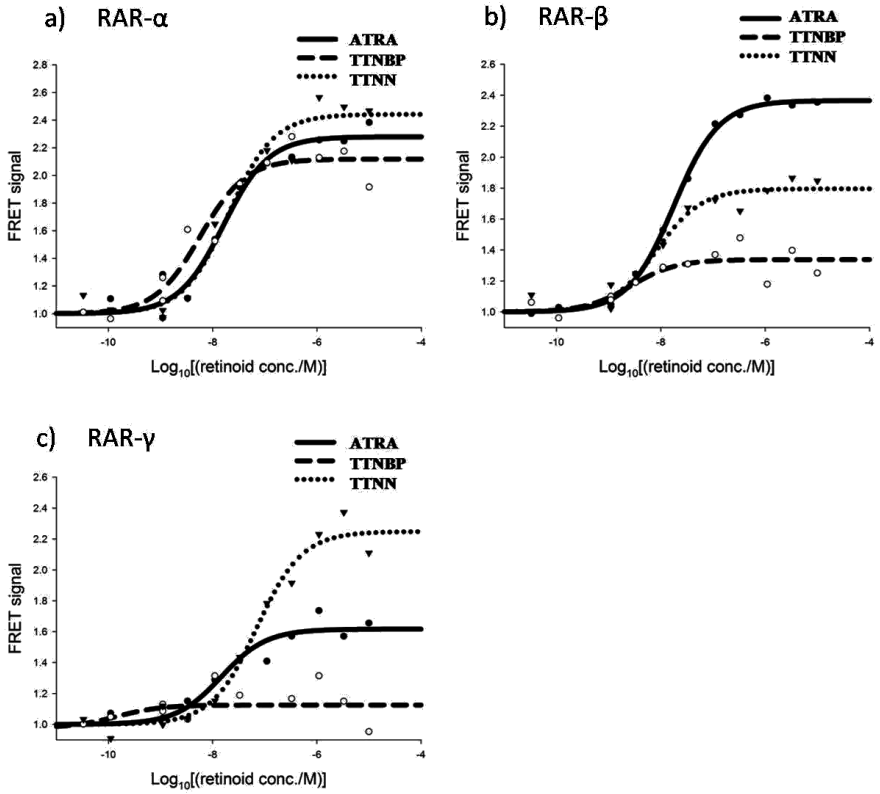

Figure 3.11: Sigmoid representation for the receptor binding assay of synthetic retinoids TTNBP and TTNN compared to natural retinoid ATRA on RARs; a) RAR-α ; b) RAR-β; and c) RAR-γ.

a)

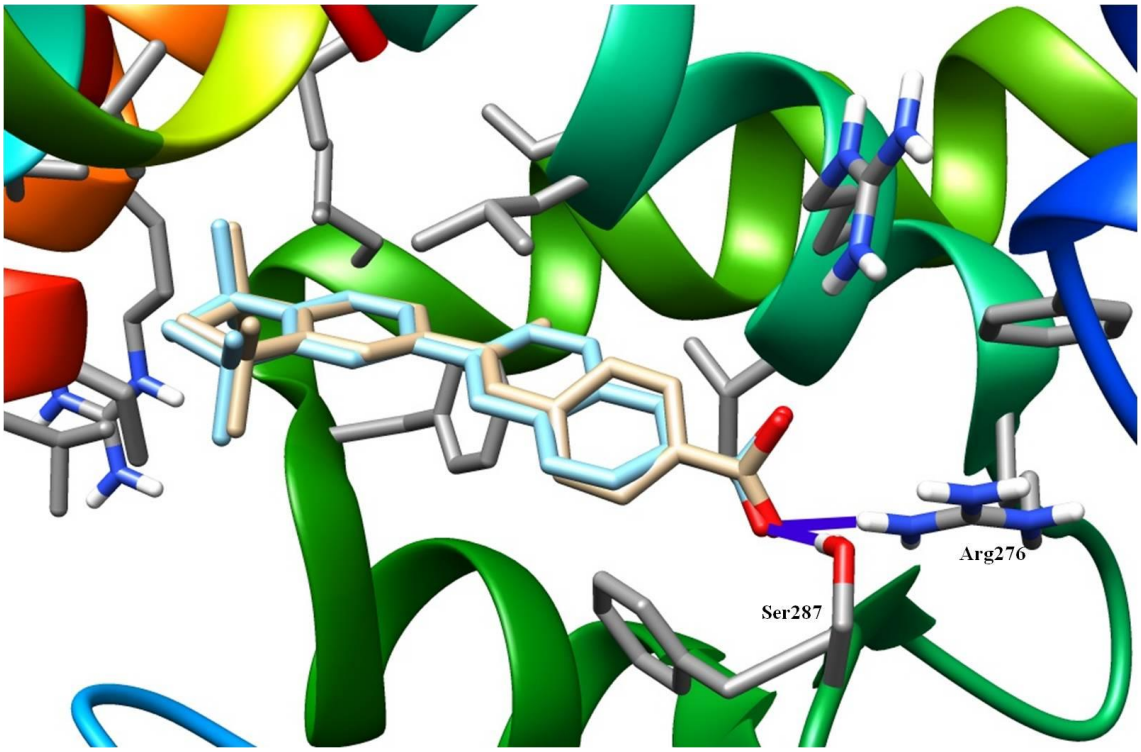

b)

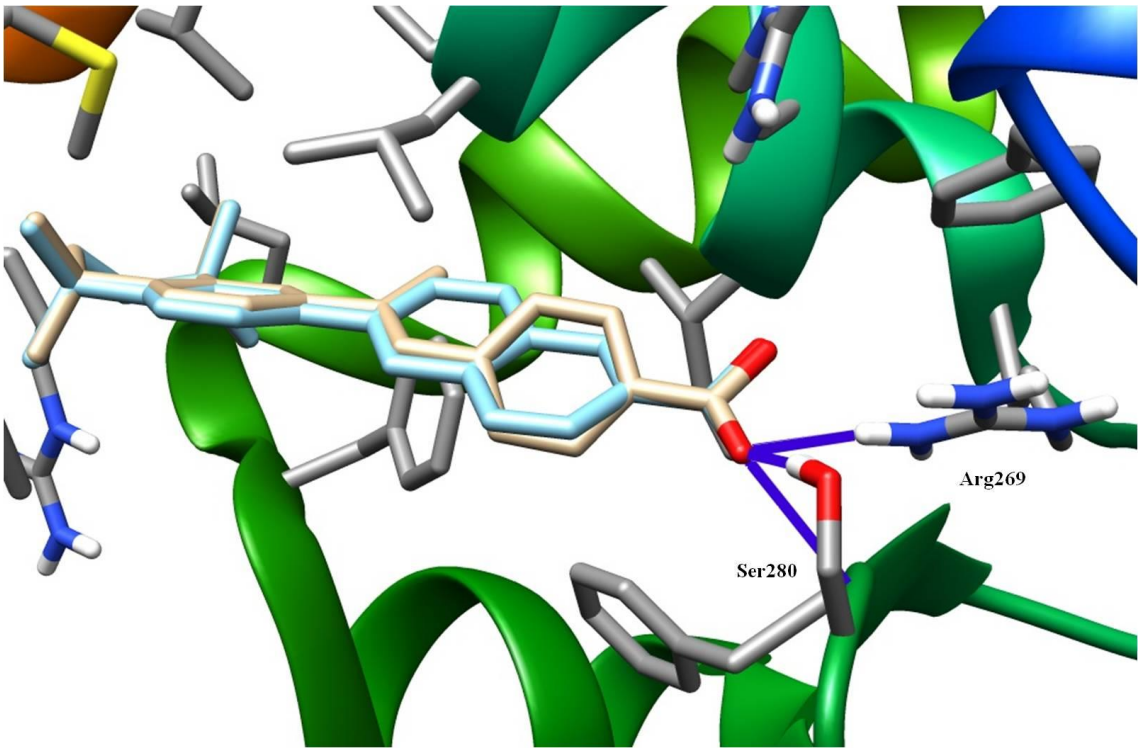

c)

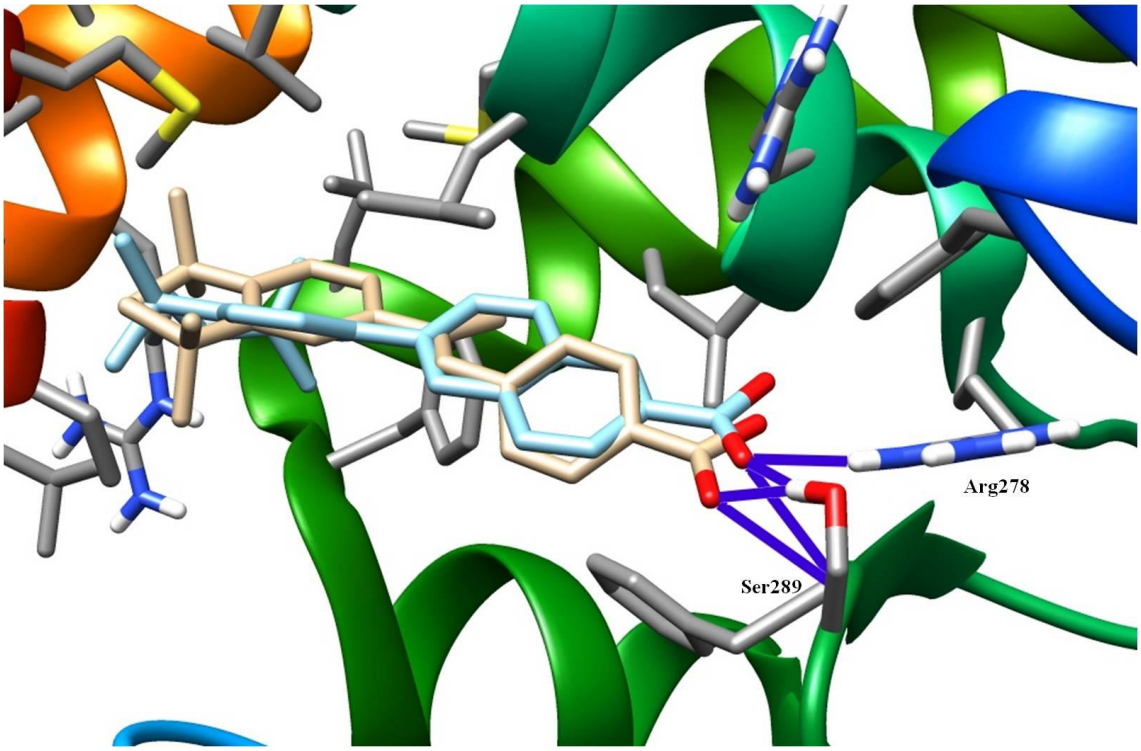

Figure 3.12: TTNBP and TTNN binding mode of interactions in its cognate RARreceptors; a) RAR-α; b) RAR-β; and c) RAR-γ. TTNBP and TTNN bind with the same mode of binding interaction to Ser and Arg residues with coincidental overlay in the binding pocket of RAR-α, -β and some twisting compared to TTNBP in RAR-γ binding pocket. TTNN is blue and TTNBP is in gold color.

3.7.2 Selective synthetic retinoids agonists (AM-580 and CD437)

Synthetic retinoids targeting all retinoic acid receptors have been developed for a variety of therapeutic applications; however, their success has been limited in part due to lack of selectivity. This is why some new RAR agonists has been developed that can distinguish between different RARs-types and in some cases, between different isoforms. The selectivity for each retinoic receptor is based on the nature of the pharmacophore region (hydrophilic or hydrophobic) and the presence of one or more sets of targeted amino acid residues that can bind selectively to specific groups in retinoid molecules. Two examples of synthetic retinoids with potential RAR-selectivity are represented in this chapter.

3.7.2.1 Am580 as RAR-α selective agonist

Interestingly, the measured EC_{50} for AM-580 on RAR-α was 3.8 nM, compared to 16 nM for ATRA (5-fold lower than that of ATRA) which indicated that AM-580 has a higher binding affinity, 5-times more than ATRA (Fig. 3.13a). The molecular observation of the LBD of RAR-α revealed that several amino acids from α-helices H1, H3, H5, H11 and H12 were directed as contact residues between the receptor and ligand. Two positions were important and could be responsible for anchoring retinoids with hydrophilic groups such as Ser287 and Ser232. These two amino acids therefore, were elements for examining RAR-α selective candidate. Molecular docking of AM-580 into the RAR-α LBD could probably help to understand the difference in binding affinity to ATRA since hydrogen bonding would not be permitted between the hydroxyl of ser232 and the hydrophobic linker of ATRA, while it can form such hydrogen bond with the amide linker in Am580. As a consequence, AM-580 might adapt a well fitted conformation in the RAR-α binding pocket to form three strong hydrogen bonds with Ser287 (2.06, 2.4 and 2.2 Å) and one strong salt bridge with Arg276 (2.0 Å) compared to one hydrogen bond and one salt bridge for ATRA (Fig.3.14).

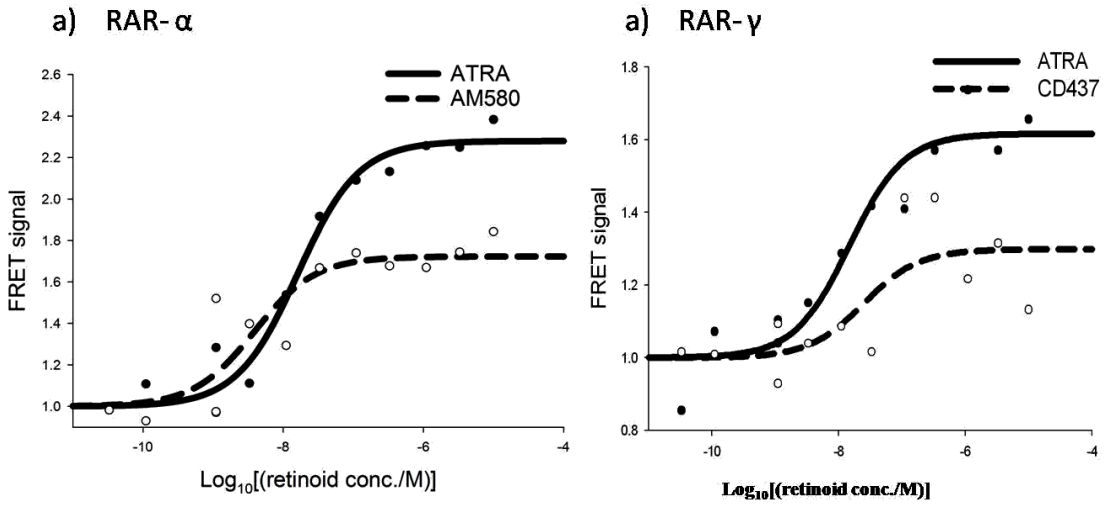

Figure 3.13: Sigmoid representation for the receptor binding assay of synthetic RAR-selective retinoids; a) EC_{50} of AM-580 was 3.8nM compared to 16nM for ATRA showed higher binding affinity of AM-580 to RAR-α; and b) EC50 of CD437 compared to ATRA showed comparable to slightly lower binding affinity of CD437 to RAR-γ.

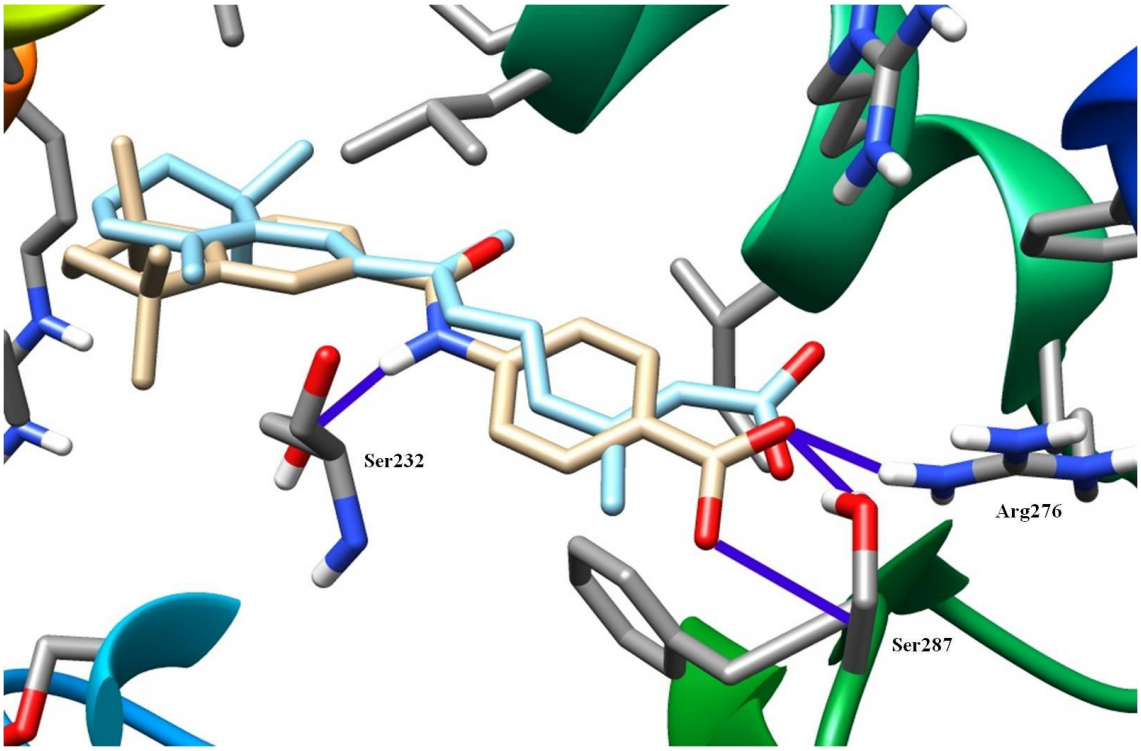

Figure 3.14: Am580 and ATRA binding mode of interactions onto its cognate receptor RAR-α showed additional hydrogen bonding of AM-580 to Ser232 which favours the higher binding selectivity and fitting of AM-580 into the LBD pocket.

3.7.2.3 CD437 as RAR-γ selective agonist

On the same concept of the presence of conserved residues in the LBD of RARs which play key roles in retinoid selectivity, it was found that Met272 was a key amino acid residue that adopts different conformations in the LBD for RAR-γ selectivity. Met272 locates above the ligand binding site and arranges itself for best hydrogen bonding between its sulphur atom and the ligand. This might add extra hydrogen bond for the ligand in LBD consequently results in higher binding affinity and a stronger interaction. Also, Lys236 was one of the backup residues in the LBD which thought to be essential either to overcome the drop in binding interaction with Ser or Arg residues or to act as one of the selective residues in the RAR-γ pocket.

CD437 was one of the admantyl bulky group retinoid derivatives that had measured EC_{50} of 25 nM, compared to 14 nM of ATRA (Fig.3.13b). The molecular docking revealed that the phenyl group side-chain of CD437 could form hydrophobic contacts with Met272, which consequently added to the overall interaction with CD437 in the LBD of RAR-γ. The admentayl side chain can also form hydrophobic contact with the surrounded Met residues in H11 and H12 which might be added to the overall interaction. In addition, CD437 also formed three hydrogen bonds; two of them with Ser289 (2.4, 2.5 Å) and one with Lys236 (2.1 Å), one salt bridge with Arg278 (2.5 Å) and this is why it was proposed that CD437 had some selective binding affinity to RAR-γ (Fig.3.15).

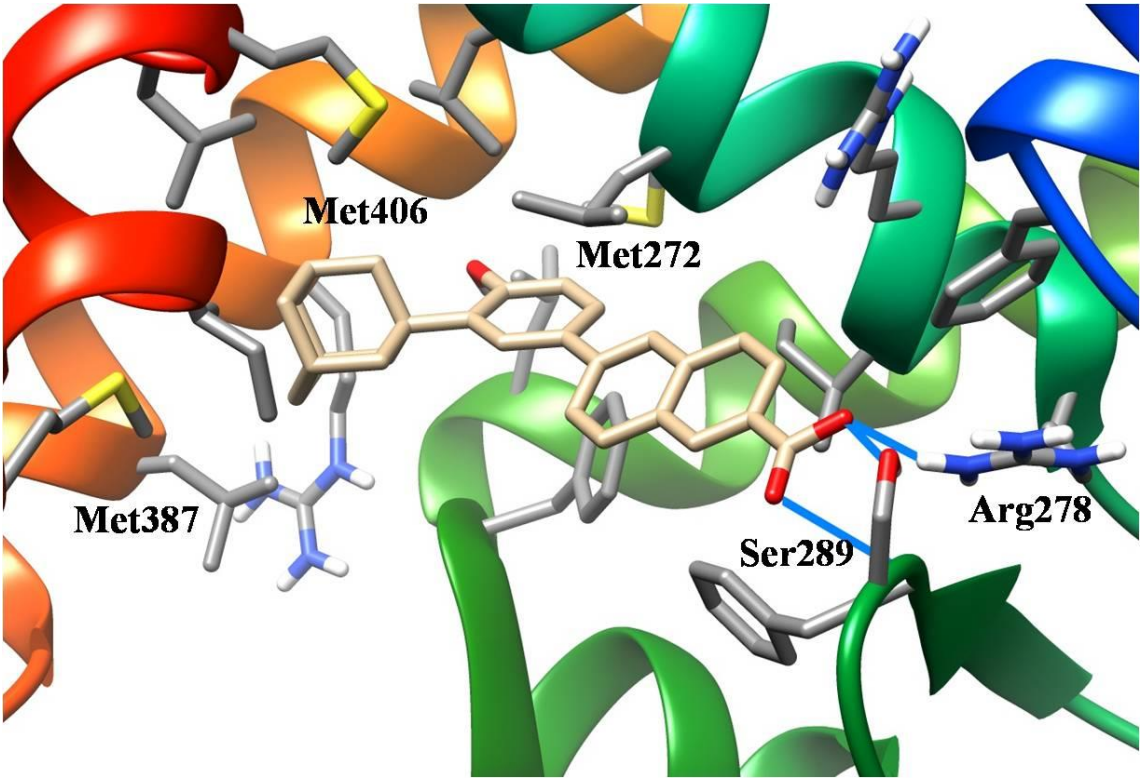

Figure 3.15: CD437 binding mode of interactions into its cognate receptor RAR-γ showed additional hydrophobic contacts between of Met272 with phenyl group and Met406, Met387 with admantyl group of CD437 which favoured the higher binding selectivity and fitting into the LBD pocket.

3.8 Molecular docking study of new synthetic retinoid analogues

The activity of natural retinoids, ATRA and 9-CRA has limited *in vitro* application because of photo induced isomerization and radical oxidation which consequently affects their stability and biological activity. The Whiting group has designed new synthetic chemical retinoid analogues that possess similar or higher activity than natural retinoids.

In this part of the chapter, we study different types of these new synthetic retinoids to understand what factors affect retinoid binding to RARs, especially as a function of the chemical structure of the small molecule ligand. To address this, receptor-binding assays are required to test predictions from structural modelling studies and explain how structural differences relate to the thermodynamics of the different ligand binding events.

3.8.1 EC19 and EC23 arotinoids

Two derivatives which are 4-(5,5,8,8-tetramethyl-5,6,7,8 tetrahydronaphthalen-2-ylethynyl)benzoic acid (EC23) and 3-(5,5,8,8-tetramethyl-5,6,7,8-tetrahydronaphthalen-2-ylethynyl)benzoic acid (EC19). In these compounds, the tetra-methylcyclo-hexanyl ring and conjugated tetraene are replaced by robust structural units; two aromatic rings (di-phenyl acetylene) and this why they called arotinoids. Another a key chemical difference between these derivatives in the position of the carboxylic group from *meta*-(EC19) and *para*-substitution (EC23) which will be studied in details.

The results of the TR-FRET receptor binding assays are shown in Fig. 3.16, with the measured EC_{50} values for each ligand with the different RAR types summarised in (table 3.7).The midpoints of the fitted curves represented the binding affinities, expressed as EC_{50}, and the level of the upper asymptote was a measure of the affinity of co-activator for the ligand-bound LBD. For RAR-α, EC23 had the highest binding affinity (EC_{50} 3.7 nM) compared to other ligands while EC19 had the lowest (EC_{50} 194 nM), with intermediate values for the RA isomers. Upper asymptotes were highest for ATRA and EC23 compared to EC19. For RAR-β, there was a narrower range of ligand binding affinities, with EC23 having the greatest affinity (EC_{50} 3.1 nM), (Table 3.7). In contrast to RAR-α, the upper asymptotes suggested that co-activator recruitment was best for ATRA but relatively inefficient for EC23. Thus, EC19 had a relatively high affinity for the RAR-β LBD and ligand binding also facilitates co-activator recruitment. For RAR-γ, ATRA and EC23 had similar high binding affinities (EC_{50} 14.7 nM and 16.7 nM, respectively) with EC19 the lowest (EC_{50} 96.4 nM). Conversely, 9-CRA had the highest asymptote suggesting greater efficiency of co-activator recruitment compared to the other ligands, with EC19 being the least effective.

Table 3.7: Comparison between EC_{50} of ATRA, synthetic retinoids EC19 and EC23 on different RARs

Retinoid analogue	*EC_{50} (nM)		
	RAR-α	RAR-β	RAR-γ
ATRA	16 ± 1%	17.6 ± 2.1%	14.7 ± 2.2%
EC19	194 ± 0.2%	12.1 ± 7%	96.4 ± 0.6%
EC23	3.7 ± 4.6%	3.1 ± 6%	16.7 ± 2%

*(EC_{50}± % S.E.M)

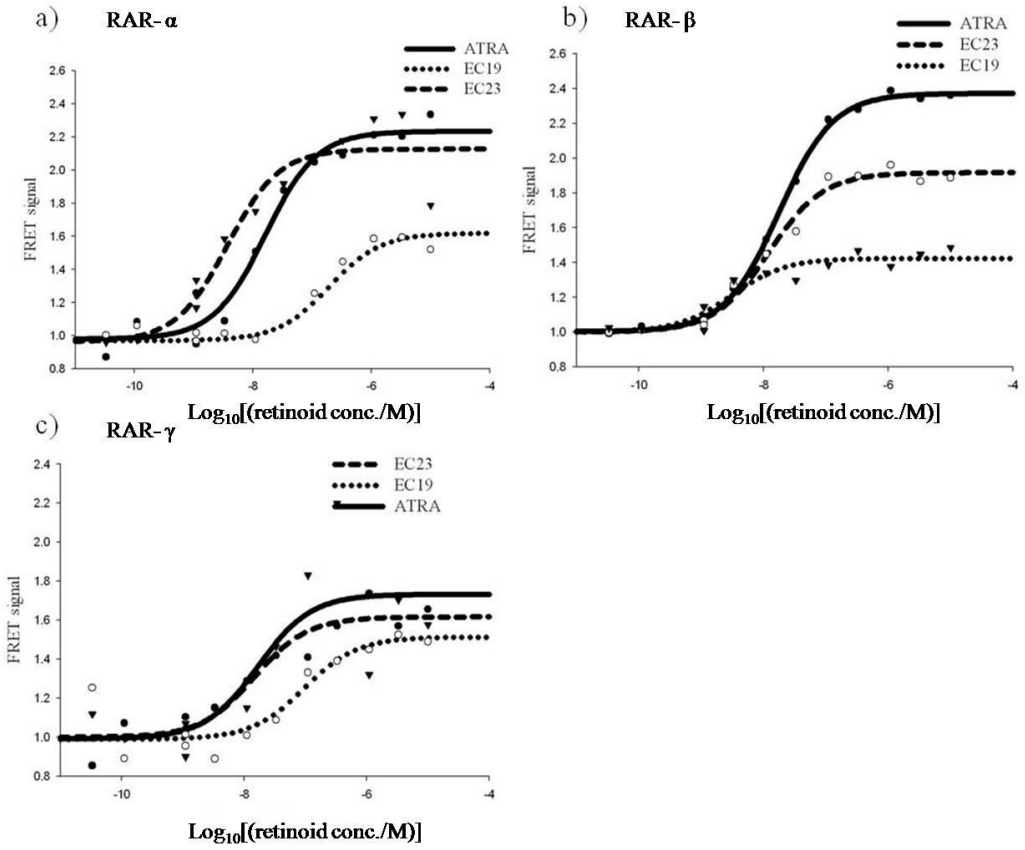

Figure 3.16: Sigmoid representation for the receptor binding assay of synthetic retinoids EC19 and EC23 compared to natural retinoid ATRA on RARs; a) RAR-α ; b) RAR-β; and c) RAR-γ.

Comparisons of EC23 and EC19 docked into the different RAR sub-types with the standard binding interactions for ATRA, showed some differences in behavior, particularly with respect to the orientation of the active carboxylate group. The *para*-substitution of the carboxylate ion facilitated a good fit of EC23 to the binding pocket in all RARs by forming a strong salt bridge with the conserved residue Arg and two hydrogen bonds with the conserved Ser residue.

In contrast, the *meta*-substitution of the carboxylate ion of EC19 altered the geometry of the molecule such that the carboxylate oxygensare too far away to form a salt bridge or hydrogen bond in the binding pocket of the RAR-α and RAR-γ (Table 3.8, Fig.3.17 and Fig. 3.19). For RAR-β, EC19 was anchored into the pocket by forming a salt bridge with Arg and a hydrogen bond with Ser, thus might give enhanced binding interactions compared to the binding interactions of EC19 with RAR-α and –γ (Fig. 3.16). The reason for such enhancement in binding interaction of EC19 to RAR-β was suggested to be due to topography and size of the LBD was different and has an extra-groove (space) compared to either RAR-α or RAR-γ; this may accommodate ligands with bulky substituents or geometries unfavourable for binding to RAR-α or RAR-γ, given sufficient anchorage by interaction with Arg and/or Ser at the other end of the pocket (Fig.3.20). The molecular modelling also suggested that the *meta*-position of the carboxylate group of EC19 caused change in orientation of the tetra-methyl-tetra-hydronaphthalene moiety which consequently formed short contacts and clashes with some residues in ligand binding pocket, such as Ile270 and Val309 in RAR-α and Ala397, Leu416, Phe230, Ala234, Met415, Phe288 and Ser289 in RAR-γ which affect the active conformation of H12, and thereby, the recruitment of co-activators and initiation of the transcription process. The differences in binding between EC19 and EC23 clearly concluded that the *para*-substitution of the carboxylic acid in EC23, *i.e.* a linear structure and ATRA-like in shape, which might create a more favourable binding interaction inside LBDs.

Table 3.8: Molecular hydrophilic binding interactions and distances in observed from molecular docking of ATRA, EC19 and EC23 on different RAR LBDs

Retinoid analogue	Molecular binding interaction (Å)					
	RAR-α		RAR-β		RAR-γ	
	Arg276	Ser287	Arg269	Ser280	Arg278	Ser289
ATRA	2.99	2.8	2.9	2.6	3	2.8
EC19	2.4	3.7	2.1	2.5	3.7	2.1, 2.6
EC23	2.2	2.7, 2.2	2.5	2.4, 2.6	2.6	2.6, 2.7

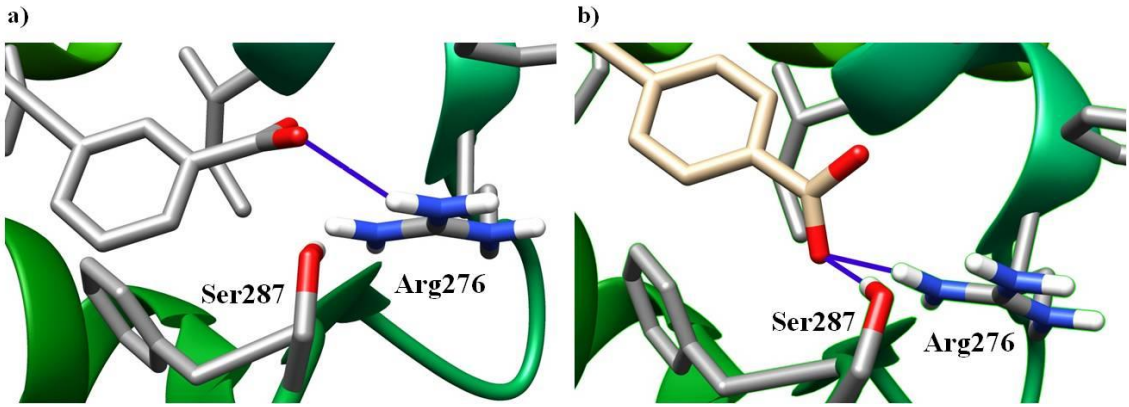

Figure 3.17: EC19 and EC23 binding mode showing interaction into its cognate receptor RAR-α; a) EC19 lost its hydrogen bond interaction with Ser287 due to twisting away from binding pocket; and b) EC23 bound to Ser287 with two strong hydrogen bonds due to best fit in LBD of RAR-α. EC19 is grey and EC23 is the brown gold colour.

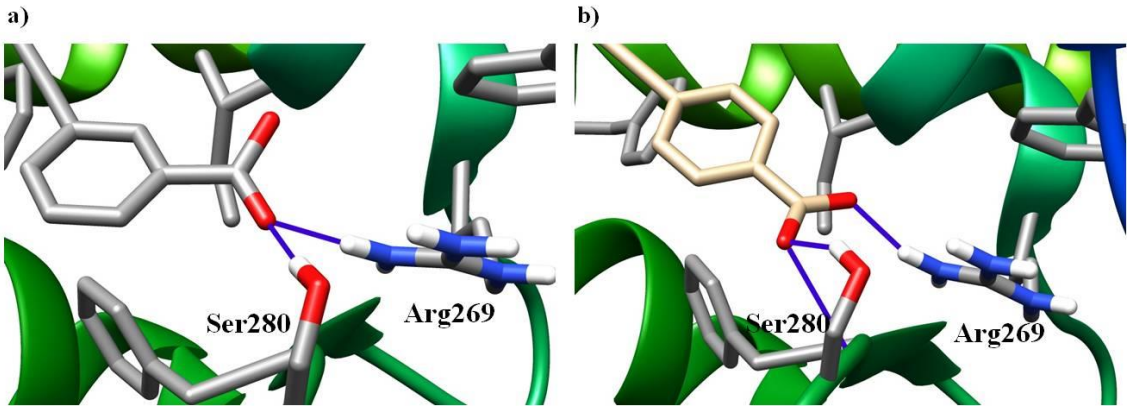

Figure 3.18: EC19 and EC23 binding mode showing interactions onto its cognate receptor RAR-β; a) EC19 bound both hydrogen bond with Ser280 and salt bridge with Arg269; and b) EC23 formed both salt bridge with Arg269 and additional hydrogen bond with Ser280 and this can account for higher binding affinity of EC23 than EC19 in LBD of RAR-β. EC19 is grey and EC23 is the brown gold colour.

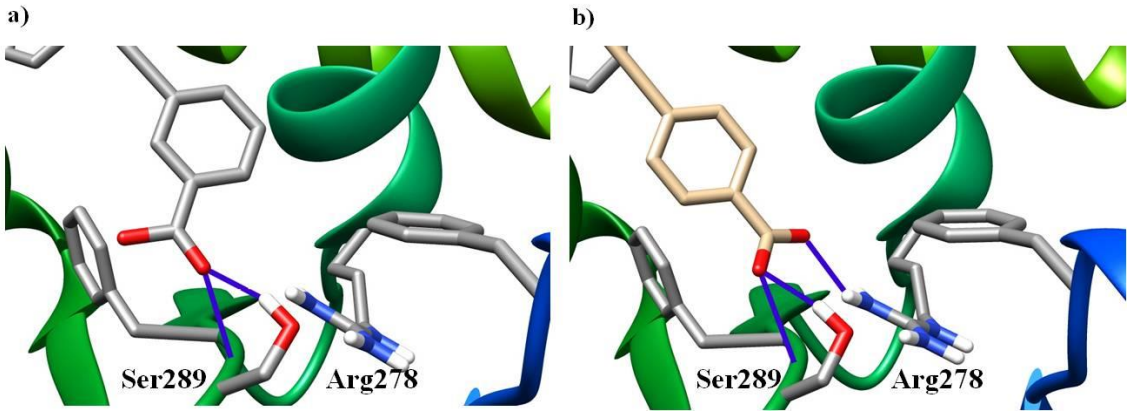

Figure 3.19: EC19 and EC23 binding mode showing interactions onto its cognate receptor RAR-γ; a) EC19 lost its salt bridge interaction with Arg278 due to twisting away from binding pocket; and b) EC23 formed this salt bridge with Arg278 due to best fit in LBD of RAR-γ. EC19 is grey and EC23 is the brown gold colour.

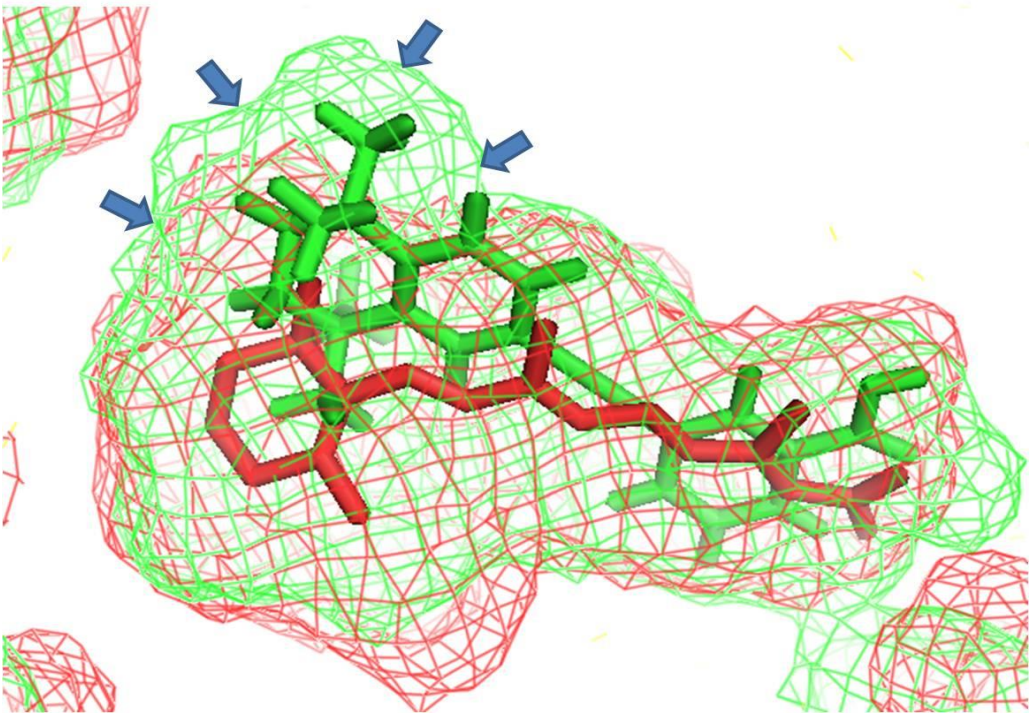

Figure 3.20: Structure overlay between binding pockets of the docked structure for EC19 in RAR-β and ATRA in RAR-γ showed the extra groove (blue arrows) in the RAR-β binding pocket (green color) that might accommodate the bulky components of EC19, compared to the RAR-γ binding pocket (red color) that lacks this groove. EC19 experiences greater steric hindrance with surrounding residues than in RAR-β binding pocket. EC19 is green and ATRA is red. Pymol was used to produce this figure.

3.8.1.1 Methyl ester of EC19 and EC23

Methyl ester derivatives of EC19 and EC23 were synthesized by the Whiting group to investigate if the ester form can enhance the activity of either EC19 or EC23 and the measured EC_{50s} for methyl esters of EC19 and EC23 showed that was no increase in binding affinity of EC19 methyl ester to any of RARs, except slightly to RAR-α, but still the binding affinity was lower than ATRA and EC23. However, methyl ester derivative of EC23 caused massive drop in binding affinity to all RARs compared to ATRA and EC23 with acid form. This matches previous observations of the binding affinity of methyl ester of ATRA (methyl retinoate) (Table 4.9) which was similarly reduced.

Molecular docking of methyl esters of EC19 and EC23 caused a drop in the binding interactions with the Ser and Arg conserved residues in the LBD of all RARs and only a small improvement in binding affinity of EC19 methyl ester was observed due to two hydrogen bond with Ser287. Also, EC23 methyl ester caused additional short contact clashes with the adjacent Arg278 and this also caused a drop in binding interactions (Fig.3.21).

Table 3.9: Comparison between EC_{50} of ATRA, synthetic retinoids EC19 and EC23 and its methyl ester derivatives on different RARs

Retinoid analogue	EC_{50} (nM)		
	RAR-α	RAR-β	RAR-γ
ATRA	16 ± 1%	17.6 ± 2.1%	14.7 ± 2.2%
EC19	194 ± 0.2%	12.1 ± 7%	96.4 ± 0.6%
EC23	3.7 ± 4.6%	3.1 ± 6%	16.7 ± 2%
EC19-methyl ester	49 ± 0.8%	30 ± 0.5%	97.7 ± 0.3%
EC23-methyl ester	20.4 ± 0.6%	14.1 ± 1.2%	847.2 ± 0.39%

*(EC_{50}± % S.E.M)

3.8.2 Thiazole derivatives (GZ-derivatives)

This was the second class of synthetic retinoids which have the conjugated tetraene replaced with a thiazole ring. The incorporation of thiazole group has the effect of creating a bend in the structure which might affect the structure activity of the resulting retinoid derivatives. In addition, these thiazole derivatives have different molecular lengths and are shorter, longer or similar to that of ATRA depending on other motifs in the molecule which is second criterion affecting the retinoid binding activity. And again, esters of these derivatives were also studied for these retinoid thiazole derivatives. Receptor binding assay studies showed that EC_{50} for all of the GZ-derivatives were higher than for ATRA, except for GZ25, on all its RAR-types, and GZ23 on RAR-β. This means that only GZ25 has similar to higher binding affinity to all the RARs compared to ATRA. Also, GZ23 has a higher binding affinity to RAR-β, similar to ATRA compared to the lower binding affinity to RAR-α and RAR-γ (Fig.3.22 and Table 3.10).

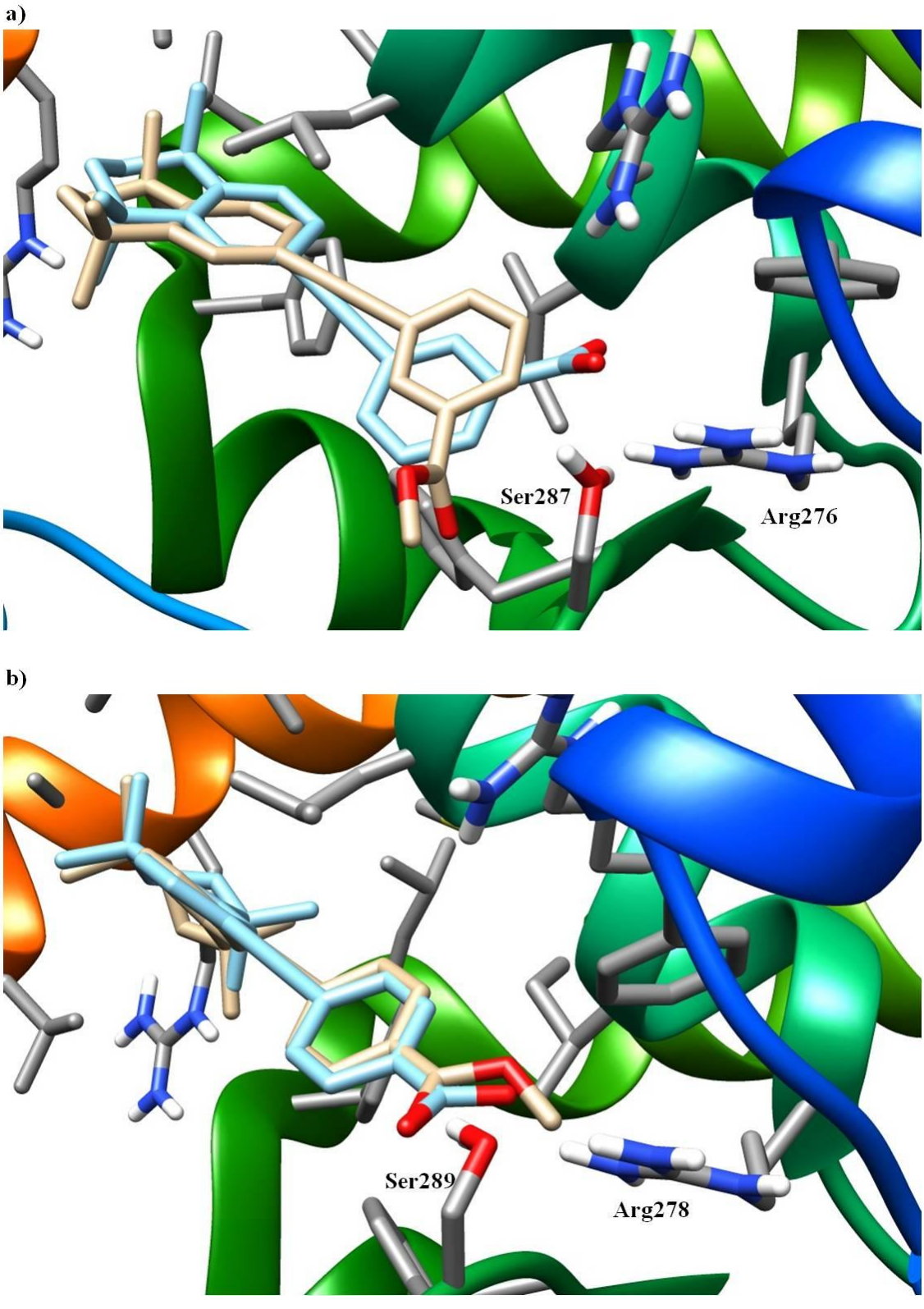

Figure 3.21: Binding mode interactions of methyl ester of EC19 and EC23 into its cognate RARreceptors; a) EC19 and EC19 methyl ester binding interaction showed different behaviour of interaction with methyl ester oriented away from both Arg276 and Ser287 in LBD of RAR-α; and b) EC23 and EC23 methyl ester with potential short contact clashes between methyl ester and Arg278 in LBD of RAR-γ. EC19/EC23 is blue and EC19/EC23 methyl ester is the gold colour.

Interestingly, to understand these differences in binding affinity, molecular lengths have been measured from the carbon atom of carboxylate /ester group to the carbon atom of the cyclohexyl side-chain by UCSF Chimera wizard, and summarized in (Table 3.10). It was suggested that some molecules were shorter than ATRA, as GZ18 and GZ24, while some were longer than ATRA as GZ22 and GZ23, and only GZ25 was similar in length to ATRA. GZ25 seemed, therefore, to be the optimal length to hit the LBD of all the RARs, as most of these derivatives formed salt bridges and hydrogen bonds with the Ser and Arg residues (Table 3.11).However, the hydrophobic pockets must also be filled with the optimum side-chain to form sufficient contact surface with residues of H11-H12 (AF-2) to keep it in the active conformation, thereby enabling the recruitment of co-activators and the initiation of the transcription process. Examples of the important residues of AF-2 that play important roles in recruitment of the co-activators are; (Arg 294, Ile270, Leu398, Met406, Val395 and TRP225 for RAR-α); (Ile266, Leu262 and Met406 for RAR-β); and (Met272, Ile275, Leu271 and Leu400 for RAR-γ). Fig.3.22a and Fig. 3.22b show the differences between the GZs derivatives in forming hydrophobic interactions with these residues based on ligands with shorter chains (as with GZ18) failed to create sufficient contact surfaces with the AF-2 residues, while increasing the number of carbons in the alkyl chain (as with GZ23) might cause steric clashes which consequently orient H12 helix in a position not active for co-activator recruitment. In addition, GZ analogues were shown to have a considerable lower EC_{50} (higher binding affinity) to RAR-α and –β compared to RAR-γ. This might be explained by the additional hydrogen bond formed between the nitrogen atom of thiazole and hydrogen atom of Ser232 (in RAR-α) and the extra groove in RAR-β that might accommodate the relatively bulky analogues of GZ derivatives.

Table 3.10: Comparison between $EC_{50}$and molecule lengthof ATRA, synthetic thiazole retinoids derivatives on different RARs

Retinoid analogue	Molecule length (Å)	*EC_{50} (nM)		
		RAR-α	RAR-β	RAR-γ
ATRA	13.11	16 ± 1%	17.6 ± 2.1%	14.7 ± 2.2%
GZ18	12.20	98.94 ± 0.2%	56 ± 1.3%	141.2 ± 0.38%
GZ22	13.93	82 ± 0.32%	136.3 ± 0.1%	38.3 ± 1%
GZ23	15.19	89 ± 0.44%	12.1 ± 0.83%	847.22 ± 0.47%
GZ24	11.52	77.5 ± 0.18%	77.8 ± 0.8%	109.2 ± 0.46%
GZ25	13.31	8.2 ± 2%	11.0 ± 1%	15 ± 1%

*(EC_{50}± % S.E.M)

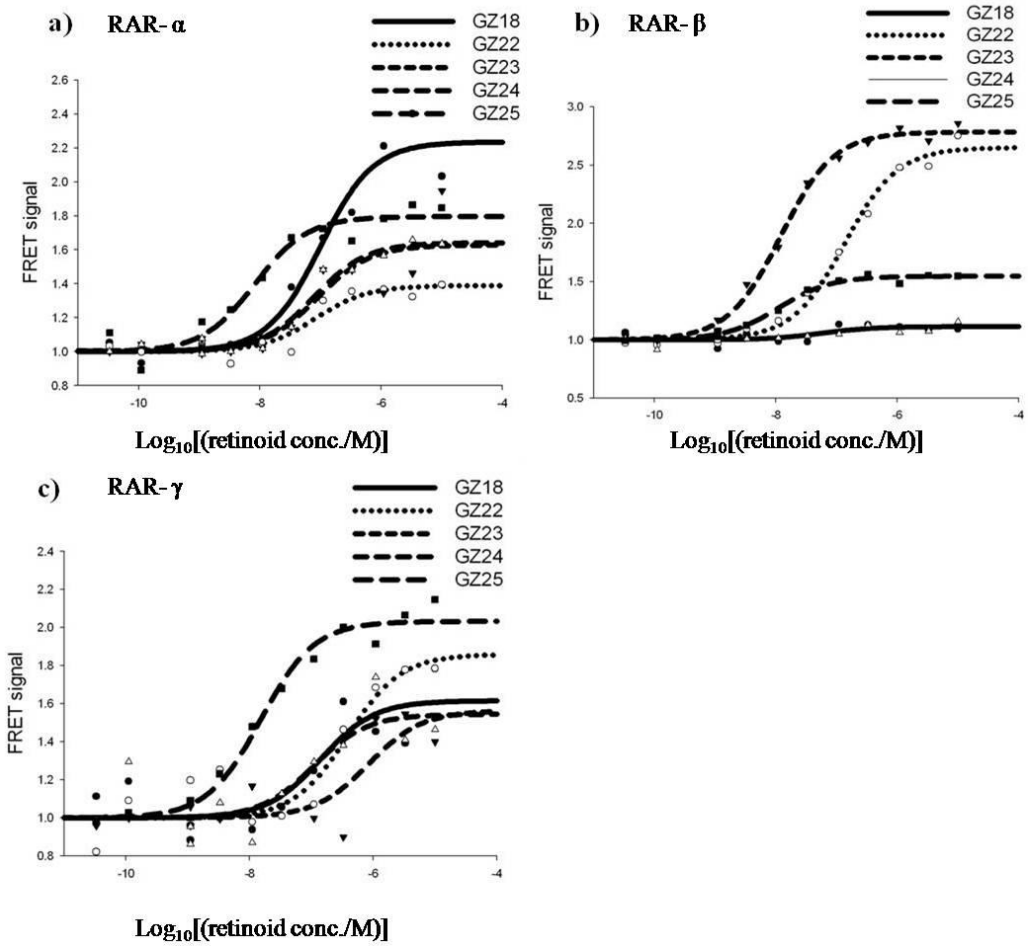

Figure 3.22: Sigmoid representation for the receptor binding assay of GZs synthetic thiazole retinoids; GZ18, GZ22, GZ23, GZ24 and GZ25 on RARs; a) RAR-α; b) RAR-β; and c) RAR-γ.

Table 3.11: Molecular hydrophilic binding interactions observed from molecular docking of GZ derivatives on different RARs

Retinoid analogue	Molecular binding interaction (Å)							
	RAR-α			RAR-β		RAR-γ		
	Arg276	Ser287	Ser232	Arg269	Ser280	Arg278	Ser289	Lys236
GZ18	2.3	2.5,2.5	2.5	2.5	2.0	1.8	2.1,2.2	2.3
GZ22	2.3	2.1,2.2	2.5	X	X	X	X	X
GZ23	2.1	2.4,2.6	2.5	2.4	2.5,2.5	X	2.4	2.4
GZ24	2.5	2.4,2.7	2.4	2.5	2.4,2.5	2.8	2.1,2.2	2.5
GZ25	2.4	2.4,2.8	2.6	2.2	2.4,2.5	2.4	2.4,2.4	2.5

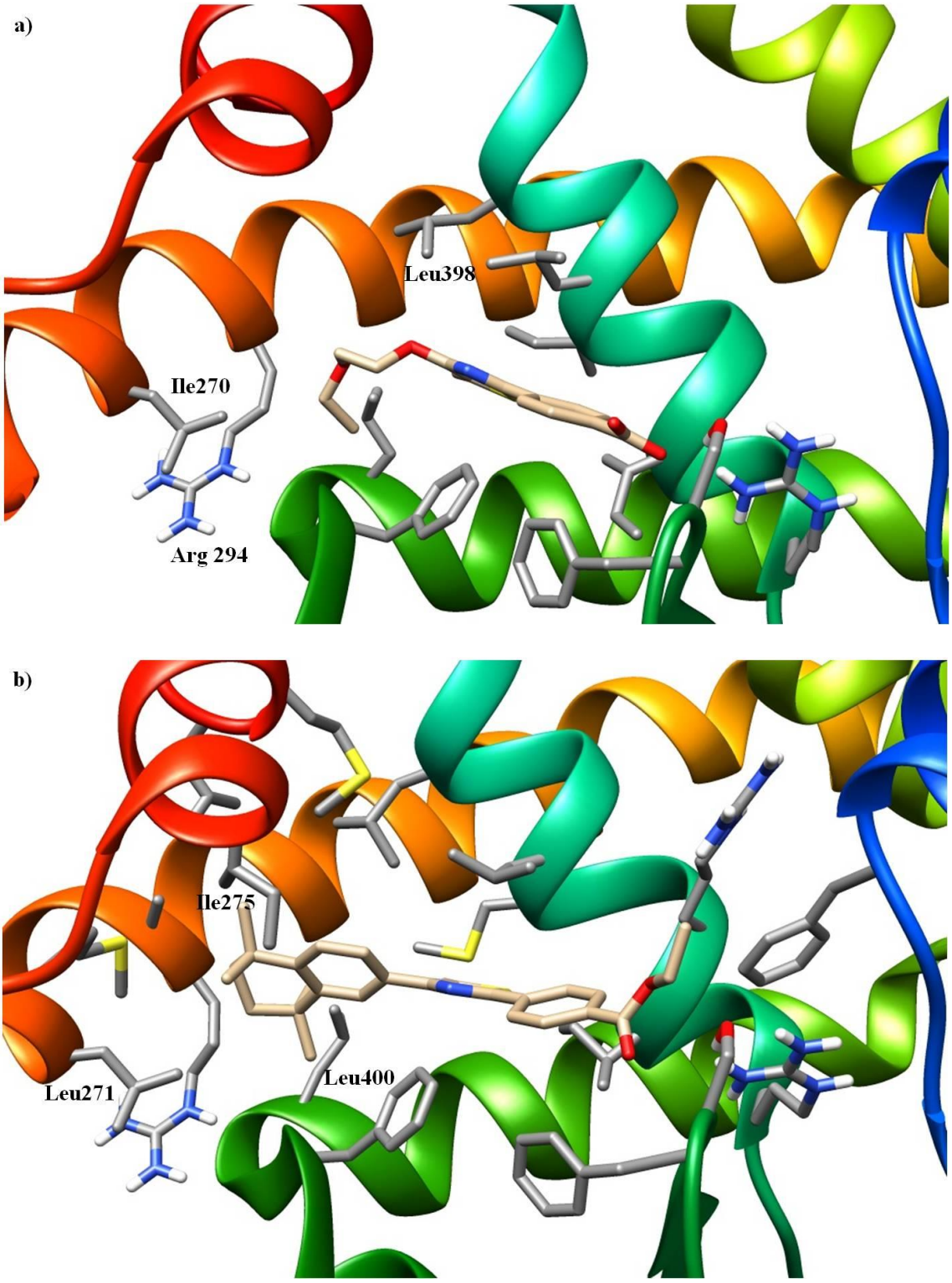

Figure 3.22: Binding mode of interactions of GZ derivatives its cognate receptor RARs; a) GZ18 binds to LBD of RAR-α fails to fill in the hydrophobic cavity and form contacts withAF-2 residues Ile270, Arg294 and Leu398; b) GZ23 bind to LBD of RAR-γ forming short contact clashes with AF-2 residues Leu271, Leu400 and Leu275. Both GZ18/GZ23 ligands are the gold colour.

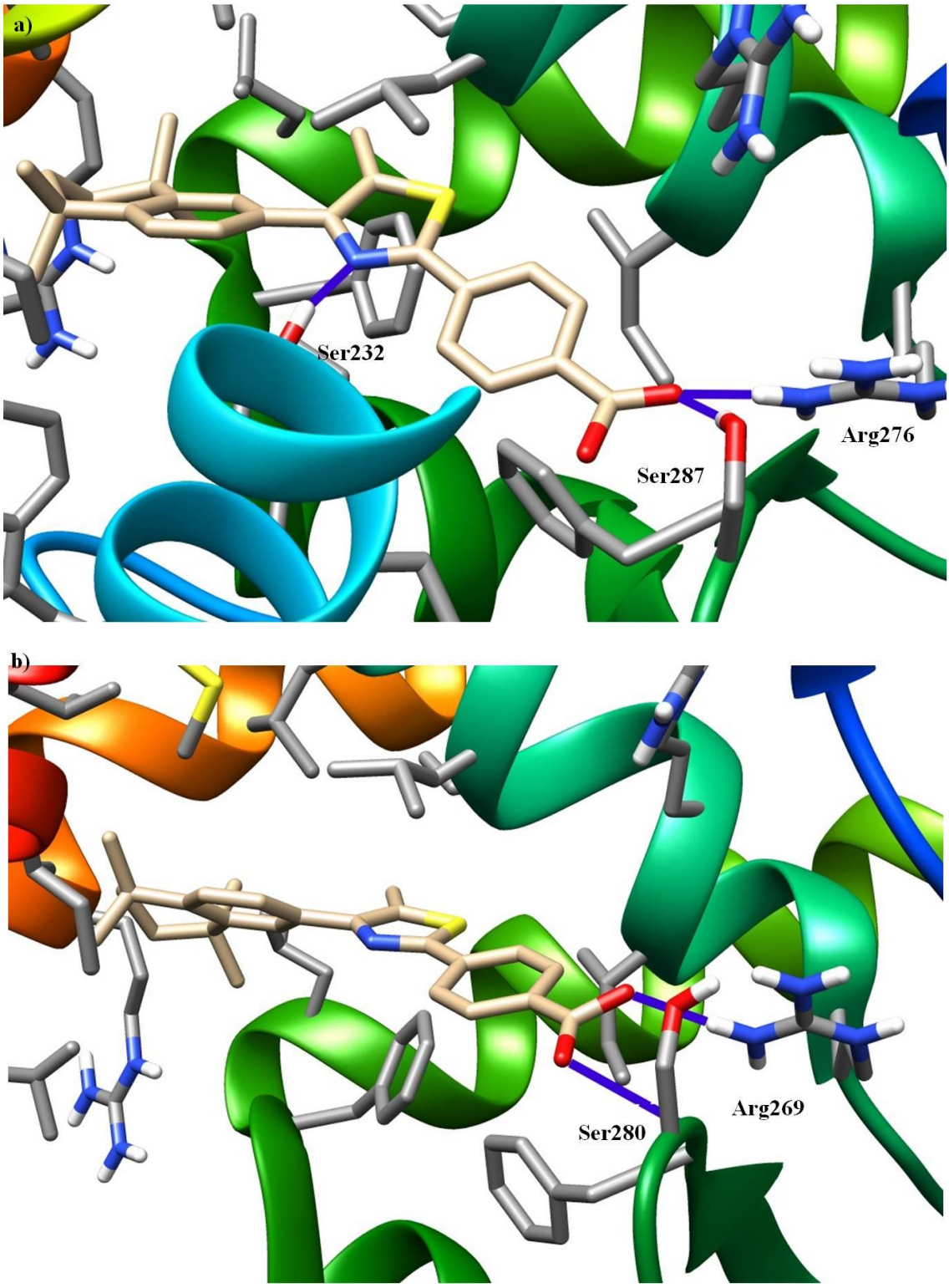

Figure 3.23: Binding mode of interactions of GZ25 derivatives its cognate receptor RARs; a) GZ25 binds to LBD of RAR-α with best fit and fill in the hydrophobic cavity and formed contacts with AF-2 residues Ile270, Arg294 and Leu398 and hydrogen bond with Ser232 similar to Am580; b) GZ25 bind to LBD of RAR-β with best fit with AF-2 residues. GZ25 is the gold colour.

In contrast, GZ25 was suggested to be the best fitting molecule, similar to ATRA in its binding interactions to LBD of all RARs, and with enhanced binding affinity to RAR-α. This was revealed from the modelling due to the formation of an extra hydrogen bond with the Ser232 conserved residue which was discussed before as one of the residues responsible for selectivity of Am580 to RAR-α. Also, the length of GZ25 was suitable for fitting into the hydrophobic space of the LBD of all the RARs and form contacts with all AF-2 residues to induce co-activator recruitment (Fig.3.23). The only exception to this was GZ23 which showed enhanced binding affinity to RAR-β, similar to ATRA, and although it had an ester group replacing the carboxylate acid form and bulk side-chain, but it might fit the LBD of RAR-β and formed the required hydrogen bonds and salt bridge with Ser280 and Arg269. Thed suggest reason for this is the extra groove found in the LBD of RAR-β, which might accommodate the bent structure of GZ23 and the extra bulk side-chain (Fig.3.24).

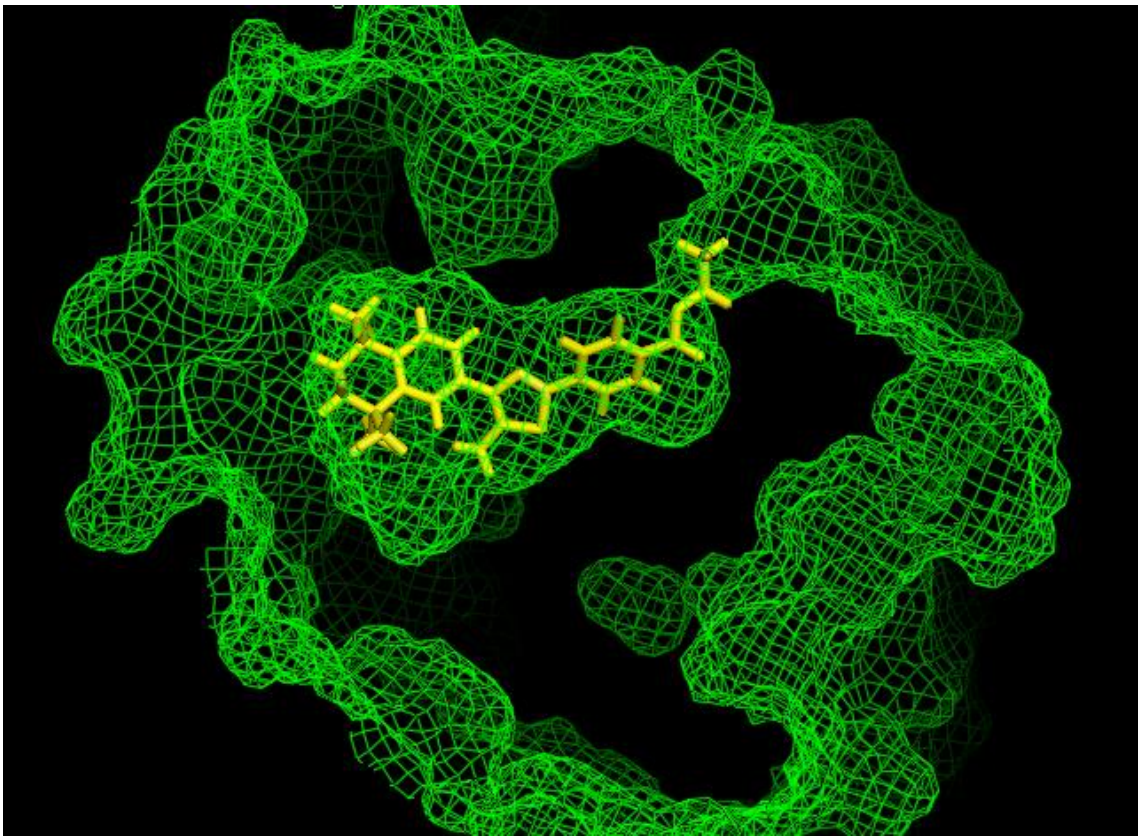

Figure 3.24: GZ23 binding into the LBD of RAR-β showed the extra groove pocket might accommodate the bent structure of GZ23 and the extra bulk of the side-chain. GZ23 is yellow colour.

3.9 COPASI biochemical simulation model

The readout of the Lanthascreen TR-FRET binding assay was based on FRET signal generated from the interaction between a terbium-labelled anti-glutathione-S-transferase (GST) antibody and a fluorescein-labelled co-activator peptide. The RAR ligand-binding domain (LBD) is a GST fusion protein and interaction between the LBD and the fluorescein-labelled co-activator peptide was driven by the binding of ligand to the LBD, and detected by the FRET signal from the terbium/fluorescein interaction when the terbium-labelled anti-GST binds the LBD fusion protein. The output of the assay thus relied on two binding interactions: ligand with LBD, and ligand-bound LBD with the co-activator peptide.

Both interactions may be affected by the fit of the ligand to the binding pocket of the LBD. COPASI[9] was used as a biochemical pathway simulator to help in building a simple model of how the FRET signal output in the assay would vary according to differential changes in the kinetics of the two binding interactions. Reactions were modelled deterministically using mass-action kinetics described by ordinary differential equations (ODE) within COPASI. The component of the model and chart for construction of the model is shown in (Fig.3.25).

This model helped us to assess the effect of different rate constants and varying ligand concentrations on the formation of the final ternary complex that was the read-out from the LanthaScreen TR-FRET assay. The two coupled equilibria given in equation1 were controlled by four rate constants, k_1-k_4. The concentration of the starting species are ligand= 10 µmol. L^{-1} to 0.03 nmol. L^{-1}, RAR= 0.0035 µmol. L^{-1} (defined by the TR-FRET assay formulation), co activator = 30 µmol. L^{-1} (defined by the TR-FRET assay formulation). The Rate constants from analogous ligand-nuclear receptor systems[318,319] were used as the starting point for calculating the EC_{50} (half maximal effective concentration) for ATRA. These rate constants (k_1=0.6 µmol. L^{-1}, k_2=0.1 min^{-1}, k_3=0.014 µmol. L^{-1} and k_4=0.2 min^{-1}) were then altered individually, or together, to model different possible scenarios. The simulation results show that the k_1/k_2 ratio reflected the affinity of the ligands for LBD, which directly affects EC_{50} values, while alteration in k_3/k_4 ratio reflected the affinity of co-activator for the ligand-LBD complex (LR), which changes both the EC_{50} and upper asymptote.

$$L+R \underset{*k_2}{\overset{*k_1}{\rightleftharpoons}} LR \qquad LR+CO.A \underset{*k_4}{\overset{*k_3}{\rightleftharpoons}} LRCO.A \quad \ldots\ldots\ldots\ldots\ldots\ldots\ldots\ldots (\mathbf{1})$$

* Where k_1, k_2 and k_3, k_4 are the rate constants controlling the rate of LR and LR.CO.A complex formation, respectively.

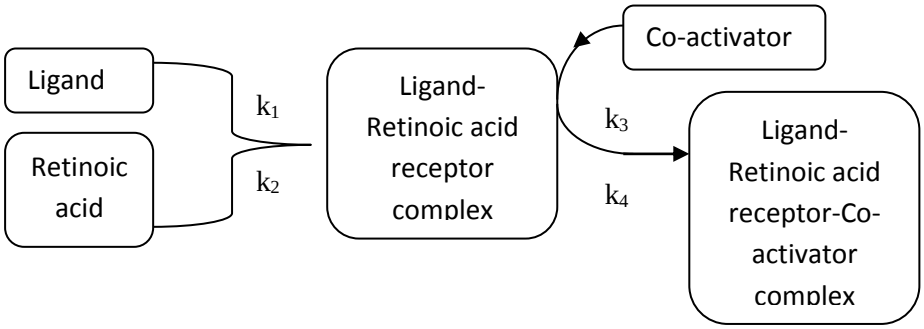

Figure 4.25: Representation of the biochemical COPASI model of the different components of reaction, binding constants and the direction of reaction.

To understand the way by which receptor binding assay data was interpreted, three different retinoids were compared to ATRA,by changing either ligand receptor binding constants or ligand receptor co-activator complex binding constants or changing both (Fig.3.26). Three main conclusions would be made from these examples; 1) Changing ligand receptor affinity alone shifts the EC_{50} but not upper asymptote; 2) changing ligand receptor co-activator affinity alone changed the upper asymptote AND $EC_{50;}$ and 3) changing both in the same direction gave a bigger effect on the $EC_{50,}$ but not on the upper asymptote. Even if the retinoid compounds had EC_{50s} lower than ATRA, but had lower k_3/k_4 ratios, then meant the retinoid compound failed to induce co-activator recruitment and this had been observed in Fig. 3.27.

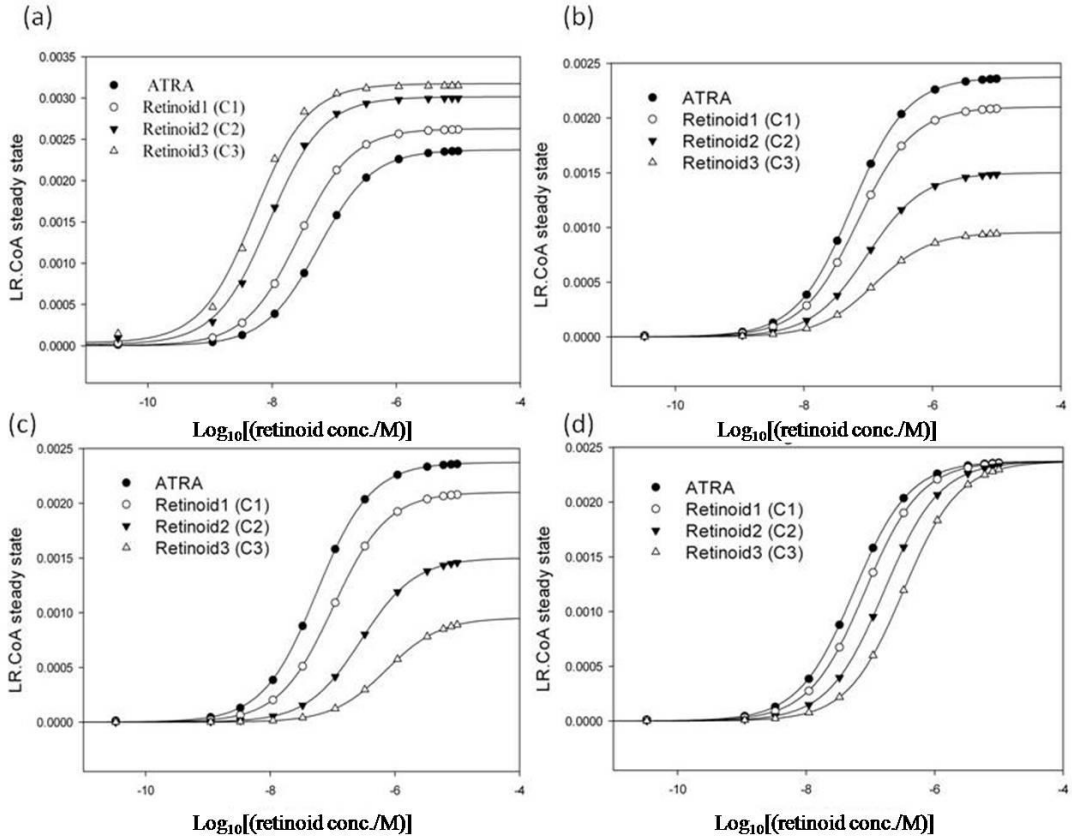

Figure 3.26: Biochemical simulation analysis of TR-FRET assay using COPASI software assumed 3 different retinoid compounds to show the effect of changes in k_1/k_2 and k_3/k_4 values on EC_{50} compared to ATRA withk_1/k_2=6, k_3/k_4= 0.07). (a) High ligand-receptor binding affinity and high induction of co-activator binding (k_1/k_2 = 10, 20, 30 and k_3/k_4 = 0.1, 0.2, 0.3) leads to low EC_{50} values in the range of 9-27 nM for the virtual compounds C1, C2, C3 which are hypothetical ATRA analogues with increasing k_1/k_2 and k_3/k_4 values. Increasing both ratios leads to decreased EC_{50} values and increasing upper asymptotes (b) Lower ligand-receptor binding affinity and co-activation binding (k_1/k_2 = 4, 2, 1 and k_3/k_4 = 0.05, 0.025, 0.0125) leads to higher EC_{50} values in the range of 102-729 nM for the virtual compounds C1, C2, C3 which are hypothetical ATRA analogues with lower k_1/k_2 and k_3/k_4 values. Decreasing both ratios leads to increased EC_{50} values and decreased upper asymptotes (c) No change in ligand-receptor binding affinity and lower co-activation binding (k_1/k_2 = 6 and k_3/k_4 = 0.05, 0.025, 0.0125) leads to higher EC_{50} values in the range of 102-729 nM for the virtual compounds C1, C2, C3 which are hypothetical ATRA analogues with lower k_3/k_4 values. Decreasing k_3/k_4 ratio leads to increased EC_{50} values and decreased upper asymptotes (d) Lower ligand-receptor binding affinity and no change in co-activation binding (k_1/k_2 = 4, 2, 1 and k_3/k_4 = 0.07) leads to higher EC_{50} values in the range of 82.6-324 nM for the virtual compounds C1, C2, C3 which are hypothetical ATRA analogues with lower k_1/k_2 values. Decreasing k_1/k_2 ratio leads to increased EC_{50} values only. Graphs were produced by Sigmaplot based on steady state calculated by COPASI and using the 3-parameter sigmoid curve f = min + (max-min)/(1+10^(logEC_{50}-x)) to fit the output.

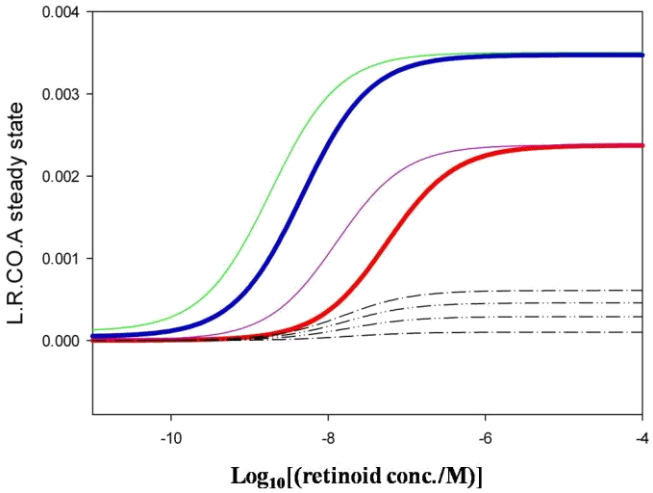

Figure 3.27: Summary of biochemical simulations for the TR-FRET assay using COPASI assuming 7 different retinoid compounds to show the relationships between ligand-receptor-co-activator affinity, EC_{50} and upper asymptote. All these compounds had lower EC_{50} compared to ATRA (red line) with different scenarios, green line (both k_1/k_2 and k_3/k_4 are higher than ATRA), blue line (similar k_1/k_2 and higher k_3/k_4 than ATRA), pink line (higher k_1/k_2 and similar k_3/k_4 to ATRA), black dashed lines (higher k_1/k_2 and lower k_3/k_4 than ATRA). Graphs were produced by Sigmaplot based on steady state calculated by COPASI and using the 3-parameter sigmoid curve f = min + (max-min)/(1+10^(logEC_{50}-x)) to fit the output.

3.9.1 Application of COPASI bio-simulation model on the TR-FRET assay data

COPASI is bio-simulation software that uses mathematical equations to simulate different biochemical reactions. It was important to understand, not only the difference between different retinoids in the measured EC_{50}, but also the ability of formation of ligand-receptor complex which was able to induce co-activator recruitment based on different binding constants k_1, k_2, k_3 and k_4. Fig. 3.14 shows the sigmoid FRET signal of EC19 and EC23 compared to ATRA and it was shown that EC19 came in higher EC_{50} than EC23 and ATRA on RAR-α and RAR-γ. This was accompanied with a corresponding low upper asymptote as well which might suggest that EC19 had both lower k_1/k_2 ratio (lower binding affinity to RAR-α and –γ) and also hada lower k_3/k_4 ratio (not able to induce co-activator recruitment). In contrast, its behaviour on RAR-β was different as it had a relatively lower EC_{50} with also, a lower asymptote which can be explained by its binding to the LBD of RAR-β. However, it might not induce co-activator recruitment in a similar way as EC23. In another example, such as the GZ derivatives in Fig. 3.19, GZ25 showed a lower EC_{50} on all the RARs compared to the other GZ derivatives, suggesting it had the higher binding affinity to the pocket, however, the upper asymptote was the highest on RAR-γ but not on RAR-α and RAR-γ. From these two examples, it can be concluded that the first part of the COPASI assumption about ligand-receptor binding affinity is based on k_1/k_2 ratio which perfectly matches the actual behaviour of measured EC_{50}.

The second part which is related to co-activator recruitment based on the k_3/k_4 ratio was not matched completely with the bio-simulation software observation as it might need further validation by addition of other factors contribute to the dynamic transactivity of RAR binding pocket.

3.10 Conclusion

In silico molecular modelling based on accurate docking algorithms by GOLD software was used to help in explaining possible binding interactions of both natural and novel synthetic retinoids. The binding modes of interactions were correlated with the retinoid binding affinities measured as EC_{50s} by a sensitive TF-FRT assay. This could be useful for suggesting and finding reasons of the differences in the biological activity of these retinoids. In this study, some synthetic retinoids were shown to have a broad range of binding to all RARs such as TTNBP and TTNN. Some were suggested to be selectively bound to one specific type of receptor, such as Am580 for RAR-α and CD437 for RAR-γ. Also, it was noticed that it might be tentatively proposed that RAR-α and -β prefer to recognise a similar ATRA conformation, whereas RAR-γ prefers to recognise a more extended, nearly all *s-trans* conformation. Understanding such factors is likely to be an important matter and one in which much further work is required in order to fully understand molecular interactions of these retinoids. For some synthetic derivatives as EC19 and EC23, changing the orientation of carboxylic group from the *para*-position of EC23 to the *meta*-position as in EC19 massively decreased the binding affinities, due to enforced changes in the orientation of this molecule within the LBD of the different RARs relative to ATRA and EC23.

In other derivatives, such as the GZ derivatives, the length of the molecule and ester form had a great impact on binding interactions and binding affinities, such as the short molecule, GZ18 did not show a proper binding to the active Ser and Arg residues in binding pocket of the RARs. Longer molecules, such as GZ22, had little impact on co-activator recruitment which might be due to the steric clashes with AF-2, while GZ25 was the optimum molecular length and similar to ATRA. The use of calculated chemical structures, receptor binding assays and molecular docking tools was suggested to be useful in order to probe, and hence, understand, the biological activity of certain synthetic retinoids. The ultimate goal is designing more specific synthetic retinoic acid derivatives, as well better understanding the downstream effects.

Chapter IV

Characterization of biological potency of synthetic retinoids for induction of neuronal cell differentiation

Characterization of biological potency of synthetic retinoids for induction of neuronal cell differentiation

4.1 Introduction

4.1.1 Retinoids for cellular differentiation

The induction of differentiation of a wide variety of human cell lines is now playing an important role in the biomedical research field, offering alternative ways of treatment of chronic diseases such as Alzheimer's.[320,321] It also provides an *in vitro* model to study the process of neuronal differentiation of many specific neuron-inducing agents, such as naturally occurring ATRA. ATRA is a developmentally regulated morphogen that has diverse roles in both *in vivo* and *in vitro* systems includes controlling the generation of primary neurons in *Xenopus,*[322] development of the hindbrain,[323] motor neuron specification[324] and limbbud formation in chick embryo.[325] Also, ATRA plays a crucial role for the *in vitro* differentiation of stem cells[326] into a range of various cell types such as neurons,[327] insulin-producing cells,[328] osteoblast[329] cells and epithelialcells.[173] This is not the only role of retinoids, but they also have a practical application in the cancer field, and there have been great advances in this area such as in promylocytic anemia and neuroblastoma. Many studies have shown that retinoids can suppress the process of carcinogenesis *in vivo* and these results are now the basis of current attempts to use retinoids for cancer prevention in humans.[330,331]

The mechanism by which retinoids exert their pleiotropic effects involves a complex signalling pathway because of presence of other main cognate receptors that are responsible for the activation of the transcriptional process. These receptors are called retinoic acid receptors, including the RARs and RXRs,[332] and these act as RXR/RAR heterodimers[333] to the polymorphic acting response elements of RA target genes.[334] These receptors can also initiate a cross-interaction with the other cell surface signaling[335,336] pathways or co-activator/co-repressors[337] to generate additional levels of complexity for the combinatorial pleiotropic effects. The goal of this chapter is to study the biological activity of new synthetic retinoid analogues and evaluate their effects in both stem cells and one cancer cell line. This can be useful to understand the difference between these compounds based on the previous information of modelling and binding assay studies in chapter 3.

4.1.1.1 TERA-2.cl.SP12 teratocarcinoma stem cells

Embryonal carcinoma (EC) is stem cells from germ tumours origin and is considered the malignant counterparts of embryonic stem (ES) cells. EC cells are a useful model to investigate the molecular mechanisms that control differentiation, especially TERA-2.cl.SP12 cell type for neural development which behave in a manner similar to human embryogenesis.[338] TERA-2.cl.SP12 was choosen as a model for cellular differentiation as it's robust model and very sensitive for differentiation by retinoids. ATRA is the active retinoid molecule that has been found to induce neuronal differentiation of these cells depend on the concentration of retinoic acid used and the time of exposure.[339] It was found that in an average of 7 days, TERA-2 cells tend to differentiate into aggregates termed neuro spheres which contain neuro progenitor cells. After 14 - 21 days of growth in suspension, neuro spheres are readily dissociated to release neural cells for growth as adherent monolayers on poly-D-lysine coated surface.[340]

During the induction of differentiation, TERA-2-derived cells rapidly lose their EC stem cell phenotype and acquire different growth characteristics and morphologies. This includes, loss of their expression of cell-surface antigens specific for pluripotent human stem cells (e.g. SSEA3, SSEA4 and TRA-1-60) and simultaneously acquiring a variety of other antigens that commonly appear on the surface of TERA-2 differentiated cells such as A2B5.[335] Notably, the expression of some intracellular markers such as nestin, NeuroD1 and Pax6 are markedly up-regulated after TERA-2-derived cells lose their pluripotency upon cellular differentiation.[340]

4.1.1.2 Neuroblastoma (SHSY5Y)

SH-SY5Y cells contain many characteristics of dopaminergic neurons and have, therefore, been used extensively to study neuron-like behavior in response to neurotoxins in the context of Parkinson disease.[340] These cells can respond well to retinoic acid exposure and differentiate into neuron-like structures, and hence, lose their carcinogenic characteristics.[341] This was interestingly seen through the resistance of un-differentiated cells by retinoic acid to oxidative stress-inducing compounds such as 6-hydroxydopamine, whereas neuronal cells are generally thought to be more susceptible.[232]

During *in vivo* neuro-differentiation of SHSY5Y, various proteins change in their expression levels as a consequence of cellular specialization. Tyrosine hydroxylase (TH) as an example, TH catalyzes the rate-limiting step in the synthesis of dopamine and other catecholamines, namely the conversion of tyrosine to dihydroxy phenylalanine. This makes TH one of the markers of choice for dopaminergic neuron's screening.[342] Also, Synaptophysin, which is an integral membrane glycoprotein, is a marker for synaptic vesicles that store and release classical neurotransmitters. Thus, its presence indicates secretory activity typical for neurons and neuroendocrine cells.[343] As a consequence for over-expression of TH and dopamine; this will stimulate the expression of Dopamine transporter (DAT) as a sodium-dependent dopamine reuptake carrier expressed only in dopaminergic neurons at early stage of SHSY5Y differentiation.[342] In addition, microtubule-associated protein 2 (MAP-2) is an abundant neuronal cytoskeletal phosphoprotein that binds to tubulin and stabilizes microtubules, essential for the development and maintenance of neuronal morphology, cytoskeleton dynamics and organelle trafficking.[344] Once the neuronal cells become mature and have dopamenrgic activity (secretion and uptake of dopamine), this needs MAP-2 as constructive protein to build and stabilize the neuron structure. All these previously mentioned markers are harmony working protein markers that are responsible for functional characterization of differentiated neuroblastoma cells. The next question will be, whether undifferentiated SHSY5Y cells are suitable for studying the early stage effects of natural and synthetic retinoids to be able to use for treatment of neuroblastoma and other neurodegenerative diseases.

In this chapter, a comparison was considered between the long-term effects on TERA-2.cl.SP12 and the early stage differentiation of SHSY5Y. This work was to assist with screening the biological effects of a large number of new synthetic retinoids that have been prepared in the search for more efficient compounds than ATRA. This screening was based mainly on any obvious morphology changes in both cell lines, quantitative changes in gene expression level that can be correlated to the differentiation products, and hence, the nature and maturity of resulting cell types. Terminally differentiated, functional neurons are a potentially valuable resource for screening other new synthetic retinoids, testing their toxicity and to use these cells as a potential source of transplantable material to correct neurodegenerative diseases.

4.2 Flow cytometry analysis of cell surface markers in TERA-2.cl.SP12 stem cell

The primary characteristic feature of TERA-2.cl.SP12 cells is their ability to maintain pluripotent behaviour of stem cells for unlimited cell passages. Several markers are characteristic for human pluripotent stem cells and these proved to be useful tools to monitor their undifferentiated phenotype. In our study, we showed that the expression of a set of important cell surface pluripotent markers such as SSEA-3 and TERA-1-60 are useful for monitoring of cell pluripotency during retinoid exposure. In addition, the neural differentiation cell marker A2B5 was an early marker that can track the stage at which differentiation occurs. The level of expression of these markers depends on the exposure time and the concentration used of these retinoid compounds.

Flow cytometry analysis of these markers was the tool of choice for the quantitative assessment for the biological potency of these retinoid analogues. The control un-treated cultures, or those treated with DMSO solvent, showed high levels of SSEA-3 and TRA-1-60 (60-70% of cells expressed these markers), which might suggest that the cells retained their un-differentiated state. The 2D plots in fig. 4.6 show thresholds determining the numbers of positively expressing cells were set against the negative control P3X antibody. Control cells treated with DMSO were gated in the lower right-hand side of the quadrant plot. This indicated that cells expressed high level of SSEA-3 and the same pattern was seen with the TRA-1-60 marker. In contrast, less than 20% of control cells expressed A2B5 and so, cells were gated in the lower left-hand side of 2D plot and histogram of A2B5 (Fig. 4.6). Cultures treated with 10 µM of ATRA or EC23, EC19 or their methyl esters for 7 days showed a significant reduction in expression of these pluripotent markers especially with ATRA and EC23 as SSEA-3 (less than 20%) and TRA-1-60 (less than 50%), (Fig. 4.7a and Fig.4.7b). This was revealed in fig. 4.6 as few gated cells expressed SSEA-3 or TRA-1-60 is in the lower right-hand side of the 2D plot.

A2B5 is another cell surface marker over-expressed as a consequence of cellular differentiation. The cultures treated with ATRA or EC23 showed the highest expression levels of A2B5 and so, gated cells were shown to be in the right-hand side of the 2D plot and histogram. This might suggest that cells exposed to ATRA and EC23 were induced to differentiate in away similar to neuronal fate (Fig. 4.7).

EC19 treated cultures showed lower expression levels of both SSEA-3 but not TRA-1-60 however; the expression level of A2B5 was remained not over-expressed. This might suggest there was specific way of cellular changes upon treatment with EC19 but the effect is different than ATRA or EC23. Only the methyl ester of EC23 was able to show higher biological potency similar to EC23 (Fig. 4.7).

For the second class of thiazole synthetic retinoids, GZ25 was the only one that displayed a profile similar to ATRA. SSEA-3 and TRA-1-60 levels were down-regulated to less than 10 % and 20 % respectively compared to control cultures. Additionally, the A2B5 level was up-regulated more than 80% compared to 60% for ATRA. This might be releated to the molecule's length of GZ25 is close to ATRA as discussed before in chapter 3. The other GZ derivatives, such as GZ18, GZ22 and GZ23 showed reduction in the level of SSEA-3 expression. This might be explained ad aconsequence of the cellular loss for its pluripotent character compared to control cultures but there was not higher increase in A2B5 as with ATRA or GZ25 cultures. Additionally, the ethyl ester analogues of GZ24 did not show any significant improvement of the biological activity than their parent acid form (Fig. 4.8).

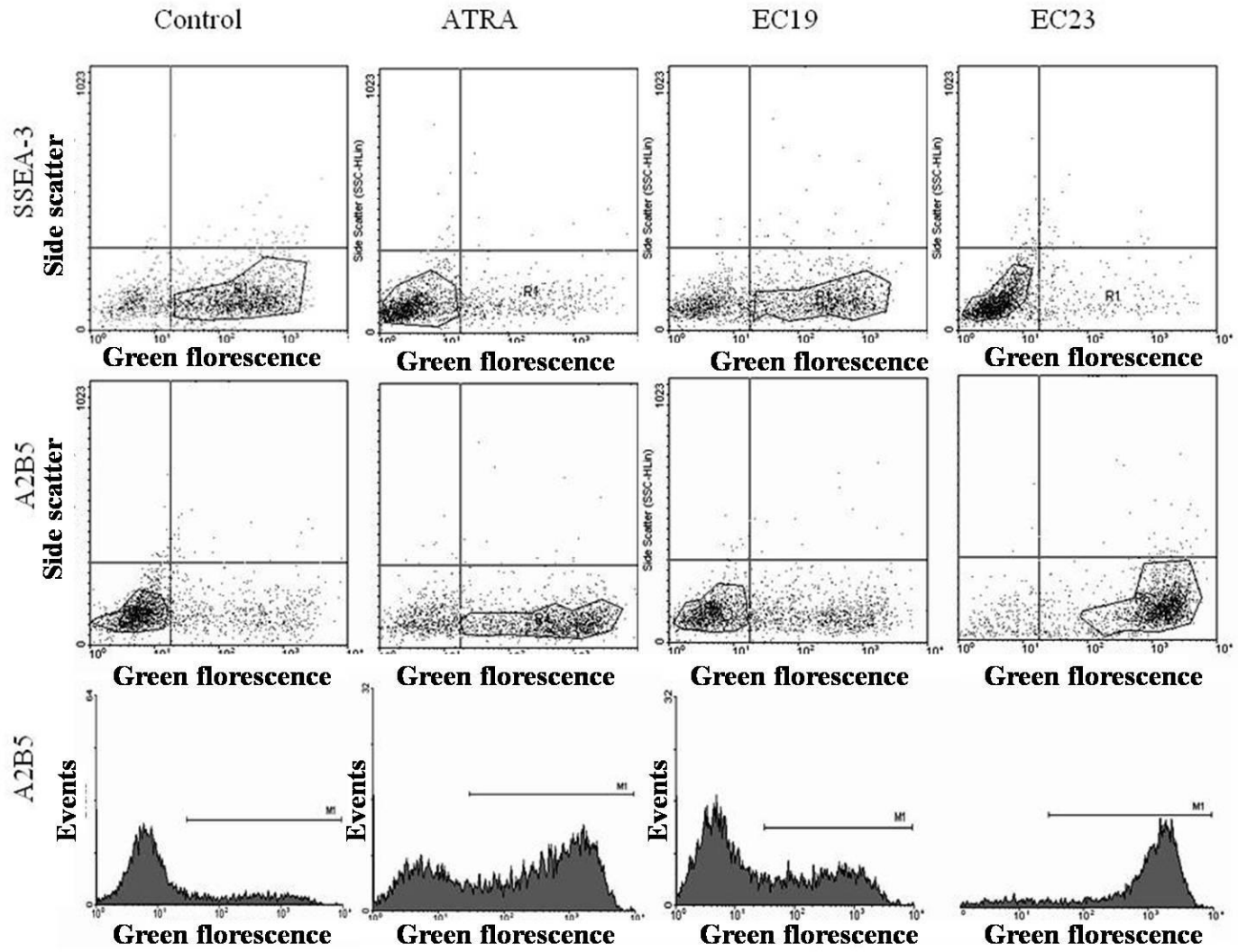

Figure 4.6: Flow cytometry analysis of TERA-2.cl.SP12 cells treated with 10µM ATRA, EC19 and EC23 after 7days, A) 2D plots and histogram representation of gated cells expressing SSEA-3 and A2B5 after treatment with retinoids. Graphs were analysed and drawn using WinMDI2.9. Results are presented as n=3.

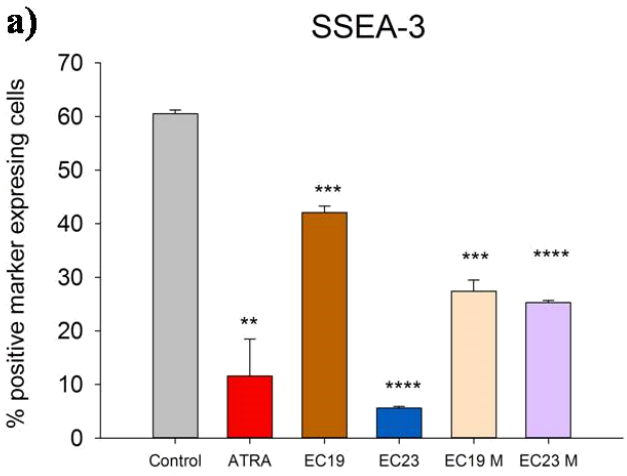

Retinoid compound	Probability	P value	Significant?
ATRA	P < 0.05	0.0021	Yes **
EC19	P < 0.05	0.0002	Yes***
EC23	P < 0.05	< 0.0001	Yes ****
EC19 M	P < 0.05	0.0001	Yes ***
EC23 M	P < 0.05	< 0.0001	Yes ****

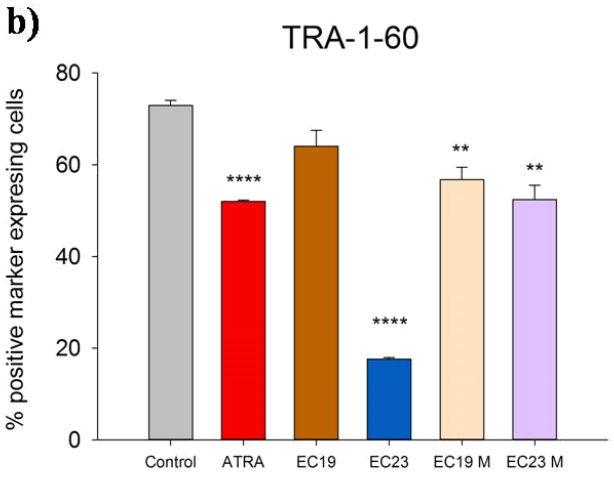

Retinoid compound	Probability	P value	Significant?
ATRA	P < 0.05	< 0.0001	Yes ****
EC19	P < 0.05	0.0708	NS
EC23	P < 0.05	< 0.0001	Yes ****
EC19 M	P < 0.05	0.0048	Yes **
EC23 M	P < 0.05	0.0033	Yes **

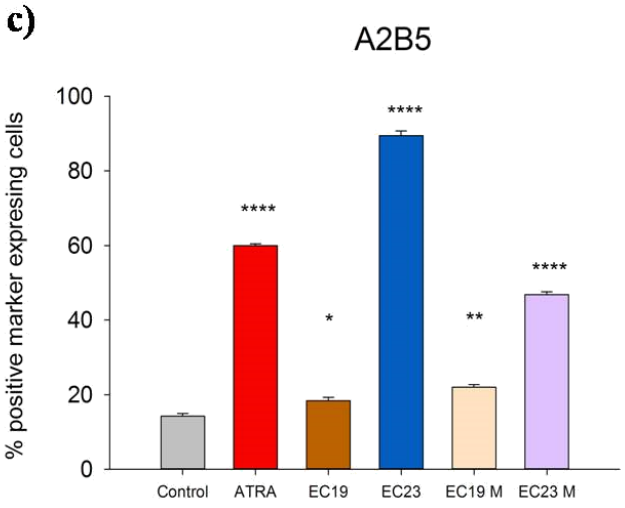

Retinoid compound	Probability	P value	Significant?
ATRA	P < 0.05	< 0.0001	Yes ****
EC19	P < 0.05	0.0243	Yes *
EC23	P < 0.05	< 0.0001	Yes ****
EC19 M	P < 0.05	0.0020	Yes **
EC23 M	P < 0.05	< 0.0001	Yes ****

Figure 4.7: Flow cytometry analysis of stem cell surface markers a) SSEA-3; b) TRA-1-60; and c) early stage neuronal marker A2B5. Control TERA-2.cl.SP12 cultures represent cells treated with 1% DMSO. TERA-2.cl.SP12 cultures were treated with 10 µM of different synthetic retinoids and analysis was done 7 days after exposure. All retinoids showed significant reduction in level of SSEA-3 and TRA-1-60 which might suggest cellular change. However, the level of A2B5 as neuronal marker compared to control was markedly increased with ATRA, EC23 and EC23 methyl ester. Results are presented as ± SEM, n = 3 and un-paired t-test followed by F-test analysis (test of varience) was used for analysis at ($p < 0.05$) in comparison to control cells treated with 0.1% DMSO.

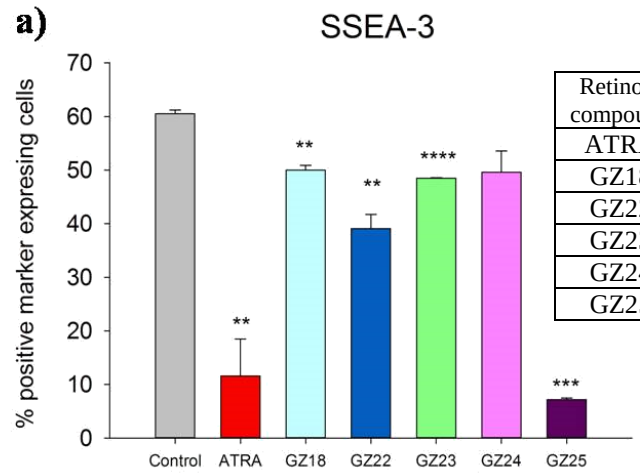

Retinoid compound	Probability	P value	Significant?
ATRA	P < 0.05	0.0021	Yes **
GZ18	P < 0.05	0.0026	Yes**
GZ22	P < 0.05	0.0015	Yes **
GZ23	P < 0.05	< 0.0001	Yes ****
GZ24	P < 0.05	0.0550	NS
GZ25	P < 0.05	< 0.0001	Yes ****

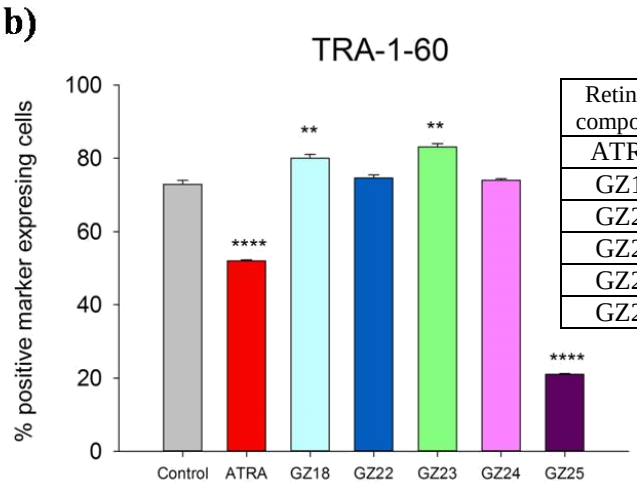

Retinoid compound	Probability	P value	Significant?
ATRA	P < 0.05	< 0.0001	Yes ****
GZ18	P < 0.05	0.0088	Yes**
GZ22	P < 0.05	0.2750	NS
GZ23	P < 0.05	0.0016	Yes **
GZ24	P < 0.05	0.3726	NS
GZ25	P < 0.05	< 0.0001	Yes ****

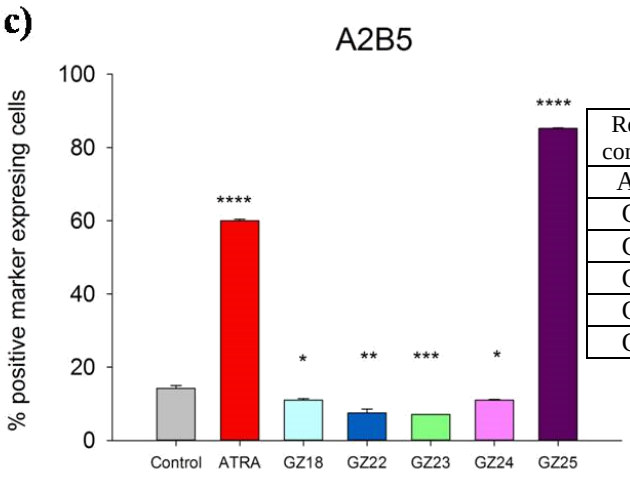

Retinoid compound	Probability	P value	Significant?
ATRA	P < 0.05	< 0.0001	Yes ****
GZ18	P < 0.05	0.0237	Yes *
GZ22	P < 0.05	0.0069	Yes **
GZ23	P < 0.05	0.0008	Yes ***
GZ24	P < 0.05	0.0170	Yes *
GZ25	P < 0.05	< 0.0001	Yes ****

Figure 4.8: Flow cytometry analysis of stem cell surface markers a) SSEA-3; b) TRA-1-60; and c) early stage neuronal marker A2B5. Control TERA-2.cl.SP12 cultures represent cells treated with 1% DMSO. Other cultures were treated with 10 µM of different thiazole synthetic retinoids and analysis was done 7 days after exposure. All retinoids showed significant reduction in level of SSEA-3 and TRA-1-60 which might suggest cellular change. However, the level of A2B5 as neuronal marker compared to control was markedly increased with ATRA, GZ25 and GZ23. Results are presented as ± SEM, n = 3 and un-paired t-test followed by F-test analysis (test of varience) was used for analysis at ($p < 0.05$) in comparison to control cells treated with 0.1% DMSO.

4.3 Immunocytochemistry analysis of TERA-2.cl.SP12

Immunocytochemistry is an important tool for visualization of some specific neuronal proteins as an indication for the induction of cellular differentiation. There are many extra- and intra-cellular proteins that are secreted upon induction of differentiation in TERA-2.cl.SP12 with specific markers for early stages; A2B5 and TUJ-1. It is convenient to compare the changes in the level of expression of these proteins with the time of exposure to retinoids. This helps in the evaluation for the potency of these molecules and to observe the stage at which differentiation occurs. On the other hand, it is also useful to investigate the non-neuronal cell types such as epithelial cell which is usually associated with differentiation of weaker acting retinoids. CK-8 is one of these markers, which is known for its specific secretion with many types of epithelial cell[345] and hence, it can be used for evaluation of retinoids' activity. Primary antibodies for TUJ-1 and CK-8 were used in this study after treatment of cells with 10 µM of different synthetic retinoids for 7, 14 and 21 days.

In Fig. 4.9, the control DMSO cultures showed low levels of expression for both neuronal markers A2B5 and TUJ-1 and epithelial marker CK-8, which might suggest that the cells were in un-differentiated pluripotent state. It was also noted that the low level of TUJ-1 in the control cells mainly coincided in the cytoplasm. Upon exposure of cells to ATRA and EC23 for 7 days, the levels of A2B5 (around the cell surface) and TUJ-1 (in the cytoplasm) were increased as an early stage of neuronal differentiation with the minimum level of CK-8. After 14 and 21 days, the level of TUJ-1 expression continued to increase with obvious formation of more mature, differentiated neuronal cells. TUJ-1 was localized in both cytoplasm and diffused also into the peripherals of neurons. Moreover, it was found that levels of CK-8 with ATRA, and EC23 treated cultures was kept low, such as most of the cells differentiated into the neuronal cell types. In contrast, EC19 did not show any increase in either the level of A2B5 or TUJ-1 after 7 days, with a minimum level of TUJ-1 positive cells even after 21 days as a late stage of exposure. However, CK-8 level increased in EC19 treated cultures after three weeks, as an indication of the epithelial fate of this cellular differentiation (Fig. 4.9).

Additionally, the biological potency of the thiazole retinoid derivatives was investigated and GZ25 was the only synthetic analogue that showed similar behaviour as ATRA and EC23. Higher levels of A2B5 and TUJ-1 were observed with GZ25 treated cultures (stained both extracellular and intracellular content) after 7 days with formation of neuron aggregates expressing TUJ-1 in peripherals (Fig. 4.10). GZ18 and GZ22 expressed minimum level of TUJ-1 up to 21 days. This might suggest the lower potency of these analogues compared to GZ25 to induce neuronal differentiation (fig 4.10). The CK-8 level was also kept low with GZ25 treated cultures even after 21 days while, GZ18 and GZ222 showed an increase in number of positive stained cells for CK-8 after 14 days and enhanced after 21 days (Fig. 4.11). This can reveal that GZ25 was potent enough to induce most of TERA-2.cl.SP12 cells into mature neurons in a way similar to ATRA and EC23 while GZ18 and GZ22 are intermediate compounds that induce a mixture of different cell types, of much lower number of neurons and higher number of epithelial cells. In conclusion, this accurate cell marker counting helped in evaluating the biological potency of these synthetic retinoids, compared to the levels of secretion of A2B5 and TUJ-1, which was also useful to differentiate the behaviour between retinoids as ATRA, EC23 and GZ25 from the other EC19, GZ18, GZ22, GZ23 and GZ24.

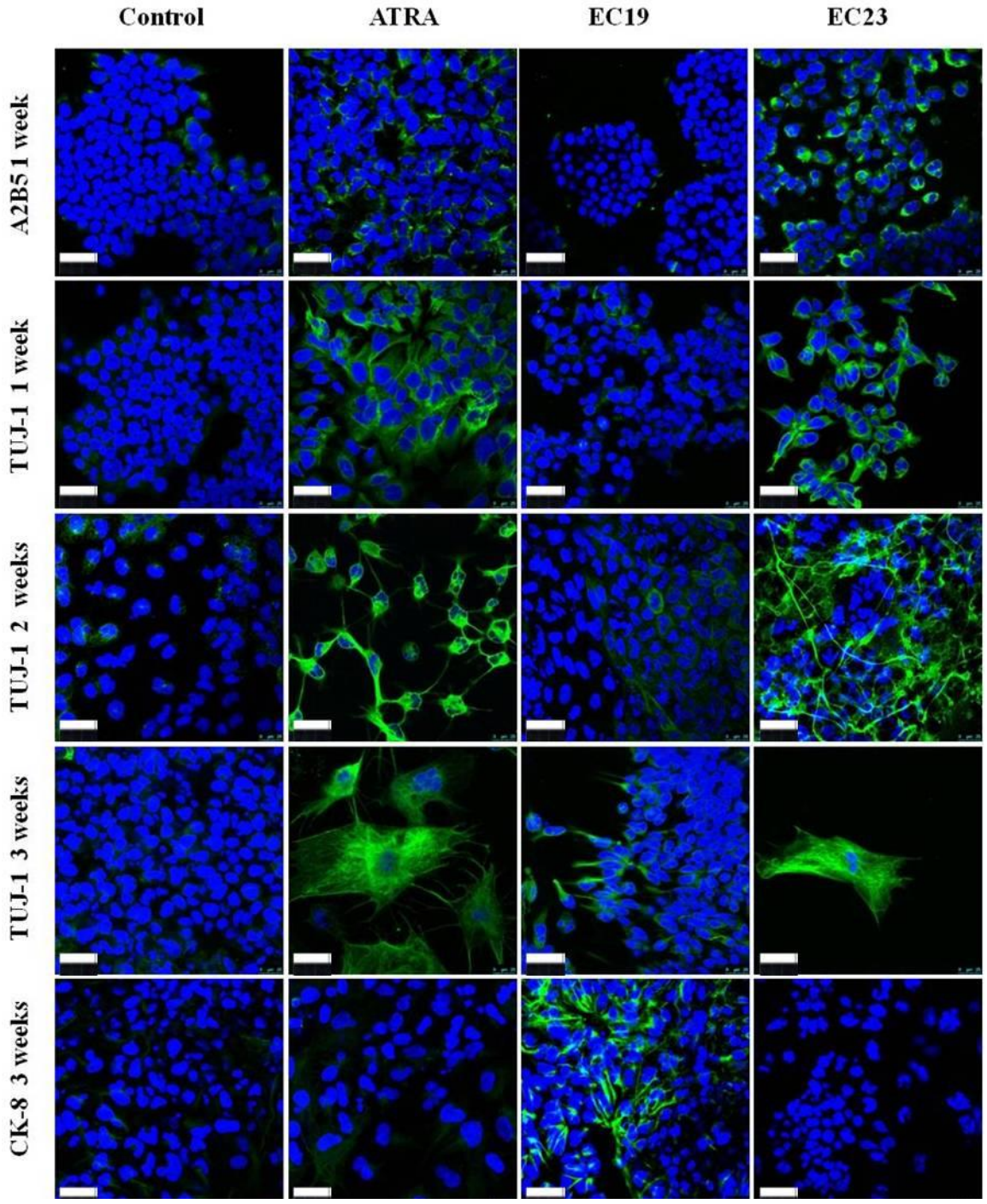

Figure 4.9: Expression of neuronal (A2B5 and TUJ-1) and epithelial (CK-8) proteins in TERA-2.cl.SP12 treated with 10 µM of ATRA and synthetic analogues; EC19 and EC23 for 7, 14 and 21 days. Cells were fixed by 4% PFA and permeabilised using 1% Triton-X-100, stained with primary antibodies for A2B5, TUJ-1 and CK-8 followed by green fluorescent IgM secondary antibody (for A2B5) and IgG Alexafluor488 (for TUJ-1 and CK-8). High levels of A2B5 and TUJ-1 were observed only with culture treated with ATRA and EC23 with the minimum level of CK-8 expression. EC19 showed high level of CK-8 expression after 21 days as a result of epithelial cell differentiation with the low level of TUJ-1. Control cells treated with DMSO did not show any expression of either marker. Scale bar; 25 µm.

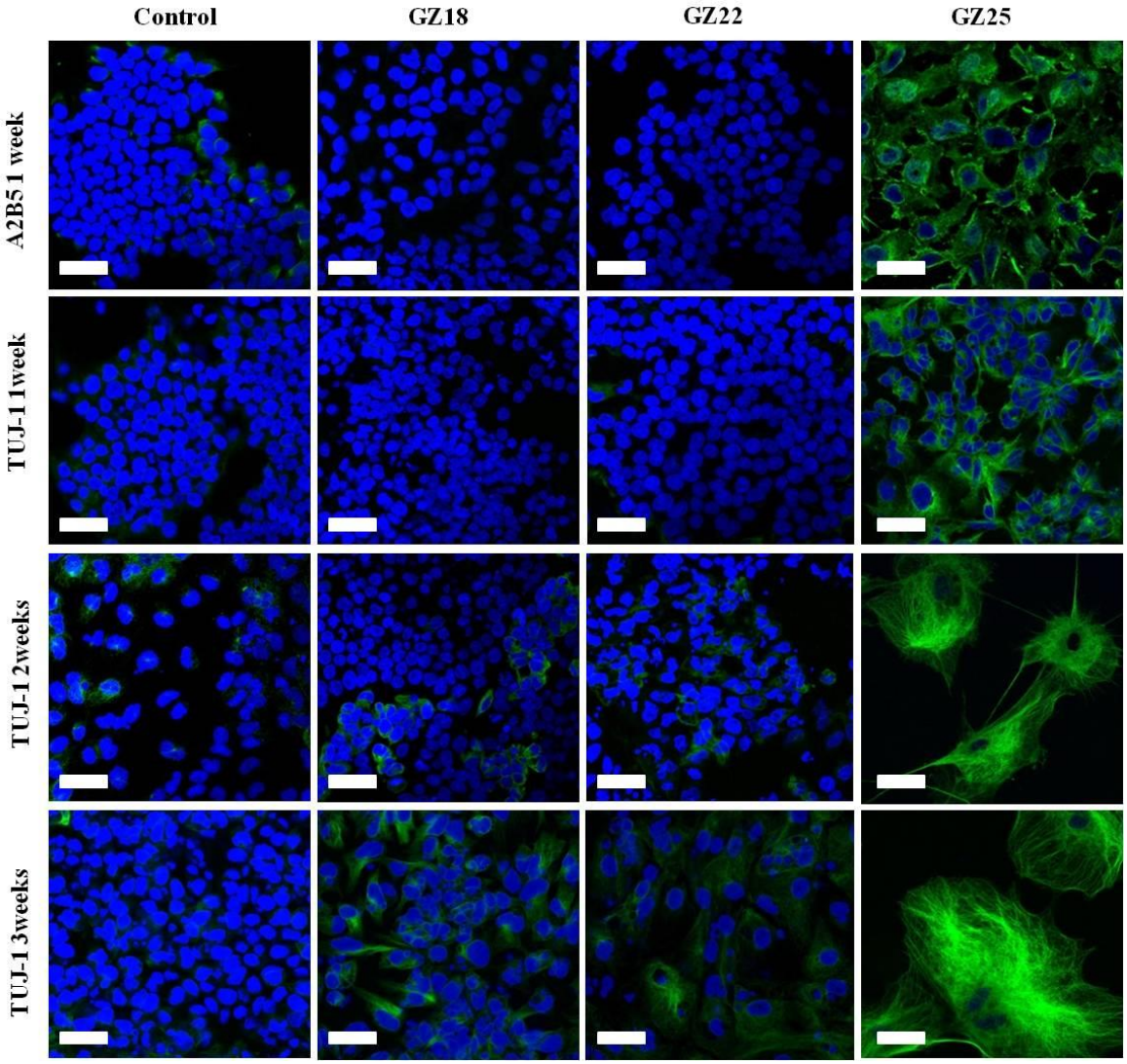

Figure 4.10: TERA-2.cl.Sp12 cells treated with 10 µM of thiazole synthetic analogues for 7, 14 and 21 days. GZ25 showed high levels of A2B5 and TUJ-1 within time of exposure and formation of neurons rosette like structure stained with TUJ-1. GZ18 and GZ22 showed high level of TUJ-1 only after 21 days as indication of late stage biological potency. Control cells treated with DMSO did not show any expression of either marker. Scale bar; 25 µm.

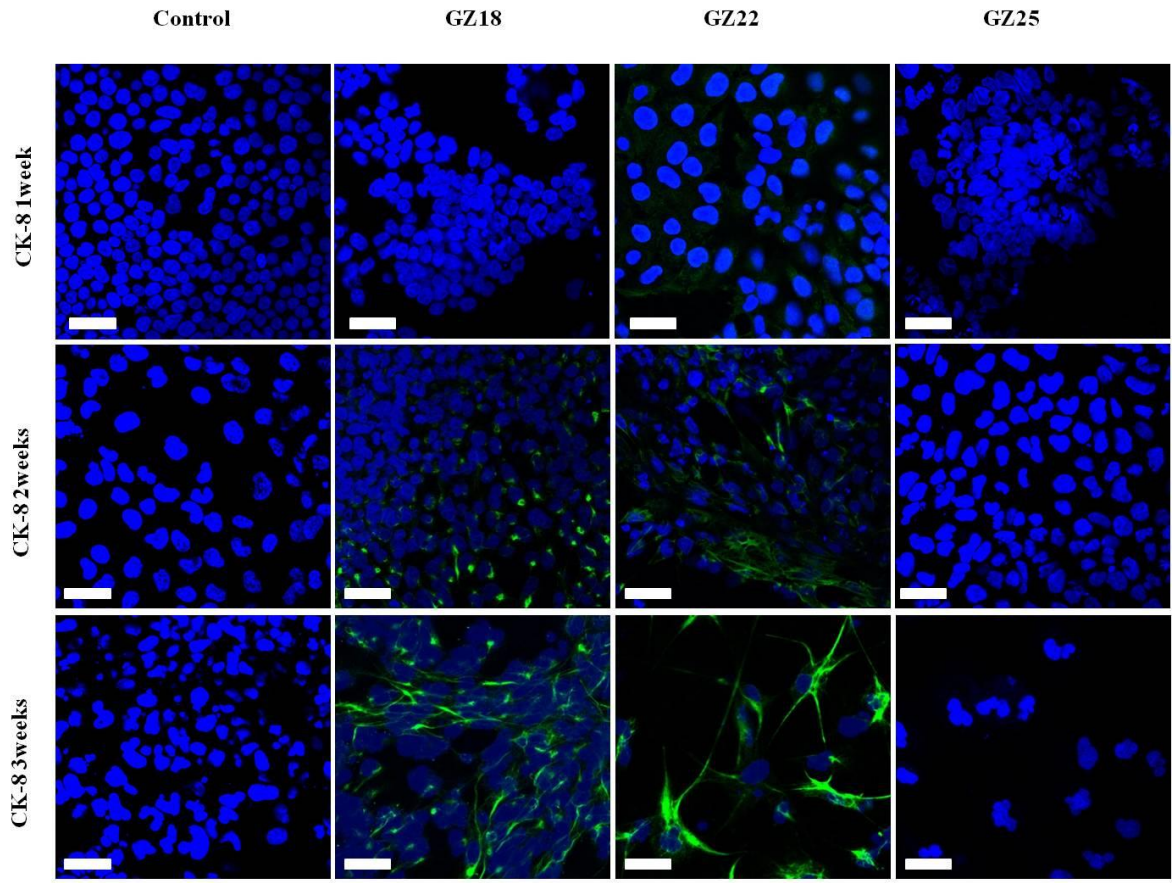

Figure 4.11: TERA-2.cl.Sp12 cells treated with 10 µM of thiazole synthetic analogues for 7, 14 and 21 days. GZ25 did not show any increase in level of CK-8 similar to control culture treated with DMSO solvent. While, GZ18 and GZ22 showed high levels of CK-8 after 14 days and increased after 21 days as a fate of epithelial cell differentiation. Scale bar; 25 µm.

4.4 Induction of cellular differentiation - gene expression analysis

The gene expression levels in TERA-2.cl.SP12 cells and SHSY5Y after retinoid treatment were analyzed using real time PCR. This can help in elucidating the biological activity and potency of ATRA and other new synthetic retinoids for induction of differentiation of both stem cells and cancer cells. During *in vivo* neuro-differentiation using retinoic acid, various genes and proteins change in their expression as a consequence of cellular specialization, In SH-SY-SY neuroblastoma cells, the expression of RAR-β is rapidly induced in response to ATRA. RAR-β gene has been relatively well characterized,[346] and its induction may be important for the retinoic acid-mediated expression of other "late" genes so that, it may be a valuable marker for evaluating the action of different synthetic retinoic acid derivatives.

Besides RAR-β gene investigation, this study investigated the expression of CYP26A1 since it is the major enzyme responsible for the metabolic breakdown of ATRA and might be some other retinoids. CYP26 is a type of cytochrome P450 group of RA-metabolizing enzymes (producing inactive hydroxylated products; 4-hydroxy-RA and 4-oxo-RA) that may explain specific cellular effects on stability of retinoids. Hence, the induction of cellular differentiation for some synthetic retinoids, the SHSY5Y neuroblastoma cell line was studied in parallel to the cellular metabolism. This can test the reliability of this model of SHSY5Y for evaluation of the biological potency of any other synthetic retinoid analogues. To address this question, a comparison was done to test the biological activity of EC19, EC23 and methyl esters analogues as synthetic retinoids in TERA-2.cl.SP12 stem cells using different neuronal markers in undifferentiated and differentiated SHSY5Y neuroblastoma cells. This helped in further investigation of the biological potency of other synthetic analogues, such as GZ derivatives, for late and early stages of induction of cellular differentiation.

Fig. 4.12 shows the difference in gene expression level of NeuroD1 (Fig. 4.12a) after TERA-2.cl.SP12 cells treated with 10 μM of different retinoids for 3, 5 and 7 days. NeuroD1 was up-regulated 5 days after treatment not with ATRA but with EC23, methyl esters of EC19, EC23 and increased significantly, after 7 days. EC19 treated cultures showed increase in level of NeuroD1 after 5 days however, it declined after 7 days compared to ATRA and EC23 treated cells. On the other hand, PAX6 was another gene responded later after NeuroD1 with over expression 10 times more in EC23 treated cultures more than ATRA. EC19 treated cultures did not show any significant up-regulation of PAX6 after 5 days and only slightly increased after 7 days (Fig. 4.12b). Interestingly, the PAX6 gene was over-expressed 100 times more in EC23 treated cultures than NeuroD1 gene. It can be suggested on the basis that the promoter region of PAX6 gene is completely under the control of retinoic acid receptor especially RAR-β, and hence, can explain the difference in magnitude and time onset. EC19 methyl ester also came in the same lower biological order of magnitude for up-regulation of PAX6 as matched with previous biological assays.

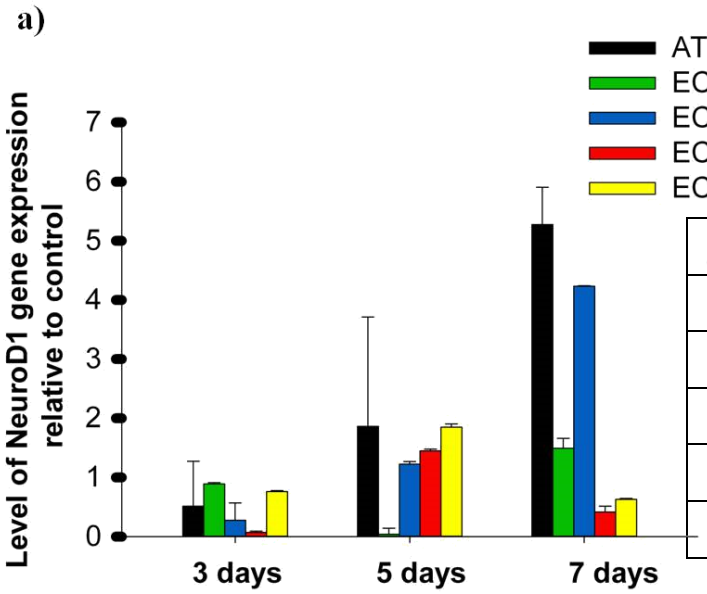

Retinoid compound	Probability	P value 5 days	P value 7 days
ATRA	P < 0.05	0.5372 NS	0.0086 Yes **
EC19	P < 0.05	0.0011 Yes **	0.0233 Yes *
EC23	P < 0.05	0.0339 Yes *	0.0002 Yes ***
EC19 M	P < 0.05	0.0001 Yes ***	0.0265 Yes ***
EC23 M	P < 0.05	0.0001 Yes ***	0.0065 Yes **

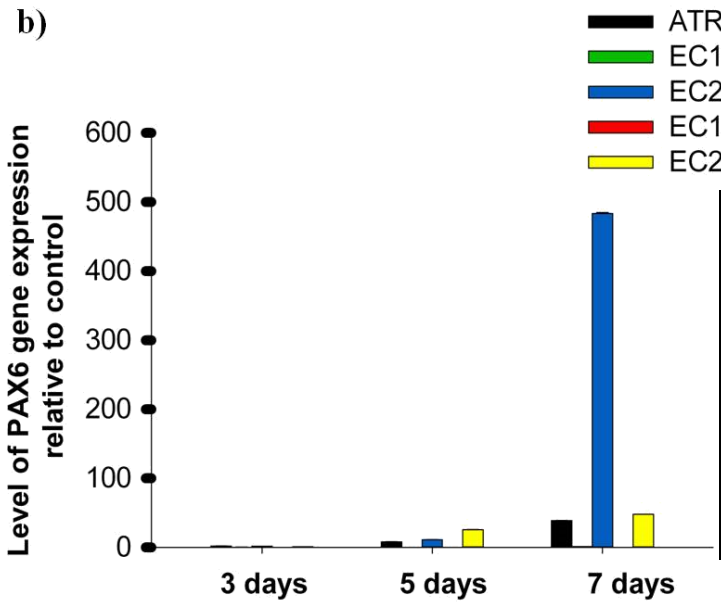

Retinoid compound	Probability	P value 5 days	P value 7 days
ATRA	P < 0.05	0.0001 Yes ****	0.0001 Yes ***
EC19	P < 0.05	0.3774 NS	0.0364 Yes *
EC23	P < 0.05	0.0001 Yes ****	0.0001 Yes ****
EC19 M	P < 0.05	0.0027 Yes **	0.2180 NS
EC23 M	P < 0.05	0.0001 Yes ****	0.0001 Yes ***

Figure 4.12: Gene expression analysis using qPCR for; a) NeuroD1 and; b) PAX6 in TERA-2.cl.SP12 treated with ATRA, EC19, EC23 and their methyl ester analogues. TERA2.cl.SP12 cells were exposed to 10 μM of different synthetic derivatives for 3, 5 and 7 days. Level of NeuroD1 increased after 7 days with cultures treated in ATRA, EC23 compared to EC19, while the cultures of methyl ester analogues of EC19 and EC23 showed decline in the level of NeuroD1 after 7 days. PAX6 gene level increased with ATRA, EC23 and EC23 methyl ester after 3, 5 and 7 days, while other analogues did not show increasing in its level. Gene profile quantification is relative to the level of gene expression in TERA2.cl.SP12 cultured with 0.1% DMSO solvent for 7 days. Data are normalized to both control 0.1% DMSO and the internal reference gene (GADPH). Statistical analysis was done by paired t-test followed by F-test (test of varience) at ($P<0.05$) in comparison to cultures treated with retinoids for 3 days. Data represent mean ± SEM, n = 3.

Gene expression analysis of RAR-α, -β and –γ on the SHSY5Y neuroblastoma cell line treated with retinoids showed different responses over a scale time of 2 to 12 hours and at concentrations of 10, 1, 0.1, 0.01 and 0.001 µM. The RAR-β gene expression level increased over time with concentration of 10 µM for both ATRA and EC23 treated cells. Based on the previous information in introduction chapter, this could suggest an early signs of cellular differentiation in neuroblastoma cells within 2 hours and the induction reached to the maximal peak after 6 – 8 hours and then declined (Fig. 4.12a). Also, it was noticed that EC23 showed higher gene expression levels than ATRA treated cells all over the time scale with 3 times magnitude higher after 6 hours of treatment. EC19 did not show any significant increase in gene expression of RAR-β at any time point of treatment with 10 µM concentration. By testing different concentrations of these retinoids within 6 hours treatment, EC23 showed the same concentration dependent effect on expression of RAR-β compared to ATRA while EC19 showed higher gene expression of RAR-β at concentrations of 0.1 and 0.01 µM (Fig. 4.13b). EC19 methyl ester did not show any significant over-expression of RAR-β over the different time scale while, EC23 methyl ester showed significant increase in RAR-β gene expression relative to control cells treated with DMSO within early treatment (2 hours) but this was declined gradually by time until 12 hours treatment (Fig. 4.13a). All these information can reveal that RAR- β can be a useful marker as early sign for cellular differentiaon in SHSY5Y neuroblastoma cells. Also, RAR- β can be used as a marker to show the difference in biological activity between the different synthetic retinoids such as EC19 and EC23.

RAR-α and RAR-γ genes showed different levels of expression in SHSY5Y cells upon treatment with 10 µM of different retinoids over time than in RAR-β gene expression. Only, ATRA increased the expression of RAR-α gene level compared to control cells after 4 hours and over-expressed by time within 12 hours with ATRA showed higher level of RAR-α compared to EC19 and EC23. While, EC23 showed an increase in RAR-α gene expression by 12 hours treatment, however, its level was not higher than ATRA (Fig. 4.14b). RAR–γ gene level increased significantly after 12 hours treatment in all retinoid treated cells however ATRA showed higher level than EC23 and EC19. It also noted that ATRA induced high level of RAR-γ gene expression compared to RAR-α after 12 hours (5 fold higher).

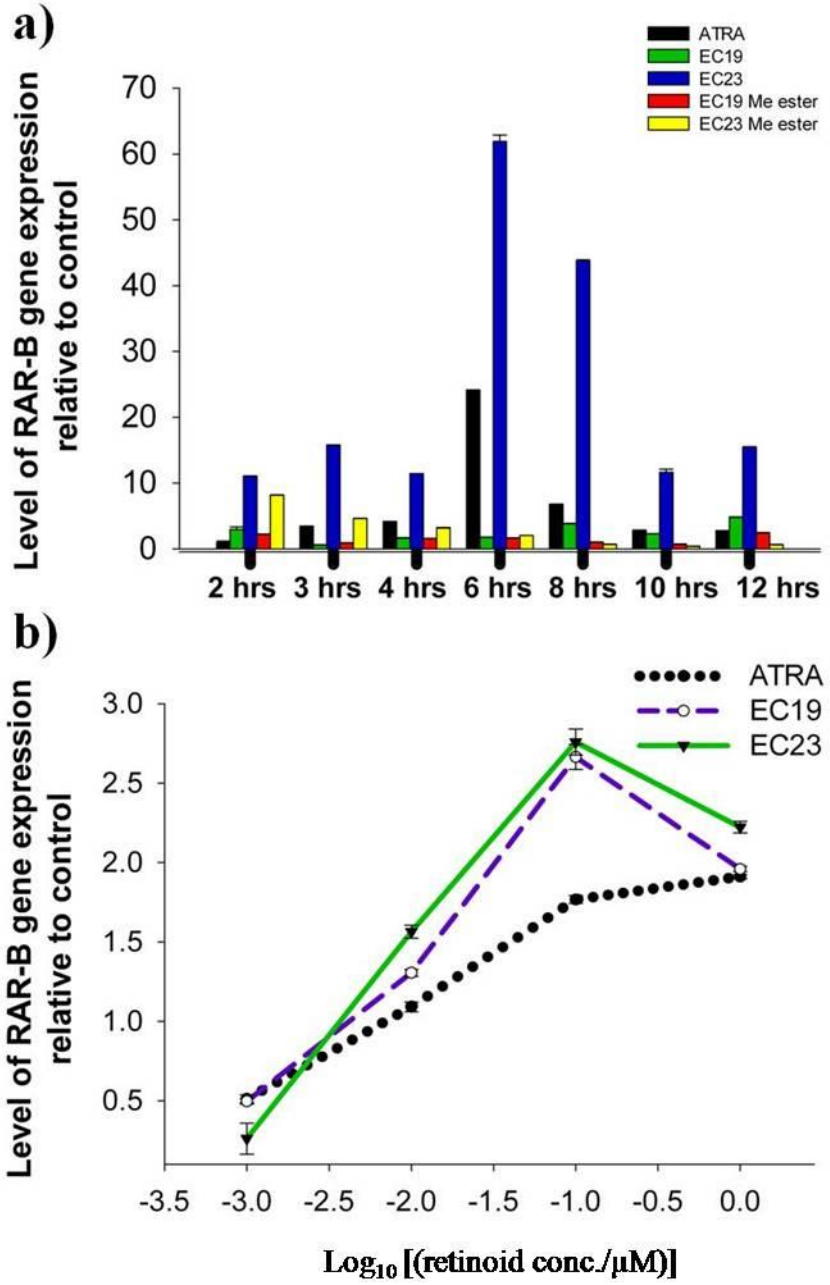

Figure 4.13: Real time PCR analysis of RAR-β gene expression in SHSY5Y cells treated with ATRA, EC19, EC23 and methyl ester analogues; a) SHSY5Y cells were exposed to 10µM of different synthetic derivatives for up to 12 hrs. ATRA and EC23 showed higher expression level compared to EC19 and other analogues over time scale with maximal peak after 6 hrs; b) SHSY5Y cells were exposed to 1, 0.1, 0.01 and 0.001µM of different synthetic derivatives for up to 8 hrs. EC23 induced higher level of RAR-β over different concentration scales. EC19 showed also slightly higher level of expression of RAR-β compared to ATRA at 0.1 and 0.01 µM concentrations. Gene profilequantification is relative to the level of gene expression in SHSY5Ycultured with DMSO solvent for 12 hrs. Data were normalized to both control 0.1% DMSO and the internal reference gene (β-actin). Data represent mean ± SEM, n = 3.

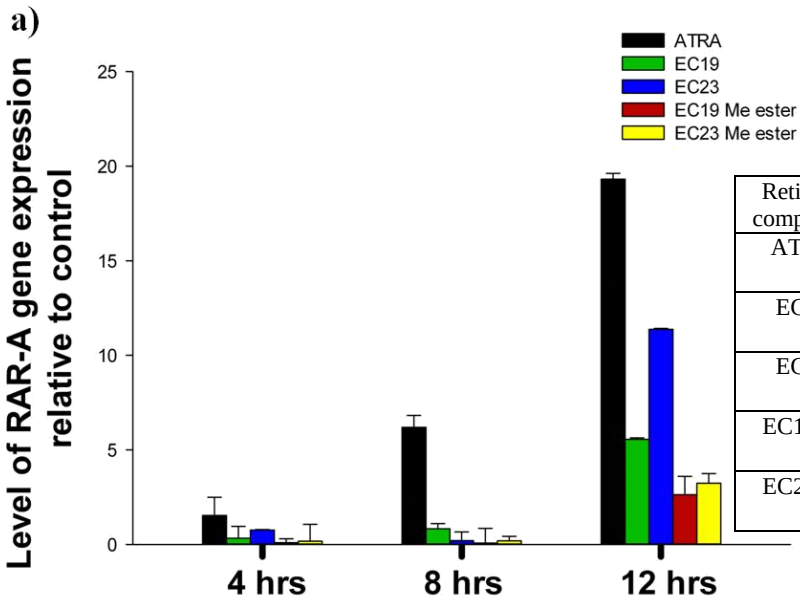

Retinoid compound	Probability	P value 8 hours	P value 12 hours
ATRA	P < 0.05	0.0151 Yes *	0.0001 Yes ***
EC19	P < 0.05	0.5023 NS	0.0011 Yes *
EC23	P < 0.05	0.2905 NS	0.034 Yes *
EC19 M	P < 0.05	0.9811 NS	0.0649 NS
EC23 M	P < 0.05	0.9898 NS	0.0415 Yes *

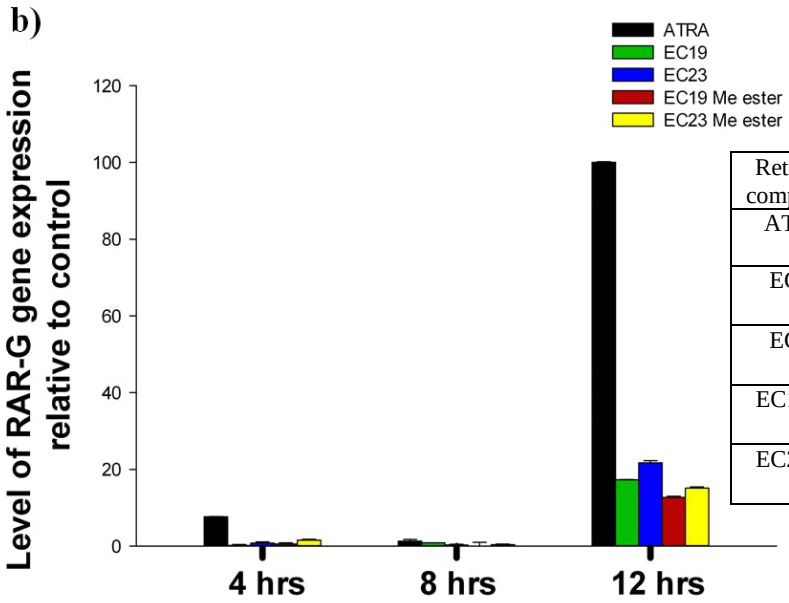

Retinoid compound	Probability	P value 8 hours	P value 12 hours
ATRA	P < 0.05	0.0001 Yes ****	0.0001 Yes ***
EC19	P < 0.05	0.0309 Yes*	0.01 Yes **
EC23	P < 0.05	0.2250 NS	0.0001 Yes ****
EC19 M	P < 0.05	0.6961 NS	0.0001 Yes ****
EC23 M	P < 0.05	0.0271 Yes *	0.0001 Yes ***

Figure 4.14: Real time PCR analysis of SHSY5Y cells which exposed to 10μM of ATRA, EC19, EC23 and methyl ester analogues for up to 12 hrs and gene expression analysis of; a) RAR-α gene and; b) RAR-γ gene. ATRA and EC23 showed slight increase in expression level of RAR-α after 4 hrs which increased significantly after 12 hrs compared to EC19 and other synthetic analogues. ATRA treated cells showed higher level of RAR-α expression than EC23. Also, ATRA and EC23 showed higher expression level of RAR-γ after 12 hrs compared to EC19 and other analogues after 12 hrs. ATRA treated cells showed 5 times higher level of RAR-γ than EC23. Gene profile quantification is relative to the level of gene expression in SHSY5Y cultured with 0.1% DMSO solvent for 4, 8 and 12 hours. Data are normalized to both control 0.1% DMSO and the internal reference gene (β-actin). Statistical analysis was done by paired t-test followed by F-test (test of varience) at ($P<0.05$) in comparison to cultures treated with retinoids for 3 days. Data represent mean ± SEM, n = 3.

The stability of these molecules in SHSY5Y cells were also investigated through the gene expression levels of CYP26A1. It was shown that 10 µM of ATRA induced quickly over-expression of CYP26A1 within 2 hours of cell uptake with the same maximal peak of gene expression after 6 hours and then, it declined gradually compared to the non-significant expression of EC19, EC23 and methyl ester analogues treated cultures (Fig.4.15a). Additionally, CYP26A1 was highly induced by ATRA over different concentration scales compared to EC19 and EC23 treated cultures (Fig. 4.15b). It is also noted, although CYP26A1 declined after 6 hours of ATRA treated cells but it was still higher than control cells treated with DMSO or even EC19 and EC23 treated cells. This may indicate that the process of cellular metabolism for ATRA is a continuous process occurs parallel to the process of induction of cellular differentiation and responsible for decline in RAR-β gene expression after 6 hours.

The data gene expression data was presented here for ATRA, EC19 and EC23 using different concentrations and time scales showed that the both TERA-2.cl.SP12 cells as relatively long time scale and SHSY5Y cells as early stage seems to useful for biological evaluation of the synthetic retinoids. Both models can demonstarte the difference between the biological potency between these synthetic analogues in term of induction of genes responsible for cellular differentiation. Moreover, ATRA was reliable for cellular metabolism through the induction of CYP26A1 gene while, the EC19 and EC23 seem to be resistant for cellular metabolism.

The second target was to evaluate the biological potency of other synthetic analogues; the GZ derivatives with special focusing on GZ18 and GZ25 compared to ATRA. It was found that GZ18 and GZ25 was able to induce higher gene expression level of NeuroD1 compared to ATRA with maximal peak up to 5 days of TERA-2.cl.SP12 cell treatment. However, this declined gradually after 7 days. Two notes are observed here, first, GZ25 was consistently potent for induction of NeuroD1 gene expression compared to GZ18 over 7 days. Second, the level of NeuroD1 gene expression gradually increased with ATRA treated cells up to 7 days, compared to the level of expression of either GZ18 or GZ25 treated cells (Fig. 4.16a). For PAX6 gene expression analysis, the level of PAX6 was slightly shown to be increased after 3 days of ATRA or GZ25 treatment with a significant increase after 7 days. Interestingly, GZ25 treated cells showed a higher induction of PAX6 gene level (5 fold higher) than ATRA treated cells (Fig. 4.16b).

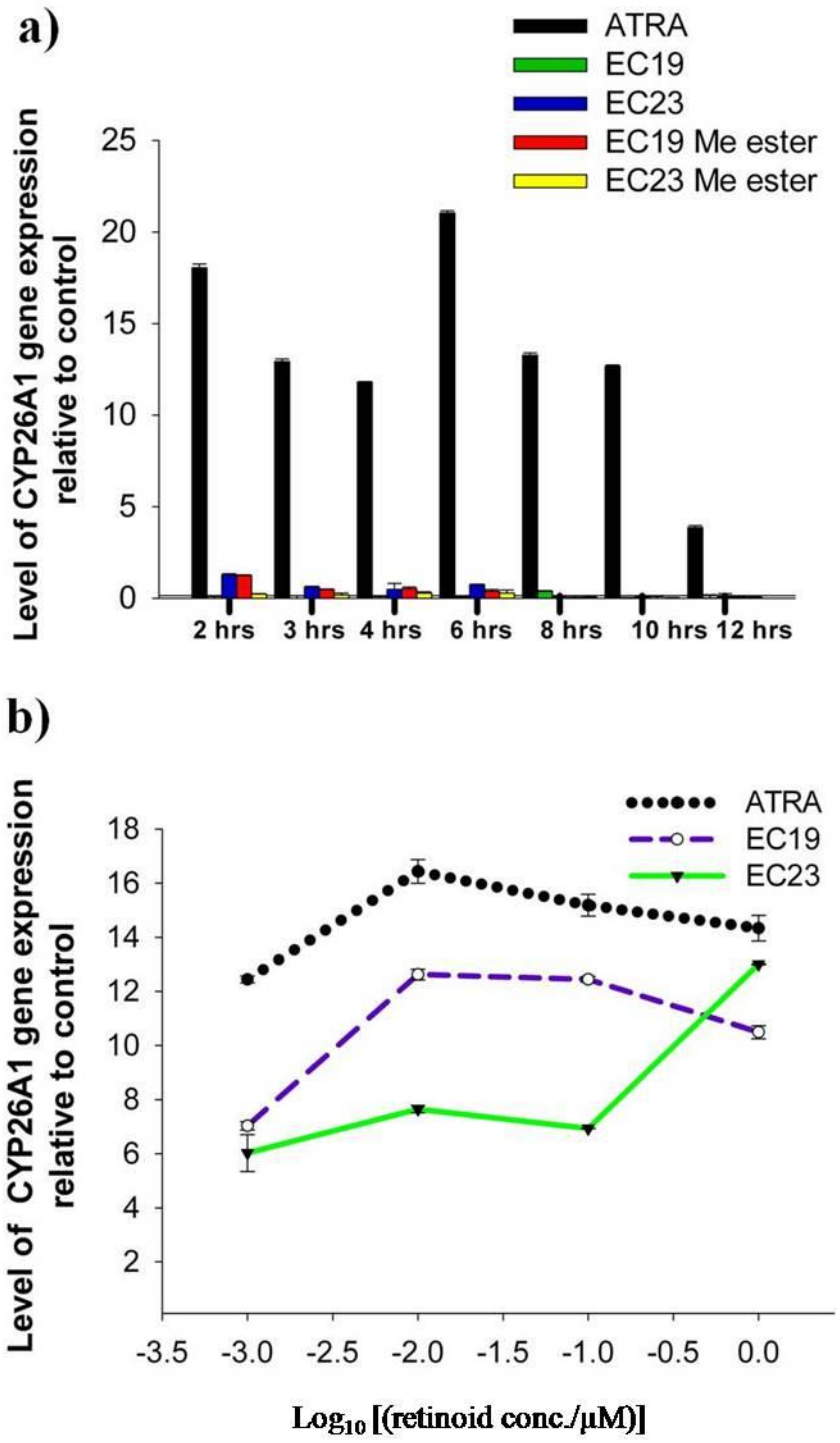

Figure 4.15: Real time PCR analysis of CYP26A1 gene expression in SHSY5Y cells treated with ATRA, EC19, EC23 and methyl ester analogues; a) SHSY5Y cells were exposed to 10 μM of different synthetic derivatives for up to 12 hours. Only ATRA showed higher expression level compared to EC23 and EC19 and other analogues over time scale with maximal peak after 6 hrs; b) SHSY5Y cells were exposed to 1, 0.1, 0.01 and 0.001 μM of different synthetic derivatives for up to 8 hours. Also ATRA induced higher level of CYP26A1 over different concentration scales. EC19 showed also slightly higher level of expression of CYP26A1 compared to ATRA at 0.001, 0.01 and 0.1 μM concentrations. Gene profile quantification is relative to the level of gene expression in SHSY5Y cultured with DMSO solvent for 12 hrs. Data are normalized to both control 0.1% DMSO and the internal reference gene (β-actin). Data represent mean ± SEM, n = 3.

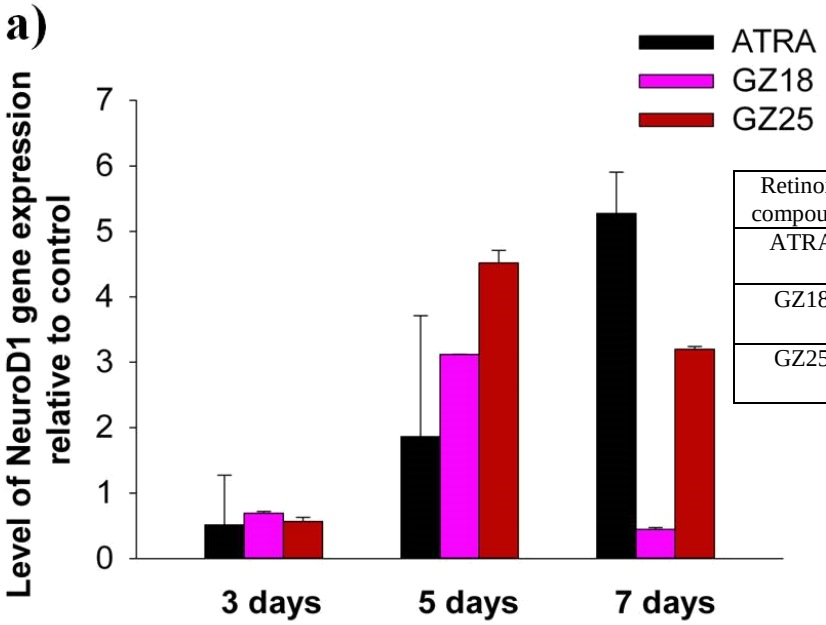

Retinoid compound	Probability	P value 5 days	P value 7 days
ATRA	P < 0.05	0.5372 NS	0.0086 Yes **
GZ18	P < 0.05	0.0001 Yes ****	0.0029 Yes **
GZ25	P < 0.05	0.0001 Yes ****	0.0001 Yes ****

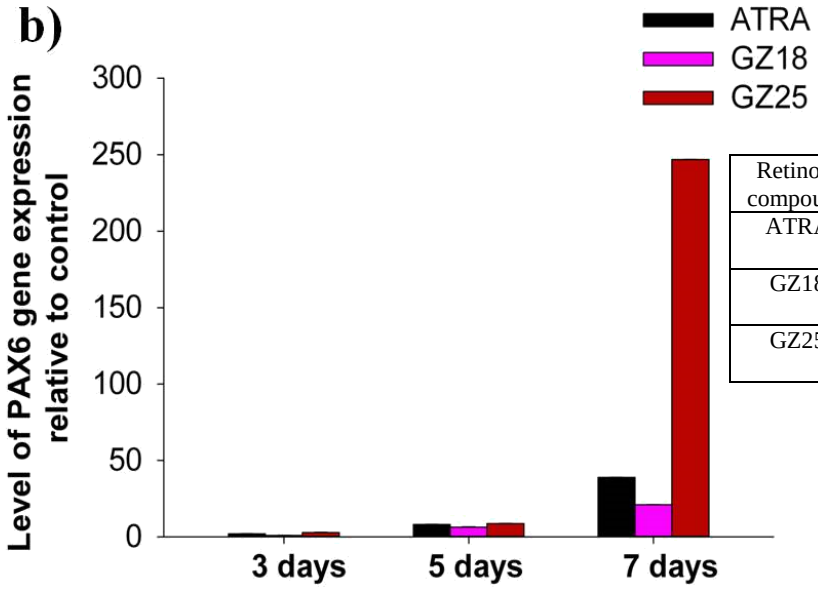

Retinoid compound	Probability	P value 5 days	P value 7 days
ATRA	P < 0.05	0.0001 Yes ****	0.0001 Yes ***
GZ18	P < 0.05	0.0001 Yes ****	0.0001 Yes ****
GZ25	P < 0.05	0.0001 Yes ****	0.0001 Yes ****

Figure 4.16: Gene expression analysis of; a) NeuroD1 and; b) PAX6 in TERA-2.cl.SP12 treated with ATRA, GZ18 and GZ25. TERA2.cl.SP12 cells were exposed to 10µM of different synthetic derivatives for 3, 5 and 7 days. Level of NeuroD1 increased significantly by time treatment with ATRA while GZ18 and GZ25 showed maximal peak of induction after 5 days and then decreased gradually. GZ25 showed markedly higher level of expression of NeuroD1 over time scale compared to GZ18. PAX6 gene level increased with ATRA and GZ25 with maximal peak at late stage (after 7 days) of induction of cellular differentiation. GZ18 showed also increase in PAX6 gene level after 7 days however, it was lower than either ATRA or GZ25. Gene profile quantification is relative to the level of gene expression in TERA2.cl.SP12 cultured with 0.1% DMSO solvent for 3, 5 and 7 days. Data are normalized to both control 0.1% DMSO and the internal reference gene (GADPH). Statistical analysis was done by paired t-test followed by F-test (test of varience) at ($P<0.05$) in comparison to cultures treated with retinoids for 3 days. Data represent mean ± SEM, n = 3.

For RAR-β gene expression analysis, biological screening of all the GZ derivatives showed that GZ25 had the higher potency for induction of RAR-β at very early stages (2 – 3 hours) compared to ATRA and other GZ analogues with maximum peak after 6 hours. However, ATRA had the higher induction potency for RAR-β gene level, compared to GZ25 and the other GZ derivatives after 6 hours. RAR-β gene level decreased gradually after 6 hours but was higher for ATRA and GZ25 treated cells compared to other GZ analogues (Fig. 4.17a). GZ18 only showed a low variable gene expression level of RAR-β along the whole time scale of culture treatment and the RAR-β level was lower than that ATRA and GZ25, and only the significant increase was observed after 12 hours. This might suggest the late response of this compound due to lower potency and this matched with delayed onset of induction for TUJ-1 markers which was observed previousely. At lower concentration scales, GZ25 was still significantly higher than GZ18 or ATRA for the induction of RAR-β gene expression (Fig. 4.17b).

For RAR-α, GZ18 and GZ25 showed a gradual increase in the level of gene expression with a maximal peak after 12 hours of SHSY5Y treatment. However, ATRA induced a higher level of RAR-α gene expression compared to GZ18 and GZ25 cultures. Furthermore, GZ25 and GZ18 showed comparably similar levels of gene expression after 12 hours, with slight enhancement with GZ18 treated cultures (Fig. 4.18a). In addition, ATRA showed a higher level of RAR-γ expression after 12 hours of neuroblastoma treated cells compared to GZ18 and GZ25. However, GZ25 showed, a markedly higher level of expression compared to GZ18 (Fig. 4.18b). GZ25 was shown to be reliable for cellular metabolism similar to ATRA as it induced high gene expression level of CYP26A1 significantly over different time scales compared to other GZ analogues. Also, the maximal peak of CYP26A1 gene induction came earlier than that for ATRA (3 hours compared to 6 hours for ATRA) (Fig. 4.19a). This also was confirmed at lower concentration levels, GZ25 was able to induce more gene expression levels of CYP26A1 compared to either ATRA or GZ18 at a concentration of 0.001 μM.

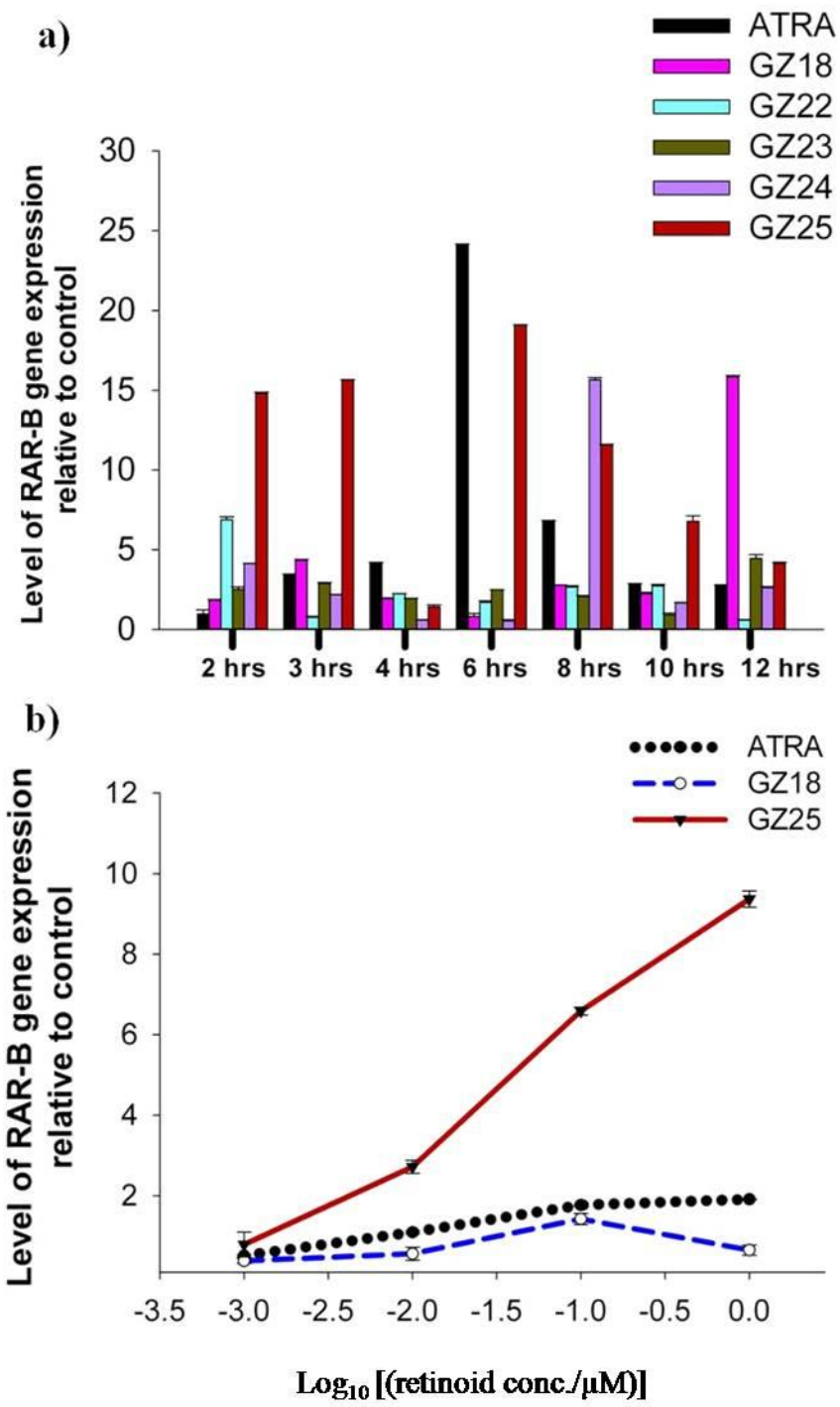

Figure 4.17: Real time PCR analysis of RAR-β gene expression in SHSY5Y cells treated with ATRA, and different GZ derivatives (GZ18, GZ22, GZ23, GZ24 and GZ25); a) SHSY5Y cells were exposed to 10 µM of different synthetic derivatives for up to 12 hours. ATRA and GZ25 showed higher expression level compared to other analogues over time scale with maximal peak after 6 hrs however, ATRA showed higher level of expression at 6 hrs than GZ25; b) SHSY5Y cells were exposed to 1, 0.1, 0.01 and 0.001 µM of ATRA, GZ18 and GZ25 for up to 8 hours. GZ25 induced higher level of RAR-β over different concentration scales, this was followed by ATRA as a second order of magnitude. GZ18 showed the lowest level of expression of RAR-β compared to GZ25 and ATRA. Data are normalized to both control 0.1% DMSO and the internal reference gene (β-actin) Data represent mean ± SEM, n = 3.

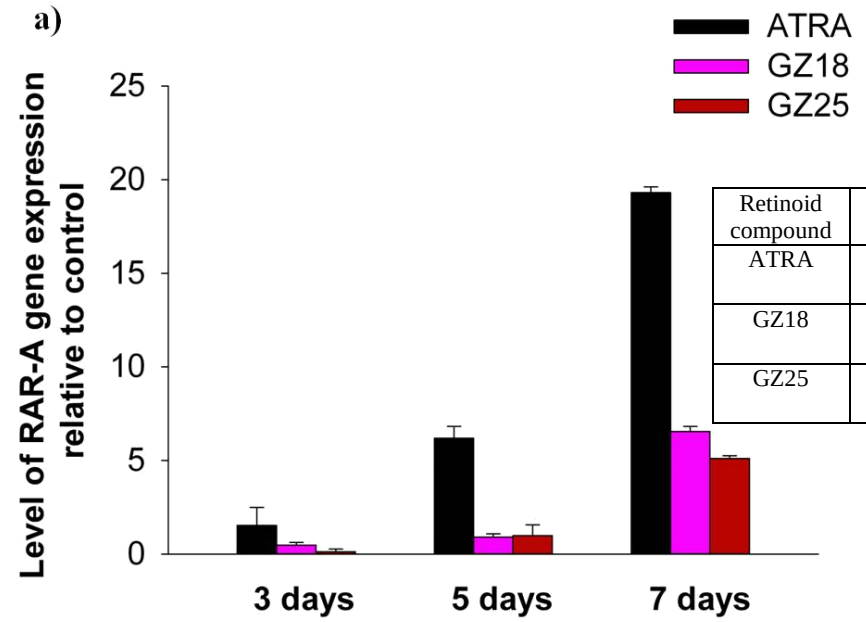

Retinoid compound	Probability	P value 5 days	P value 7 days
ATRA	P < 0.05	0.0151 Yes *	0.0001 Yes ***
GZ18	P < 0.05	0.1346 NS	0.0001 Yes ***
GZ25	P < 0.05	0.2131 NS	0.0001 Yes ***

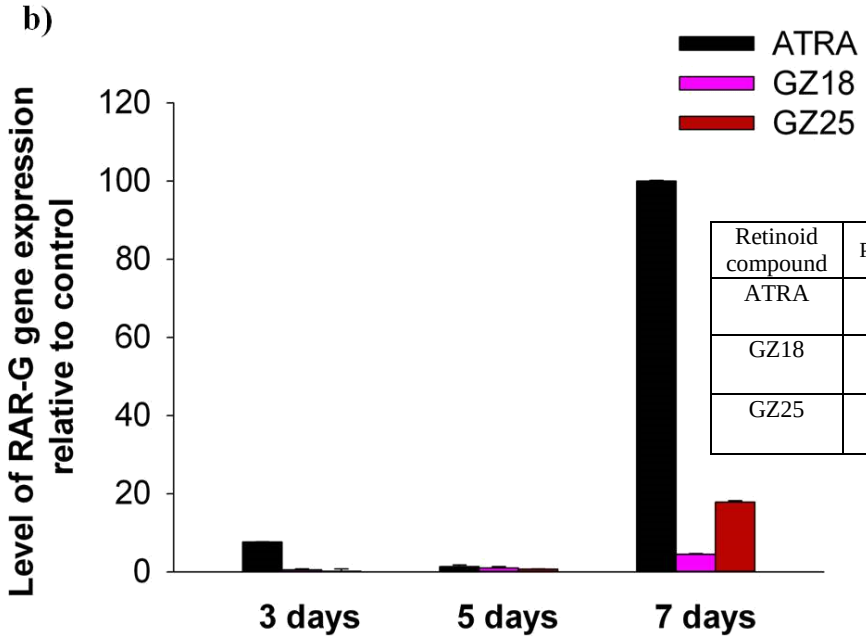

Retinoid compound	Probability	P value 5 days	P value 7 days
ATRA	P < 0.05	0.0001 Yes ****	0.0001 Yes ***
GZ18	P < 0.05	0.3244 NS	0.0002 Yes ***
GZ25	P < 0.05	0.4259 NS	0.0001 Yes ****

Figure 4.18: Real time PCR analysis of SHSY5Y cells which exposed to 10µM of ATRA, GZ18 and GZ25 for up to 12 hours and gene expression analysis of; a) RAR-α gene and; b) RAR-γ gene. ATRA induced the expression level of RAR-α after 4 hours and over-expressed after 12 hours compared to GZ18 and GZ25 whih only induced the over-expression level of RAR-α after 12 hours. GZ18 showed comparable level of expression of RAR-α to GZ25. Also, ATRA and GZ25 showed higher expression level of RAR-γ after 12 hours compared to GZ18 and ATRA treated cells showed 5 times higher level of RAR-γ than GZ25. Data are normalized to both control 0.1% DMSO and the internal reference gene (β-actin). Data represent mean ± SEM, n = 3.

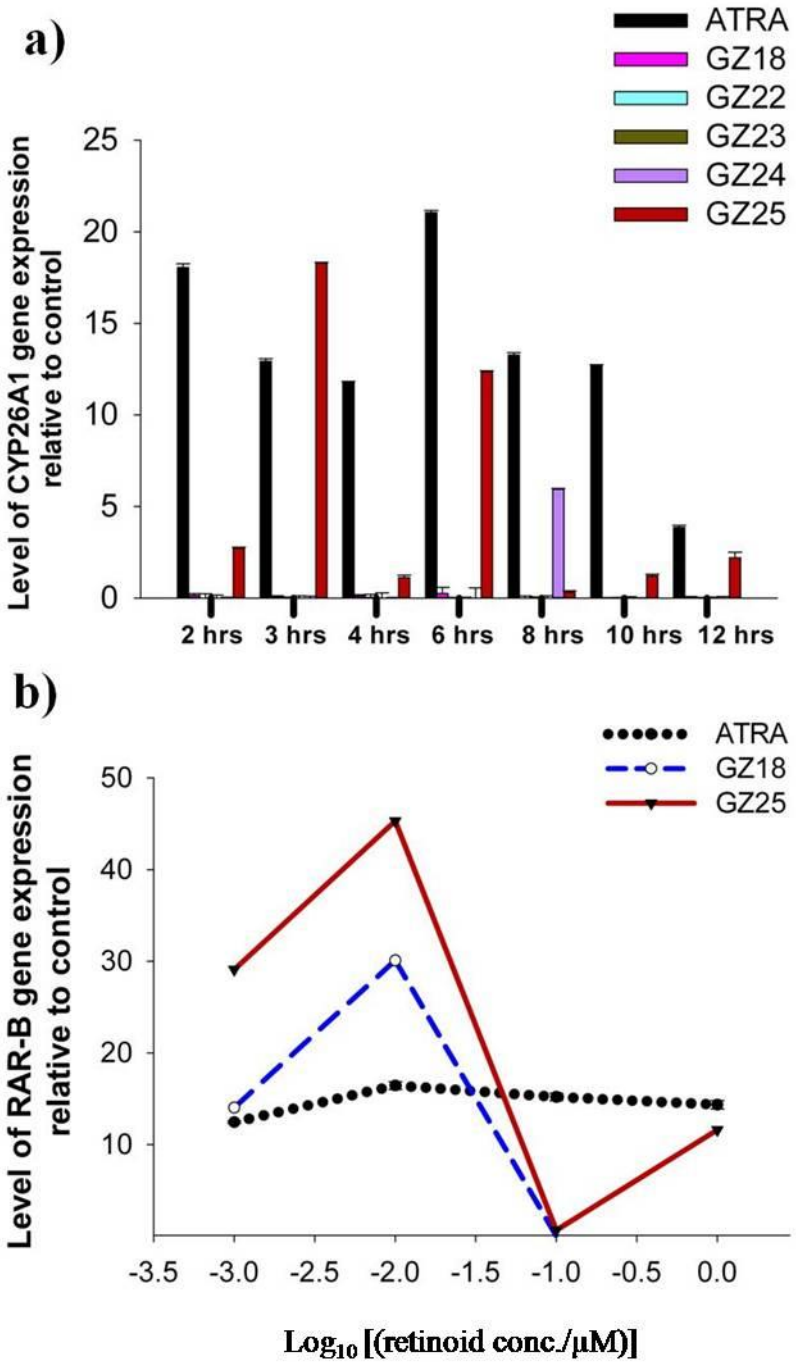

Figure 4.19: Real time PCR analysis of CYP26A1 gene expression in SHSY5Y cells treated with ATRA, GZ18 and GZ25; a) SHSY5Y cells were exposed to 10 µM of different synthetic derivatives for up to 12 hrs. GZ25 showed higher expression level similar to ATRA with maximal peak after 3 hours which was earlier than ATRA (6 hours); b) SHSY5Y cells were exposed to 1, 0.1, 0.01 and 0.001 µM of different synthetic derivatives for up to 8 hrs. Also GZ25 induced higher level of CYP26A1 at 0.001 and 0.01 µM concentration scales. GZ18 showed also slightly higher level of expression of CYP26A1 compared to ATRA at 0.001 and 0.01 µM concentrations. Data are normalized to both control 0.1% DMSO and the internal reference gene (β-actin). Data represent mean ± SEM, n = 3.

Only GZ18 was able to slightly induce gene expression of CYP26A1 at 1 and 0.1 µM but not at concentrations lower than that. This may give an indication that it is not necessarily that environmentally stable synthetic retinoid analogues would be metabolically stable as well (Fig. 5.19b).

4.5 X-gal assay analysis of EC19 and EC23

This assay was done by Prof. Peter Mccaffery's group in Aberdeen University using Sil-15 reporter cells (also called F9-RARE-lacZ cells) in the X-Gal Assay. This cell line was derived from a stable transfection of F9 teratocarcinoma cells with a plasmid containing the LacZ gene under the control of a promoter linked to a retinoic acid response element (RARE). This assay can visually detect and semi-quantify the transcriptional activity of retinoic acid and other retinoids by monitoring β-galactosidase activity produced by the reporter cells in response to the retinoic acid/retinoids in the surrounding medium. EC19 and EC23 were tested compared to control cells (as a blank) which are treated with DMSO solvent. The response of the Sil-15 reporter cell line to the two retinoids, EC23 and EC19 compared to RA was assayed at concentrations ranging from 10^{-6} M to 10^{-14} M (Fig. 4.20). EC23 was shown to be effective for induction of β-galactosidase expression and hence, a high genomic activity through RARE, while EC19 did not show any increase in induction of β-galactosidase gene at any of the concentration scale. This may give another indication for the selective and higher potency of EC23 compared to ATRA and EC19 for induction of cellular differentiation through activation of the RARE promoter and consequently, RARs.

4.6 Induction of neurite outgrowth in SHSY5Y using EC19 and EC23.

This assay was done by Prof. Peter Mccaffery's group in Aberdeen University using SH-SY5Y cells as a model to study neuronal differentiation phenotypes through measuring neurite outgrowth. The exposure time of cells with ATRA, EC19 and EC23 was long time scale to obtain more stable neuron-like properties, such as the neurite outgrowth.

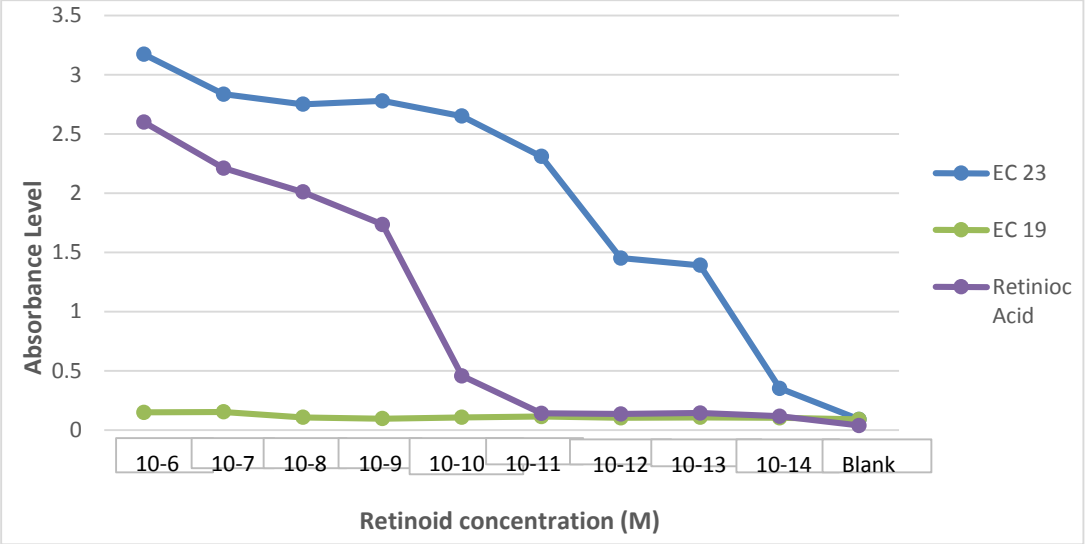

Figure 4.20: Concentration response graph of X-gal assay for evaluating ATRA, EC23 and EC19 for induction of genomic response of β-galactosidase in Sil-15 reporter cells. ATRA and EC23 showed higher absorbance level as an indication of potent induction of β-galactosidase activity through RARE at different concentration scales. EC19 was similar to blank control cells and did not show induction of β-galactosidase activity. n = 3.

The effects of EC23 and EC19 on neuronal differentiation and neurite outgrowth in SH-SY5Y cells were evaluated after 5 days at two different concentrations of 10 µM and 0.01 µM and compared to control cells treated with DMSO. Cells were fixed and stained for TUJ-1 and the mouse anti-β-III tubulin, a secondary antibody was used for fluorescent labelling of neurites for easy tracing the number and length in different fields. Fig. 4.21a and Fig. 5.22a showed that EC23 was potent enough at concentration of 10 µM to induce induction of cellular differentiation of SHSY5Y and produced high numbers of mature neurons compared to DMSO treated cells. The length of these neurons was not increased with the corresponding increase in concentration of EC23 from 0.01 µM (Fig. 4.22c and Fig.4.22d) to 10 µM (Fig.4.21c and Fig.4.21d). However, the numbers of neurons were slightly increased with the 10 µM concentration compared to 0.01 µM. In a different way; EC19 was not potent in either concentration to induce any increase in both neurite number and length for the same time of cell exposure compared to control cultures (Fig.4.23a and Fig. 4.24a). This means that EC19 was not potent even over long times of exposure to induce cellular differentiation of the SHSY5Y cells (Fig.4.23c and Fig.4.24c). Interestingly, it was noted that EC19 had the effect on SHSY5Y cells to form clumps, which was not further studied yet to investigate its biological role on cell adhesion (Fig.4.25).

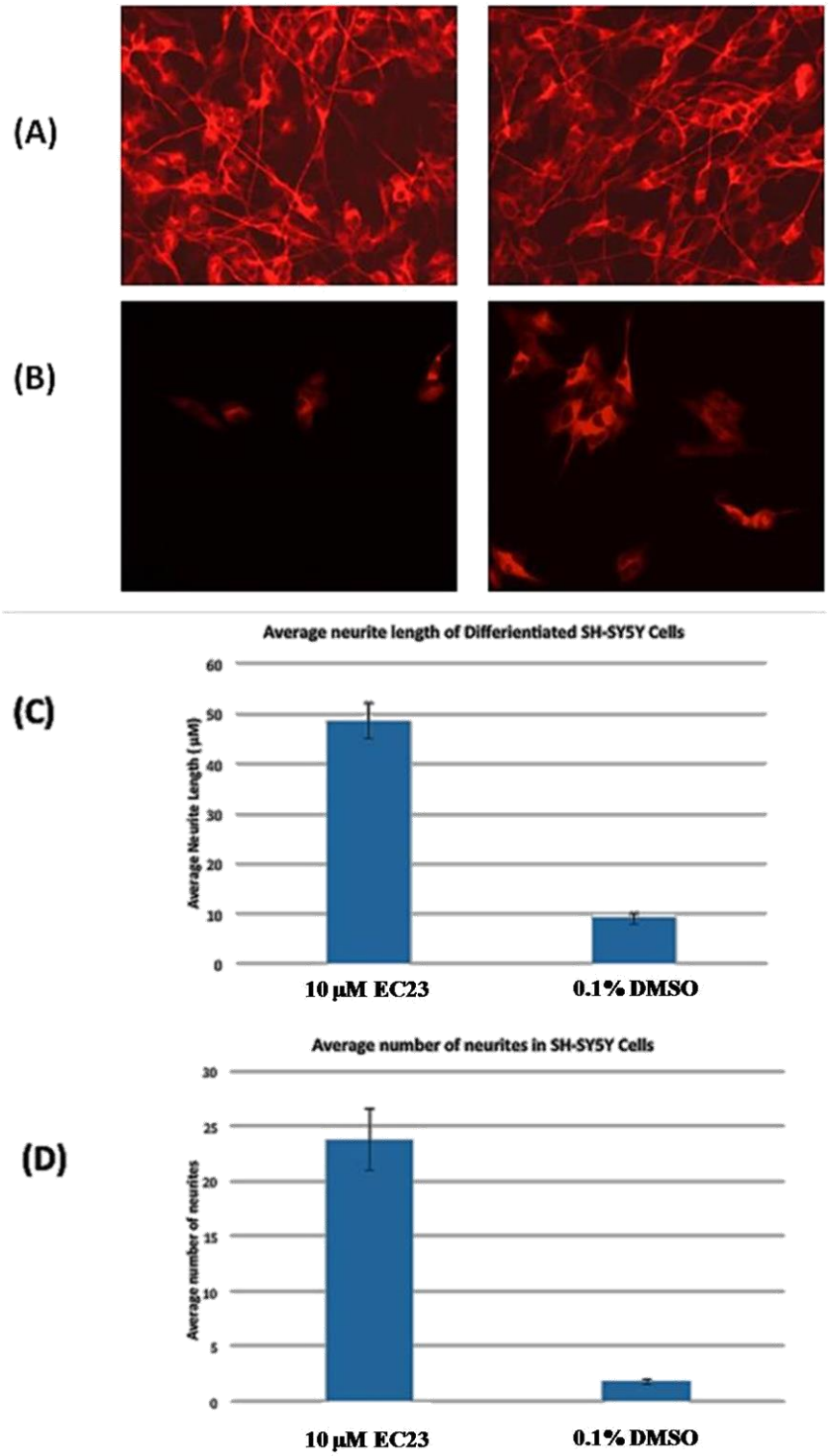

Figure 4.21: Neurite outgrowth of SHSY5Y treated with EC23 and stained for TUJ-1; A) 10 µM EC23 as it induced the differentiation of SH-SY5Y cells. B) DMSO treated SH-SY5Y cells as a control. C) The length of neurites extending from SH-SY5Y cells after 5 days of 10 µM EC23 treatment was measured and compared with the control. The average length was expressed in the graph ± SEM, n=3. Significant difference was measured by t-test (P= 0.0005). D) The total number of neurites extending from SH-SY5Y cells after 5 days of 10 µM EC23 treatment was measured and compared with the control. The average number was expressed in the graph ± SEM, n = 3(3 values of average neurite length; one value per each cover slip of the three). Significant difference was measured by Student's t-test (P = 0.0014). Scale bar 50 µm. This analysis was done by Prof. Peter Mccaffery's group in Aberdeen University, UK.

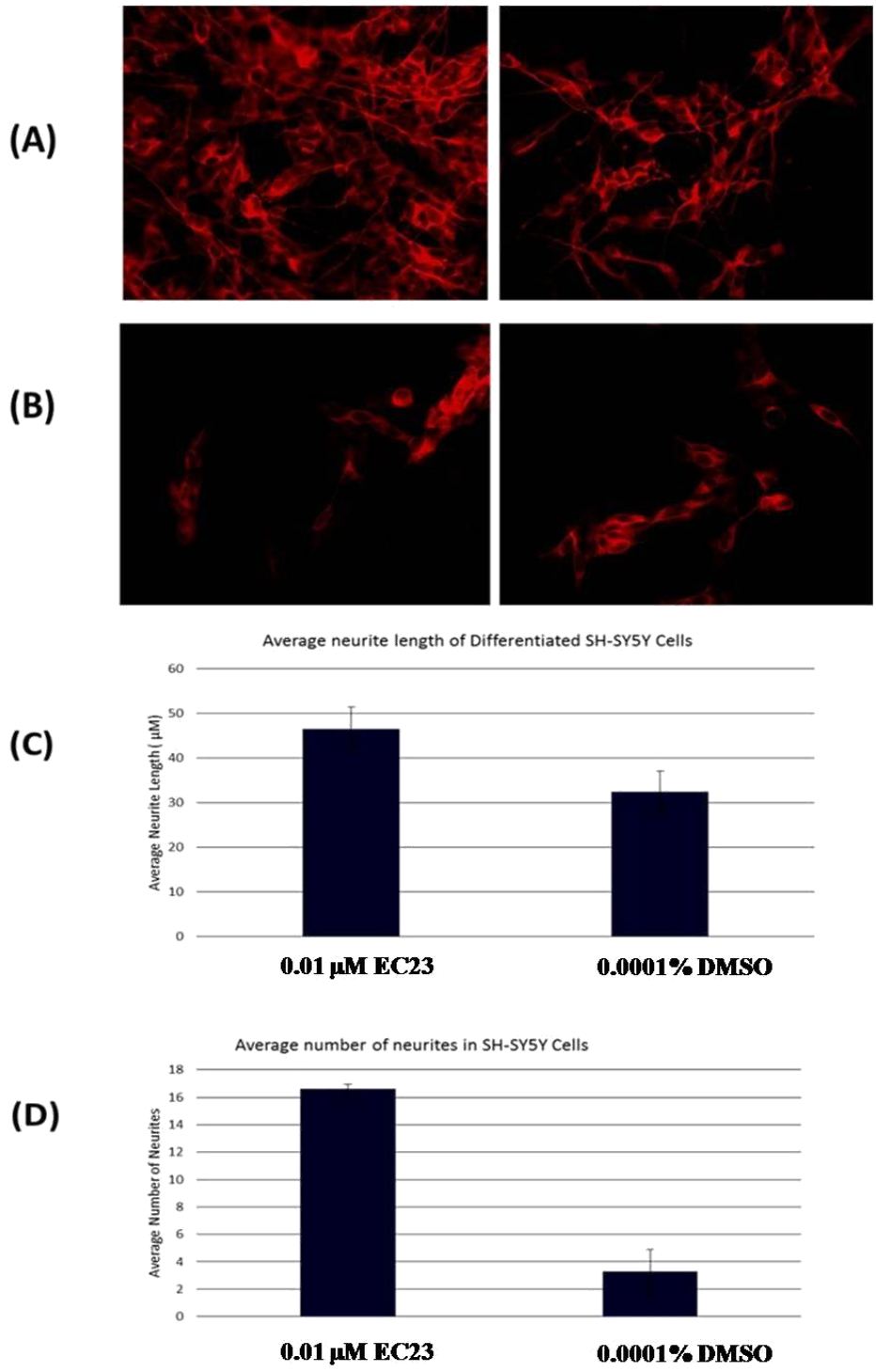

Figure 4.22: Neurite outgrowth of SHSY5Y treated with EC23 and stained for TUJ-1; A) 0.01 µM EC23 as it induced the differentiation of SH-SY5Y cells. B) DMSO treated SH-SY5Y cells as a control. C) The length of neurites extending from SH-SY5Y cells after 5 days of 0.01 µM EC23 treatment was measured and compared with the control. The average length was expressed in the graph ± SEM, n = 3. No significant difference was measured by t-test (P = 0.1701). D) The total number of neurites extending from SH-SY5Y cells after 5 days of 0.01 µM EC23 treatment was measured and compared with the control. The average number was expressed in the graph ± SEM, n = 3(3 values of average neurite length; one value per each cover slip of the three). Significant difference was measured by t-test (P = 0.0147). Scale bar 50 µm. This analysis was done by Prof. Peter Mccaffery's group in Aberdeen University, UK.

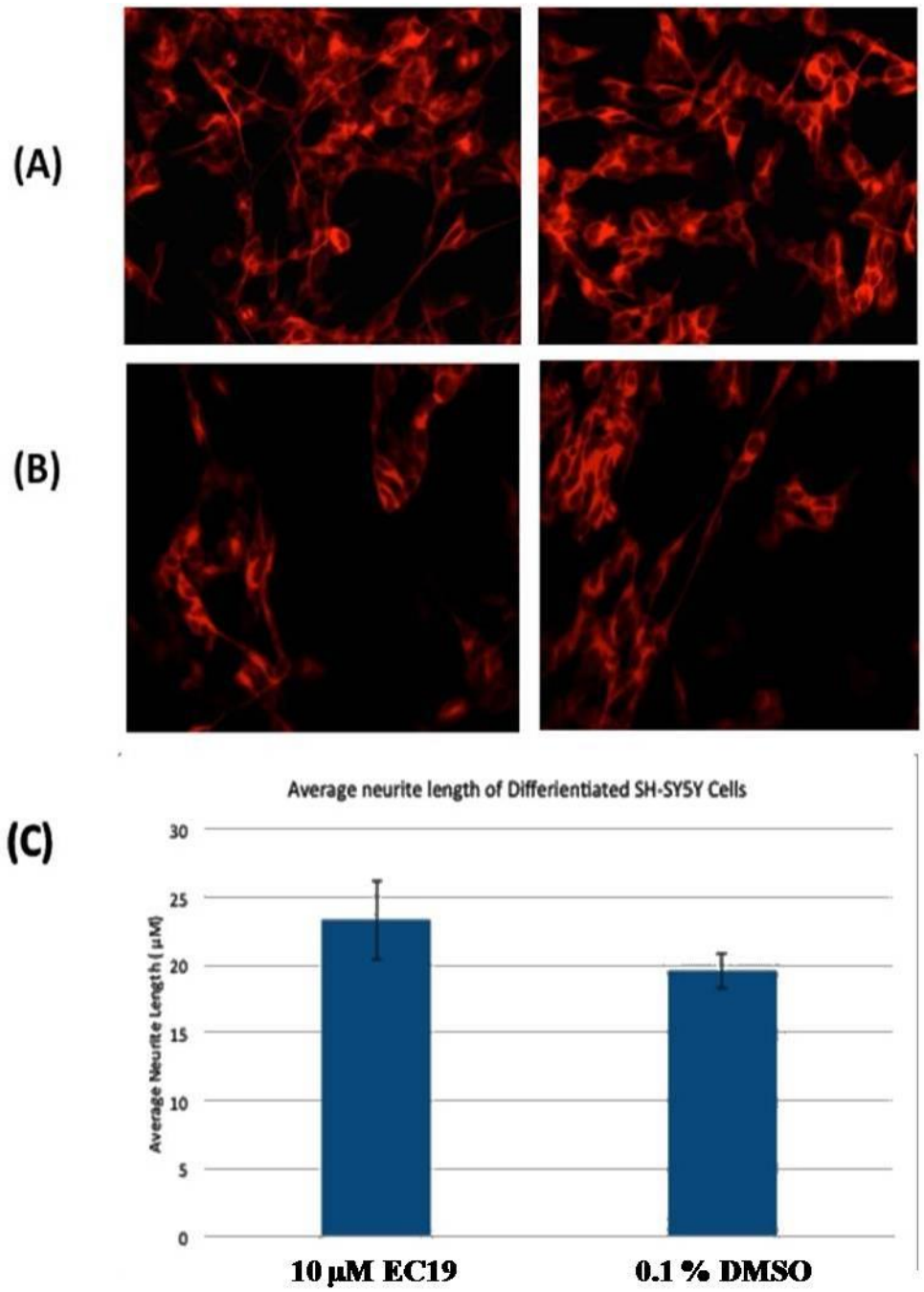

Figure 4.23: Neurite outgrowth of SHSY5Y treated with EC19 and stained for TUJ-1; A) EC19 treated SH-SY5Y cells at 10 µM. EC19 did not induce neurite outgrowth of SH-SY5Y cells. B) DMSO treated SH-SY5Y cells used as a control. C) The length of neurites extending from SH-SY5Y cells after 5 days of 10 µM EC19 treatment was measured and compared with the control. The average length was expressed in the graph ± SEM, n = 3(3 values of average neurite length; one value per each cover slip of the three). No significant difference was measured by t-test (P = 0.3043). Scale bar 50 µm. This analysis was done by Prof. Peter Mccaffery's group in Aberdeen University, UK.

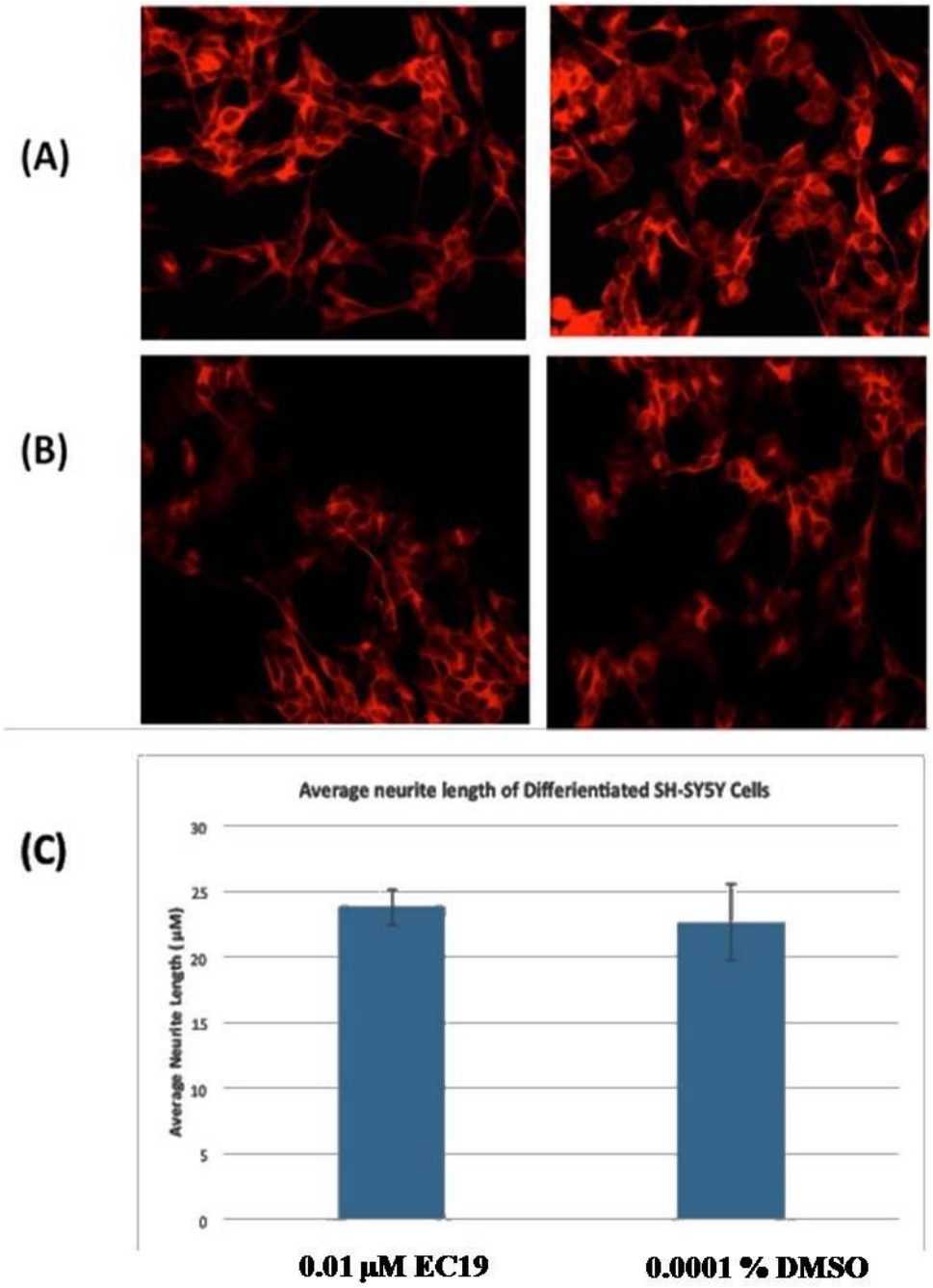

Figure 4.24: Neurite outgrowth of SHSY5Y treated with EC19 and stained for TUJ-1; A) EC19 treated SH-SY5Y cells at 0.01 µM. EC19 did not induce neurite outgrowth of SH-SY5Y cells. B) DMSO treated SH-SY5Y cells used as a control. C) The length of neurites extending from SH-SY5Y cells after 5 days of 0.01µM EC19 treatment was measured and compared with the control. The average length was expressed in the graph ± SEM, n = 3(3 values of average neurite length; one value per each cover slip of the three). No difference was measured by T-test (P = 0.6881). Scale bar 50 µm. This analysis was done by Prof. Peter Mccaffery's group in Aberdeen University, UK.

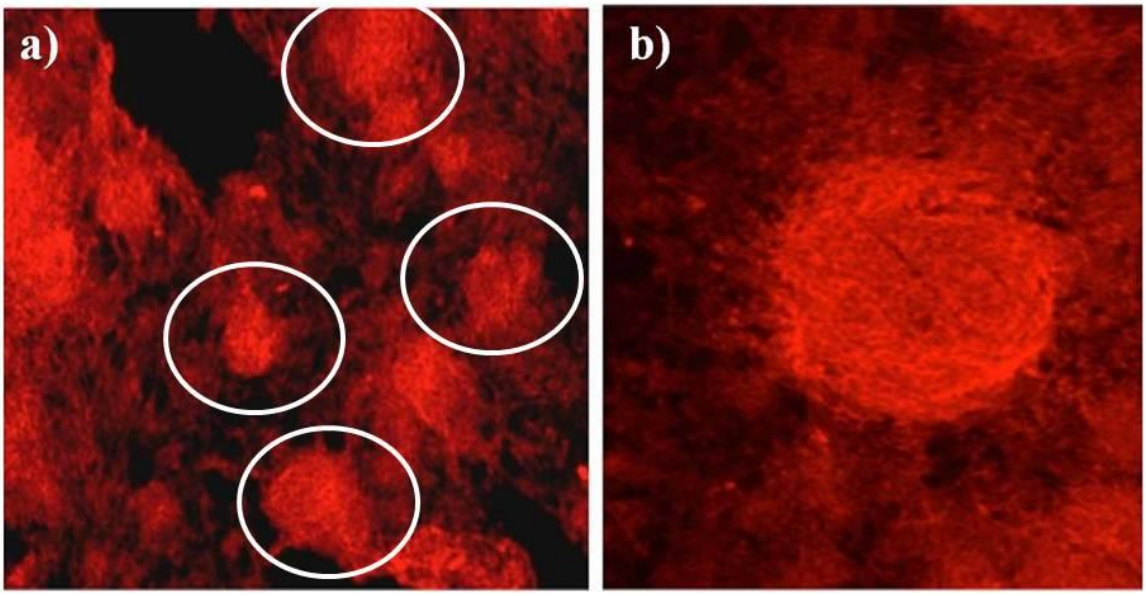

Figure 5.25: SHSY5Y cells treated with 10 µM EC19 for 5 days and then, stained for TUJ-1; a) EC19 at either lower or higher concentrations did not show any peripheral neuronal outgrowth within the different colonies, scale bar 50 µm; b) higher resolution (10 µm) showed that EC19 induced cell clump formation within each colony (showed in white circles) which might suggest induction of cellular proliferation rather than differentiation. This analysis was done by Prof. Peter Mccaffery's group in Aberdeen University, UK.

4.7 Raman spectroscopy analysis of SHSY5Y cells

There are many non-traditional preclinical tools that are accurate, high-throughput, and cost-effective those provide a unique fingerprint spectrum containing global biochemical information of the main macromolecules that compose a cell; either at the single-cell level or as an overall signal from a global cell population. The evidence for retinoids–cell interactions and hence, their efficacy can be, inferred by the acquisition of IR spectral data from treated cells. It is possible to detect discriminatory changes to the cellular IR signals even before visible morphological changes are evident, producing data of diagnostic significance for retinoid screening applications. Some previous FTIR analysis of TERA-2.cl.SP12 cells was done to investigate the biological changes occurred to stem cells upon cellular differentiation with EC19 and EC23. In this study, Raman spectroscopy, a more powerful tool with higher resolution was used to find out if any biological changes might happen upon treatment of SHSY5Y cells with EC19, EC23 and ATRA for 3 days. Prior to recording the Raman analysis of the cells, every spectrum was corrected for Raman scattering/fluorescence using a polynomial baseline fitting function.

After doing this optimization, every recorded cell spectrum had a flat baselines, which made elucidating spectral differences between the different spectra easier (gives each spectrum a common flat baseline).After, a polynomial fitting process, every spectrum was then normalised to account for the larger Raman signal intensities seen from some of the cell spectra recorded. When comparing the mean cell spectra from the different groups (retinoid treated neuroblastoma cells, ATRA and EC23 groups) and control neuroblastoma cells (control un-treated and DMSO treated neuroblastoma cells) there were few Raman band, which were different from cells that had been treated with retinoids (starred in the Fig. 4.26).

The clear spectral differences at 1570-1640 cm^{-1} from ATRA treated cell spectra when compared against control cells could be due to the C=C vibrations of the retinoid molecules still present inside the treated neuroblastoma cells. To back this up, Raman spectra recorded before from retinal and vitamin A in liver tissue and retinoic acid in literature were displayed and compared to the Raman spectrum of pure ATRA, EC19 and EC23 to confirm the region of this band. Every Raman spectra recorded for pure retinoid compounds had a high-intensity Raman band situated at 1570-1620 cm^{-1} due to the differences in compound chemical structures. This band has been previously assigned to the stretching vibrations of C=C molecules present in the molecular structures of retinoids. There is an interesting band for carbon – carbon triple bonds, which provides a strong Raman signal with frequencies typically between 2100 – 2250 cm^{-1} (Fig.4.27). By looking to Fig. 4.26, if the band at ~1602 was due to the retinoid compounds still present in and around the cell, a strong C-C triple bond should be seen from EC19 or EC23 treated cell spectra; a vibration frequency at 2100-2250 cm^{-1}, but this signal does not exist. To confirm this finding, Raman spectrum was recorded at the range of 1800-3600 cm^{-1} and there was no signal seen in the 2100-2250 cm^{-1} (fig. 4.28). Therefore, it is unlikely that this Raman band at ~1602 cm^{-1} was due to the retinoids still being bound, but is purely due to biological changes in the neuroblastoma occuring upon retinoid treatment. Furthermore, Fig.4.29a and Fig.4.29b were produced using principal component analysis (PCA) and show that the retinoid treated cells can be separated from the control cells (untreated and DMSO treated neuroblastoma cells), with spectral differences in the PC1 separation boundary, explaining differences between the retinoid treated and not treated ones.

The main spectral differences causing the separation along this boundary are due to a large increase at 1570-1640, and increases at 1220-1280, 1145 and 974-975 cm^{-1}. As previously explained, the Raman band at 1570-1640 cm^{-1} is more than likely to derive from the retinoid structures present inside the cells.

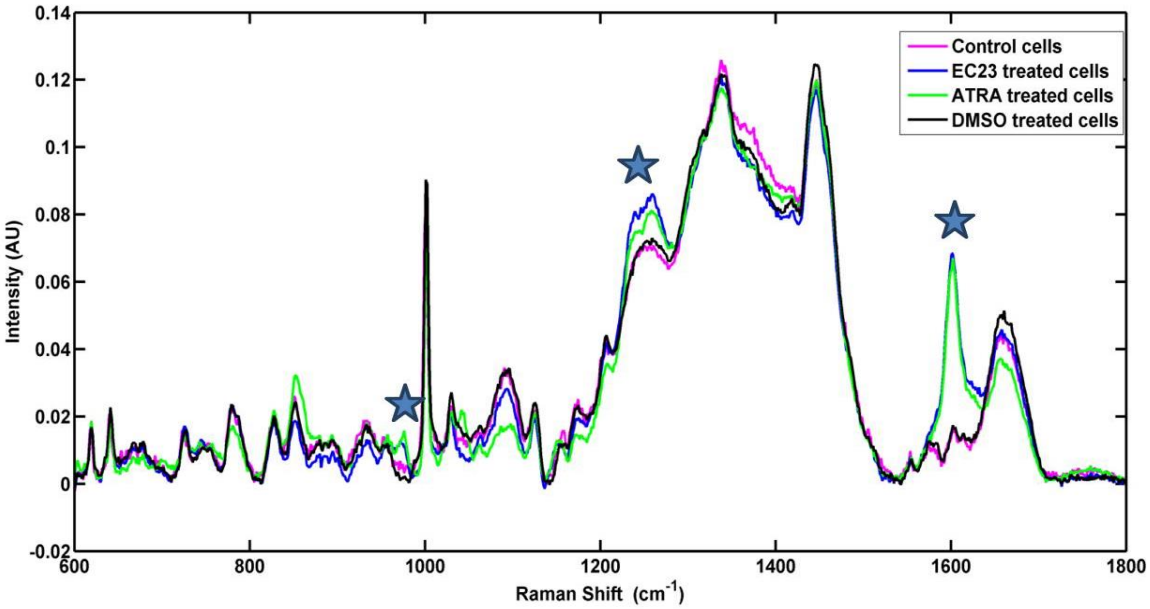

Figure 4.26: Mean Raman spectra of SHSY5Y neuroblastoma cells of un-differentiated, DMSO- treated, EC23 and ATRA treated neuroblastoma cells. Mean spectra revealed spectral differences between the retinoid treated neuroblastoma cells and the control cells from the Raman bands situated at 1570-1640, 1220-1280 and 960-980 cm^{-1}. This analysis was done by Graeme Clemens and Mathew Baker, University of Central Lancashire, UK.

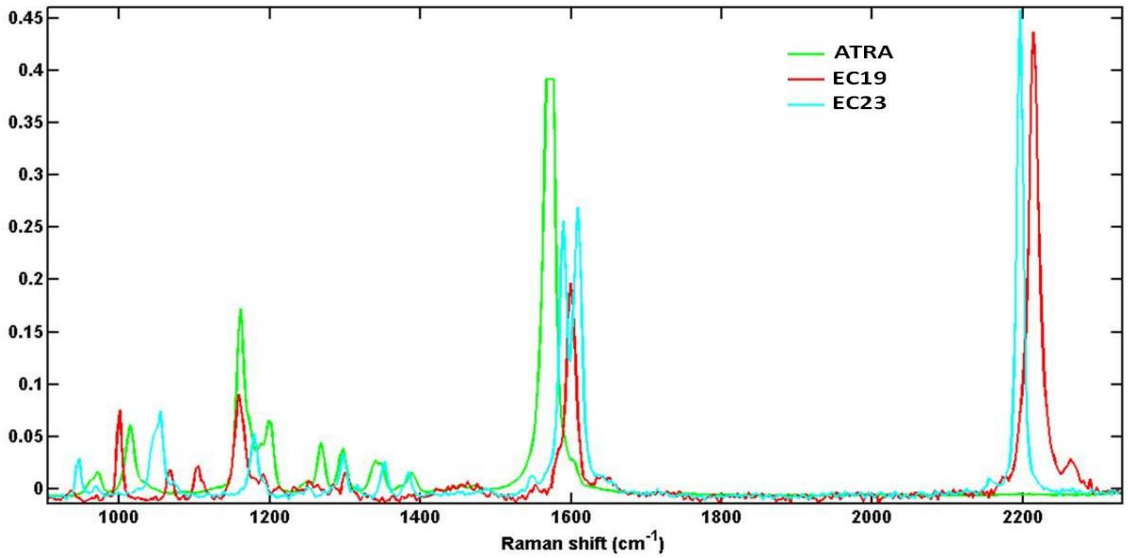

Figure 4.27: Raman spectra recorded from ATRA, EC19 and EC23 pure compounds using a 532 nm laser. The synthetic retinoids EC19 and EC23 have a strong Raman band attributed to carbon – carbon triple bond vibrations frequency between 2100 – 2250 cm^{-1}. This analysis was done by Graeme Clemens and Mathew Baker, University of Central Lancashire, UK.

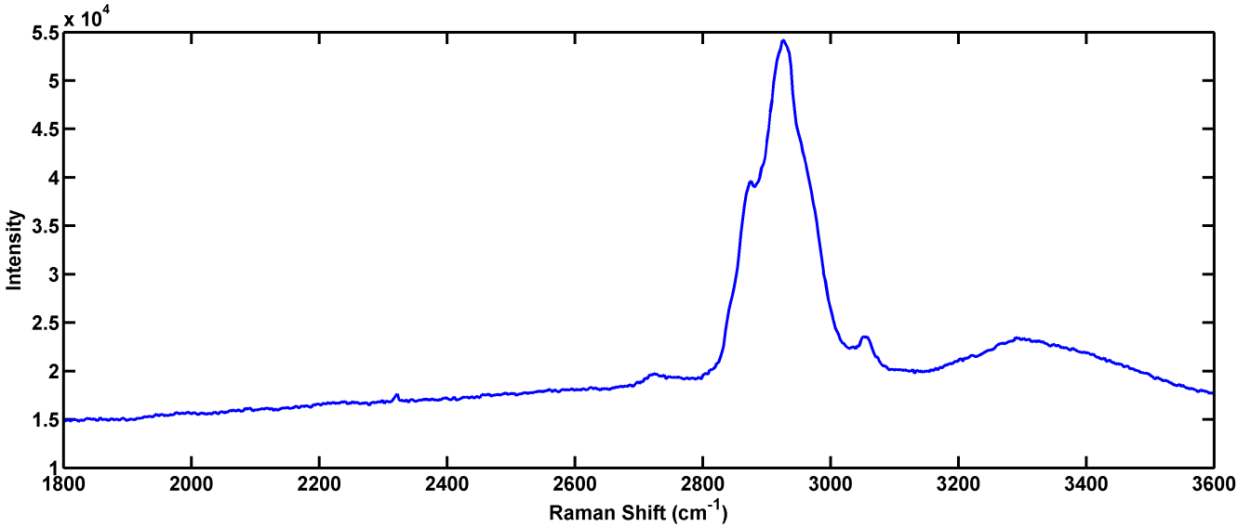

Figure 4.28: EC23 treated neuroblastoma cell Raman spectrum; using 532nm laser 1800-3600 cm^{-1} spectral range. There is no Raman signal is seen in the 2100-2250 cm^{-1} spectral range from the Raman spectrum recorded from an AH61 treated neuroblastoma cell. Therefore it can be concludedthat the increase in Raman signal ~1602 cm^{-1} from EC23 treated neuroblastoma cells is due to cellular changes as a result of cellular differentiation not any residual amount of the compound in the cells. This analysis was done by Graeme Clemens and Mathew Baker, University of Central Lancashire, UK.

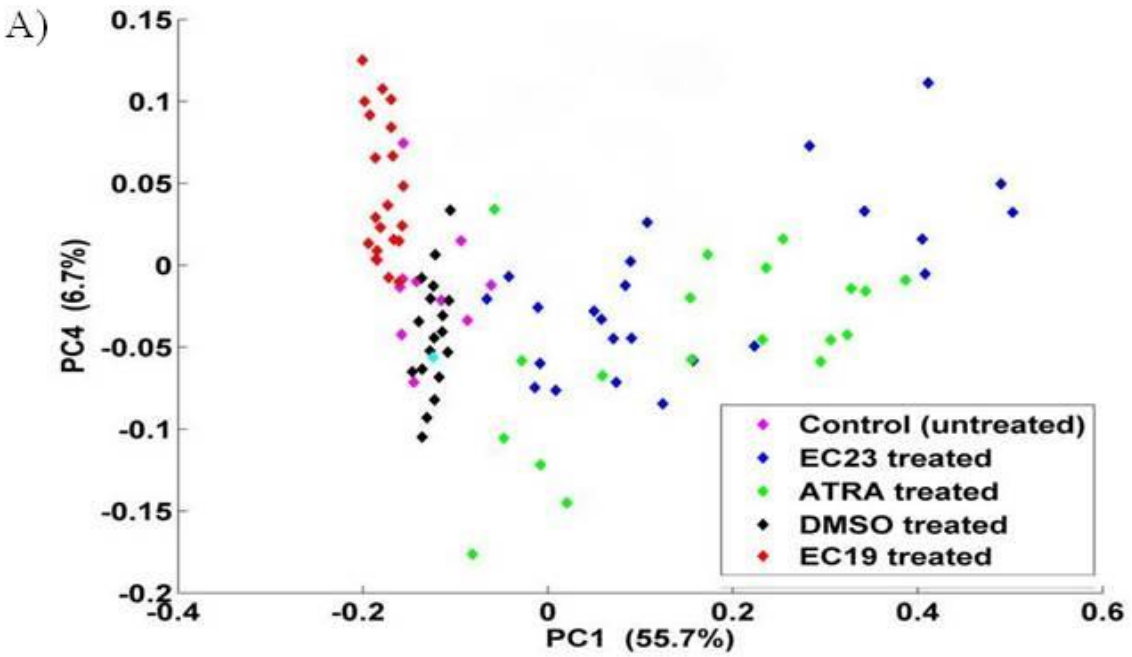

B)

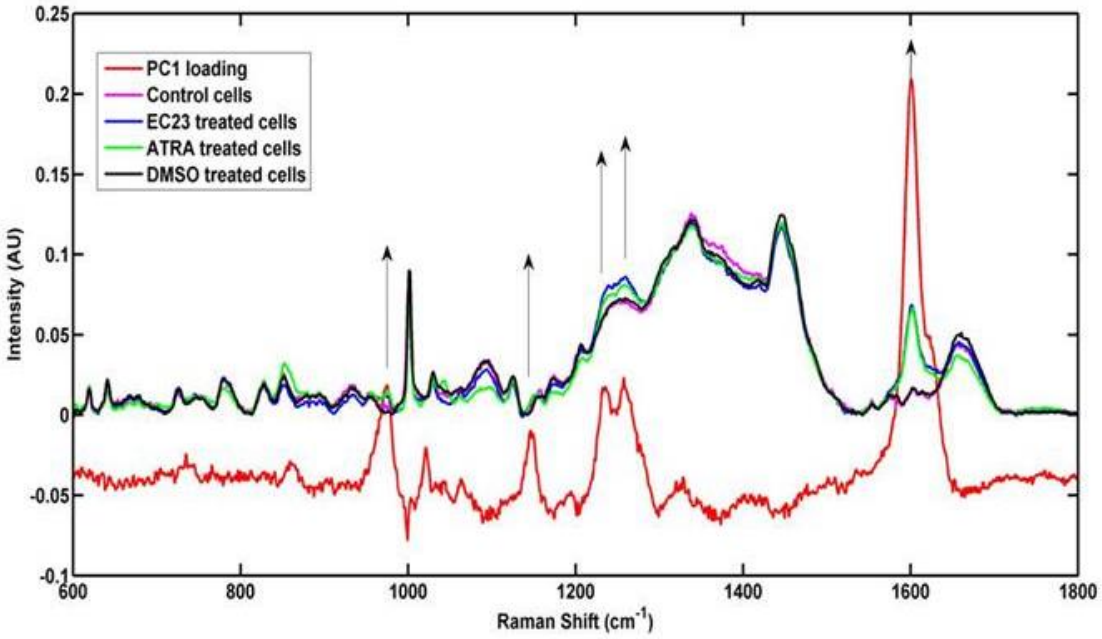

Figure 4.29: principal component spectral loading vector of SHSY5Y neuroblastoma cells treated with ATRA, EC19 and EC23 compared to control cells, A) All the peaks between retinoids and control samples at 1570-1640, 1220-1280 and 960-980 cm^{-1} were statistically analysed by transforming into set of linearly un-correlated varriables and the graph was drawn between PC1 versus PC4 as the two major variables. All the retinoid treated neuroblastoma cells of ATRA and EC23 treated cells were clearly separated from EC19, control and DMSO treated cells along these PC1 principal component vector, B) the main spectral difference causing the separation along the PC1 vector for the Raman band situated at ~1602 cm^{-1}; EC23 and ATRA treated cells all showed a much greater intensity from when compared to EC19, DMSO and control cells in addition to other discrete spectral differences as a result of the retinoids treatment. This analysis was done by Graeme Clemens and Mathew Baker, University of Central Lancashire, UK.

4.8 Conclusion

Biological characterization of synthetic retinoids is the second tool used for screening and understanding the differences in the potency of these molecules, based on the differences in their chemical structures. The validation of different biological assays was based on analysis of two synthetic analogues; EC19 and EC23 compared to ATRA and control un-differentiated cells. In TERA-2.cl.SP12 stem cells, EC23 showed similar behaviour to ATRA with higher biological potency to induce cellular differentiation at different time scales.

This included down-expression of some extracellular markers using flow cytometry such as SSEA-3 and TRA-160, and up-regulation of neuro-specific extracellular marker A2B5. Also, EC23 was potent at inducing the secretion of intracellular TUJ-1; the early stage neuro-marker is an indication of cellular differentiation. While, EC19 was less potent at showing any enhancement in activity for the induction of cellular differentiation represented as changes in the previously mentioned markers. Gene expression analysis of TERA-2.cl.SP12 stem cells showed an increase in up-regulation of both NeuroD1 and PAX6 genes with different time patterns in the case of ATRA and EC23 treated cells compared to EC19. These genes are known to be over-expressed with early formation of neurons and at late stage of cellular differentiation. Upon investigation of other classes of synthetic retinoids, the GZ derivatives, GZ25 showed biological activity similar to ATRA, this was confirmed by the previously mentioned assays.

Another biological assessment was done using the neuroblastoma cell line to investigate its efficacy as a model for biological screening of early signs of cellular differentiation of retinoids. Gene analysis was done including all RAR genes and cellular metabolic genes responsible for CYP26A1 activity and it was found that ATRA, EC23 and GZ25 were biologically potent to induce up-regulation of RAR-β gene which was reported as the main gene for induction of cellular differentiation in SHSY5Y. EC23 was suggested as a metabolically stable synthetic analogue as it showed lower induction potency to the CYP26A1 gene compared to ATRA and GZ25 at different times and concentration scales. This combined biological approach is useful for the biological characterization of future synthetic retinoid analogues at late and early stages of cellular exposure to retinoids.

Chapter V
Discussion, concluding remarks and future work

Discussion

Retinoids are essential for embryonic development and play important physiological functions, particularly in the brain and other highly developed organs.[347] These activities occur through the actions of the six known nuclear receptors, the retinoic acid receptors (RAR-α, -β and –γ) and the retinoic X receptor (RXR-α, -β and –γ).[348,349,350,351] Each of these receptors are encoded by distinct classes of genes and bind to different classes of other proteins. Indeed, most of retinoids that are used in the past for treating different diseases, *in vivo* and *in vitro* analysis are ATRA, 9-CRA and to less extend 13-CRA.[352,353] However, the reported drawbacks of using these molecules in research due to instability and cellular metabolism limits the effective use of these molecules.[354] Hence, there is a need to design and synthesise other modified molecules that are derivatives of vitamin A, with higher stability and more potency to be used in both i*n vitro* and *in vivo* applications.

The main aim of this thesis is to combine the calculated chemical structures, receptor binding assays and molecular docking tools in order to probe, and hence, understand the biological activity of newly synthesized retinoids with the ultimate goal of designing more specific synthetic retinoic acid derivatives, as well as improving our understanding of the downstream effects. Moreover, these was an urgent need to build up our knowledge about the biological activity of these molecules in different cell lines, at different concentrations and different time of exposures so as to understand the activity of these molecules in the induction of neuronal development.

Molecular docking was useful tool to conclude some important findings about the molecular interactions of retinoids in the RAR LBDs:

1. The carboxylate moiety of ATRA forms a salt bridge with the highly conserved Arg residue and hydrogen bonds with the hydroxyl group of Ser. This is similar to the binding interactions shown for the crystal structure of ATRA bound to RAR-γ.[355]
2. 9-CRA also showed interactions with all the RAR LBDs, however, it was unable to form the same salt bridge *via* the Arg-carboxylate interaction which would be stronger interactions.

Instead, Ser hydrogen bonds in all RAR binding pockets remain, together with the hydrophobic interactions around the tri-methyl-cyclohexene section of the molecule. It is because 9-CRA has a *cis*-double bond at C-9 that changes the geometry of the molecule such that the carboxylate cannot quite reach the Arg residue, consequently reducing the binding affinity compared to ATRA.

3. The ligand binding pocket of RAR-α and RAR-β, ATRA exists with in a single *s-cis* conformation which is ideal for best fitting interactions with Arg and Ser residues compared to, the *s-trans* form of 9-CRA. While in the ligand binding pocket of RAR-γ, ATRA and 9-CRA both exist in a mostly *s-trans* form with much better interactions for ATRA. This might account for previous observations for selective binding to the LBD of RAR-γ to the more extended conformation of ATRA (favorable conformation with minimum energy) compared to non-extended form in RAR-α or RAR-β and hence, the difference in binding affinity of RAR-γ than RAR-α or RAR-β.

Moreover, molecular docking was able to shed the light on some characterstics for retinoid molecules with specific activity towards one type of RARs:

1- Am580 has an amide linker region (check the list of retinoid chemical structures) that is arranged in a specific way so that the carbonyl group is oriented in a conformation in close proximity to Ser232. This allowed Am580 to form additional hydrogen bonds with Ser232 which reflect the selectivity and tight binding of this retinoid analogue to RAR-α. This was matched with previous studies showed that the serine at position 232 in RAR-α gives an explanation for the observed differences in the affinity with ATRA in this RAR type compared with that for RAR-β and –γ. This hydrogen bonding would not be permitted between the hydroxyl of serine and the hydrophobic linker of ATRA.[51,356]. This acitvity makes this compound useful for application in fighting different cancer cell lines due to the up regulation of the mRNAs coding for pro-caspase-1, -7, -8, and -9, which results in the increased synthesis of only pro-caspase-1 and -7 proteins and hence, induction of cell apoptosis.[357]

2- The selectivity of CD437 (check the list of retinoid chemical structures) to RAR-γ as it has adamantyl group side-chain with a strongly lipophilic effect. This group can form a hydrophobic network with residues in the H12 helix, such as, Phe304, Leu386, Leu407, Met406 and Ile403 which play a critical role for accommodating different ligands in this region.[358] In addition, Met272 is a fairly hydrophobic amino acid and typically found buried within the binding pocket of RAR-γ. It adopts a conformation suitable to form a stacking interaction with the aromatic moiety of CD437. The hydroxyl group also showed a hydrogen bond interaction with Met406; however, it was a weak interaction (distance in the range of 4 Å). This also matches with previous observation for the activity of this compound to induce apoptosis in a variety of human cell types, including cancer cell lines. [359, 360,361]

The second approach was to measure EC_{50s} of these compounds in the RAR LBDs in term of binding affinities of these compounds and ability to induce the co activator recruitment succesifully. This can help to discriminate between different RAR receptor types because their specificities as drivers of biological responses were poorly defined:

1- All the three RARs bind ATRA with similarly high affinities with the highest affinity were found with RAR-γ.[362] For 9-CRA, the natural retinoid isomer of ATRA, showed also similar binding to all RAR types with relatively lower binding affinity compared to ATRA due to the bednt structure of 9-CRA at carbon 9. All these differences could be explaine based on the previous observation of molecular binding interactions of these molecues. Many studies suggested that under physiological conditions, RAR-γ would selectively bind ATRA over 9-CRA.[363,364] The preference for ATRA by RAR-γ was found to result from ATRA having a slower off-rate compared to 9-CRA. Thus, once ATRA binds to RAR-γ, it remains bound for a longer time than 9-CRA before dissociates. This difference in the off-rate between ATRA and 9-CRA is such that, at equilibrium, in the presence of a mixture of ATRA and 9-CRA, very little 9-CRA is bound to RAR-γ, unless the concentration of 9-CRA exceeded that of ATRA by at least more than 2 fold. This can be explained by the difference in term of higher binding affinity of RAR-γ to ATRA than 9-CRA.

2- TTNBP was shown to be a potent synthetic analogue of retinoic acid that is known from several studies to have pan-agonist potency to bind and transactivate all RAR types.[365,366,367]

This was revealed from the lowest measured EC_{50}s for this compound compared to ATRA. It can be suggested from modelling study that this has a both hydrophobic side-chain in addition to replacement for the polyene linker group which makes it anchored by network of hydrogen bonds identical to that formed with ATRA with one extra hydrogen bond with Ser residue in each RAR pocket in addition to the van der Waals contacts with residues lining the LBP.

3- RAR selective Compounds such as Am580 and CD437 showed lower EC_{50} for RAR-α and RAR- γ respectively. This was correlated to the specific binding interactions of these compounds in the RAR LBDs as it was revealed from the molecular modeling study.

In addition, COPASI biosimulation software was helpful in understanding the shape of the sigmoidal curves and the different level of higher asymptoes resulted from the receptor binding assay studies as it can be concluded that:

1- There are four important parameters control the interactions of retinoids with RAR; k_1,k_2, k_3 and k_4. (k_1/k_2) ratio represented the binding affinity of the retinoid ligands to RAR LBDs. Also, the (k_3/k_4) ratio represents the binding affinity of the formed ligand-receptor complex to the co-activator.

2- The nature of the ligand- receptor complex is a crucial element for further binding to the co-activator, and hence, the success of the transcription process. In other words, if the retinoid compound fits properly in the RAR LBD, this will trigger the succesiful binding to co-activator and hence, lower EC_{50} and higher upper asymptote. There are two possibilites for the higher upper asymptote in this case, the succesiful binded co-activator will be in close proximity to the conformational structure of retinoid-receptor complex and hence, the signal propagation in FRET assay will be high. The other probability that there will be high number of best fit retinoid-receptor complex which will consequently bind with many of co-activators availble and also this will also induce higher signal propagation in FRET assay.

3- It was found that some compounds may be able to bind succesifully to the RAR LBDs however, they had lower upper asympotes and this might be explained as the retinoid-receptor complexs formed can not induce co-activator binding or co-activator binds in away different than the typical retinoid agonist.

Gathering all these information together was useful to understand the molecular and cellular activity of the new synthetic retinoid analogues, EC, GZ and their methyl ester derivatives (check the list of retinoid chemical structures) in different biological systems of TERA-2.cl.SP12 and SHSY5Y cells.

EC19 and EC23 differ from each other only in the position of carboxylic acid group on the terminal substituted ring; EC23 was designed to mimic ATRA, and the *meta*-position carboxylic acid of EC19 has the effect of changing the geometry of the molecule in a similar manner to the alkene geometry differences between ATRA and 9-CRA. EC23 and EC19 docked into the different RARs with binding interactions which were different to those of ATRA, particularly with respect to the orientation of the crucial carboxylate group. The *para*-substitution of the carboxylate facilitated an excellent fit of EC23 into the binding pocket in all the RARs by forming a strong salt bridge with the conserved Arg residue, with the addition of two further hydrogen bonds with the conserved Ser residue. This binding mode is very similar to that of ATRA, and in contrast to that of the *meta*-substitution of the carboxylate in EC19. In this case, the different geometry of the phenyl carboxylate alters the orientation of the entire molecule in the LBD, such that neither a salt bridge nor, a hydrogen bond is possible in the LBDs of either RAR-α or –γ. This was correlated with the measured EC_{50}, EC23 had the strongest binding affinity compared to EC19 that had the lowest EC_{50}.

However, for RAR-β, EC19 has both the topography and size that is more complementary with the binding pocket because of the additional space (extra groove compared with either RAR-α or -γ) in the LBD of RAR-β[67] and hence, it had a relatively high affinity for the RAR-β LBD, and ligand binding also facilitates co-activator recruitment with higher upper asymptote.

The binding pose of EC19 within the LBD of RAR-β was found to be stabilised by the formation of a salt bridge interaction with Arg and hydrogen bonds with Ser, but modelling also showed change in the orientation of EC19, resulting in the tetra-methyl-tetra-hydronaphthalene moiety forming short contacts and clashes with some key residues in the LBD, *i.e.* with residues Ile270 and Val395 in RAR-α[355,368,369] and Ala397, Leu416, Phe230, Ala234, Met415, Phe288 and Ser289 in RAR-γ but not with RAR-β residues.[355,370]

Such interactions are likely to affect the active conformation of H12, and thereby, the recruitment of co-activators and initiation of the transcription process. Having examined and compared ATRA, 9-CRA, EC23 and EC19, in order to confirm the key role of the carboxylate interaction with the Arg and Ser residues, the corresponding methyl esters of EC19 and EC23 were synthesized[371] and investigated to see if the ester form reduced the activity of either EC19 or EC23. There was no increase in, the binding affinity of EC19 methyl ester to any of the RARs, except slightly to RAR-α, but the binding affinity was lower than for both ATRA and EC23 in their free acid forms. For the methyl ester of EC23, there was a massive drop in the binding affinity to all the RARs compared to both ATRA and EC23 in their acid forms.

The second class of synthetic retinoids accommodates the alkoxythiazoles, *i.e.* the GZ derivatives (check the list of retinoid chemical structures). These compounds were synthesized[372] with the aim to selectively bind to RAR-β. The idea was that the RAR-β binding site was larger due to the presence of an additional cavity between H5 and H10.[67] It may be postulated, therefore, that ligands with larger side-chains are able to occupy the additional space within the RAR-β retinoid binding site, and hence, may show selectivity for this subtype. Receptor binding affinity showed that GZ25, and its ester derivatives, were the only ones able to bind efficiently to RAR-β binding pocket. Our suggestion for the enhanced binding affinity of these two derivatives matched previous studies claiming that the tetramethyl-1,2,3,4-tetra-hydronaphthyl side-chain can be accommodated by the RAR-β pocket and form favourable interactions with Leu407, Met406, and Ile403 to keep, the important helix-12 (AF-2) in the active conformation with minimal steric clashes.[373]

In addition, the position of the thiazole group within these derivatives was optimal to allow all the GZ derivatives to form additional hydrogen bonds with the Ser232 residue and this was reflected also in the higher binding affinity of GZ25 to RAR-α.

However, GZ25 was the one with higher binding affinity and best fitting in RAR LBDs, which can be explained in terms of the similar molecule length as ATRA, and hence, can produce the same binding interactions in the RAR-α binding pocket. The other GZ derivatives did not properly fit within the binding pocket either, due to the extended molecular length which (causing additional strain inside binding pocket, such as GZ23), or shorter molecules that could not hit all the hydrophobic contacts within lipophilic region in RAR-α, such as GZ18, GZ22 and GZ24.

Biological evaluation of these EC and GZ derivatives showed that the overall higher binding affinity of EC23 and GZ25 to all RARs was the sarting point for further up-regulation of RAR-β level in SHSY5Y neuroblastoma cell line in early stage within 2 hours of treatment. RAR-β is well known to be a major regulatory factor in the induction of cellular differentiation in many cell lines.[374] Decreased expression of RAR-β plays a key role in the maintenance of malignant phenotypes in many cancerous cells such as human pancreatic adenocarcinoma, and therefore, it represents a novel target for experimental strategies in the treatment of cancer and evaluation of retinoids.[375] EC23 and GZ25 were potent enough in a concentration dependent manner, with 10 μM to 1 nM showing the higher potency compared to ATRA, EC19 and their methyl esters. Also, Many studies showed that PAX6 gene expression is controlled by the promoter region of the RARs (RARE), especially RAR-β and so, its expression is regulated by their activation.[376,377,378] This was observed in TERA-2.cl.SP12 as EC23 and GZ25 were able to induce higher level of PAX6 after 7 days as indicated by the determination of neuro-differentiation. The levels were 5 and 10 fold higher than for ATRA. Neither EC19 nor its ester derivatives or other GZ derivatives, showed any significant increase in the level of PAX6. Also, for further confirmation for the role of RARE and PAX6 for the difference in biological potency of these compounds, an X-gal assay was done using the LacZ gene under control of RARE which consequently was affected by RAR-β gene expression. EC23 and ATRA showed higher potency to induce β-galactosidase activity than EC19 over different concentration scales up to 10^{-14} M, and hence, this showed the higher induction of RAR gene levels reflected in the activity of RARE promoter region.[379]

The effect of these compounds on RAR-α and RAR-γ was also studied and showed that retinoic acid induced over-expression of RAR-α and RAR-γ was more than EC23 and GZ25, and it was observed in previous research work that RAR-α and RAR-γ have a major role in formation of heterodimer complex with RXR. These complexes increase the retinoic acid metabolism by activation of CRABPII.[380] This was confirmed as ATRA was highly susceptible to cellular metabolism more than EC23, EC19 and induced higher gene levels of CYP26A1 up to 12 hours and at lower concentration scales.

However, RAR- α and RAR- γ are still have biological roles for synergism with RAR-β for the induction of cellular differentiation and this is what was revealed from their higher levels after 12 hours in EC23 and GZ25 treated cultures compared to EC19 and other GZ analogues.

The long term observation for the biological effect of these compounds on both SHSY5Y and TERA-2.cl.SP12 showed that EC23 and GZ25 at concentration of 10 µM, was able to induce neurite outgrowth in SHSY5Y while not at lower concentrations while, EC19 and other GZ analoges were not able to induce any of neurite outgrowth at any concentration scale. This might be explained in terms of over-expression of NeuroD1 gene and supported by many studies, in addition to the role of Nav2 gene under control of NeuroD1 to stimulate neuronal extensions.[381] Also, literature showed that ATRA was able to induce neurite outgrowth at a concentration range of 1-10 µM[382,224] which coincided with what we observed for the optimum activity of 10 µM EC23 compared to 10 µM EC19, which only drives cells into clump formation in SHSY5Y. In TERA-2.cl.SP12, neurite outgrowth with EC23 and GZ25 was supported by up-regulation of TUJ-1, the neurofilament protein which is highly expressed in neural tissue as an indication for more committed neural phenotypes at different stages of neural development.[383,384] While, EC19 was different in the way induction for cellular differentiation was observed and large numbers of lump cells stained for CK-8 after 14 days as indication of epithelial cell fate. These results might explain why EC23 can successfully induce stem cell and SHSY5Y differentiation resulting in neural cells similarly to ATRA, at lower concentration. However, since EC19 binds only RAR-β reasonably efficiently, or other GZ derivatives have lower RAR binding affinities this suggests that neurogenesis in response to EC23 might be driven more *via* a combination of all the RAR receptors.

In summary, some new synthetic retinoids analogues, including EC23 and GZ25, were characterized in two different cell models. They have the potential biological activity to be more potent and more stable than ATRA to reduce any disadvantages of using ATRA for *in vitro* differentiation. The comparison was done for biological potency of these compounds in TERA-2.cl.SP12 stem cells and SHSY5Y neuroblastoma cells and it was shown that there are some common similarities in the mechanism of neuronal cell differentiation.

The main reasons for the higher biological activity of these compounds are the *para*-position of the carboxylate group that makes the compounds best-fit in the RAR LBDs. Also, the optimum molecular length plays key role to hit the essential binding residues inside RAR pockets and minimize the possible ligand steric clashes. The higher binding affinitiy to all RARs and particulary RAR-β is essentail for successful up-regulation of other markers such as PAX6, NeuroD1 and TUJ-1 and hence, induction of neuronal cell differentiation. All these information can help in designing more compounds with more potent and selective biological activity towards one type of RAR for possible therapeutic use. Table 5.1 summarizes the key observations in binding data, biological characterizations and suggestions from molecular docking between natural and different synthetic retinoids.

Table 5.1: The key observations in evaluation of new synthetic retinoids compared to ATRA.

Retinoid	RAR binding affinity	Biological characterization features	Molecular docking suggestions
ATRA	Binds to all RARs with relatively higher binding affinity to RAR-γ	Induces higher level of RAR-α, RAR-γ and CYP26A1 genes in SHSY5Y cells. Induce neurite outgrowth and over-expression of A2B5, TUJ-1 proteins and NeuroD1 gene in TERA-2 cells.	In RAR-α and RAR-β, ATRA exists with *s-cis* conformation, While in RAR-γ, it exist in a mostly *s-trans* form.
EC23	The strongest binding affinity to all RARs compared to ATRA.	Induces the highest level of RAR-β followed by RAR-α, RAR-γ genes in SHSY5Y cells. Induce neurite outgrowth and over-expression of A2B5, TUJ-1 proteins in TERA-2.cl.SP12 cells. Induce neurite outgrowth in SHSY5Y cells at 10 µM concentration.	The *para*-position carboxylic acid fit the molecule in a similar way as ATRA.
EC19	Lowest binding affinity to RAR-α and RAR-γ with relatively high affinity for the RAR-β.	Induces the lowest RAR-α, RAR-β, RAR-γ, CYP26A1, NeuroD1, PAX6 genes in SHSY5Y and TERA-2 cells respectively. It Can not Induce neurite outgrowth in SHSY5Y cells. It induces epithelial cell differentiation in TERA-2 cells confirmed by high level of CK-8.	The *meta*-position carboxylic acid has the effect of changing the geometry of the molecule in a similar manner to bent structure of 9-CRA. EC19 can fit in RAR-β due to extra space in binding pocket.
GZ25	The strongest binding affinity to all RARs compared to ATRA and simillar to EC23.	Induce the highest level of RAR-β followed by RAR-α, RAR-γ genes in SHSY5Y cells. Also, it is reliable for cellular metabolism by CYP26A1. Induce neurite outgrowth and over-expression of TUJ-1 proteins in TERA-2.cl.SP12 cells.	It has similar molecule length as ATRA and form additional hydrogen bond with Ser232 in RAR-α to fit and fill in the RAR binding pocket.

Concluding remarks

In this study, the use of calculated 3D structures of ligand chemical structures and their conformations, receptor binding assays and molecular docking tools have been combined to understand the biological activity of certain synthetic retinoids in comparison with natural systems. Two synthetic analogues, EC23 and GZ25 were highlighted to have higher binding affinities to all RAR types, confirmed by the molecular docking structures using GOLD docking software. COPASI bio-simulation models were useful to understand the kinetic parameters behind the ligand binding interactions and co-activator recruitment. These finding support the major aim of the designing more stable and potent synthetic retinoids to further understand the retinoic acid signalling pathway and *in vitro* differentiation.

Molecular docking highlighted important interactions of these molecules, with the *para*-position of carboxylate in EC23 being essential for the optimum fitting in the RAR LBDs. Arg and Ser residues played a crucial role for the formation of hydrophilic interaction networks with carboxylate moiety. The quality of the retinoid-receptor complex had an impact on the co-activator recruitment, and hence, the transcriptional process.

Upon biological screening, the potency of EC23 and GZ25 was reflected in the ability of these compounds to induce cellular differentiation in stem cells and cancerous cells. TERA-2.cl.SP12 cells were useful model for prolonged investigations of synthetic retinoid effects on extracellular and intracellular marker expression. Additionally, gene expression profiles using NeuroD1 and PAX6 showed the difference in biological potency of these molecules. SHSY5Y neuroblastoma cells were developed as a model for early screening of synthetic retinoids using the RAR-β gene as a rapid and promising marker, which was induced by EC23 and GZ25 in away similar to ATRA with enhanced over-expression, as indicated in the difference in potency. When cellular metabolism was compared with chemical and environmental stability, it was found that the two factors were not necessirely correlated. This was shown in GZ25 which was sensitive for cellular metabolism by CYP26A1, though it was environmentally stable.

7.2 Future work

- Molecular docking studies need to be continued by calculation of molecular binding interactions between retinoid ligands and the interacting residues inside the RAR LBDs. Many interaction factors, such as entropy and induction of molecular conformational changes induced during interactions, must be included in the docking calculations. This could help in using the overall fitness score for assessing the biological potency of retinoids in quicker and more precise way.

- Accurate quantification of synthetic retinoids is required to measure level of these compounds both inside cells and in the media, so that their fate can be monitored. These compounds are lipophilic, and they are not easily measured by traditional protocols or to purify them purely in aqueous solution or cell extracts. Also, identification and quantification of the possible metabolites of these compounds is required, especially using the isolated microsome systems and accurate mass spectrometric analysis.

- Raman spectroscopy analysis of live cells, such as neuroblastoma treated with these compounds, is required for the accurate assessment of the biological response of the cells to retinoids.

- Further biological characterization of these synthetic retinoids, on neuroblastoma is required to understand the different mechanisms that control the process of cellular differentiation and neurite outgrowth.

- Detailed *in vitro* and *in vivo* toxicity studies are needed for these synthetic retinoids in comparison to ATRA. This can help in the identification of one or more of compounds as potential drugs, for treatment of cancer.

Chapter VI

References

References

1. Böhm, H. J. (1996). Computational tools for structure-based ligand design. *Prog. Biophys. Mol. Biol*, *66*, 197–210.
2. Kuntz, I. D., Blaney, J. M., Oatley, S. J., Langridge, R., & Ferrin, T. E. (1982). A geometric approach to macromolecule-ligand interactions. *J. Mol. Biol.*, *161*, 269–288.
3. Morris, G. M., Goodsell, D. S., Halliday, R. S., Huey, R., Hart, W. E., Belew, R. K. & Olson, A. J. (1998). Automated docking using a Lamarckian genetic algorithm and an empirical binding free energy function. *J. Comput. Chem.*, *19*, 1639–1662.
4. Totrov, M., & Abagyan, R. (1997). Flexible protein-ligand docking by global energy optimization in internal coordinates. *Protein Struct. Funct. Genet.*, *29*, 215–220.
5. Venkatachalam, C. M., Jiang, X., Oldfield, T., & Waldman, M. (2003). Ligand Fit: A novel method for the shape-directed rapid docking of ligands to protein active sites. *J. Mol. Graph. Model.*, *21*, 289–307.
6. Jain, A. N. (2007). Surflex-Dock 2.1: robust performance from ligand energetic modeling, ring flexibility, and knowledge-based search. *J. Comput. Aided Mol. Des.*, *21*, 281–306.
7. Kramer, B., Rarey, M., & Lengauer, T. (1999). Evaluation of the FlexX incremental construction algorithm for protein- ligand docking. *Protein Struct. Funct. Genet.*, *37*, 228–241.
8. Nissink, J. W. M., Murray, C., Hartshorn, M., Verdonk, M. L., Cole, J. C., & Taylor, R. (2002). A new test set for validating predictions of protein-ligand interaction. *Protein Struct. Funct. Genet.*, *49*, 457–471.
9. Friesner, R. A., Murphy, R. B., Repasky, M. P., Frye, L. L., Greenwood, J. R., Halgren, T. A., Sanschagrin, P. C. & Mainz, D. T. (2006). Extra precision glide: Docking and scoring incorporating a model of hydrophobic enclosure for protein-ligand complexes. *J. Med. Chem.*, *49*, 6177–6196.
10. Friesner, R. A., Banks, J. L., Murphy, R. B., Halgren, T. A., Klicic, J. J., Mainz, D. T., Repasky, M. P., Knoll, E. H., Shelley, M., Perry, J. K., Shaw, D. E., Francis, P. & Shenkin, P. S. (2004). Glide: A New Approach for Rapid, Accurate Docking and Scoring. 1. Method and Assessment of Docking Accuracy. *J. Med. Chem*, *47*, 1739–1749.

11. Cho, A. E., Guallar, V., Berne, B. J., & Friesner, R. (2005). Importance of accurate charges in molecular docking: Quantum Mechanical/Molecular Mechanical (QM/MM) approach. *J. Comput. Chem.*, *26*, 915–931.
12. Kua, J., Zhang, Y., &McCammon, J. A. (2002). Studying enzyme binding specificity in acetylcholinesterase using a combined molecular dynamics and multiple docking approach. *J. Am. Chem. Soc.*, *124*, 8260–8267.
13. Ota, N., & Agard, D. A. (2001). Binding mode prediction for a flexible ligand in a flexible pocket using multi-conformation simulated annealing pseudo crystallographic refinement. *J. Mol. Biol*., *314*, 607–617.
14. Ferrari, A. M., Wei, B. Q., Costantino, L., & Shoichet, B. K. (2004). Soft docking and multiple receptor conformations in virtual screening. *J. Med. Chem*., *47*, 5076–5084.
15. Cavasotto, C. N., & Abagyan, R. A. (2004). Protein Flexibility in Ligand Docking and Virtual Screening to Protein Kinases. *J. Mol. Biol*., *337*, 209–225.
16. Lin, B. C., Hong, S. H., Krig, S., Yoh, S. M., & Privalsky, M. L. (1997). A conformational switch in nuclear hormone receptors is involved in coupling hormone binding to corepressor release. *Mol Cell Biol*, *17*, 6131–6138.
17. Leid, M., Kastner, P., & Chambon, P. (1992). Multiplicity generates diversity in the retinoic acid signalling pathways. *Trends Bioch. Sci., 17*, 427–433.
18. Kastner, P., Leid, M. & Chambon, P. The role of nuclear retinoicacid receptors in the regulation of gene expression. Marcel Dekker Inc. publisher. New York. 1994.
19. Mangelsdorf, D. J., Umesono, K. & Evans, R. M. The Retinoid Receptors. In *The Retinoids (second edition)*. Raven Press publisher. NY. 1994.
20. Lohnes, D., Mark, M., Mendelsohn, C., Dollé, P., Dierich, A., Gorry, P., Gansmuller, A. & Chambon, P. (1994). Function of the retinoic acid receptors (RARs) during development (I). Craniofacial and skeletal abnormalities in RAR double mutants. *Development, 120*, 2723–2748.
21. Giguere, V., Ong, E. S., Segui, P., & Evans, R. M. Identification of a receptor for the morphogen retinoic acid. *Nature, 330*, 624–629.
22. Petkovich, M., Brand, N. J., Krust, A., & Chambon, P. (1987). A human retinoic acid receptor which belongs to the family of nuclear receptors. *Nature*, *330*, 444–450.

23. Chambon, P. (1996). A decade of molecular biology of retinoic acid receptors. *FASEB J., 10,* 940–954.
24. Kastner, P., Mark, M., Ghyselinck, N., Krezel, W., Dupé, V., Grondona, J. M., & Chambon, P. (1997). Genetic evidence that the retinoid signal is transduced by heterodimeric RXR/RAR functional units during mouse development. *Development , 124,* 313–326.
25. Mark, M., Ghyselinck, N. B., Wendling, O., Dupé, V., Mascrez, B., Kastner, P., & Chambon, P. (1999). A genetic dissection of the retinoid signalling pathway in the mouse. *Proc. Nutr. Soc., 58,* 609–613.
26. Mark, M., Ghyselinck, N. B., &Chambon, P. (2006). Function of retinoid nuclear receptors: lessons from genetic and pharmacological dissections of the retinoic acid signaling pathway during mouse embryogenesis. *Rev. Pharmacol. Toxicol., 46,* 451–480.
27. Kurokawa, R., DiRenzo, J., Boehm, M., Sugarman, J., Gloss, B., Rosenfeld, M. G., Heyman, R. A. & Glass, C. K. (1994). Regulation of retinoid signalling by receptor polarity and allosteric control of ligand binding. *Nature, 371,* 528–531.
28. Rastinejad, F. (2001). Retinoid X receptor and its partners in the nuclear receptor family. *Curr. Opin. Struct. Biol., 11,* 33–8.
29. Tabin, C. (1995). The initiation of the limb bud: growth factors, Hox genes, and retinoids. *Cell, 80,* 671–674.
30. Dupe, V., Davenne, M., Brocard, J., Dolle, P., Mark, M., Dierich, A., Chambon, P. & Rijli, F. M. (1997). *In vivo* functional analysis of the Hoxa-1 3' retinoic acid response element (3'RARE). *Development, 124,* 399–410.
31. Boncinelli, E., Simeone, A., Acampora, D., & Mavilio, F. (1991). HOX gene activation by retinoic acid. *Trends Genet., 7,* 329–334.
32. Mangelsdorf, D. J., Ong, E. S., Dyck, J. A., & Evans, R. M. (1990). Nuclear receptor that identifies a novel retinoic acid response pathway. *Nature, 345,* 224–229.
33. Rowe, A., Eager, N. S., & Brickell, P. M. (1991). A member of the RXR nuclear receptor family is expressed in neural-crest-derived cells of the developing chick peripheral nervous system. *Development, 111,* 771–778.

34. Levin, A. A., Sturzenbecker, L. J., Kazmer, S., Bosakowski, T., Huselton, C., Allenby, G., Speck, J., Kratzeisen, C., Rosenberger, M. & Lovey, A. (1992). 9-cis retinoic acid stereoisomer binds and activates the nuclear receptor RXR alpha. *Nature, 355*, 359–361.
35. Brocard, J., Kastner, P., &Chambon, P. (1996). Two novel RXR alpha isoforms from mouse testis. *Biochem. Biophys. Res. Commun., 229*, 211–218.
36. Nagata, T., Kanno, Y., Ozato, K., & Taketo, M. (1994). The mouse Rxrb gene encoding RXR beta: genomic organization and two mRNA isoforms generated by alternative splicing of transcripts initiated from CpG island promoters. *Gene, 142*, 183–189.
37. Chambon, P. (2005). The nuclear receptor superfamily: a personal retrospect on the first two decades. *Mol. Endocrinol., 19*, 1418–28.
38. Bastien, J., & Rochette-Egly, C. (2004). Nuclear retinoid receptors and the transcription of retinoid-target genes. *Gene, 328*, 1–16.
39. McGrane, M. M. (2007). Vitamin A regulation of gene expression: molecular mechanism of a prototype gene. *J. Nutr. Biochem., 18*, 497–508.
40. Balmer, J. E. (2002). Gene expression regulation by retinoic acid. *J. Lipid Res., 43*, 1773–1808.
41. Blomhoff, R., & Blomhoff, H. K. (2006). Overview of retinoid metabolism and function. *J. Neurobiol., 66*, 606–630.
42. Perissi, V., & Rosenfeld, M. G. (2005). Controlling nuclear receptors: the circular logic of cofactor cycles. *Nat. Rev. Mol. Cell Biol., 6*, 542–554.
43. Hu, X., & Lazar, M. A. (2000). Transcriptional repression by nuclear hormone receptors. *Trends Endocrinol. Metab., 11*, 6–10.
44. McKenna, N. J., & O'Malley, B. W. (2002). Combinatorial Control of Gene Expression by Nuclear Receptors and Coregulators. *Cell, 108*, 465–474.
45. Germain, P., Iyer, J., Zechel, C., & Gronemeyer, H. (2002). Co-regulator recruitment and the mechanism of retinoic acid receptor synergy. *Nature, 415*, 187–192.
46. Altucci, L., & Gronemeyer, H. (2001). The promise of retinoids to fight against cancer. *Nat. Rev. Can., 1*, 181–193.
47. Henderson, A. P. Small Molecules for Controlling Stem Cell Differentiation. Durham E-theses. Durham University.2011.

48. Germain, P., Chambon, P., Eichele, G., Evans, R. M., Lazar, M. A., Leid, M., De Lera, A. R., Lotan, R., Mangelsdorf, D. J. & Gronemeyer, H. (2006). International Union of Pharmacology. LX. Retinoic acid receptors. *Pharmacol. Rev.*, *58*, 712–725.
49. Renaud, J. P., Rochel, N., Ruff, M., Vivat, V., Chambon, P., Gronemeyer, H., & Moras, D. (1995). Crystal structure of the RAR-γ ligand-binding domain bound to all-trans retinoic acid. *Nature*, *378*, 681 – 689.
50. Pogenberg, V., Guichou, J. F., Vivat-Hannah, V., Kammerer, S., Pérez, E., Germain, P.,de Lera, A. R.,Gronemeyer, H., Royer, C. A. & Bourguet, W. (2005). Characterization of the interaction between retinoic acid receptor/retinoid X receptor (RAR/RXR) heterodimers and transcriptional coactivators through structural and fluorescence anisotropy studies. *J. Biol. Chem.*, *280*, 1625–1633.
51. Ostrowski, J., Roalsvig, T., Hammer, L., Marinier, A., Starrett, J. E., Yu, K. L., & Reczek, P. R. (1998). Serine 232 and methionine 272 define the ligand binding pocket in retinoic acid receptor subtypes. *J. Biol. Chem.*, *273*, 3490–3495.
52. Renaud, J. P., Rochel, N., Ruff, M., Vivat, V., Chambon, P., Gronemeyer, H., & Moras, D. (1995). Crystal structure of the RAR-gamma ligand-binding domain bound to all-trans retinoic acid. *Nature*, *378*, 681–689.
53. Gampe, R. T., Montana, V. G., Lambert, M. H., Miller, A. B., Bledsoe, R. K., Milburn, M. V, Kliewer, S. A., Willson, T. M. & Xu, H. E. (2000). Asymmetry in the PPARgamma/RXRalpha crystal structure reveals the molecular basis of heterodimerization among nuclear receptors. *Mol. Cell*, *5*, 545–555.
54. Egea, P. F., Mitschler, A., Rochel, N., Ruff, M., Chambon, P., & Moras, D. (2000). Crystal structure of the human RXRalpha ligand-binding domain bound to its natural ligand: 9-cis retinoic acid. *EMBO J.*, *19*, 2592–2601.
55. Shiau, A. K., Barstad, D., Loria, P. M., Cheng, L., Kushner, P. J., Agard, D. A., & Greene, G. L. (1998). The Structural Basis of Estrogen Receptor/Coactivator Recognition and the Antagonism of This Interaction by Tamoxifen. *Cell*, *95*, 927–937.
56. Tairis, N., Gabriel, J. L., Gyda, M., Soprano, K. J., & Soprano, D. R. (1994). Arg269 and Lys220 of retinoic acid receptor-beta are important for the binding of retinoic acid. *J. Biol. Chem.*, *269*, 19516–19522.

57. Bourguet, W., Ruff, M., Chambon, P., Gronemeyer, H., & Moras, D. (1995). Crystal structure of the ligand-binding domain of the human nuclear receptor RXR-alpha. *Nature*, *375*, 377–382.
58. Vivat, V., Zechel, C., Wurtz, J. M., Bourguet, W., Kagechika, H., Umemiya, H.,Shudo, K.,Moras, D., Gronemeyer, H. & Chambon, P. (1997). A mutation mimicking ligand-induced conformational change yields a constitutive RXR that senses allosteric effects in heterodimers. *EMBO J.*, *16*, 5697–5709.
59. Voegel, J. J., Heine, M. J. S., Tini, M., Vivat, V., Chambon, P., & Gronemeyer, H. (1998). The coactivator TIF2 contains three nuclear receptor-binding motifs and mediates transactivation through CBP binding-dependent and -independent pathways. *EMBO J.*, *17*, 507–519.
60. Egea, P. F., Mitschler, A., Rochel, N., Ruff, M., Chambon, P., & Moras, D. (2000). Crystal structure of the human RXRα ligand-binding domain bound to its natural ligand: 9-cis retinoic acid. *EMBO J.*, *19*, 2592–2601.
61. Darimont, B. D., Wagner, R. L., Apriletti, J. W., Stallcup, M. R., Kushner, P. J., Baxter, J. D.,Baxter, J. D., Fletterick, R. J. & Yamamoto, K. R. (1998). Structure and specificity of nuclear receptor-coactivator interactions. *Genes and Development*, *12*, 3343–3356.
62. Mailfait, S., Thoreau, E., Belaiche, D., Formstecher, P., & Sablonnière, B. (2000). Critical role of the H6-H7 loop in the conformational adaptation of all- *trans* retinoic acid and synthetic retinoids within the ligand-binding site of RARα. *J. Mol. Endocrinol.*, 24, 353–364.
63. Durand, B., Saunders, M., Gaudon, C., Roy, B., Losson, R., & Chambon, P. (1994). Activation function 2 (AF-2) of retinoic acid receptor and 9-cis retinoic acid receptor: presence of a conserved autonomous constitutive activating domain and influence of the nature of the response element on AF-2 activity. *EMBO J.*, *13*, 5370–5382.
64. Saitou, M., Narumiya, S., & Kakizuka, A. (1994). Alteration of a single amino acid residue in retinoic acid receptor causes dominant-negative phenotype. *J. Biol. Chem.*, *269*, 19101–19107.

65. Ostrowski, J., Hammer, L., Roalsvig, T., Pokornowski, K., & Reczek, P. R. (1995). The N-terminal portion of domain E of retinoic acid receptors alpha and beta is essential for the recognition of retinoic acid and various analogs. *Proc. Natl. Acad. Sci*., *92*, 1812–1816.
66. Wurtz, J. M., Bourguet, W., Renaud, J. P., Vivat, V., Chambon, P., Moras, D., & Gronemeyer, H. (1996). A canonical structure for the ligand-binding domain of nuclear receptors. *Nat. Struct. Biol.*, *3*, 87–94.
67. Germain, P., Kammerer, S., Pérez, E., Peluso-Iltis, C., Tortolani, D., Zusi, F. C.Starrett, J., Lapointe, P., Daris, J. P., Marinier, A., de Lera, A. R., Rochel, N. & Gronemeyer, H. (2004). Rational design of RAR-selective ligands revealed by RARbeta crystal stucture. *EMBO Rep.*, *5*, 877–882.
68. Zhang, X. K., Lehmann, J., Hoffmann, B., Dawson, M. I., Cameron, J., Graupner, G., Hermann, T., Tran, P. & Pfahl, M. (1992). Homodimer formation of retinoid X receptor induced by 9-cis retinoic acid. *Nature*, *358*, 587–591.
69. Egea, P. F., Mitschler, A., & Moras, D. (2002). Molecular recognition of agonist ligands by RXRs. *Mol. Endocrinol*., *16*, 987–997.
70. Bourguet, W., Vivat, V., Wurtz, J. M., Chambon, P., Gronemeyer, H., & Moras, D. (2000). Crystal structure of a heterodimeric complex of RAR and RXR ligand-binding domains. *Mol. Cell*, *5*, 289–298.
71. Sussman, F., & de Lera, A. R. (2005). Ligand recognition by RAR and RXR receptors: binding and selectivity. *J. Med. Chem*., *48*, 6212–6219.
72. Kleywegt, G. J., & Alwyn Jones, T. (1994). Detection, delineation, measurement and display of cavities in macromolecular structures. *ActaCryst. D, Bio.Cryst.*, *50*, 178–185.
73. Philippsen A. (1999). DINO: visualizing structural biology, 18, 12-53. http://www.dino3d.org
74. Barnard, J. H., Collings, J. C., Whiting, A., Przyborski, S. A., & Marder, T. B. (2009). Synthetic retinoids: structure-activity relationships. *Chem. J.*, *15*, 11430–11442.
75. Bastien, J. & Rochette-Egly, C. (*2004*). *Gene, 328*,1-16.

76. Maltman, D. J., Christie, V. B., Collings, J. C., Barnard, J. H., Fenyk, S., Marder, T. B., Whiting, A. & Przyborski, S. A. (2009). Proteomic profiling of the stem cell response to retinoic acid and synthetic retinoid analogues: identification of major retinoid-inducible proteins. *Mol. BioSys.*, *5*, 458–471.
77. Dawson, M. I., Chan, R. L., Derdzinski, K., Hobbs, P. D., Chao, W. R., & Schiff, L. J. (1983). Synthesis and pharmacological activity of 6-[(E)-2-(2,6,6-trimethyl-1-cyclohexen-1-yl)ethen-1-yl]- and 6-(1,2,3,4-tetrahydro-1,1,4,4-tetramethyl-6-naphthyl)-2-naphthalenecarboxylic acids. *J. Med. Chem*., *26*, 1653–1656.
78. Crettaz, M., Baron, A., Siegenthaler, G., & Hunziker, W. (1990). Ligand specificities of recombinant retinoic acid receptors RAR alpha and RAR beta. *Biochem. J.*, *272*, 391–397.
79. Agarwal, C., Chandraratna, R. A., Teng, M., Nagpal, S., Rorke, E. A., & Eckert, R. L. (1996). Differential regulation of human ectocervical epithelial cell line proliferation and differentiation by retinoid X receptor- and retinoic acid receptor-specific retinoids. *Cell Growth Differ.*, *7*, 521–530.
80. Newton, D. L., Henderson, W. R., & Sporn, M. B. (1980). Structure-activity relationships of retinoids in hamster tracheal organ culture. *Cancer Res*., *40*, 3413–3425.
81. Miller, D. A., Stephens-Jarnagin, A., & DeLuca, H. F. (1985). The epithelial differentiating activity in vivo of (E)-4-[2-(5,6,7,8-tetrahydro-5,5,8,8-tetramethyl-2-naphthylenyl) -1-propenyl]benzoic acid and 4,4-difluororetinoic acid. *Biochem. J*., *227*, 311–316.
82. Loeliger P., Bollag W., Mayer H. (1980). Arotinoids, a new class of highly active retinoids. *Eur. J. Med. Chem*., 1980, *15*, 9–15.
83. Anding, A. L., Nieves, N. J., Abzianidze, V. V, Collins, M. D., Curley, R. W., &Clagett-Dame, M. (2011). 4-Hydroxybenzyl modification of the highly teratogenic retinoid, 4-[(1E)-2-(5,5,8,8-tetramethyl-5,6,7,8-tetrahydro-2-naphthalenyl)-1-propen-1-yl]benzoic acid (TTNPB), yields a compound that induces apoptosis in breast cancer cells and shows reduced teratogenicity. *Chem. Res. Toxicol*., *24*, 1853–1861.
84. Delescluse, C., Cavey, M. T., Martin, B., Bernard, B. A., Reichert, U., Maignan, J., Darmon, M. & Shroot, B. (1991). Selective High-Affinity Retinoic Acid Receptor-Alpha or Receptor-Beta-Gamma Ligands. *Mol. Pharmacol.*, *40*, 556–562.

85. Sasaki, T., Shimazawa, R., Sawada, T., Iijima, T., Fukasawa, H., Shudo, K., Hashimoto, Y. & Iwasaki, S. (1995). Determination of the photoaffinity-labeled site on the ligand-binding domain of retinoic acid receptor alpha. *Biochem. Biophys. Res. Commun.*, *207*, 444–451.
86. Guldberg C.M., Waage P. (1864). Studies Concerning Affinity.*Videnskabs-Selskabet , 92*, 35–41.
87. Waage P. (1864). Experiments for Determining the Affinity Law, *Videnskabs-Selskabet*, 13, 1-*92*.
88. Guldberg C.M. (1864). Concerning the Laws of Chemical Affinity. *Videnskabs-Selskabet, 111*.
89. Alsop, D., Brown, S., & Van Der Kraak, G. (2001). Development of a retinoic acid receptor-binding assay with rainbow trout tissue: characterization of retinoic acid binding, receptor tissue distribution, and developmental changes. *Gen. Comp. Endocrinol.*, *123*, 254–267.
90. Bissonnette, R. P., Brunner, T., Lazarchik, S. B., Yoo, N. J., Boehm, M. F., Green, D. R., &Heyman, R. A. (1995). 9-cis retinoic acid inhibition of activation-induced apoptosis is mediated via regulation of fas ligand and requires retinoic acid receptor and retinoid X receptor activation. *Mol. Cell Biol.*, *15*, 5576–5585.
91. Boehm, M. F., McClurg, M. R., Pathirana, C., Mangelsdorf, D., White, S. K., Hebert, J., Winn, D., Goldman, M. E. &Heyman, R. A. (1994). Synthesis of high specific activity [3H]-9-cis-retinoic acid and its application for identifying retinoids with unusual binding properties. *J. Med. Chem.*, *37*, 408–414.
92. Turton, J. A., Hicks, R. M., Gwynne, J., Hunt, R., & Hawkey, C. M. (1985). Retinoid toxicity. *Ciba Found. Symp.*, *113*, 220–251.
93. Sen, S., Jaakola, V. P., Heimo, H., Kivelä, P., Scheinin, M., Lundstrom, K., & Goldman, A. (2002). Development of a scintiplate assay for recombinant human α2B-adrenergic receptor. *Anal. Biochem.*, *307*, 280–286.
94. Del Corral, R. D., Olivera-Martinez, I., Goriely, A., Gale, E., Maden, M., & Storey, K. (2003). Opposing FGF and retinoid pathways control ventral neural pattern, neuronal differentiation, and segmentation during body axis extension. *Neuron, 40*, 65–79.
95. Gilbert, S. F. Developmental Biology. 6th ed. Sunderland (MA), UK. 2000.

96. Ben-Tabou de-Leon, S., & Davidson, E. H. (2007). Gene regulation: gene control network in development. *Annu. Rev. Biophys. Biomol. Struct., 36*, 191-212.
97. Khillan, J. S. (2014). Vitamin A/retinol and maintenance of pluripotency of stem cells. *Nutrients*, *6*, 1209–1222.
98. Gunther, S. (1973). The therapeutic value of retinoic acid in chronic discoid, acute guttate, and erythrodermic psoriasis: clinical observations on twenty-five patients. *Br. J. Dermatol.*, *89*, 515–517.
99. Fredriksson, T. (1971). Antipsoriatic Activity of Retinoic Acid (Vitamin A Acid). *Dermatology*, *142*, 133–136.
100. Fenaux, P., Wang, Z. Z., & Degos, L. (2007). Treatment of acute promyelocytic leukemia by retinoids.*Curr. Top. Microbiol. Immunol., 313*, 101–28.
101. Tang, X.-H., & Gudas, L. J. (2011). Retinoids, retinoic acid receptors, and cancer. *Ann. Rev. Pathol.*, *6*, 345–64.
102. Smith, M. A., Parkinson, D. R., Cheson, B. D., & Friedman, M. A. (1992). Retinoids in cancer therapy. *J. Clin. Onc.*, *10*, 839–864.
103. Freemantle, S. J., Spinella, M. J., & Dmitrovsky, E. (2003). Retinoids in cancer therapy and chemoprevention: promise meets resistance. *Oncogene*, *22*, 7305–7315.
104. Penniston, K. L., & Tanumihardjo, S. A. (2006). The acute and chronic toxic effects of vitamin A. *Am. J. Clin. Nutr.*, *83*, 191–201.
105. Curley, R. W., & Fowble, J. W. (1988). Photoisomerization of retinoic acid and its photoprotection in physiologic-like solutions. *Photochem. Photobiol., 47*, 831–835.
106. Murayama, A., Suzuki, T., & Matsui, M. (1997). Photoisomerization of retinoic acids in ethanol under room light: a warning for cell biological study of geometrical isomers of retinoids. *J. Nutr. Sci. Vitaminol., 43*, 167–176.
107. Furr, H. C. (2004). Analysis of Retinoids and Carotenoids: Problems Resolved and Unsolved. *J. Nutr.*, *134*, 281–285.
108. Kistler, A. (1981). Structure-activity relationship of retinoids in fetal rat bone cultures. *Calcif. Tissue Int.*, *33*, 249–254.
109. Jetten, A. M., & Jetten, M. E. R. (1979). Possible role of retinoic acid binding protein in retinoid stimulation of embryonal carcinoma cell differentiation. *Nature*, *278*, 180–182.

110. Manaut, F., Sanz, F., José, J., & Milesi, M. (1991). Automatic search for maximum similarity between molecular electrostatic potential distributions. *J. Comput. Aided Mol. Des.*, *5*, 371–380.

111. Kistler, A. (1984). Structure-activity relationship of retinoids on the differentiation of cultured chick foot skin. *Rouxs Arch. Dev. Biol.*, *194*, 9–17.

112. Bachmair, F., Hoffmann, R., Daxenbichler, G., & Langer, T. (2000). Studies on structure-activity relationships of retinoic acid receptor ligands by means of molecular modeling. *Vitam. Horm.*, *59*, 159–215.

113. Charpentier, B., Bernardon, J.M., Eustache, J., Millois, C., Martin, B., Michel, S., & Shroot, B. (1995). Synthesis, Structure-Affinity Relationships, and Biological Activities of Ligands Binding to Retinoic Acid Receptor Subtypes. *J. Med. Chem.*, *38*, 4993–5006.

114. Maden, M. (2000). The role of retinoic acid in embryonic and post-embryonic development. *Proceed. Nutr. Soc.*, *59*, 65–73.

115. Silveira, E. R., & Moreno, F. S. (1998). Natural retinoids and β-carotene: from food to their actions on gene expression. *J. Nutr. Biochem.*, *9*, 446–456.

116. Li, Y., Wongsiriroj, N., & Blaner, W. S. (2014). The multifaceted nature of retinoid transport and metabolism. *Hepatobiliary Surg. Nutr.*, *3*, 126–139.

117. MacDonald, P. N., & Ong, D. E. (1988). Evidence for a lecithin-retinol acyltransferase activity in the rat small intestine. *J. Biol. Chem.*, *263*, 12478–12482.

118. Siegenthaler, G. (1996). Extra-and intracellular transport of retinoids: a reappraisal. *Horm. Res.*, *45*, 122–127.

119. Newcomer, M. E., & Ong, D. E. Retinol Binding Protein and Its Interaction with Transthyretin. Landes Bioscience. Austin, USA. 2000.

120. Ross, A. C. (1993). Cellular metabolism and activation of retinoids: roles of cellular retinoid-binding proteins. *FASEB J.*, *7*, 317–327.

121. Lidén, M., & Eriksson, U. (2006). Understanding retinol metabolism: structure and function of retinol dehydrogenases. *J. Biol. Chem.*, *281*, 13001–13004.

122. Napoli, J. L. (1996). Biochemical Pathways of Retinoid Transport, Metabolism, and Signal Transduction. *Clin. Immunol. Immunopathol.*, *80*, S52–S62.

123. Das, B. C., Thapa, P., Karki, R., Das, S., Mahapatra, S., Liu, T.-C.,& Evans, T. (2014). Retinoic acid signaling pathways in development and diseases. *Bioorg. Med. Chem.*, *22*, 673–683.

124. Ross, A. C., & Zolfaghari, R. (2011). Cytochrome P450s in the regulation of cellular retinoic acid metabolism. *Annu. Rev. Nutr.*, *31*, 65–87.

125. Cerignoli, F., Guo, X., Cardinali, B., Rinaldi, C., Casaletto, J., Frati, L., Screpanti, I., Gudas, L. J., Gulino, A., Thiele, C. J. & Giannini, G. (2002). retSDR1, a short-chain retinol dehydrogenase/reductase, is retinoic acid-inducible and frequently deleted in human neuroblastoma cell lines. *Cancer Res.*, *62*, 1196–1204.

126. Gallego, O., Belyaeva, O. V, Porté, S., Ruiz, F. X., Stetsenko, A. V, Shabrova, E. V,Kostereva, N. V., Farrés, J., Parés, X. &Kedishvili, N. Y. (2006). Comparative functional analysis of human medium-chain dehydrogenases, short-chain dehydrogenases/reductases and aldo-keto reductases with retinoids. *Biochem. J.*, *399*, 101–109.

127. Ruiz, F. X., Moro, A., Gallego, O., Ardèvol, A., Rovira, C., Petrash, J. M.,Parés, X. & Farrés, J. (2011). Human and rodent aldo-keto reductases from the AKR1B subfamily and their specificity with retinaldehyde. *Chem. Biol. Interact.*, *191*, 199–205.

128. Ray, W. J., Bain, G., Yao, M., & Gottlieb, D. I. (1997). CYP26, a Novel Mammalian Cytochrome P450, Is Induced by Retinoic Acid and Defines a New Family. *J. Biol. Chem.*, *272*, 18702–18708.

129. White, J. A., Beckett-Jones, B., Guo, Y. D., Dilworth, F. J., Bonasoro, J., Jones, G., & Petkovich, M. (1997). cDNA cloning of human retinoic acid-metabolizing enzyme (hP450RAI) identifies a novel family of cytochromes P450. *J. Biol. Chem.*, *272*, 18538–18541.

130. Chen, S., Zhang, Q., Wu, X., Schultz, P. G., & Ding, S. (2004). Dedifferentiation of lineage-committed cells by a small molecule. *J. Am. Chem. Soc.*, *126*, 410–411.

131. Álvarez, R., Vaz, B., Gronemeyer, H., & de Lera, Á. R. (2014). Functions, therapeutic applications, and synthesis of retinoids and carotenoids. *Chem. Rev.*, *114*, 1–125.

132. Paiva, S. A., & Russell, R. M. (1999). Beta-carotene and other carotenoids as antioxidants. *J. Am. Coll. Nutr.*, *18*, 426–33.

133. Sagha, M., & Vardin, M. M. (2015). Opposing Biological Functions of Retinoic Acid in Normal Embryonic Development. *Stem Cell and Translational Investigation*, *2*, 1–3.

134. Alizadeh, F., Bolhassani, A., Khavari, A., Bathaie, S. Z., Naji, T., & Bidgoli, S. A. (2014). Retinoids and their biological effects against cancer. *Int. Immunopharmacol., 18*, 43–9.

135. Han, G., Chang, B., Connor, M. J., & Sidell, N. (1995). Enhanced potency of 9-cis versus all-trans-retinoic acid to induce the differentiation of human neuroblastoma cells. *Differentiation, 59*, 61–9.

136. Boik J. Natural compounds in cancer therapy. 1st ed. Princeton, MN: Oregon Medical Press, 2001.

137. Ponthan, F., Johnsen, J. I., Klevenvall, L., Castro, J., & Kogner, P. (2003). The synthetic retinoid Ro 13-6307 induces neuroblastoma differentiation in vitro and inhibits neuroblastoma tumour growth in vivo. *Int. J. Cancer*, *104*, 418–424.

138. Qiao, J., Paul, P., Lee, S., Qiao, L., Josifi, E., Tiao, J. R., & Chung, D. H. (2012). PI3K/AKT and ERK regulate retinoic acid-induced neuroblastoma cellular differentiation. *Biochem. Biophys. Res. Commun., 424*, 421–426.

139. Vreeland, A. C., Levi, L., Zhang, W., Berry, D. C., & Noy, N. (2014). Cellular retinoic acid-binding protein 2 inhibits tumor growth by two distinct mechanisms. *J. Biol. Chem., 289*, 34065–34073.

140. Polvani, S., Tarocchi, M., Tempesti, S., & Galli, A. (2014). Nuclear receptors and pathogenesis of pancreatic cancer. *J. Gastroenterol., 20*, 12062–12081.

141. Chung, S. S. W., & Wolgemuth, D. J. (2004). Role of retinoid signaling in the regulation of spermatogenesis. *Cytogenet. Genome Res., 105*, 189–202.

142. Henning, P., Conaway, H. H., & Lerner, U. H. (2015). Retinoid receptors in bone and their role in bone remodeling. *Front. Endocrinol., 6*, 31-43.

143. Ono, K., Yoshiike, Y., Takashima, A., Hasegawa, K., Naiki, H., & Yamada, M. (2004). Vitamin A exhibits potent antiamyloidogenic and fibril-destabilizing effects in vitro. *Exper. Neurol., 189*, 380–392.

144. Reiner, D. J., Yu, S.-J., Shen, H., He, Y., Bae, E., & Wang, Y. (2014). 9-Cis retinoic acid protects against methamphetamine-induced neurotoxicity in nigrostriatal dopamine neurons. *Neurotoxicity Res., 25*, 248–261.

145. Takasaki, J., Ono, K., Yoshiike, Y., Hirohata, M., Ikeda, T., Morinaga, A., & Yamada, M. (2011). Vitamin A has anti-oligomerization effects on amyloid-β in vitro. *J. Alzheimer's Dis., 27*, 271–280.

146. Bhat, P. V., & Manolescu, D.-C. (2008). Role of Vitamin A in Determining Nephron Mass and Possible Relationship to Hypertension. *J. Nutr., 138*, 1407–1410.
147. Cvekl, A., & Wang, W.-L. (2009). Retinoic acid signaling in mammalian eye development. *Exper. Eye Res., 89*, 280–291.
148. Halme, A., Cheng, M., & Hariharan, I. K. (2010). Retinoids regulate a developmental checkpoint for tissue regeneration in Drosophila. *Curr. Biol., 20*, 458–463.
149. Durston, A. J., Timmermans, J. P., Hage, W. J., Hendriks, H. F., de Vries, N. J., Heideveld, M., & Nieuwkoop, P. D. (1989). Retinoic acid causes an anteroposterior transformation in the developing central nervous system. *Nature, 340*, 140–144.
150. Kessel, M., & Gruss, P. (1991). Homeotic transformations of murine vertebrae and concomitant alteration of Hox codes induced by retinoic acid. *Cell, 67*, 89–104.
151. Kudoh, T., Wilson, S. W., & Dawid, I. B. (2002). Distinct roles for Fgf, Wnt and retinoic acid in posteriorizing the neural ectoderm. *Developm., 129*, 4335–4346.
152. Uehara, M., Yashiro, K., Takaoka, K., Yamamoto, M., & Hamada, H. (2009). Removal of maternal retinoic acid by embryonic CYP26 is required for correct Nodal expression during early embryonic patterning. *Genes Developm. 23*, 1689–98.
153. White, R. J., & Schilling, T. F. (2008). How degrading: Cyp26s in hindbrain development. *Developm. Dynam., 237*, 2775–2790.
154. Ribes, V., Stutzmann, F., Bianchetti, L., Guillemot, F., Dollé, P., & Le Roux, I. (2008). Combinatorial signalling controls Neurogenin2 expression at the onset of spinal neurogenesis. *Developm. Biol., 321*, 470–481.
155. Begemann, G., & Meyer, A. (2001). Hindbrain patterning revisited: timing and effects of retinoic acid signalling. *BioEssays, 23*, 981–986.
156. Gavalas, A. (2002). ArRAnging the hindbrain. *Trends Neurosc., 25*, 61–64.
157. Krumlauf, R. (1993). Hox genes and pattern formation in the branchial region of the vertebrate head. *Trends in Genetics, 9*, 106–112.
158. Marshall, H., Nonchev, S., Sham, M. H., Muchamore, I., Lumsden, A., & Krumlauf, R. Retinoic acid alters hindbrain Hox code and induces transformation of rhombomeres 2/3 into a 4/5 identity. *Nature, 360*, 737–741.

159. Chen, Y., Pan, F. C., Brandes, N., Afelik, S., Sölter, M., & Pieler, T. (2004). Retinoic acid signaling is essential for pancreas development and promotes endocrine at the expense of exocrine cell differentiation in Xenopus. *Developm. Biol.*, *271*, 144–160.

160. Bayha, E., Jørgensen, M. C., Serup, P., & Grapin-Botton, A. (2009). Retinoic Acid Signaling Organizes Endodermal Organ Specification along the Entire Antero-Posterior Axis. *PLoS ONE*, *4*, 5845-5860.

161. Öström, M., Loffler, K. A., Edfalk, S., Selander, L., Dahl, U., Ricordi, C.,& Edlund, H. (2008). Retinoic Acid Promotes the Generation of Pancreatic Endocrine Progenitor Cells and Their Further Differentiation into β-Cells. *PLoS ONE*, *3*, 2841-2848.

162. Heine, U. I., Roberts, A. B., Munoz, E. F., Roche, N. S., & Sporn, M. B. (1985). Effects of retinoid deficiency on the development of the heart and vascular system of the quail embryo. *Virchows Arch B Cell Pathol Incl Mol Pathol.*, *50*, 135–52.

163. Lin, S.-C., Dollé, P., Ryckebüsch, L., Noseda, M., Zaffran, S., Schneider, M. D., & Niederreither, K. (2010). Endogenous retinoic acid regulates cardiac progenitor differentiation. *Proc Natl Acad Sci* , *107*, 9234–9239.

164. Wingert, R. A., & Davidson, A. J. (2008). The zebrafish pronephros: a model to study nephron segmentation. *Kidney Intern.*, *73*, 1120–1127.

165. Cartry, J., Nichane, M., Ribes, V., Colas, A., Riou, J.-F., Pieler, T., & Umbhauer, M. (2006). Retinoic acid signalling is required for specification of pronephric cell fate. *Dev Biol.*, *299*, 35–51.

166. Rosselot, C., Spraggon, L., Chia, I., Batourina, E., Riccio, P., Lu, B., … Mendelsohn, C. (2010). Non-cell-autonomous retinoid signaling is crucial for renal development. *Development*, *137*, 283–292.

167. Lopez-Real, R. E., Budge, J. J. R., Marder, T. B., Whiting, A., Hunt, P. N., & Przyborski, S. A. (2014). Application of synthetic photostable retinoids induces novel limb and facial phenotypes during chick embryogenesis in vivo. *J. Anat.*, *224*, 392–411.

168. Chamorro-Premuzic, T., von Stumm, S., & Furnham, A. Essential Developmental Biology. *The Wiley-Blackwell, Oxford, UK*.2013.

169. Janesick, A., Wu, S. C., & Blumberg, B. (2015). Retinoic acid signaling and neuronal differentiation. *Cell. Mol. Life Sci.*, 1559–1576.

170. Mongan, N. P., & Gudas, L. J. (2007). Diverse actions of retinoid receptors in cancer prevention and treatment. *Differentiation*, *75*, 853–870.

171. Pacherník, J., Bryja, V., Esner, M., Kubala, L., Dvorák, P., & Hampl, A. (2005). Neural differentiation of pluripotent mouse embryonal carcinoma cells by retinoic acid: inhibitory effect of serum. *Physiol. Res.*, *54*, 115–22.

172. Abranches, E., Silva, M., Pradier, L., Schulz, H., Hummel, O., Henrique, D. & Bekman, E. (2009). Neural differentiation of embryonic stem cells in vitro: a road map to neurogenesis in the embryo. *PloS One*, *4*, 6286-6300.

173. Rohwedel, J., Guan, K., & Wobus, A. M. (1999). Induction of cellular differentiation by retinoic acid in vitro. *Cells Tissues Organs*, *165*, 190–202.

174. Pearson, S., Cuvertino, S., Fleury, M., Lacaud, G., & Kouskoff, V. (2015). In vivo repopulating activity emerges at the onset of hematopoietic specification during embryonic stem cell differentiation. *Stem Cell Rep.*, *4*, 431–444.

175. Niakan, K. K., Han, J., Pedersen, R. A., Simon, C., & Pera, R. A. R. (2012). Human pre-implantation embryo development. *Development*, *139*, 829–841.

176. Zhu, Z., & Huangfu, D. (2013). Human pluripotent stem cells: an emerging model in developmental biology. *Development*, *140*, 705–717.

177. Thomson, J. a., Itskovitz-Eldor, J., Shapiro, S. S., Waknitz, M. A., Swiergiel, J. J., Marshall, V. S., & Jones, J. M. (1998). Embryonic Stem Cell Lines Derived from Human Blastocysts. *Science*, *282*, 1145–1147.

178. Svendsen, C. N. (2013). Back to the future: how human induced pluripotent stem cells will transform regenerative medicine. *Hum. Mol. Genet.*, *22*, 32–38.

179. Aubert, J., Dunstan, H., Chambers, I., & Smith, A. (2002). Functional gene screening in embryonic stem cells implicates Wnt antagonism in neural differentiation. *Nat. Biotechnol.*, *20*, 1240–1245.

180. Kim, M., Habiba, A., Doherty, J. M., Mills, J. C., Mercer, R. W., & Huettner, J. E. (2009). Regulation of mouse embryonic stem cell neural differentiation by retinoic acid. *Dev. Biol.*, *328*, 456–471.

181. Barberi, T., Klivenyi, P., Calingasan, N. Y., Lee, H., Kawamata, H., Loonam, K., Perrier, A. L., Bruses, J., Rubio, M. E., Topf, N., Tabar, V., Harrison, N. L., Beal, M. F., Moore, M. A. &Studer, L. (2003). Neural subtype specification of fertilization and nuclear transfer embryonic stem cells and application in parkinsonian mice. *Nat. Biotechnol.*, *21*, 1200–1207.

182. Glaser, T., & Brüstle, O. (2005). Retinoic acid induction of ES-cell-derived neurons: the radial glia connection. *Trends. Neurosci., 28*, 397–400.

183. Hansen, D. V, Rubenstein, J. L. R., & Kriegstein, A. R. (2011). Deriving excitatory neurons of the neocortex from pluripotent stem cells. *Neuron*, *70*, 645–460.

184. Clagett-Dame, M., McNeill, E. M., & Muley, P. D. (2006). Role of all-trans retinoic acid in neurite outgrowth and axonal elongation. *J. Neurobiol., 66*, 739–756.

185. Sarkar, S. A., & Sharma, R. P. (2002). All-trans-retinoic acid-mediated modulation of p53 during neural differentiation in murine embryonic stem cells. *Cell Biol. Toxicol., 18*, 243–257.

186. Lin, T., Chao, C., Saito, S., Mazur, S. J., Murphy, M. E., Appella, E., & Xu, Y. (2005). p53 induces differentiation of mouse embryonic stem cells by suppressing Nanog expression. *Nat. Cell Biol.*, 7, 165–171.

187. Jain, A. K., Allton, K., Iacovino, M., Mahen, E., Milczarek, R. J., Zwaka, T. P., Kyba, M. & Barton, M. C. (2012). p53 regulates cell cycle and microRNAs to promote differentiation of human embryonic stem cells. *PLoS Biol., 10*, 1001268-1001284.

188. Aylon, Y., Sarver, A., Tovy, A., Ainbinder, E., & Oren, M. (2014). Lats2 is critical for the pluripotency and proper differentiation of stem cells. *Cell Death Differ., 21*, 624–633.

189. Gudas, L. J., & Wagner, J. A. (2011). Retinoids regulate stem cell differentiation. *J. Cell. Physio., 226*, 322–330.

190. Okada, Y., Shimazaki, T., Sobue, G., & Okano, H. (2004). Retinoic-acid-concentration-dependent acquisition of neural cell identity during in vitro differentiation of mouse embryonic stem cells. *Dev. Biol., 275*, 124–142.

191. Gajović, S., St-Onge, L., Yokota, Y., & Gruss, P. (1997). Retinoic acid mediates Pax6 expression during in vitro differentiation of embryonic stem cells. *Differentiation*, *62*, 187–192.

192. Kumar, M., Bagchi, B., Gupta, S. K., Meena, A. S., Gressens, P., & Mani, S. (2007). Neurospheres derived from human embryoid bodies treated with retinoic Acid show an increase in nestin and ngn2 expression that correlates with the proportion of tyrosine hydroxylase-positive cells. *Stem Cells Dev., 16*, 667–681.

193. Chiu, F. C., Feng, L., Chan, S. O., Padin, C., & Federoff, J. H. (1995). Expression of neurofilament proteins during retinoic acid-induced differentiation of P19 embryonal carcinoma cells. *Brain Res. Mol. Brain Res.*, *30*, 77–86.

194. Babuška, V., Kulda, V., Houdek, Z., Pešta, M., Cendelín, J., Zech, N.Pacherník, J., Vožeh, F., Uher, P. & Králíčková, M. (2010). Characterization of P19 cells during retinoic acid induced differentiation. *Prague Med. Rep.*, *111*, 289–299.

195. Varju, P., Katarova, Z., Madarász, E., & Szabó, G. (2002). Sequential induction of embryonic and adult forms of glutamic acid decarboxylase during in vitro-induced neurogenesis in cloned neuroectodermal cell-line, NE-7C2. *J. Neurochem.*, *80*, 605–615.

196. Burdon, T., Smith, A., & Savatier, P. (2002). Signalling, cell cycle and pluripotency in embryonic stem cells. *Trends Cell Biol.*, *12*, 432–438.

197. Purton, L. E., Bernstein, I. D., & Collins, S. J. (1999). All-trans retinoic acid delays the differentiation of primitive hematopoietic precursors (lin-c-kit+Sca-1(+)) while enhancing the terminal maturation of committed granulocyte/monocyte progenitors. *Blood*, *94*, 483–495.

198. Calleja, E. M., & Warrell, R. P. (2000). Differentiating agents in pediatric malignancies: all-trans-retinoic acid and arsenic in acute promyelocytic leukemia. *Curr. Oncol. Rep.*, *2*, 519–523.

199. Ghiaur, G., Yegnasubramanian, S., Perkins, B., Gucwa, J. L., Gerber, J. M., & Jones, R. J. (2013). Regulation of human hematopoietic stem cell self-renewal by the microenvironment's control of retinoic acid signaling. *Proc. Natl. Acad. Sci.*, *110*, 16121–16126.

200. Purton, L. E., Bernstein, I. D., & Collins, S. J. (2000). All-trans retinoic acid enhances the long-term repopulating activity of cultured hematopoietic stem cells. *Blood*, *95*, 470–477.

201. Rönn, R. E., Guibentif, C., Moraghebi, R., Chaves, P., Saxena, S., Garcia, B., & Woods, N.-B. (2015). Retinoic Acid Regulates Hematopoietic Development from Human Pluripotent Stem Cells. *Stem Cell Rep.*, *4*, 269–281.

202. Topletz, A. R., Thatcher, J. E., Zelter, A., Lutz, J. D., Tay, S., Nelson, W. L., & Isoherranen, N. (2012). Comparison of the function and expression of CYP26A1 and CYP26B1, the two retinoic acid hydroxylases. *Biochem. Pharmacol.*, *83*, 149–63.

203. Ye, L., Fan, Z., Yu, B., Chang, J., Al Hezaimi, K., Zhou, X., Park, N. H. & Wang, C.-Y. (2012). Histone demethylases KDM4B and KDM6B promotes osteogenic differentiation of human MSCs. *Cell Stem Cell*, *11*, 50–61.

204. Paik, S., Jung, H. S., Lee, S., Yoon, D. S., Park, M. S., & Lee, J. W. (2012). miR-449a regulates the chondrogenesis of human mesenchymal stem cells through direct targeting of lymphoid enhancer-binding factor-1. *Stem Cells Dev.*, *21*, 3298–3308.

205. Tiaden, A. N., Breiden, M., Mirsaidi, A., Weber, F. A., Bahrenberg, G., Glanz, S., Cinelli, P., Ehrmann, M. & Richards, P. J. (2012). Human serine protease HTRA1 positively regulates osteogenesis of human bone marrow-derived mesenchymal stem cells and mineralization of differentiating bone-forming cells through the modulation of extracellular matrix protein. *Stem Cells*, *30*, 2271–2282.

206. Gong, M., Bi, Y., Jiang, W., Zhang, Y., Chen, L., Hou, N., Chen, J. & Li, T. (2013). Retinoic acid receptor beta mediates all-trans retinoic acid facilitation of mesenchymal stem cells neuronal differentiation. *Int. J. Biochem. Cell Biol.*, *45*, 866–875.

207. Bi, Y., Gong, M., Zhang, X., Zhang, X., Jiang, W., Zhang, Y., Chen, J., Liu, Y., Chuan He, T. &Li, T. (2010). Pre-activation of retinoid signaling facilitates neuronal differentiation of mesenchymal stem cells. *Dev. Growth Differ.*, *52*, 419–431.

208. Sartore, R. C., Campos, P. B., Trujillo, C. A., Ramalho, B. L., Negraes, P. D., Paulsen, B. S., Meletti, T., Costa, E. S., Chicaybam, L., Bonamino, M. H. , Ulrich, H. &Rehen, S. K. (2011). Retinoic acid-treated pluripotent stem cells undergoing neurogenesis present increased aneuploidy and micronuclei formation. *PloS One*, *6*, 20667-20677.

209. Hu, B.-Y., Weick, J. P., Yu, J., Ma, L.-X., Zhang, X.-Q., Thomson, J. A., & Zhang, S.-C. (2010). Neural differentiation of human induced pluripotent stem cells follows developmental principles but with variable potency. *Proc. Natl. Acad. Sci.*, *107*, 4335–4340.

210. Lamas, N. J., Johnson-Kerner, B., Roybon, L., Kim, Y. A., Garcia-Diaz, A., Wichterle, H., & Henderson, C. E. (2014). Neurotrophic requirements of human motor neurons defined using amplified and purified stem cell-derived cultures. *PloS One*, *9*, 110324-110337.

211. Horschitz, S., Matthäus, F., Groß, A., Rosner, J., Galach, M., Greffrath, W., Treede, R. D., Utikal, J., Schloss, P. & Meyer-Lindenberg, A. (2015). Impact of preconditioning with retinoic acid during early development on morphological and functional characteristics of human induced pluripotent stem cell-derived neurons. *Stem Cell Res.*, *15*, 30–41.

212. Toma, J. S., Shettar, B. C., Chipman, P. H., Pinto, D. M., Borowska, J. P., Ichida, J. K.,Fawcett, J. P., Zhang, Y., Eggan, K. & Rafuse, V. F. (2015). Motoneurons derived from induced pluripotent stem cells develop mature phenotypes typical of endogenous spinal motoneurons. *J. Neuros.*, *35*, 1291–1306.

213. Thomson, S. R., Wishart, T. M., Patani, R., Chandran, S., & Gillingwater, T. H. (2012). Using induced pluripotent stem cells (iPSC) to model human neuromuscular connectivity: promise or reality. *J. Anat.*, *220*, 122–130.

214. Devlin, A.-C., Burr, K., Borooah, S., Foster, J. D., Cleary, E. M., Geti, I., Vallier, L., Shaw, C. E., Chandran, S. & Miles, G. B. (2015). Human iPSC-derived motoneurons harbouring TARDBP or C9ORF72 ALS mutations are dysfunctional despite maintaining viability. *Nature Commun.*, *6*, 5999-6011.

215. Zeineddine, D., Hammoud, A. A., Mortada, M., & Boeuf, H. (2014). The Oct4 protein: more than a magic stemness marker. *Am. J. Stem Cells*, *3*, 74–82.

216. Zhong, X., Gutierrez, C., Xue, T., Hampton, C., Vergara, M. N., Cao, L.-H., Peters, A., Park, T. S., Zambidis, E. T., Meyer, J. S., Gamm, D. M., Yau, K. W. & Canto-Soler, M. V. (2014). Generation of three-dimensional retinal tissue with functional photoreceptors from human iPSCs. *Nature Commun.*, *5*, 4047-4078.

217. Andrews, P. W., Matin, M. M., Bahrami, A. R., Damjanov, I., Gokhale, P., & Draper, J. S. (2005). Embryonic stem (ES) cells and embryonal carcinoma (EC) cells: opposite sides of the same coin. *Biochem. Soc. Trans.*, *33*, 1526–1530.

218. Plet, a, Evain, D., & Anderson, W. B. (1982). Effect of retinoic acid treatment of F9 embryonal carcinoma cells on the activity and distribution of cyclic AMP-dependent protein kinase. *J. Biol. Chem.*, *257*, 889–893.

219. Jones-Villeneuve, E. M., McBurney, M. W., Rogers, K. a, & Kalnins, V. I. (1982). Retinoic acid induces embryonal carcinoma cells to differentiate into neurons and glial cells. *J. Cell Biol.*, *94*, 253–262.

220. Simões, P. D., & Ramos, T. (2007). Human pluripotent embryonal carcinoma NTERA2 cl.D1 cells maintain their typical morphology in an angiomyogenic medium. *J. Negat. Results Biomed., 6*, 5-14.

221. Przyborski, S. A., Christie, V. B., Hayman, M. W., Stewart, R., & Horrocks, G. M. (2004). Human embryonal carcinoma stem cells: models of embryonic development in humans. *Stem Cells Dev., 13*, 400–408.

222. Andrews, P. W., Damjanov, I., Simon, D., Banting, G. S., Carlin, C., Dracopoli, N. C., & Føgh, J. (1984). Pluripotent embryonal carcinoma clones derived from the human teratocarcinoma cell line Tera-2. *Lab. Invest., 50*, 147–162.

223. Clemens, G., Flower, K. R., Henderson, A. P., Whiting, A., Przyborski, S. A., Jimenez-Hernandez, M., Ball, F., Bassan, P., Cinque, G. & Gardner, P. (2013). The action of all-trans-retinoic acid (ATRA) and synthetic retinoid analogues (EC19 and EC23) on human pluripotent stem cells differentiation investigated using single cell infrared microspectroscopy. *Mol. BioSys., 9*, 677–692.

224. Clemens, G., Flower, K. R., Gardner, P., Henderson, A. P., Knowles, J. P., Marder, T. B., Whiting, A. & Przyborski, S. (2013). Design and biological evaluation of synthetic retinoids: probing length vs. stability vs. activity. *Mol. BioSys., 9*, 3124–3134.

225. Soprano, D. R., Teets, B. W., & Soprano, K. J. (2007). Role of retinoic acid in the differentiation of embryonal carcinoma and embryonic stem cells. *Vit. Horm., 75*, 69–95.

226. Mills, K. J., Vollberg, T. M., Nervi, C., Grippo, J. F., Dawson, M. I., & Jetten, A. M. (1996). Regulation of retinoid-induced differentiation in embryonal carcinoma PCC4.aza1R cells: effects of retinoid-receptor selective ligands. *Cell Growth Differ., 7*, 327–337.

227. Jeong, Y., & Mangelsdorf, D. J. (2009). Nuclear receptor regulation of stemness and stem cell differentiation. *Exp. Mol. Med., 41*, 525–537.

228. Johnson, J. E., Zimmerman, K., Saito, T., & Anderson, D. J. (1992). Induction and repression of mammalian achaete-scute homologue (MASH) gene expression during neuronal differentiation of P19 embryonal carcinoma cells. *Development, 114*, 75–87.

229. Shahhoseini, M., Taei, A., Mehrjardi, N. Z., Salekdeh, G. H., & Baharvand, H. (2010). Epigenetic analysis of human embryonic carcinoma cells during retinoic acid-induced neural differentiation. *Biochem. Cell Biol.*, *88*, 527–538.

230. Fujikura, J., Yamato, E., Yonemura, S., Hosoda, K., Masui, S., Nakao, K.,Miyazaki, Ji. J. & Niwa, H. (2002). Differentiation of embryonic stem cells is induced by GATA factors. *Genes Dev.*, *16*, 784–789.

231. Andrew Tee, P. Y. L. G. M. M. and T. L. *Neuroblastoma - Present and Future*. InTech. U.S.A. 2012.

232. Cheung, Y.-T., Lau, W. K.-W., Yu, M.-S., Lai, C. S.-W., Yeung, S.-C., So, K.-F., & Chang, R. C.-C. (2009). Effects of all-trans-retinoic acid on human SH-SY5Y neuroblastoma as in vitro model in neurotoxicity research. *Neurotoxicol.*, *30*, 127–135.

233. Park, S. H., Kim, S., Park, C. J., Jang, S., Chi, H. S., Koh, K. N., Im, H. J. & Seo, J. J. (2013). Presence of differentiating neuroblasts in bone marrow is a favorable prognostic factor for bone marrow metastatic neuroblastoma at diagnosis. *Ann. Lab. Med.*, *33*, 89–96.

234. Acosta, S., Lavarino, C., Paris, R., Garcia, I., de Torres, C., Rodríguez, E., Beleta, H. &Mora, J. (2009). Comprehensive characterization of neuroblastoma cell line subtypes reveals bilineage potential similar to neural crest stem cells. *BMC Dev. Biol.*, *9*, 12-26.

235. Goldstein, M. N., Burdman, J. A., & Journey, L. J. (1964). Long-Term Tissue Culture of Neuroblastomas. II. Morphologic Evidence for Differentiation and Maturation. *J. Natl. Cancer Inst.*, *32*, 165–199.

236. Armstrong, J. L., Martin, S., Illingworth, N. A., Jamieson, D., Neilson, A., Lovat, P. E., Redfern, C. P. & Veal, G. J. (2012). The impact of retinoic acid treatment on the sensitivity of neuroblastoma cells to fenretinide. *Oncol. Rep.*, *27*, 293–298.

237. Lovat, P. E., Irving, H., Pearson, A. D. J., Redfern, C. P. F., Malcolm, A. J., Annicchiarico-Petruzzelli, M., Redfern, C. P.& Melino, G. (1997). Apoptosis of N-Type Neuroblastoma Cells after Differentiation With 9-cis-Retinoic Acid and Subsequent Washout.*J. Natl. Cancer Inst.*, *89*, 446–452.

238. Giannini, G., Dawson, M. I., Zhang, X., & Thiele, C. J. (1997). Activation of three distinct RXR/RAR heterodimers induces growth arrest and differentiation of neuroblastoma cells. *J. Biol. Chem.*, *272*, 26693–26701.

239. Cheung, B., Hocker, J. E., Smith, S. A., Norris, M. D., Haber, M., & Marshall, G. M. (1998). Favorable prognostic significance of high-level retinoic acid receptor beta expression in neuroblastoma mediated by effects on cell cycle regulation. *Oncogene*, *17*, 751–759.

240. Redfern, C. P., Lovat, P. E., Malcolm, A. J., & Pearson, A. D. (1994). Differential effects of 9-cis and all-*trans*-retinoic acid on the induction of retinoic acid receptor-beta and cellular retinoic acid-binding protein II in human neuroblastoma cells. *Biochem. J.*, *304*, 147–54.

241. Hewson, Q. C., Lova, P. E., Malcolm, A. J., Pearson, A. D., & Redfern, C. P. (2000). Receptor mechanisms mediating differentiation and proliferation effects of retinoids on neuroblastoma cells. *Neurosc. Lett.*, *279*, 113–116.

242. Kaplan, D. R., Matsumoto, K., Lucarelli, E., & Thiele, C. J. (1993). Induction of TrkB by retinoic acid mediates biologic responsiveness to BDNF and differentiation of human neuroblastoma cells. *Neuron*, *11*, 321–331.

243. Ichimiya, S., Nimura, Y., Seki, N., Ozaki, T., Nagase, T., & Nakagawara, A. (2001). The vitamin A analogues: 13-cis retinoic acid, 9-cis retinoic acid, and Ro 13-6307 inhibit neuroblastoma tumour growth in vivo. *Med. Pediatr. Oncol.*, 36, 127–131.

244. Cosgaya, J. M., Garcia-Villalba, P., Perona, R., & Aranda, A. (2002). Comparison of the Effects of Retinoic Acid and Nerve Growth Factor on PC12 Cell Proliferation, Differentiation, and Gene Expression. *J. Neurochem.*, *66*, 89–98.

245. Scheibe, R. J., Ginty, D. D., & Wagner, J. A. (1991). Retinoic acid stimulates the differentiation of PC12 cells that are deficient in cAMP-dependent protein kinase. *J. Cell Biol.*, *113*, 1173–1182.

246. Jackson, G. R., Morgan, B. C., Werrbach-Perez, K., & Perez-Polo, J. R. (1991). Antioxidant effect of retinoic acid on PC12 rat pheochromocytoma. *Int. J. Dev. Neurosc.*, *9*, 161–170.

247. Bennett, J. M., Catovsky, D., Daniel, M. T., Flandrin, G., Galton, D. A., Gralnick, H. R., & Sultan, C. (1976). Proposals for the classification of the acute leukaemias. French-American-British (FAB) co-operative group. *Br. J. Haematol.*, *33*, 451–458.

248. Breitman, T. R., Collins, S. J., & Keene, B. R. (1981). Terminal differentiation of human promyelocytic leukemic cells in primary culture in response to retinoic acid. *Blood*, *57*, 1000–1004.

249. Degos, L., & Wang, Z. Y. (2001). All-*trans*-retinoic acid in acute promyelocytic leukemia. *Oncogene*, *20*, 7140–7145.

250. Adamson, P. (1996). All-Trans-Retinoic Acid Pharmacology and Its Impact on the Treatment of Acute Promyelocytic Leukemia. *Oncologist*, *1*, 305–314.

251. Hatake, K., Uwai, M., Ohtsuki, T., Tomizuka, H., Izumi, T., Yoshida, M., & Miura, Y. (1997). Rare but important adverse effects of all-*trans*-retinoic acid in acute promyelocytic leukemia and their management. *Int. J. Hematol.*, *66*, 13–19.

252. Zhou, G.-B., Zhang, J., Wang, Z.-Y., Chen, S.-J., & Chen, Z. (2007). Treatment of acute promyelocytic leukaemia with all-trans retinoic acid and arsenic trioxide: a paradigm of synergistic molecular targeting therapy. *Philos. Trans. R. Soc. Lond., B, Biol. Sci.*, *362*, 959–971.

253. Zhu, J., Shi, X. G., Chu, H. Y., Tong, J. H., Wang, Z. Y., Naoe, T., Waxman, S., Chen, S. J. & Chen, Z. (1995). Effect of retinoic acid isomers on proliferation, differentiation and PML relocalization in the APL cell line NB4. *Leukemia*, *9*, 302–309.

254. Kirino, T., Brightman, M. W., Oertel, W. H., Schmechel, D. E., & Marangos, P. J. (1983). Neuron-specific enolase as an index of neuronal regeneration and reinnervation. *J. Neurosci.*, *3*, 915–923.

255. Matranga, V., Oliva, D., Sciarrino, S., D'Amelio, L., & Giallongo, A. (1993). Differential expression of neuron-specific enolase mRNA in mouse neuroblastoma cells in response to differentiation inducing agents. *Cell Mol. Neurobiol.*, *13*, 137–145.

256. Marrelli, M., Paduano, F., & Tatullo, M. (2015). Human periapical cyst-mesenchymal stem cells differentiate into neuronal cells. *J. Dental Res.*, *94*, 843–852.

257. Encinas, M., Iglesias, M., Liu, Y., Wang, H., Muhaisen, A., Ceña, V., Gallego, C. &Comella, J. X. (2000). Sequential treatment of SH-SY5Y cells with retinoic acid and brain-derived neurotrophic factor gives rise to fully differentiated, neurotrophic factor-dependent, human neuron-like cells. *J. Neurochem.*, *75*, 991–1003.

258. Sarnat, H. B., Nochlin, D., & Born, D. E. (1998). Neuronal nuclear antigen (NeuN): a marker of neuronal maturation in the early human fetal nervous system. *Brain Dev.*, *20*, 88–94.

259. Kim, K. K., Adelstein, R. S., & Kawamoto, S. (2009). Identification of neuronal nuclei (NeuN) as Fox-3, a new member of the Fox-1 gene family of splicing factors. *J. Biol. Chem.*, *284*, 31052–31061.

260. Gusel'nikova, V. V, & Korzhevskiy, D. E. NeuN as a Neuronal Nuclear Antigen and Neuron Differentiation Marker. *Acta Naturae*, *7*, 42–47.

261. Farooqui, A. A., Antony, P., Ong, W.-Y., Horrocks, L. A., & Freysz, L. (2004). Retinoic acid-mediated phospholipase A2 signaling in the nucleus. *Brain Res. Rev.*, *45*, 179–195.

262. Dehmelt, L., Smart, F. M., Ozer, R. S., & Halpain, S. (2003). The role of microtubule-associated protein 2c in the reorganization of microtubules and lamellipodia during neurite initiation. *J. Neurosci.*, *23*, 9479–9490.

263. Soltani, M. H., Pichardo, R., Song, Z., Sangha, N., Camacho, F., Satyamoorthy, K., Sangueza, O. P. & Setaluri, V. (2005). Microtubule-associated protein 2, a marker of neuronal differentiation, induces mitotic defects, inhibits growth of melanoma cells, and predicts metastatic potential of cutaneous melanoma. *Am. J. Pathol.*, *166*, 1841–1850.

264. Zhang, L., Yan, L., Zhang, Y., Wu, N., & Shen, Y. (2010). Role of acetylated p53 in regulating the expression of map2 in retinoic acid-induced P19 cells. *Chin. Med. Sci. J.*, *25*, 71–75.

265. Yu, S., Levi, L., Siegel, R., & Noy, N. (2012). Retinoic acid induces neurogenesis by activating both retinoic acid receptors (RARs) and peroxisome proliferator-activated receptor β/δ (PPARβ/δ). *J. Biol. Chem.*, *287*, 42195–42205.

266. Hamada-Kanazawa, M., Ishikawa, K., Nomoto, K., Uozumi, T., Kawai, Y., Narahara, M., & Miyake, M. (2004). Sox6 overexpression causes cellular aggregation and the neuronal differentiation of P19 embryonic carcinoma cells in the absence of retinoic acid. *FEBS Lett.*, *560*, 192–198.

267. Erceg, S., Laínez, S., Ronaghi, M., Stojkovic, P., Pérez-Aragó, M. A., Moreno-Manzano, V., Moreno-Palanques, R., Planells-Cases, R. &Stojkovic, M. (2008). Differentiation of human embryonic stem cells to regional specific neural precursors in chemically defined medium conditions. *PloS One*, *3*, 2122-2132.

268. Tondreau, T., Lagneaux, L., Dejeneffe, M., Massy, M., Mortier, C., Delforge, A., & Bron, D. (2004). Bone marrow-derived mesenchymal stem cells already express specific neural proteins before any differentiation. *Differentiation*, *72*, 319–326.

269. Guo, J., Walss-Bass, C., & Ludueña, R. F. (2010). The beta isotypes of tubulin in neuronal differentiation. *Cytoskeleton, 67,* 431–441.

270. Laferrière, N. B., & Brown, D. L. (1996). Expression and posttranslational modification of class III beta-tubulin during neuronal differentiation of P19 embryonal carcinoma cells. *Cell Motil. Cytoskeleton, 35*, 188–99.

271. Chae, J. H., Stein, G. H., & Lee, J. E. (2004). NeuroD: the predicted and the surprising. *Mol. Cells*, *18*, 271–288.

272. Gao, Z., Ure, K., Ables, J. L., Lagace, D. C., Nave, K.-A., Goebbels, S., Eisch A. J.& Hsieh, J. (2009). Neurod1 is essential for the survival and maturation of adult-born neurons. *Nat. Neurosci., 12*, 1090–1092.

273. Liu, Y., Encinas, M., Comella, J. X., Aldea, M., & Gallego, C. (2004). Basic helix-loop-helix proteins bind to TrkB and p21 (Cip1) promoters linking differentiation and cell cycle arrest in neuroblastoma cells. *Mol. Cell. Biol.*, *24*, 2662–2672.

274. Uruno, A., Saito-Hakoda, A., Yokoyama, A., Kogure, N., Matsuda, K., Parvin, R., Shimizu, K., Sato, I., Kudo, M., Yoshikawa, T., Kagechika, H., Iwasaki, Y., Ito, S. & Sugawara, A. (2014). Retinoic acid receptor-α up-regulates proopiomelanocortin gene expression in AtT20 corticotroph cells. *Endocr. J., 61*, 1105–1114.

275. Suzuki, S., Namiki, J., Shibata, S., Mastuzaki, Y., & Okano, H. (2010). The neural stem/progenitor cell marker nestin is expressed in proliferative endothelial cells, but not in mature vasculature. *J. Histochem. Cytochem.*, *58*, 721–730.

276. Park, D., Xiang, A. P., Mao, F. F., Zhang, L., Di, C.-G., Liu, X.-M., Shao, Y., Ma, B. F., Lee, J. H., Ha, K. S., Walton, N. & Lahn, B. T. (2010). Nestin is required for the proper self-renewal of neural stem cells. *Stem Cells, 28*, 2162–2171.

277. Strojnik, T., Røsland, G. V., Sakariassen, P. O., Kavalar, R., & Lah, T. (2007). Neural stem cell markers, nestin and musashi proteins, in the progression of human glioma: correlation of nestin with prognosis of patient survival. *Surg. Neurol. Int.*, *68*, 133–143.

278. Xu, J., Wang, H., Liang, T., Cai, X., Rao, X., Huang, Z., & Sheng, G. (2012). Retinoic acid promotes neural conversion of mouse embryonic stem cells in adherent monoculture. *Mol. Biol. Rep.*, *39*, 789–795.

279. Hämmerle, B., Yañez, Y., Palanca, S., Cañete, A., Burks, D. J., Castel, V., & Font de Mora, J. (2013). Targeting neuroblastoma stem cells with retinoic acid and proteasome inhibitor. *PloS One*, *8*, 76761-76776.

280. Shen, S., Kruyt, F. A., den Hertog, J., van der Saag, P. T., & Kruijer, W. (1991). Mouse and human retinoic acid receptor beta 2 promoters: sequence comparison and localization of retinoic acid responsiveness. *DNA Seq.*, *2*, 111–119.

281. Dollé, P., Ruberte, E., Leroy, P., Morriss-Kay, G., & Chambon, P. (1990). Retinoic acid receptors and cellular retinoid binding proteins. I. A systematic study of their differential pattern of transcription during mouse organogenesis. *Development*, *110*, 1133–1151.

282. Corcoran, J., So, P. L., Barber, R. D., Vincent, K. J., Mazarakis, N. D., Mitrophanous, K. A., Kingsman, S. M. & Maden, M. (2002). Retinoic acid receptor beta 2 and neurite outgrowth in the adult mouse spinal cord in vitro. *J. Cell Sci.*, *115*, 3779–3786.

283. Corcoran, J., Shroot, B., Pizzey, J., & Maden, M. (2000). The role of retinoic acid receptors in neurite outgrowth from different populations of embryonic mouse dorsal root ganglia. *J. Cell Sci.*, *113*, 2567–2574.

284. Goncalves, M. B. C. V, Agudo, M., Connor, S., McMahon, S., Minger, S. L., Maden, M., & Corcoran, J. P. T. (2009). Sequential RARbeta and alpha signalling in vivo can induce adult forebrain neural progenitor cells to differentiate into neurons through Shh and FGF signalling pathways. *Dev. Biol.*, *326*, 305–313.

285. Tsuchida, T., Ensini, M., Morton, S. B., Baldassare, M., Edlund, T., Jessell, T. M., & Pfaff, S. L. (1994). Topographic organization of embryonic motor neurons defined by expression of LIM homeobox genes. *Cell*, *79*, 957–970.

286. Goncalves, M. B. C. V, Boyle, J., Webber, D. J., Hall, S., Minger, S. L., & Corcoran, J. P. T. (2005). Timing of the retinoid-signalling pathway determines the expression of neuronal markers in neural progenitor cells. *Dev. Biol.*, *278*, 60–70.

287. Grunt, T. W., Tomek, K., Wagner, R., Puckmair, K., & Zielinski, C. C. (2007). The DNA-binding epidermal growth factor-receptor inhibitor PD153035 and other DNA-intercalating cytotoxic drugs reactivate the expression of the retinoic acid receptor-beta tumor-suppressor gene in breast cancer cells. *Differentiation*, *75*, 883–90.

288. Lin, Y., Zhu, M., Zhou, S., Xie, X., & Li, M. (2010). Effects of alpha-fetoprotein on the expression of TRAIL death receptor-2 and its role on resisting the cytotoxicity of TRAIL in hepatoma cells. *Chin. J. Hepatol.*, *18*, 745–750.

289. Khuri, F. R., Lotan, R., Kemp, B. L., Lippman, S. M., Wu, H., Feng, L., Lee, J. J., Cooksley, C. S., Parr, B., Chang, E., Walsh, G. L., Lee, J. S., Hong, W.K. & Xu, X. C. (2000). Retinoic Acid Receptor-Beta as a Prognostic Indicator in Stage I Non-Small-Cell Lung Cancer. *J. Clin. Oncol.*, *18*, 2798–2804.

290. Vivat-Hannah, V., You, D., Rizzo, C., Daris, J. P., Lapointe, P., Zusi, F. C., Marinier, A., Lorenzi, M.V. &Gottardis, M. M. (2001). Synergistic cytotoxicity exhibited by combination treatment of selective retinoid ligands with taxol (Paclitaxel). *Cancer Res.*, *61*, 8703–8711.

291. Koster, A. J., & Klumperman, J. (2003). Electron microscopy in cell biology: integrating structure and function. *Nat. Rev. Mol. Cell Biol.*, 6–10.

292. Hanrieder, J., Phan, N. T. N., Kurczy, M. E., & Ewing, A. G. (2013). Imaging mass spectrometry in neuroscience. *ACS Chem. Neurosci.*, *4*, 666–679.

293. Boxer, S. G., Kraft, M. L., & Weber, P. K. (2009). Advances in Imaging Secondary Ion Mass Spectrometry for Biological Samples. *Annu Rev Biophys.*, *38*, 53–74.

294. Notingher, I. (2007). Raman Spectroscopy Cell-based Biosensors. *Sensors*, *7*, 1343-1358.

295. Gardiner, D., Graves, P. Practical Raman Spectroscopy. Wiley, 1989.

296. Chan, J., Fore, S., Wachsmann-Hogiu, S., & Huser, T. (2008). Raman spectroscopy and microscopy of individual cells and cellular components. *Laser Photon. Rev.*, *2*, 325-349.

297. Schie, I. W., & Huser, T. *Comprehensive Physiology*. (R. Terjung, Ed.) *Comprehensive Physiology* (Vol. 3). John Wiley & Sons, Inc. Hoboken, 2013.

298. Notingher, I., Jell, G., Lohbauer, U., Salih, V., & Hench, L. L. (2004). In situ non-invasive spectral discrimination between bone cell phenotypes used in tissue engineering. *J. Cell. Biochem.*, *92*, 1180–1192.

299. Chan, J. W., Lieu, D. K., Huser, T., & Li, R. A. (2009). Label-free separation of human embryonic stem cells and their cardiac derivatives using Raman spectroscopy. *Anal. Chem.*, *81*, 1324–1331.

300. Schulze, H. G., Konorov, S. O., Caron, N. J., Piret, J. M., Blades, M. W., & Turner, R. F. B. (2010). Assessing differentiation status of human embryonic stem cells noninvasively using Raman microspectroscopy. *Anal. Chem.*, *82*, 5020–5027.

301. Shao, Y., Molnar, L. F., Jung, Y., Kussmann, J., Ochsenfeld, C., Brown, S. T., Gilbert, A. T. B., Slipchenko, L. V., Levchenko, S. V., O'Neill, D. P., Di Stasio Jr, R. A., Lochan, R. C., Wang, T., Beran, G. J. O., Besley, N. A., Herbert, J. M., Lin, C. Y., Voorhis, T. V., Chien, S. H., Sodt, A., Steele, R.P., Rassolov, V.A., Maslen,P.E., Korambath, P. P., Adamson, R. D., Austin, B., Baker, J., Byrd, E. F. C., Dachsel, H., Doerksen, R. J., Dreuw, A., Dunietz, B. D., Dutoi, A. D., Furlani, T. R. Gwaltney, S. R., Heyden,A., Hirata, S., Hsu, C., Kedziora, G., Khalliulin, R. Z., Klunzinger, P., Lee, A. M., Lee, M. S., Liang, W., Lotan, I., Nair, N., Peters, B., Proynov, E. I., Pieniazek, P.A., Rhee, Y. M., Ritchie, J., Rosta, E., Sherrill, C. D., Simmonett, A. C., Subotnik, J. E., Woodcock III, H. L., Zhang, W., Bell, A. T., Chakraborty, A. K., Chipman, D. M., Keil, F. J., Warshel, A., Hehre, W. J., Schaefer III, H. F., Kong, J., Krylov, A. I., Gilla, P. M. W. & Head-Gordon, M. (2006). Advances in methods and algorithms in a modern quantum chemistry program package. *Phys. Chem. Chem. Phys.*, *8*, 3172–3191.

302. Gardiner, E. J., Willett, P. & Artymiuk, P. J. (2001). Protein docking using a genetic algorithm. *Proteins*, *44*, 44–56.

303. Pettersen, E. F., Goddard, T. D., Huang, C. C., Couch, G. S., Greenblatt, D. M., Meng, E. C. & Ferrin, T. E. (2004). UCSF Chimera - A visualization system for exploratory research and analysis. *J. Comput. Chem.*, *25*, 1605–1612.

304. Baker, E. N., & Hubbard, R. E. (1984). Hydrogen Bonding in Globular Proteins. *Prog. Biophys. Molec. Biol.*, *44*, 97–179.

305. Chang, C. y, Norris, J. D., Grøn, H., Paige, L. A., Hamilton, P. T., Kenan, D. J., Fowlkes, D. & McDonnell, D. P. (1999). Dissection of the LXXLL nuclear receptor-coactivator interaction motif using combinatorial peptide libraries: discovery of peptide antagonists of estrogen receptors alpha and beta. *Mol. Cell Biol.*, *19*, 8226-8239.

306. Zhang, J. H. (1999). A Simple Statistical Parameter for Use in Evaluation and Validation of High Throughput Screening Assays. *J. Biomol. Screen.*, *4*, 67-73.

307. Hoops, S., Gauges, R., Lee, C., Pahle, J., Simus, N., Singhal, M., Xu, L. & Mendes, P., Kummer, U. (2006). COPASI - A complex Pathway Simulator. *Bioinformatics*, *22*, 3067–3074.

308. Waage, P., & Gulberg, C. M. (1986). Studies concerning affinity. *J. Chem. Educ.*, *63*, 1044 -1047.

309. Przyborski, S. A. (2001). Isolation of human embryonal carcinoma stem cells by immunomagnetic sorting. *Stem Cells, 19*, 500–504.

310. Constantinescu, R., Constantinescu, A. T., Reichmann, H., & Janetzky, B. (2007). Neuronal differentiation and long-term culture of the human neuroblastoma line SH-SY5Y. *J. Neural Transm. Suppl., 72*, 17–28.

311. Kramer, B., Rarey, M., &Lengauer, T. (1999). Evaluation of the FLEXX incremental construction algorithm for protein-ligand docking. *Proteins, 37*, 228–241.

312. Ewing, T. J., Makino, S., Skillman, A. G., & Kuntz, I. D. (2001). DOCK 4.0: search strategies for automated molecular docking of flexible molecule databases. *J. Comput. Aided Mol. Des., 15*, 411–428.

313. Jones, G., Willett, P., Glen, R. C., Leach, A. R., & Taylor, R. (1997). Development and validation of a genetic algorithm for flexible docking. *J. Mol. Biol., 267*, 727–748.

314. Christie, V. B., Barnard, J. H., Batsanov, A. S., Bridgens, C. E., Cartmell, E. B., Collings, J. C., Marder, T. B., Przyborski, S., Redfern, C. P. F. & Whiting, A. (2008). Synthesis and evaluation of synthetic retinoid derivatives as inducers of stem cell differentiation. *Org. Biomol. Chem., 6*, 3497–3507.

315. Bourhis, L. J., Dolomanov, O. V., Gildea, R. J., Howard, J. A. K. & Puschmann, H. (2015). The anatomy of a comprehensive constrained, restrained refinement program for the modern computing environment – Olex2 dissected. *ActaCrystallogr. A, Found. Adv.***,** *71*, 59–75.

316. Pettersen, E. F., Goddard, T. D., Huang, C. C., Couch, G. S., Greenblatt, D. M., Meng, E. C. & Ferrin, T. E. (2004). UCSF Chimera - A visualization system for exploratory research and analysis. *J. Comput. Chem., 25*, 1605–1612.

317. Zhang, Z. P., Shukri, M., Gambone, C. J., Gabriel, J. L., Soprano, K. J., Soprano, D. R. (2000). Role of Ser (289) in RARgamma and its homologous amino acid residue of RARalpha and RARbeta in the binding of retinoic acid. *Arch. Biochem. Biophys., 380*, 339–346.

318. Lavery, D. N., & McEwan, I. J. (2008). Functional characterization of the native NH2 terminal transactivation domain of the human androgen receptor: binding kinetics for interactions with TFIIF and SRC-1a. *Biochemistry, 47*(11), 3352–3359.

319. Kwok, K. C., & Cheung, N. H. (2010). Measuring binding kinetics of ligands with tethered receptors by fluorescence polarization and total internal reflection fluorescence. *Anal.Chem.*, *82*(9), 3819–3825.

320. Mahairaki, V., Ryu, J., Peters, A., Chang, Q., Li, T., Park, T. S., Burridge, P. W., Talbot, C. C., Jr Asnaghi, L., Martin, L. J., Zambidis, E. T. & Koliatsos, V. E. (2014). Induced pluripotent stem cells from familial Alzheimer's disease patients differentiate into mature neurons with amyloidogenic properties. *Stem Cells Dev.*, *23*, 2996–3010.

321. Rosenberg, L., & Vinik, A. I. (1989). Induction of endocrine cell differentiation: a new approach to management of diabetes. *J. Lab. Clin. Med.*, *114*, 75–83.

322. Sharpe, C., & Goldstone, K. (2000). The control of Xenopus embryonic primary neurogenesis is mediated by retinoid signalling in the neurectoderm. *Mech. Dev.*, *91*, 69–80.

323. Begemann, G., & Meyer, A. (2001). Hindbrain patterning revisited: timing and effects of retinoic acid signalling. *BioEssays, 23*, 981–986.

324. Novitch, B. G., Wichterle, H., Jessell, T. M., & Sockanathan, S. (2003). A requirement for retinoic acid-mediated transcriptional activation in ventral neural patterning and motor neuron specification. *Neuron*, *40*, 81–95.

325. Thaller, C., & Eichele, G. Identification and spatial distribution of retinoids in the developing chick limb bud. *Nature*, *327*, 625–628.

326. Schuldiner, M., Eiges, R., Eden, A., Yanuka, O., Itskovitz-Eldor, J., Goldstein, R. S., & Benvenisty, N. (2001). Induced neuronal differentiation of human embryonic stem cells. *Brain Res.*, *913*, 201–205.

327. Andrews, P. W. (1984). Retinoic acid induces neuronal differentiation of a cloned human embryonal carcinoma cell line in vitro. *Dev. Biol.*, *103*, 285–293.

328. Jiang, W., Shi, Y., Zhao, D., Chen, S., Yong, J., Zhang, J., Qing, T., Sun, X., Zhang, P., Ding, M., Li, D. & Deng, H. (2007). In vitro derivation of functional insulin-producing cells from human embryonic stem cells. *Cell Res.*, *17*, 333–344.

329. Yamashita, A., Takada, T., Narita, J., Yamamoto, G., & Torii, R. (2005). Osteoblastic differentiation of monkey embryonic stem cells in vitro. Cloning *Stem Cells*, *7*, 232–237.

330. Connolly, R. M., Nguyen, N. K., & Sukumar, S. (2013). Molecular pathways: current role and future directions of the retinoic acid pathway in cancer prevention and treatment. *Clin. Cancer Res., 19*, 1651–1659.

331. Liu, S.-M., Chen, W., & Wang, J. (2014). Distinguishing between cancer cell differentiation and resistance induced by all-trans retinoic acid using transcriptional profiles and functional pathway analysis. *Sci. Rep., 4*, 5577-5585.

332. Rowe, A. (1997). Retinoid X receptors. *Int. J. Biochem. Cell Biol., 29*, 275–278.

333. Mangelsdorf, D. J., & Evans, R. M. (1995). The RXR heterodimers and orphan receptors. *Cell*, *83*, 841–850.

334. Chambon, P. (1994). The retinoid signaling pathway: molecular and genetic analyses. *Semin. Cell Biol., 5*, 115–125.

335. Gang, E. J., Bosnakovski, D., Figueiredo, C. A., Visser, J. W., &Perlingeiro, R. C. R. (2007). SSEA-4 identifies mesenchymal stem cells from bone marrow. *Blood*, *109*, 1743–1751.

336. Storch, A., Ludolph, A. C., & Schwarz, J. (2004). Dopamine transporter: involvement in selective dopaminergic neurotoxicity and degeneration. *J. Neural Transm., 111*, 1267–1286.

337. Gillespie, R. F., & Gudas, L. J. (2007). Retinoid regulated association of transcriptional co-regulators and the polycomb group protein SUZ12 with the retinoic acid response elements of Hoxa1, RARbeta (2), and Cyp26A1 in F9 embryonal carcinoma cells. *J. Mol. Biol., 372*, 298–316.

338. Tonge, P. D., & Andrews, P. W. (2010). Retinoic acid directs neuronal differentiation of human pluripotent stem cell lines in a non-cell-autonomous manner. *Differentiation*, *80*, 20–30.

339. Lee, V. M., & Andrews, P. W. (1986). Differentiation of NTERA-2 clonal human embryonal carcinoma cells into neurons involves the induction of all three neurofilament proteins. *Neuroscience*, *6*, 514–521.

340. Xie, H., Hu, L., & Li, G. (2010). SH-SY5Y human neuroblastoma cell line: in vitro cell model of dopaminergic neurons in Parkinson's disease. *Chin. Med. J., 123*, 1086–1092.

341. Abemayor, E., & Sidell, N. (1989). Human neuroblastoma cell lines as models for the in vitro study of neoplastic and neuronal cell differentiation. *Environ. Health Perspect., 80*, 3–15.

342. Hashemi, S. H., Li, J.-Y., Ahlman, H., & Dahlström, A. (2003). SSR2 (a) receptor expression and adrenergic/cholinergic characteristics in differentiated SH-SY5Y cells. *Neurochem. Res., 28*, 449–460.

343. Gaardsvoll, H., Obendorf, D., Winkler, H., & Bock, E. (1988). Demonstration of immunochemical identity between the synaptic vesicle proteins synaptin and synaptophysin/p38. *FEBS Lett., 242*, 117–120.

344. Tahirovic, S., &Bradke, F. (2009). Neuronal Polarity. *Cold Spring Harb.Perspect. Biol., 1*, 1644–1661.

345. Böcker, W., Moll, R., Poremba, C., Holland, R., Van Diest, P. J., Dervan, P., & Buchwallow, I. B. (2002). Common adult stem cells in the human breast give rise to glandular and myoepithelial cell lineages: a new cell biological concept. *Lab Invest. , 82*, 737–746.

346. Sidell, N., Chang, B., Yamashiro, J. M., & Wada, R. K. (1998). Transcriptional upregulation of retinoic acid receptor beta (RAR beta) expression by phenylacetate in human neuroblastoma cells. *Exp Cell Res., 239*, 169–174.

347. Lee, H.-P., Casadesus, G., Zhu, X., Lee, H., Perry, G., Smith, M. A., Gustaw-Rothenberg, K.& Lerner, A. (2009). All-trans retinoic acid as a novel therapeutic strategy for Alzheimer's disease. *Expert Rev. Neurother., 9*, 1615–1621.

348. Gericke, J., Ittensohn, J., Mihály, J., Alvarez, S., Alvarez, R., Töröcsik, D.,de Lera, A. R.&Rühl, R. (2013). Regulation of retinoid-mediated signaling involved in skin homeostasis by RAR and RXR agonists/antagonists in mouse skin. *PLoS ONE, 8*, 62643-62654.

349. Li, D., Li, T., Wang, F., Tian, H., & Samuels, H. H. (2002). Functional evidence for retinoid X receptor (RXR) as a nonsilent partner in the thyroid hormone receptor/RXR heterodimer. *Mol. Cell. Biol., 22*, 5782–5792.

350. Schenk, T., Stengel, S., & Zelent, A. (2014). Unlocking the potential of retinoic acid in anticancer therapy. *Br. J. Cancer, 111*, 2039–2045.

351. Heyman, R. A., Mangelsdorf, D. J., Dyck, J. A., Stein, R. B., Eichele, G., Evans, R. M., & Thaller, C. (1992). 9-cis retinoic acid is a high affinity ligand for the retinoid X receptor. *Cell, 68*, 397–406.

352. Díaz, C., Vargas, E., & Gätjens-Boniche, O. (2006). Cytotoxic effect induced by retinoic acid loaded into galactosyl-sphingosine containing liposomes on human hepatoma cell lines. *Int. J. Pharm., 325*, 108–115.

353. Gudas, L. J., & Wagner, J. A. (2011). Retinoids regulate stem cell differentiation. *J. Cell. Physiol*., *226*, 322–330.

354. de Thé, H., & Chen, Z. (2010). Acute promyelocytic leukaemia: novel insights into the mechanisms of cure. *Nat. Rev. Cancer*, *10*, 775–783.

355. Lamour, F. P., Lardelli, P., & Apfel, C. M. (1996). Analysis of the ligand-binding domain of human retinoic acid receptor alpha by site-directed mutagenesis. *Mo. Cell. Biol.*, *16*, 5386–5392.

356. Gianní, M., Li Calzi, M., Terao, M., Guiso, G., Caccia, S., Barbui, T., Rambaldi, A. & Garattini, E. (1996). AM-580, a stable benzoic derivative of retinoic acid, has powerful and selective cyto-differentiating effects on acute promyelocyticleukemia cells. *Blood*, *87*, 1520–15231.

357. Tamura, K., Kagechika, H., Hashimoto, Y., Shudo, K., Ohsugi, K., & Ide, H. (1990). Synthetic retinoids, retinobenzoic acids, Am80, Am580 and Ch55 regulate morphogenesis in chick limb bud. *Cell Differ. Dev.*, *32*, 17–26.

358. Gluyas, J. B. G., Burschka, C., Dörrich, S., Vallet, J., Gronemeyer, H., & Tacke, R. (2012). Disila-analogues of the synthetic retinoids EC23 and TTNN: synthesis, structure and biological evaluation. *Org. Biomol. Chem.*,*10*, 6914–6929.

359. Holmes, W. F., Dawson, M. I., Robert Soprano, D., & Soprano, K. J. (2000). Induction of apoptosis in ovarian carcinoma cells by AHPN/CD437 is mediated by retinoic acid receptors. *J. Cel. Physio.*, *185*, 61–67.

360. Boisvieux-Ulrich, E., Sourdeval, M., & Marano, F. (2005). CD437, a synthetic retinoid, induces apoptosis in human respiratory epithelial cells via caspase-independent mitochondrial and caspase-8-dependent pathways both up-regulated by JNK signalling pathway. *Exp. Cell Res.*, *307*, 76–90.

361. Umemura, K., Watanabe, K., Ono, K., Yamaura, M., & Yoshimura, J. (1997). Total synthesis of antibiotic karnamicin B1. *Tetrahedron Lett.*, *38*, 4811–4814.

362. Allenby, G., Janocha, R., Kazmer, S., Speck, J., Grippo, J. F., & Levin, A. A. (1994). Binding of 9-cis-retinoic acid and all-trans-retinoic acid to retinoic acid receptors alpha, beta, and gamma. Retinoic acid receptor gamma binds all-trans-retinoic acid preferentially over 9-cis-retinoic acid. *J. Biol. Chem.*, *269*, 16689–16695.

363. Idres, N., Marill, J., Flexor, M. A., & Chabot, G. G. (2002). Activation of retinoic acid receptor-dependent transcription by all-trans-retinoic acid metabolites and isomers. *J. Biol. Chem.*, *277*, 31491–31498.

364. Kosztin, D., Izrailev, S. & Schulten, K. (1999). Unbinding of Retinoic Acid from its Receptor Studied by Steered Molecular Dynamics. *Biophys. J.*, *76*, 188–197.

365. Eigler, T., Ben-Shlomo, A., Zhou, C., Khalafi, R., Ren, S.-G., & Melmed, S. (2014). Constitutive somatostatin receptor subtype-3 signaling suppresses growth hormone synthesis. *Mol. Endocrinol.*, *28*, 554–564.

366. Thacher, S. M., Standeven, A. M., Athanikar, J., Kopper, S., Castilleja, O., Escobar, M., Beard, R. L. & Chandraratna, R. A. S. (1997). Receptor Specificity of Retinoid-Induced Epidermal Hyperplasia: Effect of RXR-Selective Agonists and Correlation with Topical Irritation. *J. Pharmacol. Exp. Ther.*, *282*, 528–534.

367. Agarwal, C., Chandraratna, R. A., Johnson, A. T., Rorke, E. A., & Eckert, R. L. (1996). AGN193109 is a highly effective antagonist of retinoid action in human ectocervical epithelial cells. *J. Biol. Chem.*, *271*, 12209–12212.

368. Géhin, M., Vivat, V., Wurtz, J.-M., Losson, R., Chambon, P., Moras, D., & Gronemeyer, H. (1999). Structural basis for engineering of retinoic acid receptor isotype-selective agonists and antagonists. *Chem. Biol.*, *6*, 519–529.

369. Kam, R. K. T., Deng, Y., Chen, Y., & Zhao, H. (2012). Retinoic acid synthesis and functions in early embryonic development. *Cell Biosci.*, *2*, 11-25.

370. Mailfait, S., Thoreau, E., Belaiche, D., & FormstecherAnd B Sablonniè, P. (2000). Critical role of the H6-H7 loop in the conformational adaptation of all-trans retinoic acid and synthetic retinoids within the ligand-binding site of RARalpha. *J. Mol. Endocrinol.*, *24*, 353–364.

371. Christie, V. B., Barnard, J. H., Batsanov, A. S., Bridgens, C. E., Cartmell, E. B., Collings, J. C., Marder, T. B., Przyborski, S., Redfern, C. P. F. & Whiting, A. (2008). Synthesis and evaluation of synthetic retinoid derivatives as inducers of stem cell differentiation. *Org. Biomol. Chem.*, *6*, 3497–3507.

372. Lund, B. W., Piu, F., Gauthier, N. K., Eeg, A., Currier, E., Sherbukhin, V., Brann, M. R., Hacksell, U. & Olsson, R. (2005). Discovery of a potent, orally available, and isoform-selective retinoic acid beta2 receptor agonist. *J. Med. Chem.*, *48*, 7517–7519.

373. Lund, B. W., Knapp, A. E., Piu, F., Gauthier, N. K., Begtrup, M., Hacksell, U., & Olsson, R. (2009). Design, synthesis, and structure-activity analysis of isoform-selective retinoic acid receptor beta ligands. *J. Med. Chem.*, *52*, 1540–1545.

374. Roy, B., Taneja, R., & Chambon, P. (1995). Synergistic activation of retinoic acid (RA)-responsive genes and induction of embryonal carcinoma cell differentiation by an RA receptor alpha (RAR alpha)-, RAR beta-, or RAR gamma-selective ligand in combination with a retinoid X receptor-specific ligan. *Mol. Cell. Biol.*, *15*, 6481–6487.

375. Ozpolat, B., Mehta, K., & Lopez-Berestein, G. (2005). Regulation of a highly specific retinoic acid-4-hydroxylase (CYP26A1) enzyme and all-trans-retinoic acid metabolism in human intestinal, liver, endothelial, and acute promyelocytic leukemia cells. *Leuk. Lymphoma*, *46*, 1497–1506.

376. Kaiser, A., Herbst, H., Fisher, G., Koenigsmann, M., Berdel, W. E., Riecken, E. O., & Rosewicz, S. (1997). Retinoic acid receptor beta regulates growth and differentiation in human pancreatic carcinoma cells. *Gastroenterol.*, *113*, 920–929.

377. Králová, J., Czerny, T., Spanielová, H., Ratajová, V., & Kozmik, Z. (2002). Complex regulatory element within the gammaE- and gammaF-crystallin enhancers mediates Pax6 regulation and is required for induction by retinoic acid. *Gene*, *286*, 271–282.

378. Chauhan, B. K., Yang, Y., Cveklová, K., & Cvekl, A. (2004). Functional interactions between alternatively spliced forms of Pax6 in crystallin gene regulation and in haploinsufficiency. *Nucleic Acids Res.*, *32*, 1696–1709.

379. Hansen, S. M., Berezin, V., & Bock, E. (2008). Signaling mechanisms of neurite outgrowth induced by the cell adhesion molecules NCAM and N-cadherin. *Cell. Mol. Life Sci.*, *65*, 3809–3821.

380. Muley, P. D., McNeill, E. M., Marzinke, M. A., Knobel, K. M., Barr, M. M., & Clagett-Dame, M. (2008). The atRA-responsive gene neuron navigator 2 functions in neurite outgrowth and axonal elongation. *Dev. Neurobiol.*, *68*, 1441–1453.

381. Shiohira, H., Kitaoka, A., Shirasawa, H., Enjoji, M., & Nakashima, M. (2010). Am80 induces neuronal differentiation in a human neuroblastoma NH-12 cell line. *Int. J. Mol. Med.*, *26*, 393–399.

382. Marshall, N. J., Goodwin, C. J., & Holt, S. J. (1995). A critical assessment of the use of microculture tetrazolium assays to measure cell growth and function. *Growth Regul., 5*, 69–84.

383. Moll, R. (1993). Cytokeratins as markers of differentiation. Expression profiles in epithelia and epithelial tumors. *Veröffentlichungen Aus Der Pathologie*, *142*, 1–197.

384. Wang, Y., Hayward, S., Cao, M., Thayer, K., & Cunha, G. (2001). Cell differentiation lineage in the prostate. *Differentiation*, *68*, 270–279.